University of Bath

PHD

Use of HiTRAN inserts to reduce fouling from crude oils

Takemoto, Tsuneo

Award date:
1993

Awarding institution:
University of Bath

Link to publication

Alternative formats
If you require this document in an alternative format, please contact:
openaccess@bath.ac.uk

Copyright of this thesis rests with the author. Access is subject to the above licence, if given. If no licence is specified above, original content in this thesis is licensed under the terms of the Creative Commons Attribution-NonCommercial 4.0 International (CC BY-NC-ND 4.0) Licence (https://creativecommons.org/licenses/by-nc-nd/4.0/). Any third-party copyright material present remains the property of its respective owner(s) and is licensed under its existing terms.

Take down policy
If you consider content within Bath's Research Portal to be in breach of UK law, please contact: openaccess@bath.ac.uk with the details. Your claim will be investigated and, where appropriate, the item will be removed from public view as soon as possible.

Download date: 06. May. 2023

Use of HiTRAN Inserts to Reduce Fouling from Crude Oils

Submitted by Tsuneo Takemoto

for the Degree of Ph.D

of the University of Bath

1993

Copyright

"Attention is drawn to the fact that copyright of this thesis rests with its author. This copy of the thesis has been supplied on condition that anyone who consults it is understood to recognise that its copyright rests with its author and that no quotation from the thesis and no information derived from it may be published without the prior written consent of the author.

This thesis may not be consulted, photocopied or lent to other libraries without the permission of the author and Cal Gavin Ltd for five years from the date of acceptance of the thesis."

T. Takemoto

UMI Number: U601819

All rights reserved

INFORMATION TO ALL USERS
The quality of this reproduction is dependent upon the quality of the copy submitted.

In the unlikely event that the author did not send a complete manuscript
and there are missing pages, these will be noted. Also, if material had to be removed,
a note will indicate the deletion.

UMI U601819
Published by ProQuest LLC 2013. Copyright in the Dissertation held by the Author.
Microform Edition © ProQuest LLC.
All rights reserved. This work is protected against
unauthorized copying under Title 17, United States Code.

ProQuest LLC
789 East Eisenhower Parkway
P.O. Box 1346
Ann Arbor, MI 48106-1346

UNIVERSITY OF BATH
LIBRARY
34 14 JUL 1993
PHD
S074300

To Noriko and Norifumi

SUMMARY

Fouling experiments have been carried out with light Arabian crude oil (containing 10% waxy residue from a crude oil tank) flowing inside 3/4 inch OD, 14 BWG heat exchanger grade tubes of a pilot-scale recycle flow test rig. Use of two identical parallel test sections, maintained at constant heat fluxes, has allowed direct comparisons to be made of the effects of heat flux, surface temperature, flow velocity and the presence of HiTRAN inserts. The presence of an insert can substantially reduce the extent of fouling and the effect is not simply one of reducing the surface temperature. A greater reduction in fouling appears to occur with an insert of higher loop density and it seems that the presence of an insert can alter the hydrodynamics in a beneficial manner. Crucial factors could be enhanced shear removal of deposits and the suppression of nucleation as well as reductions in both the residence time and the volume of fluid which is at a temperature in excess of that of the bulk fluid.

A simple film-based fouling model has been developed to account for the initial fouling rate in both a bare tube and a tube fitted with an insert. It is proposed that the initial fouling rate is dependent on the film heat transfer coefficient h_i, the average fluid velocity V_m, and the surface temperature T as follows:

$$\frac{dR_f(0)}{dt} = \frac{\alpha}{h_i * V_m} \int_o^1 \frac{1}{y} \exp\left(-\frac{E}{RT(y)}\right) dy$$

For the two parallel test sections operating at the same bulk temperature and the same initial surface temperature in the same Run, the ratio of the initial fouling rates is given by:

$$\frac{\left(\frac{dR_f(0)}{dt}\right)_1}{\left(\frac{dR_f(0)}{dt}\right)_2} * \frac{(h_{i1} * V_{m1})}{(h_{i2} * V_{m2})} - 1$$

The ratio of asymptotic fouling resistances is given by

$$\frac{R_{fi}^*}{R_{f2}^*} * \frac{(h_{i1}V_{m1})^2}{(h_{i2}V_{m2})^2} - 1$$

These relationships have been tested on two different crude oils with flow in both the fully convective regime and the subcooled nucleate boiling regime at surface temperatures in the range of 197°C to 239°C and fluid velocities in the range of 0.5 ms^{-1} to 1.1 ms^{-1}, with and without inserts of different density. Agreement with the experimental data is very good.

Further pilot-scale experiments, complemented by field trials on crude preheat trains, are now required to elucidate further the actual mechanisms of fouling reduction and to optimise insert configurations.

ACKNOWLEDGEMENTS

I am most grateful to Professor B D Crittenden for his supervision throughout the course of my study and for his constructive criticism and fruitful discussion especially during the preparation of my thesis.

I would like to express my sincere gratitude to Dr S T Kolaczkowski for his help in the preparation of the experimental apparatus and for his encouragement over the course of my study.

Thanks are particularly due to the two Pat McDonalds (Senior and Junior) for their help in acquiring the experimental data.

I am grateful to the Asahi Chemical Industry Co Ltd, Japan for the sponsorship of my stay and research. I would also like to thank Cal Gavin Ltd, Birmingham, for the sponsorship of the project and for supplying the HiTRAN inserts.

Finally I would like to express my thanks to everybody who has helped in accomplishing this work.

TABLE OF CONTENTS

LIST OF TABLES

LIST OF FIGURES

NOMENCLATURE

A	constant in Chapter 3 (s^{-2})
A	surface area in Chapter 1 (m^2)
A_c	cross sectional area of the fin (m^2)
A_s	surface area of the fin (m^2)
A_t	surface area based on d_t (m^2)
a	constant
b	constant
C_b	concentration of reactant and/or precursor in the bulk fluid (kg m^{-3})
C_f	friction coefficient
C_p	specific heat (J kg^{-1} $°C^{-1}$)
C_{pb}	concentration of reactant or precursor in the bulk fluid (kg m^{-3})
$C_p(x)$	concentration of reactant or precursor at the position x from the wall
C_{sf}	concentration of foulant at fluid/solid interface (kg m^{-3})
C	constant
C_1	constant
C_2	constant
D	foulant material (in Chapter 1)
D	diameter of the fin (in Appendix 4) (m)
D_p	diffusivity of precursor (m^2 s^{-1})
d_i	inside diameter of tube (m)
d_o	outside diameter of tube (m)

d_t	diameter based on the distance between two diametrically opposed wall thermocouples (m)
dq_{conv}	heat transferred by convection from length dx of the wire fin (W)
E	activation energy (kJ mol^{-1})
F	correction factor for temperature difference
f	Moody's friction factor
G	mass velocity (kg s^{-1} m^{-2})
H_i	thermal coefficient (W m^{-2} K^{-1})
h	heat transfer coefficient between fluid and wire (Wm^{-2} K^{-1})
h_i	in-tube heat transfer coefficient (W m^{-2} K^{-1})
j_H	Colburn's j factor
k	thermal conductivity of fluid (general) (W m^{-1} $°C^{-1}$)
k	thermal conductivity of the fin (in Appendix 4) (Wm^{-1} $°C^{-1}$)
k_b	thermal conductivity of the bulk fluid (Wm^{-1} $°C^{-1}$)
k_d	thermal conductivity of the deposit (W m^{-1} $°C^{-1}$)
k_{eff}	effective thermal conductivity (W m^{-1} $°C^{-1}$)
k_f	thermal conductivity of foulant (W m^{-1} $°C^{-1}$) (in Chapter 1)
k_f	thermal conductivity of the fluid (Wm^{-1} $°C^{-1}$) (in Chapter 3)
k_t	mass transfer coefficient for reactant or precursor (ms^{-1})
k_{tf}	mass transfer coefficient for foulant (ms^{-1})
k	reaction velocity constant (ms^{-1})
LMTD	log mean temperature difference (°C)
m	constant defined by equation (A4.14)
m_1	constant

m_2	constant
N_f	mass flux of foulant (kg m^{-2} s^{-1})
Nu	Nusselt number
P	precursor
Δp	pressure drop (Nm^{-2})
Pr	Prandtl number
Q	heat supplied (W)
q	heat flux (Wm^{-2})
q_f	heat transferred by fin (W)
q_x	heat transferred to the fluid at the position x (W)
q_{x+dx}	heat transferred to the fluid at the position x + dx (W)
R	gas constant (kJ mol^{-1} K^{-1})
Re	Reynolds number
R_f	fouling resistance (m^2 K W^{-1})
$R_f(1)$	fouling resistance at the end of Run (m^2 K W^{-1})
$R_f(2)$	fouling resistance measured after the increase in flow velocity (m^2 K W^{-1})
R_f^*	asymptotic fouling resistance (m^2 K W^{-1})
R_w	wall resistance (m^2 K W^{-1})
ΔR_f	change of fouling resistance (%)
Sc	Schmidt number
St	Stanton number
sg	specific gravity
T	temperature (general) (°C)

T_b	bulk temperature (°C)
T_{bc}	bulk temperature in clean condition (°C)
T_{bd}	bulk temperature in fouled condition (°C)
T_{bi}	inlet bulk temperature of the test section (°C)
T_{bo}	outlet bulk temperature of the test section (°C)
T_f	film temperature $T_f = (T_b + T_{sc})$ /2 (°C)
T_s	surface temperature (°C)
T_{sc}	clean surface temperature (°C)
T_w	wall temperature (°C)
T_{wc}	wall temperature in clean condition (°C)
T_{wd}	wall temperature in fouled condition (°C)
T^*	critical temperature (°C)
T (x)	temperature at the position x from the wall (°C)
U	local heat transfer coefficient (W m^{-2} K^{-1}) (in Chapter 2)
U	overall heat transfer coefficient (W m^{-2} K^{-1}) (in Chapter 1)
U_c	clean overall heat transfer coefficient (W m^{-2} K^{-1})
U_d	dirty overall heat transfer coefficient (W m^{-2} K^{-1})
U_t	overall heat transfer coefficient (W m^{-2} K^{-1}) (in Appendix 3)
V_b	volume of bulk fluid (m^3)
V_d	volume of deposit (m^3)
V_m	mean velocity of the fluid (ms^{-1})
V(x)	velocity of the fluid at the position x from the wall (ms^{-1})
WK	Watson K value
x	dimension of the test section (m)

x	distance from the wall (m)
X	ratio of k_b to k_d
X_d	thickness of deposit (m)
y	dimension of the test section (m)
y	non-dimensional distance defined by equation (3.25)
z	dimension of the test section (m)
α	constant in the summary (ms^{-2})
β_1	constant (m)
β_2	constant defined by equation (3.31)
β_3	constant defined by equation (3.36)
δ_m	thickness of the diffusion boundary layer (m)
δ_T	thickness of the thermal boundary layer (m)
$\theta(x)$	residence time at the position x from the wall (in Section 3.2) (s)
$\theta(x)$	temperature difference between fluid and fin at the position x (in Appendix 4) (°C)
θ_s	temperature difference defined by equation (A4.17) (°C)
μ	viscosity of the fluid (Pa.s)
μ_f	viscosity of the fluid at film temperature (Pa.s)
π_1	defined by equation (3.26)
π_2	defined by equation (3.30)
ρ	density of the fluid (kg m^{-3})
ρ_a	density of the fluid at the average temperature of T_{bi} and T_{bo} (kg m^{-3})
ρ_d	density of deposit (kg m^{-3})
ρ_f	density of foulant (kg m^{-3})

ρ_{15c}	density of fluid at 15°C (kg m^{-3})
τ	shear stress at the wall (Nm $^{-2}$)
Ψ	function of deposit structure
Ψ_d	fractional volume of the deposit defined by equation (3.12)

1. HYDROCARBON FOULING AND HEAT TRANSFER ENHANCEMENT

1.1 Introduction

Fouling is defined as the build-up of undesired material on a surface. Somerscales (1988) in a discussion of the history of fouling of heat transfer surfaces indicates that the phenomenon has been recognised as a problem for a long time. Despite the new knowledge that has been accumulating over the past 20 years, fouling remains one of the most poorly understood aspects of heat transfer design and operation. This lack of understanding inevitably leads to an increase in a number of costs, the extent of each of which is dependent on the particular processing application (Pritchard (1988), Rebello (1988) and Bott (1990)):

(1) Increased capital investment

The inclusion of an allowance for the fouling resistance in the heat transfer design results in an increase in the design surface area. In addition, a unit which fouls heavily might need to be positioned in a more accessible location for maintenance and/or be fitted with on-line cleaning. Duplication of equipment might also be required for a unit in a critical process location.

(2) Additional energy requirements

Shortfalls in energy exchange as a result of fouling are often compensated for by burning additional primary fuels in furnaces and heaters. Also if fouling creates a significant pressure drop there will be an increase in power requirements for pumping.

(3) Additional maintenance requirements

There will be a need periodically to clean equipment, either in-situ or by dismantling to improve heat transfer efficiency. In addition, repairs might need to be effected following damage caused if, due to the gradual build-up of the deposit thickness, the pressure at the inlet end is increased beyond that expected at the design stage.

(4) Loss of production

Heat transfer equipment which is isolated for cleaning cannot be used for production. In addition, the accumulation of deposits may limit thermal and pumping performance to an extent that throughput must be decreased.

(5) The use of antifoulant additives

Antifoulants for many processes are available from specialist chemical companies. However, the cost of implementing and monitoring an antifoulant chemical campaign is expensive and it is difficult to determine its effectiveness, particularly for the oil industries.

Although the total cost of fouling is not always appreciated, total fouling-related costs in the UK and USA have been estimated to be as follows:

UK (1979) : £3 x 10^8 to £5 x 10^8 (Thackery (1979))

USA (1985) : \$8 x 10^9 to \$10 x 10^9 (Garrett-Price *et al* (1985))

For an oil refinery, the Exxon Chemical Company estimated the fouling related expense in a hypothetical 100,000 bbl per day oil refinery in 1979 to be nearly \$10 million per annum (Van Nostrand *et al*, 1982). The above figures give ample incentive for research into fouling and there is no doubt that a better understanding of the phenomenon would lead to substantial cost savings.

1.2 General background

Fouling references of general interest which reflect the current state of knowledge are provided by Somerscales and Knudsen (1981), Chenoweth and Impagliazzo (1981), Suitor and Pritchard (1984) and Melo *et al* (1988). Fouling processes have been classified by Epstein (1981, 1983) into the following generally accepted categories.

(1) Precipitation fouling: the precipitation of inverse solubility salts (such as $CaC0_3$, $CaS0_4$, $Ca_3(P0_4)_2$, $CaSi0_3$, $Ca(0H)_2$, $Mg(0H)_2$, $MgSi0_3$, Na_2S0_4 and Li_2C0_3 in water) onto a superheated transfer surface. Though more severe under boiling conditions, precipitation also occurs when hard water or

aqueous solutions undergo sensible heating. This is often referred to as scaling.

(2) Particulate fouling: the accumulation of particles suspended in a liquid onto a heat transfer surface. This includes gravitational settling of relatively large particles onto a horizontal heat transfer surface (sedimentation fouling), as well as deposition of colloidal particles by other mechanisms onto a surface at any other inclination.

(3) Chemical reaction fouling: deposits formed by chemical reactions at or close to the heat transfer surface in which the surface material itself is not a reactant. Polymerisation, cracking and coking of hydrocarbons are prime examples.

(4) Corrosion fouling: the heat transfer surface itself reacts to produce corrosion products which foul the surface and may foster the attachment of other potential fouling materials.

(5) Biofouling: biological organisms which attach themselves to the heat transfer surface and which may generate adherent slimes.

(6) Freezing fouling: the solidification of a pure liquid or constituents of a liquid solution onto a subcooled transfer surface. This may be considered to be a category of precipitation fouling.

Fouling problems which occur in industrial processes often involve two or more mechanisms. For example, in oil refineries chemical reaction fouling may be accompanied by particulate fouling and corrosion fouling.

Epstein (1983) has proposed a general sequence of fouling events which may play a role in all types of fouling:

(1) Initiation, which may include surface conditioning

(2) Transport of foulant

(3) Attachment to the surface

(4) Release of the deposit

(5) Aging of the deposit on the surface

This classification of primary types and successive events, shown in Figure 1.1 as Epstein's 5 by 5 matrix, provides both a conceptual framework for the study of fouling and a focus for research. Bohnet (1987) assessed the extent of the current knowledge on fouling in each element, as shown in Figure 1.2. For chemical reaction fouling it appears that the extent of knowledge still lies between scant and poor.

1.3 Fouling from hydrocarbons

Using Epstein's 5 by 5 matrix, hydrocarbon fouling is generally regarded to be a sub-category of chemical reaction fouling. Particulate fouling and corrosion fouling

	1. Crystallization Fouling	2. Particulate Fouling	3. Chemical-Reaction Fouling	4. Corrosion Fouling	5. Biological Fouling
1. Initiation	1,1	1,2	1,3	1,4	1,5
2. Transport	2,1	2,2	2,3	2,4	2,5
3. Attachment	3,1	3,2	3,3	3,4	3,5
4. Removal	4,1	4,2	4,3	4,4	4,5
5. Aging	5,1	5,2	5,3	5,4	5,5

Figure 1.1 Fouling matrix by Epstein (1983)

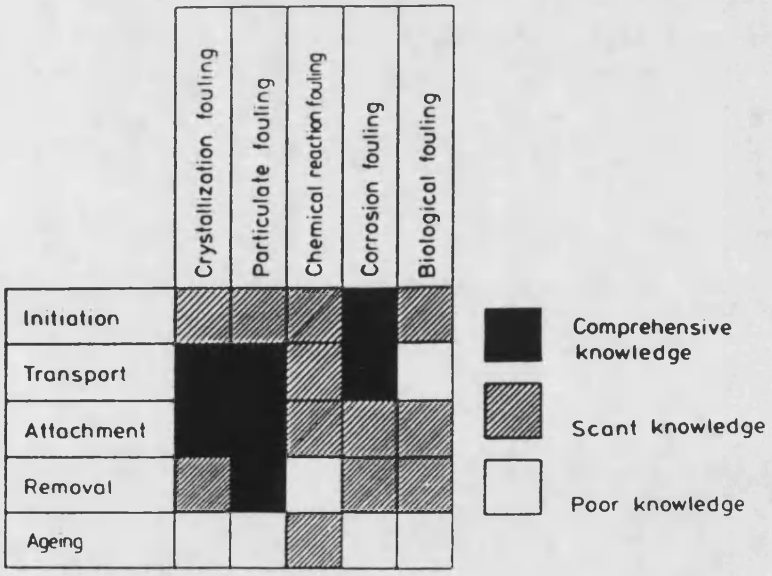

Figure 1.2 Bohnet's assessment (1987) of state of knowledge of fouling matrix

are possibly involved as well.

1.3.1 Mechanisms

The recent critical review by Watkinson (1988) shows that in many cases the complex reaction mechanisms associated with the fouling process can be considered to occur in two-steps in which soluble precursors are first formed, and then precipitation of higher molecular weight polymerised products occurs. The insoluble species may be produced in the fluid in the bulk, or close to or at the heat exchange surface. The generation of precursors in aerated organic fluids is believed to occur primarily by autoxidation at temperatures below 650 K or by thermal decomposition (pyrolysis) at higher temperatures, especially in the absence of oxygen. Subsequent precipitation occurs following the polymerisation of precursors.

In hydrocarbon fouling three types of chemical reaction may be involved, namely thermal decomposition, autoxidation and polymerisation.

(1) Thermal decomposition (Fitzer *et al* (1971))

At high temperatures, over 650K, and particularly in the gas phase, thermal cracking can proceed. By this mechanism coke can be formed via synthesis reactions of the intermediate products from degradation reactions. Such a mechanism clearly applies to thermal or steam cracking furnaces.

(a) Degradation reactions

In cracking reactions, paraffins decompose to one paraffin and one olefin:

$$2R_1\text{-}CH_2\text{-}CH_2\text{-}CH_2\text{-}CH_2\text{-}R_2 \begin{cases} \nearrow & R_1\text{-}CH_2\text{-}CH_3 + R_2\text{-}CH = CH_2 \\ \searrow & R_1\text{-}CH{=}CH_2 + R_2\text{-}CH_2\text{-}CH_3 \end{cases} \quad (1.1)$$

In dehydrogenation reactions, hydrogen is split off, causing the formation of a double bond without changing the chain length of the original paraffin, *e g*

$$CH_3\text{-}CH_2\text{-}CH_2\text{-}CH_3 \begin{cases} \nearrow & CH_3\text{-}CH{=}CH\text{-}CH_3 \\ \searrow & CH_3\text{-}CH_2\text{-}CH{=}CH_2 \end{cases} \quad (1.2)$$

The pyrolytic cracking of a C-C or C-H bond can take place by way of radical or ion formation. In the absence of a catalyst thermal pyrolysis will proceed primarily by the radical mechanism.

(b) Synthesis reactions

The synthesis of larger molecules can occur by way of cyclisation, aromatisation and ring condensation. Higher polycyclic aromatic molecules can be formed via condensation reactions of aromatics formed from the cyclisation reactions of olefins. Aromatisation takes place preferentially at temperatures above 950K. Condensation leading to polycyclic compounds in the liquid phase can occur at temperatures between 650K and 750K. Cross-linking reactions between polycyclic aromatics can

occur at temperatures below 650K. Possible mechanisms of synthesis reactions are the Diels-Alder and radical pyrocondensation reactions.

The pyrolytic processes of hydrocarbons are schematically illustrated in Figure 1.3

(2) Autoxidation (Emanuel *et al* (1967)), Reich and Stivala (1969))

At temperatures below 650K it is generally accepted that gum and deposit formation, particularly from liquid hydrocarbons, is due to free radical autoxidation reactions (Brooks (1926), Canapary (1961), Braun (1977), Crittenden and Khater (1984)). Autoxidation is initiated by hydrogen abstraction from the parent molecule RH by a free radical $\dot{X}$:

$$R - H + \dot{X} \rightarrow R\cdot + HX \qquad (1.3)$$

Reaction of the substrate radical with molecular oxygen and further hydrogen abstraction results in a chain reaction involving peroxyl radicals and hydroperoxide molecules:

$$\dot{R} + 0_2 \rightarrow ROO\cdot \qquad (1.4)$$

$$ROO\cdot + RH \rightarrow ROOH + \dot{R} \qquad (1.5)$$

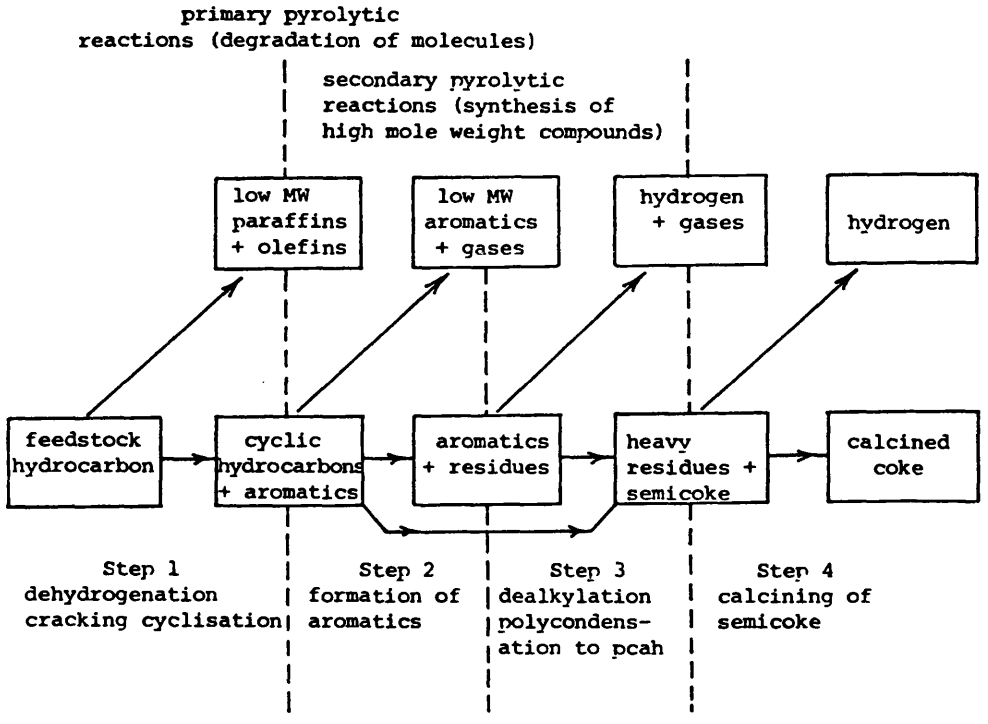

Figure 1.3 Schematic of hydrocarbon pyrolysis (Fitzer et al (1971))

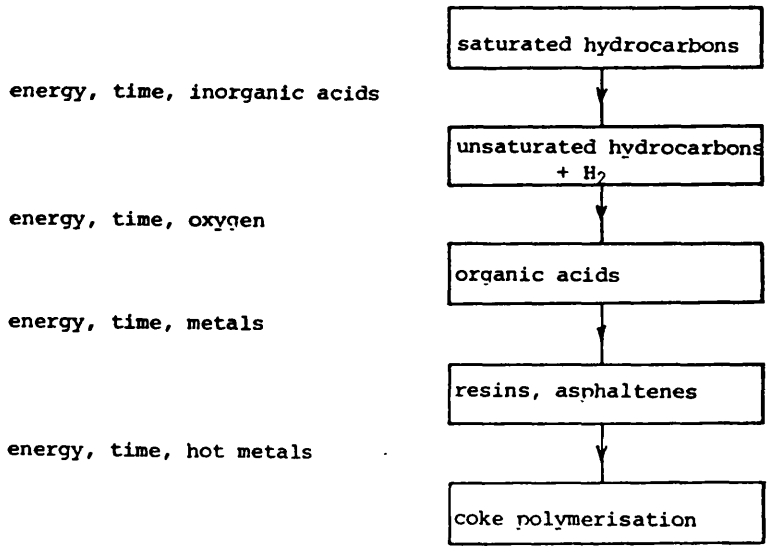

Figure 1.4 Successive degradation of hydrocarbon to coke (Eaton and Lux (1983))

Possible termination steps are:

$$2R\cdot \rightarrow R - R \qquad (1.6)$$

$$R\cdot + ROO\cdot \rightarrow R - 0 - 0 - R \qquad (1.7)$$

$$2ROO\cdot \rightarrow R - 0 - 0 - R + 0_2 \qquad (1.8)$$

Transition metals such as cobalt, manganese, iron, copper and nickel can catalyse the reaction by increasing the rate of hydroperoxide homolysis and by participating in free radical formation reactions. The autoxidation mechanism is summarised by Eaton and Lux (1983) as shown in Figure 1.4.

(3) Polymerisation

Polymerisation reactions consist of three basic steps:

(a) radical formation and chain initiation

$$XH \rightarrow \dot{X} + \dot{H} \qquad (1.9)$$

$$R - CH - CH_2 + \dot{X} \rightarrow R - \dot{C}H - CH_2 - X \qquad (1.10)$$

b) chain propagation

$$R - \underset{\displaystyle CH_2X}{\underset{|}{\dot{C}H}} + n\,(R - CH = CH_2) \rightarrow R - \underset{\displaystyle CH_2}{\underset{|}{CH}}\,[\,\overset{\displaystyle R}{\overset{|}{CH_2}} - CH\,]_n\,\overset{\displaystyle R}{\overset{|}{CH_2}} - CH\cdot \qquad (1.11)$$

(c) termination

$$R - \underset{\displaystyle CH_2}{\underset{|}{CH}}\,[\,CH_2 - \overset{\displaystyle R}{\overset{|}{CH}}\,]_n\,CH_2 - \overset{\displaystyle R}{\overset{|}{\dot{C}H}} + \dot{H} \rightarrow R - \underset{\displaystyle CH_2}{\underset{|}{CH}}\,[\,\overset{\displaystyle R}{\overset{|}{CH_2}} - CH\,]_n\,\overset{\displaystyle R}{\overset{|}{CH_2}} - CH_2 \qquad (1.12)$$

Oxygen, halides, sulphides, nitrogen compounds, certain metals and metallic compounds are known to initiate polymerisation reactions (Lenz (1982)).

1.3.2 Fouling models

Recent reviews of thermal fouling models and chemical reaction fouling models are provided by Epstein (1988) and Crittenden *et al* (1987b), respectively. Chemical reaction fouling models are summarised chronologically in Table 1.1. All have been developed for heat transfer applications and are related to in-tube fouling only. Several (Nelson (1934), Fernandez-Baujin and Solomon (1976), Crittenden and

Table 1.1 Chemical reaction fouling models

Authors	Application	Deposition term	Removal term	Remarks
Nelson (1934)	Oil refining	Rate is directly dependent upon thickness of thermal boundary layer	None considered	Fouling rate can be reduced by increasing fluid velocity
Atkins (1962)	Fired heaters in oil industry	Constant monthly increase in coke resistance for various refinery streams	None considered	Two layer concept - porous coke adjacent to fluid and hard coke adjacent to wall
Nijsing (1964)	Organic coolant in nuclear reactors	Hydrodynamic boundary layer and diffusion partial differential equations: (1)instaneous first order reaction in zone close to wall (2)very rapid crystallisation at hot surface	Product diffusion back to the fluid bulk is an integral part of the differential equations	(1)Solution with diffusion control fits plant data; fouling rate predicted to increase with velocity (2)Extended to consider colloidal transfer to the hot syrface
Watkinson and Epstein (1970)	Liquid phase fouling from gas oil	Mass transfer and adhesion of suspended particles: (1)sticking probability proportioal to exp(-E/RT) (2) sticking probability inversely proportional to hydrodynamic forces on particle as it reaches wall	First order Kern and Seaton shear removal term	(1)Correct prediction of initial rate dependence on velocity (2)Incorrect prediction of asymptotic resistance on velocity
Jackman and Aris (1971)	Vapour phase pyrolysis	Kinetics control - two reactions: (1)first order dissociation of A into products (2)zero order coke formation	None considered	(1)Quasi-steady-state assumption (2)Untested
Fernandez-Bauijn and Solomon (1976)	Vapour phase pyrolysis	Kinetics and/or mass transfer control with fist order reaction	None considered	Solution with mass transfer control fits plant run-time data, fouling rate increases with velocity

Table 1.1 continued...

Table 1.1 continued

Authors	Application	Deposition term	Removal term	Remarks
Sundaram and Froment (1979)	Vapour phase pyrolysis of ethane	Kinetics control (1)at surface temperature (2)first order in propylene concentration, a product of primary cracking reactions	None considered	(1)Quasi-steady-state assumption (2)Good agreement between industrial and numerically simulated data
Crittenden and Kolaczkowski (1979a,b)	Hydrocarbons in general	Kinetics and/or mass transfer control with first order reaction	(1)Diffusion of foulant back into fluid bulk (2)First order Kern and Seaton shear removal term	(1)Limited testing (2)Complex - many parameters (3)Extended to two layer concept proposed by Atkins
Crittenden et al (1987b)	Dilute solution polymerisation of styrene	Non-zero order kinetics	(1)Diffusion of foulant back into fluid bulk (2)First order Kern and Seaton shear removal term	
Kolaczkowski et al (1988)	Crude oils	Kinetics control	First order Kern and Seaton shear removal term	Demonstrated interractive nature of fouling in process networks
Crittenden et al (1992)	Crude oils	Kinetics control	None considered	Plant data used to obtain coefficients in predictive models; good fits obtained
Panchal and Watkinson (1993)	Autoxidation of indene in kerosine	Kinetics and/or mass transfer control Non-zero order kinetics	Nono considered	Models are developed for three fouling mechanisms on the basis ofthe region where generation of precursor occures (1)in the bulk fluid (2)in the thermal boundary layer (3)at the wall surface

Kolaczkowski (1979 a, b), Panchal and Watkinson (1993)) are based on the film theory of mass and heat transfer.

Nelson (1934) was the first to provide a fouling model for oil refinery equipment. He suggested that the rate of coking (fouling) is directly dependent on the volume of the fluid in the film at the heat transfer surface. The volume of this film, which is exposed to higher temperatures than the bulk for a fluid being heated, is proportional to the thickness of the thermal boundary layer.

The model developed by Crittenden and Kolaczkowski (1979a) was established to account for chemical reaction fouling in general. The deposition of foulant materials, D, is assumed to involve:

(1) transport of the foulant precursor, P, present in the fluid bulk in a direction normal to the tube surface,

(2) chemical decomposition and/or polymerisation close to or at the heat surface,

(3) possible transport of products including foulant away from the reaction zone.

Foulant material is assumed to be formed by the irreversible reaction:

$$P \rightarrow D + \text{light products} \qquad (1.13)$$

The removal or release of deposits by the shearing action of the fluid, which was originally proposed by Kern and Seaton (1959), was included in the model. Finally, the fouling rate could be expressed as:

$$\frac{dR_f}{dt} = \frac{1}{\rho_f k_f}\left[\frac{C_b}{\frac{1}{k_t} + \frac{1}{k}} - k_{tf} C_{sf}\right] - \frac{\tau}{k_f \psi} R_f \qquad (1.14)$$

in which

ρ_f	is density of foulant (kg m^{-3})
k_f	is thermal conductivity of foulant (kW m^{-1} K^{-1})
k_t	is mass transfer coefficient for reactant or precursor (ms^{-1})
k_{tf}	is mass transfer coefficient for foulant (ms^{-1})
C_b	is concentration of reactant or precursor in the bulk (kg m^{-3})
C_{sf}	is concentration of foulant at fluid/solid interface (kg m^{-3})
k	is reaction velocity constant (ms^{-1})
τ	is shear stress at the wall (Nm^{-2})
ψ	is a function of deposit structure

This model was tested in a system which comprised the polymerisation of 1% styrene in kerosine (Crittenden *et al* (1987a)). The interfacial concentration C_{sf} was obtained by fitting data to the model. The variation of C_{sf} with temperature was found to be as expected.

Equation (1.14) implies a complex dependency of fouling rate on mass flow rate.

Table 1.2 shows that the effect of mass velocity on fouling is dependent upon the balance between mass transfer and kinetics. In the case where back diffusion of precursors and shear removal of deposits are negligible and mass transfer controls the deposition rate, the dependency of the fouling rate on mass velocity is the same as the Nijsing (1964) and the Fernandez-Baujin and Solomon (1976) models. Crittenden and Kolaczkowski (1979b) extended their model to take into account two layers as in the mechanism proposed by Atkins (1962). However, this model has not been tested yet.

Very recently, Panchal and Watkinson (1993) have developed a general fouling model which can be applied to situations in which the chemical reactions for precursor generation take place in the bulk fluid, in the thermal boundary layer or at the wall surface. The chemical reactions which result in fouling are assumed to occur via a two step mechanism:

Reactants (soluble)	→	Precursor (sparingly soluble)	→	Foulant (insoluble)	(1.15)

The model was used to examine the experimental data for fouling deposition via poly-peroxide produced by the autoxidation of indene in kerosine. Comparison of experimental data with predictions indicated that the model more accurately predicted the fouling resistances when based on the reaction taking place in the thermal boundary layer than when based on the other locations. It is claimed that this approach is the first step towards the development of a comprehensive fouling model in which the effects of particulates, inorganic salts and the presence of

Table 1.2 Scenarios of deposition and removal in mass transfer and kinetics model (Crittenden (1988a))

deposition term		release/removal term		effect of increasing w (at given T_w)
		precursor back diffusion	foulant shear removal	
T_w low	kinetics control	√	-	reduces dR_f/dt
d small	$k << k_t$	-	-	little effect
w high		-	√	reduces dR_f/dt
T_w high	precursor diffusion	√	-	increases dR_f/dt
d large	control	-	-	increases dR_f/dt
W low	$k >> k_t$	-	√	complex

complex substances such as asphaltene can be included.

1.3.3 Factors influencing fouling

Overall fouling rates are strongly affected by temperatures, velocity, pressure and composition. Those parameters which affect fouling and are, in turn, affected by fouling are summarised in Figure 1.5.

1.3.3.1 Time

The fouling process is a transient condition. Possible variations of fouling resistance with time are shown in Figure 1.6. For hydrocarbon fouling the dependency on time has been found to be linear (Atkins (1962), Watkinson and Epstein (1969), Smith (1969), Vranos *et al* (1981), Lambourn and Durrieu (1983), Crittenden and Khater (1984), Crittenden *et al* (1992)), falling rate (Butler *et al* (1949), Weiland *et al* (1949)), asymptotic (Watkinson and Epstein (1969), Eaton and Lux (1983)) or falling rate + linear (Shah *et al* (1976), Sundaram and Froment (1979)). In general it is not possible to determine whether or not an initial fouling behaviour would eventually yield either a falling rate behaviour or an asymptotic behaviour, unless a sufficiently long period of operation is provided. During the initial stages of fouling, a period in which the fouling resistance is not appreciable or even negative, has been observed by several investigators (Bott and Gudmundsson (1978), Crittenden and Khater (1984), Ritter (1984)). Possible reasons for the occurrence of negative fouling resistances have been investigated in

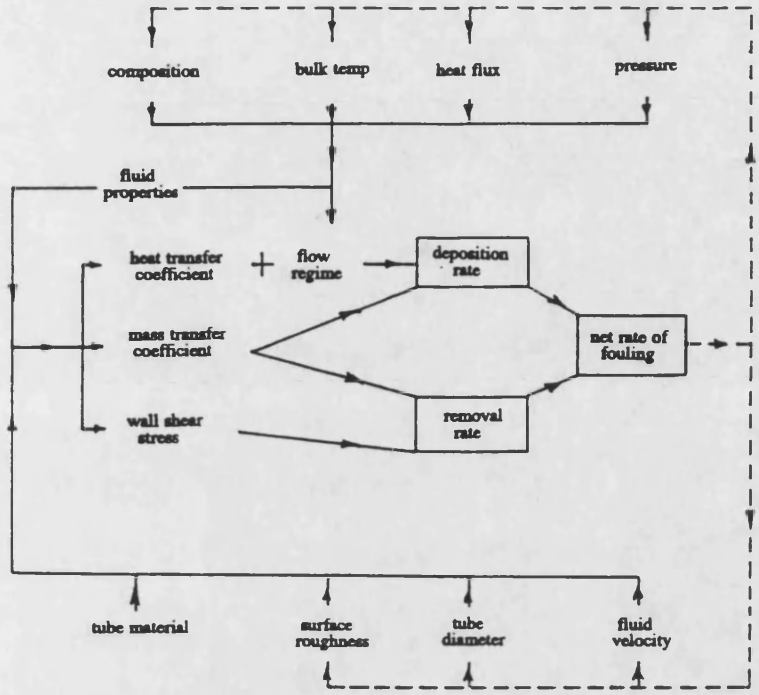

Figure 1.5 Prameters affecting and affected by deposition (Crittenden et al (1987a))

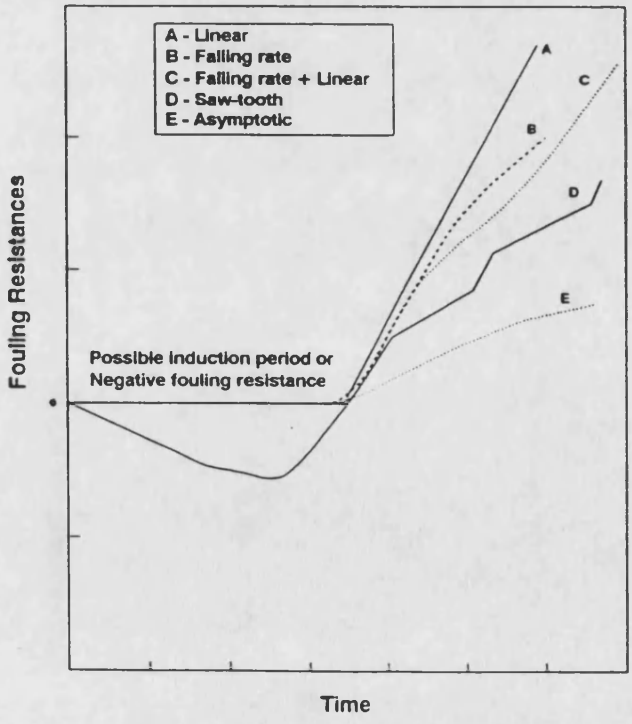

Figure 1.6 Effect of time on fouling resistance

detail by Crittenden and Alderman (1983 and 1992).

1.3.3.2 Flow velocity

The effect of velocity on hydrocarbon fouling has been fully discussed by Crittenden (1988b). It is a generally accepted rule in the oil and chemical industries that the problem of fouling from hydrocarbons can be reduced to some extent by use of a high velocity. However, Table 1.3 shows complex effects of fluid velocity on fouling and thus this simple rule may not always be applicable. Changing the flow velocity can affect fouling in a number of ways:

(1) Use of a higher velocity, which increases a film heat transfer coefficient, can also increase the mass transfer rate of precursors to the hot surface.

(2) Use of a higher velocity, which reduces the thickness of the thermal boundary layer, decreases the residence time of fouling precursors which are exposed to temperatures higher than that of the bulk fluid.

(3) Use of a higher velocity increases the shear stress at the wall leading to possible removal of deposits.

(4) Changing the fluid velocity alters the surface temperature on which the chemical reaction fouling rate is strongly dependent.

For a given heat flux, q and bulk temperature, T_b, the surface temperature, T_s, is given by:

Table 1.3 Effect of flowrate on deposition rate

Authors	Dependence of deposition rate on increasing flowrate	System studied	Tube diameter (m)	Temperature range (C)	Flowrate range	Comments
Nelson (1958)	decreases	desalted,wet and corrosive crude oils	not specified	to greater than 260	0.3<m/s<2.1	industrial plant data
Chantry and Church (1958)	decreases	forced circulation reboilers	not specified	not specified	3 <m/s< 10	
TEMA (1968)	decreases	various gas,gasoline and refinery streams	not specified	120 to 260	< 0.6m/s to > 1.2m/s	
Watkinson and Epstein (1969)	decreases	liquid sour gas oils	0.0087	146 to 204	9800 < Re < 41900	
Smith (1969)	increases	liquid aviation kerosene	0.0021 - 0.0028	160 to 260	4500 < Re < 10000	ASTM fuel coker
Chen and Maddock (1973)	increases	cracking furnace for ethylene	0.05 - 0.2	900 to 1000	not specified	kinetics may control at lower temperatures
Fernandez-Baujin (1976)	increases	vapour phase pyrolysis of naphtha and light gas oil	not specified	high	not specified	comparison of model with plant data
Veranos et al (1981)	increases	liquid jet fuels	0.0018 - 0.0048	149 to 260	600 < Re < 10000	rate (Re)^0.6
Shah et al (1976)	increases or decreases	vapour phase thermal cracking of n-octane	0.0046 - 0.0064	750 to 800	0.1 < space/ time < 1s	maximun in rate-flowrate relationship
Crittenden et al (1987a)	increases or decreases	dilute solution polymerisation of stylene	0.02	22 to 249	1000 < Re < 5200	maximun in rate-flowrate relationship

$$T_s - T_b + \frac{q}{h_i} \qquad (1.16)$$

in which h_i is the film heat coefficient.

From equation (1.16), an increase in fluid velocity for a given heat flux reduces the surface temperature. However, for a given heat exchanger in which the outlet temperature must be maintained for operational reasons, the thermal duty and hence the heat flux are proportional to mass velocity, whilst the film heat transfer coefficient is proportional to mass velocity raised to the power 0.8. Thus:

$$T_s - T_b + aG^{0.2} \qquad (1.17)$$

in which G is mass velocity and a is a constant.

In this case the surface temperature can be increased by increasing the mass velocity. Smith (1969) worked with constant inlet and outlet temperatures (which is the case considered above). Thus the local surface temperatures in Smith's experiments would have increased slightly as the mass flow rate was increased and hence his results cannot be solely attributable to velocity. In other experiments, increases in fouling rate which occur as the flow velocity is increased, are probably due to the mass transfer effect in which precursors can be conveyed faster to the hot surface.

1.3.3.3 Temperature

The effect of temperature, which is one of the most important variables of all in hydrocarbon fouling, is complex because the mechanisms by which fouling occurs are complex. However, many studies (Atkins (1962), Taylor (1969), Watkinson and Epstein (1969), Crittenden *et al* (1987a), Crittenden *et al* (1992)) show that the initial fouling rate increases exponentially with absolute temperature. Data are normally correlated by Arrhenius-type equations:

$$\textit{fouling rate} \propto \exp\left(-E/RT_s\right) \tag{1.18}$$

in which E is the activation energy and R is the gas constant.

Activation energies obtained from hydrocarbon fouling studies are shown in Table 1.4. Values over 40 kJ mol^{-1} indicate the predominance of chemical mechanisms. On the other hand an activation energy below 40 kJ mol^{-1} probably indicates that physical mechanisms, such as precipitation and particle adhesion, are important as well as chemical mechanisms. More complicated relationships between fouling rate and surface temperature, similar to that shown in Figure 1.7, have been found in three studies (Taylor (1974), Vranos (1981), Crittenden and Khater (1987)). In each case the reason for the decrease in deposition rate at a critical temperature, labelled T*, was associated with the transition from liquid phase to vapour phase on the hot surface. Other types of complex rate-temperature relationship have been reported (Taylor *et al* (1968, 1978), Taylor (1974, 1976), Braun (1977)).

Table 1.4 Activation energies for chemical reaction fouling

fluid	activation energy kJ/mol	surface temperature range, C	reference
liquid jet fuels	42	149 - 260	Vranos et al (1981)
pure n-paraffins	40	93 - 260	Taylor(1969)
styrene polymerisation	39	22 - 98	Crittenden et al(1987a)
sour gas oils	120	146 - 204	Watkinson and Epstein(1969)
'light' crude oils	33	160 - 280	Crittenden et al(1992)
'heavy' crude oils	21	160 - 280	Crittenden et al(1992)

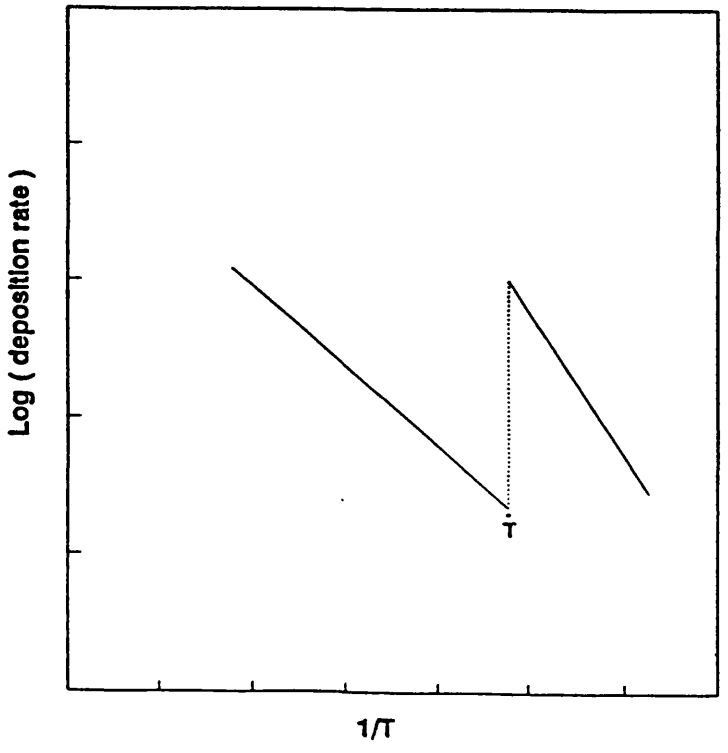

Figure 1.7 Arrhenius plot showing change of mechanism

Studies of the effect of bulk temperature and temperature difference (between bulk and surface) are rare. Eaton and Lux (1983) found that with their probe an increased oil temperature caused a decrease in fouling for the same probe temperature. For example at a probe temperature of 267°C, fouling of paraffin oils was rapid with a bulk temperature of 38°C but no observable fouling occurred when the bulk fluid was at 267°C. They suggested that the possible reason for this was that less oxygen was dissolved in the oil at the higher bulk temperature and/or the solubility of the deposit in the bulk fluid was higher at the higher bulk temperature. In contrast, Panchal and Watkinson (1993) found that the fouling rate from indene was increased as the bulk temperature was increased for a given clean surface temperature. They concluded that fouling probably occurred in the fluid bulk as well as at the wall. Clearly further study of the effect of bulk temperature is required.

1.3.3.4 Pressure and boiling

Hydrocarbon fouling studies involving phase change are relatively rare. The most detailed study of fouling in this field was carried out by Crittenden and Khater (1984). They found that the fouling rate from vaporising air-saturated kerosine increased in general with increasing pressure over the range 1 to 2.5 bar. Pressure controls not only the onset of boiling of kerosine but also the solubility of oxygen or air in the liquid phase. Therefore, increasing the oxygen content in the kerosine and suppressing vaporisation by raising the pressure were believed to cause increases in fouling rates for the liquid phase.

Vranos (1981) found that the boiling regime certainly has a marked effect on the thermal decomposition of a puddle of air-saturated n-hexadecane. Although decomposition rates were not reported, an increased decomposition rate apparently coincided with the onset of film boiling, which was observed visually, and with the simultaneous surface-catalysed decomposition of hexadecyl hydroperoxides originating in the liquid phase.

For hydrocarbon fouling, fouling rates in boiling and non-boiling situations have not been directly compared before, although Shalhi (1993) did explore the effect of various dissolved gases. Lack of adequate control of the system pressure however meant that Shalhi was unable to interpret the fouling data in an unambiguous manner. Clearly further investigation is necessary to elucidate the effect of the heat transfer regime on fouling.

1.3.3.5 The presence of impurities

The effect of impurities on fouling has been reviewed in detail by Watkinson (1988). The species causing fouling are not only the primary or major components of the fluid but also a wide range of species such as dissolved oxygen, oxygenated compounds, sulphur compounds, nitrogen compounds, dissolved metallic ions and tube wall materials. Such trace components may trigger and accelerate decomposition and polymerisation reactions. It is well known that for hydrocarbon streams the presence of dissolved oxygen and/or oxygenated compounds causes autoxidation to occur, particularly in the liquid phase.

1.4 Fouling in oil refineries

Oil refinery heat transfer equipment often suffers from fouling. In order to help ensure efficient recovery of energy from product streams, several investigations have been made of crude oil preheating (Nelson (1939), Butler *et al* (1949), Weiland *et al* (1949), Canapary (1961), Lawler (1979), Lambourn and Durrieu (1983), Dickakian and Seay (1988), Dickakian (1989), Crittenden *et al* (1992)).

1.4.1 Deposit composition

The deposit composition is obviously a clue to identifying the mechanisms occurring in crude oil fouling. Example compositions of deposits formed in industrial heat exchangers (Dickakian (1989), Crittenden *et al* (1992)) and in a laboratory scale stirred apparatus (Eaton and Lux (1983)) are shown in Tables 1.5(a), (b) and (c). The analyses show general similarities with deposits containing both organic and inorganic materials. Substantial amounts of iron and sulphur in the inorganic fractions have been found. Iron is almost certainly due to corrosion reactions, whilst sulphur probably originates from the crude oils themselves. The organic fractions have been found to contain resins, asphaltenic materials and cokes. From these analyses it may be inferred that the fouling mechanisms include organic reactions as well as chemical and physical processes involving inorganic species.

Table 1.5(a) Deposit analyses (Crittenden et al (1992))

fraction wt%	E7A	E8A	E9A	E10A
n-heptane-soluble	49.8	22.6	56.2	57.4
toluene-soluble	1.9	1.1	1.6	1.2
loss on ignition at 820K	32.8	37.2	24.6	25.3
remaining ash	15.5	39.1	17.6	16.1
Total	100.0	100.0	100.0	100.0
components in ash wt%				
iron	35.5	28.1	37.1	42.2
sulphur	29.0	18.3	27.4	28.0
sodium	20.0	29.6	21.7	18.0
calcium	7.7	3.3	4.1	5.6
zinc	2.6	1.0	2.8	3.1
magnesium	1.3	0.5	0.6	—
chlorine	—	14.1	1.1	0.6
others	3.9	5.1	5.2	2.5
Total	100.0	100.0	100.0	100.0

*courtesy of BP Research

Table 1.5(b) Deposit analyses (Dickakian (1989))

CHARACTERIZATION OF CRUDE OIL HEAT EXCHANGER DEPOSIT

1. COMPOSITION ANALYSIS	CRUDE SIDE	RESID SIDE
Residual Oil (%)	26.8	38.6
C_7-Asphaltene (%)	5.9	14.1
Coke Content (%)	42.5	7.9
Inorganic Material (%)	24.8	39.4
2. INORGANIC COMPOSITION		
Al (%)	5.5	3.1
Si (%)	3.0	2.1
P (%)	2.3	6.8
S (%)	7.9	8.7
Ca (%)	8.3	12.3
Fe (%)	55.4	68.1
Zn (%)	5.1	0.9
Co (%)	4.8	1.1
Ni (%)	0.2	0.1
V (%)	0.4	0.1
Co (%)	0.8	0.3
Ti (%)	0.9	0.5
Ba (%)	5.2	1.1
3. ELEMENTAL ANALYSIS		
Carbon (wt%)	49.70	56.36
Hydrogen (wt%)	6.79	7.78
Oxygen (wt%)	8.80	4.40
Nitrogen (wt%)	0.254	0.416
Sulfur (wt%)	2.17	3.56

Table 1.5(c) Deposit analyses (Eaton and Lux (1983))

Location And Oil Type	Moisture & Volatile	Pentane Sol	Toluene Sol.	Coke	Ash	Major (>10%) Portion of Ash	Minor (>1%) Portion of Ash
Blue Island, IL Crude (Field Dep.)	5.1	22.6	6.5	56.6	9.2	--	Fe,Na,Ca,Cl,S
Wichita, KS Crude (Field Dep.)	18.1	31.1	3.0	29.4	18.4	--	Fe,Na,Ca,Cl,S,P
Oklahoma Crude (Field Dep.)	2.8	11.9	3.0	28.3	54.3	Fe	Na,Cl,S
Cat. Cycle Oil HDS (Field Dep.)	11.3	16.9	2.6	34.7	34.5	Fe	Na,S,Al
Zueitina Crude (Lab Dep.)	--	51.5	9.4	35.3	3.8	--	Fe,Cl
Saharan Crude (Lab Dep.)	--	25.5	4.4	64.7	5.4	--	Fe,S
Synthetic Crude (HCl + Paraffin oil) (Lab Dep.)	--	59.1	0.2	23.6	17.1	--	Fe,Cl
Synthetic Crude (Pitch, Xylene, Paraffin oil, Pentane) (Lab Dep.)	1.2	19.8	3.2	73.8	2.0	S	Fe

1.4.2 Role of resins and asphaltenes in crude oil fouling

The presence of resins and asphaltenes has been reported to be a key factor in fouling from crude oil (Eaton and Lux (1983), Lambourn and Durrieu (1986), Dickakian and Seay (1988), Rowson *et al* (1991)). Asphaltenes are defined as a fraction of crude oil which is insoluble in non-polar solvents such as pentane, but soluble in solvents of high surface tension such as pyridine and toluene. Asphaltenes are dark brown to black friable solids that have no definite melting point. Their compositions vary over narrow ranges of 82 ± 3% carbon and 8.1 ± 0.7% hydrogen (Speight (1980)). They have high average molecular weights and very broad molecular weight distributions, for example 430 to 5170 (Dickakian and Seay (1988)).

Resins are dark coloured, semi-solid or solid, very adhesive materials of high molecular weight in the range 250 to 600, with typical compositions of 85 ± 3% carbon and 10.5 ± 1% hydrogen. Aromatisation is less advanced in resins than in asphaltenes. It has been suggested that asphaltenes are polymeric homologs of condensed aromatics found in resins and indeed that asphaltenes are produced by oxidative condensation (Speight (1980)):

$$\text{Oils} \rightarrow \text{Resins} \rightarrow \text{Asphaltenes} \qquad (1.19)$$

The solubility of asphaltenes has been related to fouling rate in several studies of crude oil fouling (Eaton and Lux (1983), Lambourn and Durrieu (1983), Dickakian

and Seay (1988), Dickakian (1989), Rowson *et al* (1991)). Eaton and Lux (1983) examined the effect of the presence of both resins and asphaltenes. They found that the presence of 5% asphaltic pitch (containing 16% asphaltenes) in a paraffin oil caused a profound increase in fouling rate but this was not the case when resins were present. They suggested that significant fouling occurred when resins were subjected to degradation to asphaltenes. They also found that when asphaltenes were completely solubilised in crude oil, no fouling occurred.

Rowson *et al* (1991) investigated the relative fouling characteristics of various blends of Arabian light crude and Cooper basin condensate. They found that the fouling increased substantially as the condensate concentration was increased above 30%, reaching a maximum at 90%. They suggested that this effect was due to an increased asphaltene content although they did not show the relationship between asphaltene solubility and blend ratio.

Dickakian and Seay (1988) reported that asphaltene precipitation and subsequent carbonisation is the major mechanism in crude oil heat exchanger fouling. However the mere presence of asphaltenes does not necessarily mean a crude oil will foul as asphaltenes may remain soluble in crude oil. Thus they proposed that crude oil fouling in heat exchangers proceeds in the following manner:

(1) Incompatibility between the asphaltenes and the oil initiates precipitation of some asphaltenes.

(2) The precipitated asphaltenes adhere to the hot metal surface.

(3) The asphaltenes then carbonise into infusible coke.

Lambourn and Durrieu (1983) found a complex relationship between solubility of asphaltenes and temperature and noted that colloidal particles containing 30 - 50% asphaltenes were associated with the deposit in crude oil heaters.

In summary the precipitation of asphaltenes seems to be essential for fouling from crude oil to occur.

1.4.3 Magnitude of fouling resistances in industrial heat exchangers

Example fouling resistance-time curves for oil refinery exchangers are shown in Figures 1.8 to 1.11. These data are based on overall heat transfer coefficients and thus may incorporate fouling on both sides of the heat transfer surface. Figures 1.8 to 1.11 show that fouling resistances generally appear not to reach asymptotic values, possibly because the extent to which the fouling proceeded in a linear or falling rate manner resulted in shut-down and cleaning well before asymptotic conditions could be reached. Another possibility is that deposit removal mechanisms may not be significant and thus asymptotic fouling would not occur.

The values of fouling resistance recommended for design purposes by TEMA are about 0.35 - 1.23 $m^2K\ kW^{-1}$ (0.002 - 0.007 hr - ft^2 °F Btu^{-1}). Therefore, it is clear that TEMA values can be exceeded after very short periods of operation. A common criticism is that the values of fouling resistance recommended by TEMA

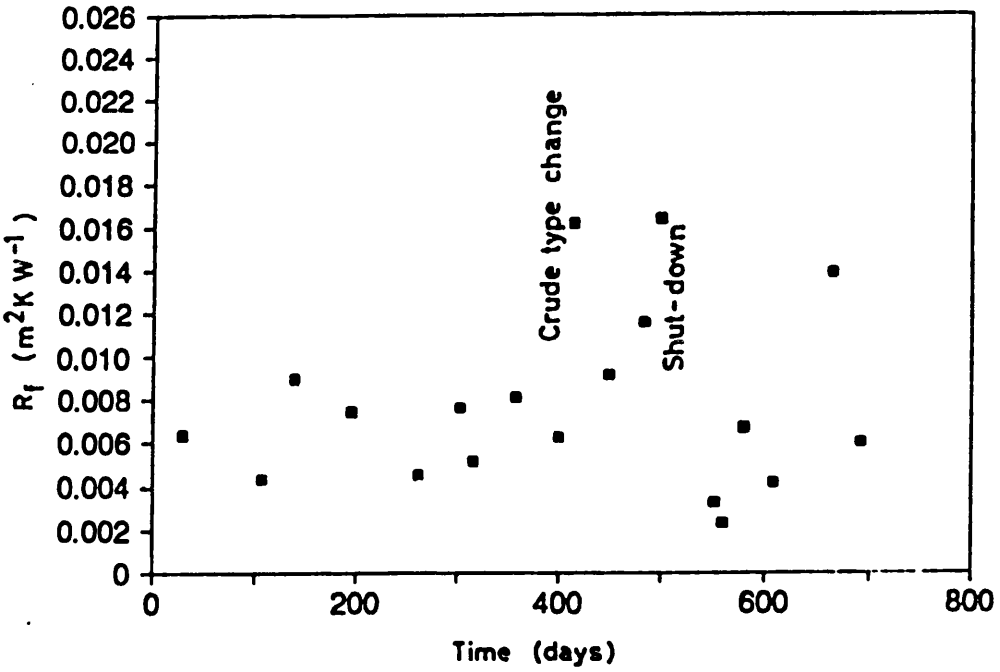

Exchanger E8AB: fouling resistance as a function of time.

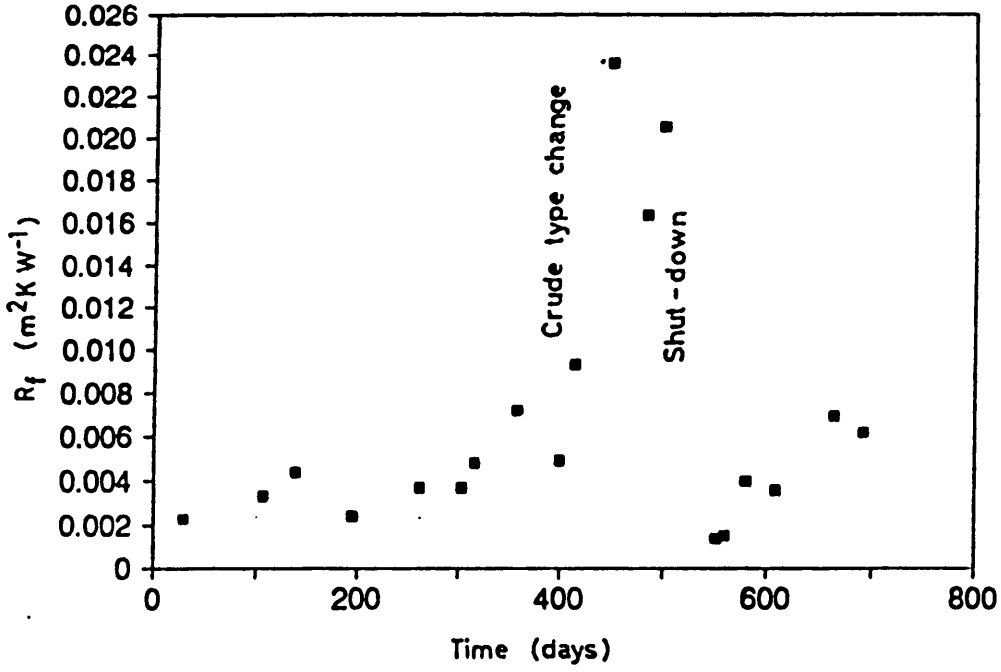

Exchanger E10AB: fouling resistance as a function of time.

Figure 1.8 Fouling resistances for crude oil preheat exchangers (Crittenden et al (1992))

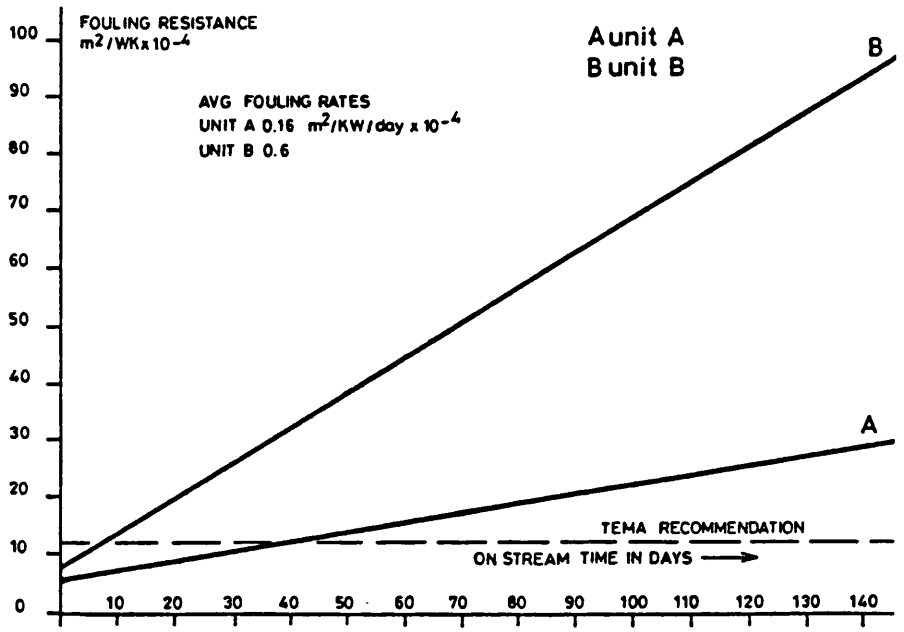

Figure 1.9 Fouling resistances for crude/residue exchangers provided by Lambourn and Durrieu (1983)

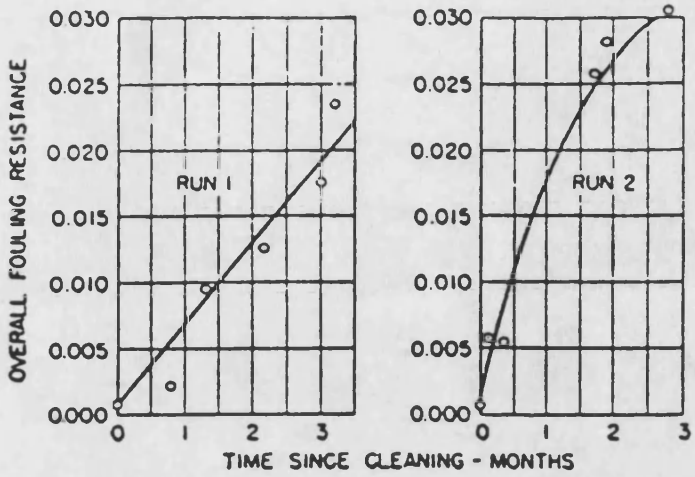

CORRELATION OF FOULING RESISTANCE WITH TIME, PIPE-STILL EXCHANGER, FURNACE OIL—WHOLE CRUDE
(Feed in tube side heated from 275 F to 330 F.)

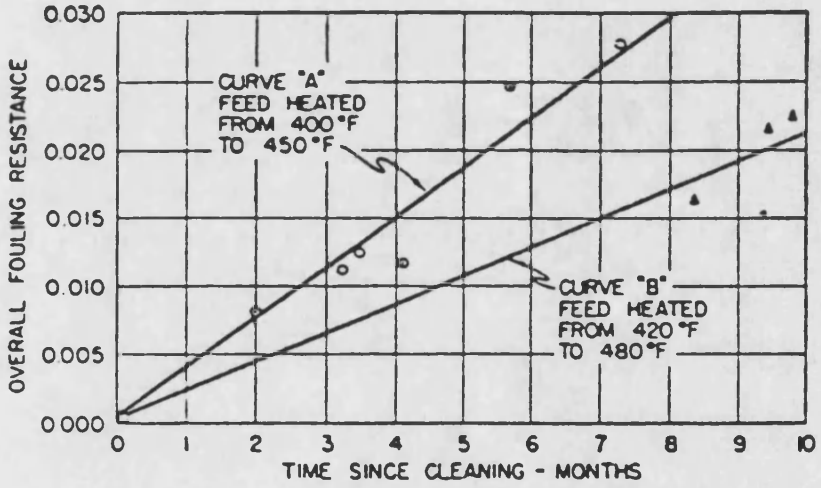

CORRELATION OF FOULING RESISTANCE WITH TIME, PIPE-STILL EXCHANGER, REDUCED CRUDE—FLASHED CRUDE
(Flashed crude in tube side being heated.)

Figure 1.10 Industrial fouling data provided by Butler et al (1949)

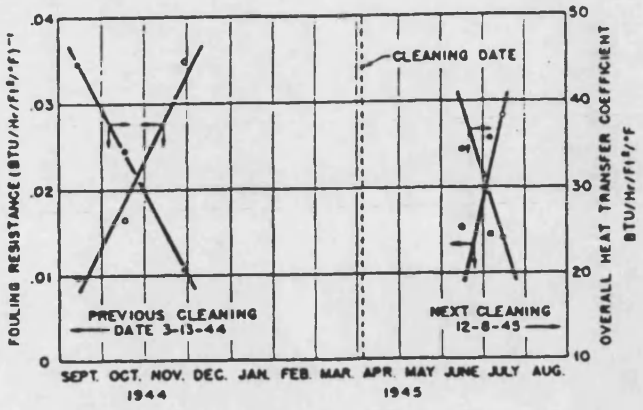

Absorption Oil Coolers

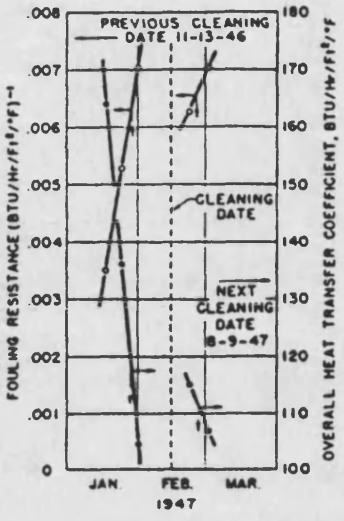

Depropanizer Reflux Condensers

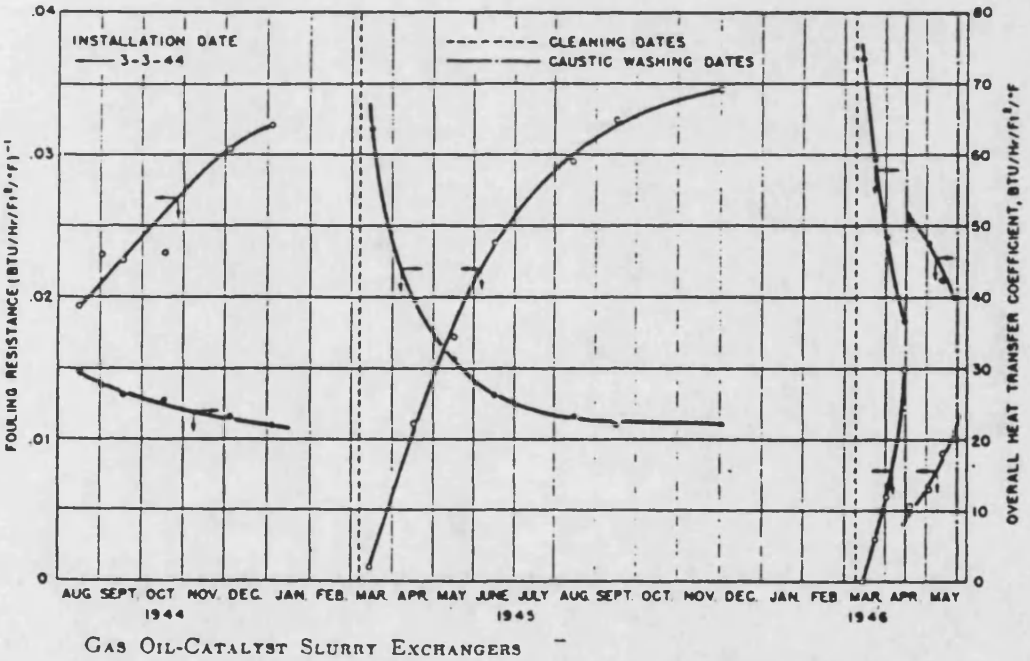

Gas Oil-Catalyst Slurry Exchangers

Figure 1.11 Industrial fouling data provided by Weiland et al (1949)

pay only scant regard to the effect of process variables such as temperature, flow rate or composition. The recent review by Chenoweth (1990) of the fouling section of the TEMA standards still does not provide the necessary systematic overhaul of the fouling tables.

1.5 Research methods

Research methods used for studies on fouling may be divided into two categories, *i.e.* those which interpret industrial plant data and those in which the data is obtained from specially designed laboratory-scale equipment.

1.5.1 Industrial plant data

Data obtained from full scale commercial heat exchangers can be used to evaluate the magnitude of fouling resistances. Unfortunately use of industrial plant for this purpose creates many limitations and restrictions. For example, Crittenden *et al* (1988) listed the following principal disadvantages in using oil refinery data in fouling research:

(1) It is not possible to carry out the desired scientific experiments without interfering with the normal business of production;

(2) Since fouling in oil refineries may occur gradually over periods exceeding a year, it is quite likely that the process operating parameters will have changed many times before the "experiment" can be terminated, *i.e.* when the

plant is shut down for cleaning and maintenance and the exchanger surfaces can be inspected;

(3) The instrumentation is usually much more limited and perhaps less accurate than that which would be possible to use in the research laboratory.

Crittenden *et al* (1988) also demonstrated that a small error in exchanger end temperature readings and an inaccuracy in flow rate measurement could yield, in some cases, as high as 100% error in the overall heat transfer coefficient as calculated from equation (1.20) and consequently this could seriously affect the accuracy of the computed fouling resistance.

$$U = \frac{Q}{A_o F\ (LMTD)} \qquad (1.20)$$

in which U is the overall heat transfer coefficient

A_o is the heat transfer surface area based on the outside diameter of the tubes

LMTD is the log mean temperature difference

F is the correction factor

The practical difficulties described above normally mean that it is necessary to compliment fouling studies made on industrial plant with laboratory-scale experimentation.

1.5.2 Laboratory studies

Comprehensive reviews of laboratory-scale experimentation techniques are provided by Epstein (1981), Knudsen (1981) and Chenoweth (1988). Carefully controlled laboratory-scale studies have been carried out to determine the dependency of fouling rate on parameters such as surface and bulk temperature, flow rate, feedstock composition, equipment geometry and metallurgy. The data obtained from well instrumented fouling apparatus is expected to have a reasonably good accuracy, and therefore could be used to develop scientific fouling models. Even so, laboratory studies are also fraught with practical problems.

Firstly, fouling in commercial exchangers, particularly in oil refinery heat exchangers, can take weeks or months to reach significant levels. Thus it is usually necessary in the laboratory to modify one or more of the operating parameters so that an accelerated test lasting only hours or days can be achieved. A common approach is to use actual feedstocks and realistic temperatures, pressures and metallurgy but to reduce greatly the fluid flow rate and thereby to reduce the equipment size, power requirements and the problem of safety in the laboratory. Experiments which are carried out at a reduced flow rate often yield deposits which are dissimilar in composition to those found in industrial exchangers. Laboratory-scale deposits from crude oils generally have unrealistically high organic contents (Crittenden (1988b)). It is quite likely therefore that modification of the operating parameters in laboratory-scale experiments can alter the balance of mechanisms by which the fouling occurs.

Secondly, once through systems may require substantial amounts of feedstock, in particular when the duration of the test is long. Where hydrocarbons are used as the feedstock in the laboratory, recirculating systems have been more widely used than once through systems due to both the safety problems and the high operating cost of once-through systems. For hydrocarbon fouling, continued recirculation of feedstock could affect its composition and lead to a loss of, or further formation of fouling precursors (Wilson and Watkinson (1992)). Such changes might create fouling resistances and fouling rates which differ from those found in actual refinery heat exchangers (Crittenden *et al* (1993)).

Since both research methods contain their separate practical problems, it is clear that both laboratory-scale studies and industrial plant studies are required to complement each other.

1.6 Single phase heat transfer enhancement techniques

Techniques for improving heat transfer rates in process equipment are referred to as heat transfer augmentation, enhancement or intensification. The need for energy conservation has led to a substantial growth in research and development in this subject which has now developed to a stage that makes it is of serious consideration for heat transfer applications in which transfer rates are otherwise low. A number of surveys have been published *e.g.* those by Bergles (1985, 1988) and Webb (1987).

Techniques to augment heat transfer can be classified as passive methods, which require no direct application of external power, or active schemes, which require external power (Bergles (1985)). The majority of commercially interesting augmentation techniques are passive ones because they are less expensive and easier to apply than active ones. Since the current study is concerned with the application of one of the passive techniques, the discussion is limited to this type only. Briefly, the following passive methods are available:

(1) Rough surfaces are produced in many configurations such as sand grains, transverse grooves, spiral fluting, threading, knurling and so on. The configuration is generally chosen to promote turbulence rather than to increase the heat transfer surface area.

(2) Extended surfaces include externally and/or internally finned tubes.

(3) Displaced enhancement devices are inserted into the flow channel. The heated surface is left essentially intact but the fluid dynamics near the surface are altered by an insert which may comprise static mixers, rings, disks or balls. The HiTRAN insert (Gough and Rogers (1982)) which is a type of coiled wire turbulence promoter, falls into this category and is described in detail in section 1.6.1.

(4) Swirl-flow devices include a number of geometrical arrangements or tube inserts for forced flow which create rotating and/or secondary flows. They

include inlet vortex generators, twisted-tape inserts and axial-core inserts with screw-type windings.

(5) Additives for liquids include solid particles and gas bubbles in single phase flows.

Two or more of the above techniques may be utilised simultaneously to produce an enhancement larger than that produced by either of the techniques. This is termed compound augmentation.

1.6.1 HiTRAN inserts

Figure 1.12 shows the HiTRAN insert used in this study. The insert is designed to position a matrix of wire filaments onto the inside wall of a tube. The filaments are supported by a central spine to form a skeletal structure through which the tube-side fluid flows. In addition to supporting the filaments, the central spine provides the means of pulling the insert into and out of the tube. The insert design enables the filaments to be sprung onto the tube wall to achieve good wire-wall contacts (Gough and Rogers (1982), Saunders (1988)).

The performance of the HiTRAN insert has been described by Cal Gavin Ltd., the manufacturers (Gough and Rogers (1982, 1987, 1991), Rogers *et al* (1989)), and by others (Oliver and Aldington (1988), Shalhi (1993)).

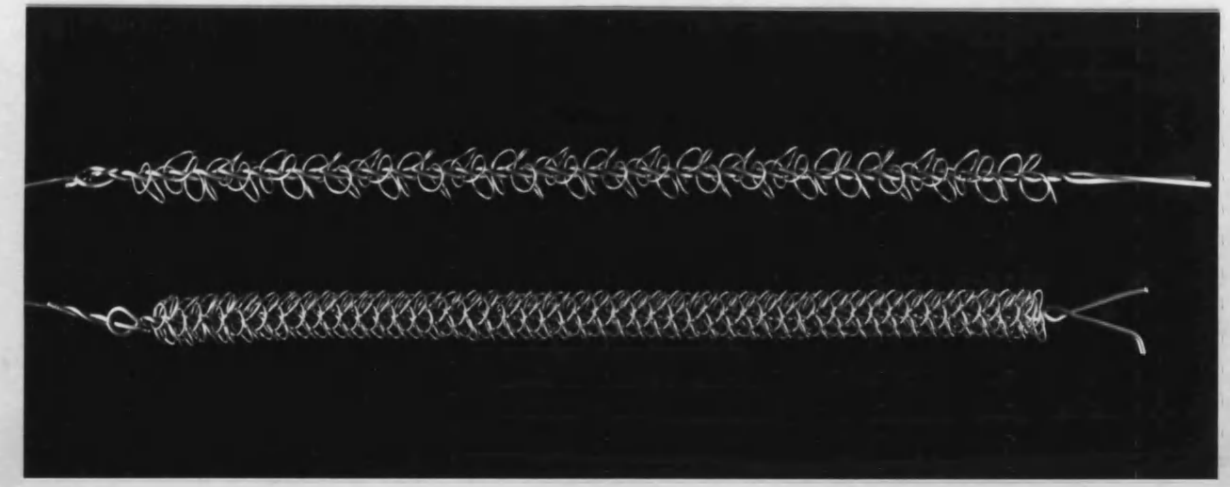

Figure 1.12 Photograph of HiTRAN inserts
top:low density insert, bottom:high density insert

With a HiTRAN insert in place heat transfer can be increased by between 2 to 10 times that for a bare tube at a Reynolds number of 10000 (Gough and Rogers (1987)). Inserts provide the best improvement in heat transfer performance in the laminar and transition flow regimes. In the laminar flow regime the increase in heat transfer factor (over that for a bare tube) is increased by an increase in Reynolds number. At a given Reynolds number the heat transfer factor can be increased by increasing the relative loop density (which is defined as the number of wire loops per unit length of an insert). However, the ratio of heat transfer factor to friction factor has been found to decrease with an increase in insert loop density (Gough and Rogers (1982)).

Oliver and Aldington (1988) investigated the heat transfer and friction factor characteristics over the range of Reynolds numbers from 5 to 1600 and Prandtl numbers from 40 to 550, using Newtonian and non-Newtonian liquids. For the Newtonian liquid (a glycerol/water mixture), heat transfer enhancement by a factor of up to five was obtained, compared with the empty tube case. However the pressure drop was correspondingly increased by a factor of up to 20. They obtained correlations of heat transfer and friction factor, f, for the tube fitted with the medium density insert as follows:-

$$Nu = 0.232\ Re^{0.54}\ Pr^{0.46} \qquad (1.21)$$

$$ln\ (f) = 5.57 - 1.32\ (ln\ Re) + 0.0627\ (ln\ Re)^2 \qquad (1.22)$$

Data on non-Newtonian fluids was also reported but this subject is beyond the scope of this study.

More recently Shalhi (1993) carried out an extensive study of the effect of HiTRAN inserts on heat transfer and friction factor with Santotherm 55 (a heat transfer oil) over the ranges of Reynolds number 500 to 34000 and Prandtl number 30 to 187. HiTRAN inserts enhanced the heat transfer factor over that of the bare tube case by between 1.3 and 5.8 times and the concomitant increase in the pressure drop was between 8.5 and 50 times, depending on the Reynolds number and the insert used. Shalhi obtained correlations of heat transfer and friction factor for both the bare tube and the tube fitted with various densities of HiTRAN insert. The correlations were tested successfully with data obtained using Arabian light crude oil under similar operating conditions.

1.6.2 Fouling with augmented tubes

As stated before, augmentation has been one of the most active and intensive research areas of heat transfer. However augmentation techniques are normally only considered to be appropriate for equipment in which fouling is not expected to occur. The reasons for this are probably firstly that the fouling characteristics of augmented surfaces are poorly understood and secondly that, if augmented tubes

foul, they will not be easy to clean.

Research investigations on augmented tube fouling are rather sparse and are summarised in Table 1.6. For particulate fouling Webb and Kim (1989, 1991) showed that an enhanced tube fouled almost the same as a smooth tube at Reynolds numbers over 26000. At lower Reynolds number, however, the enhanced tube showed higher fouling resistances. They inspected the tube surface visually after several flushing tests to find that the deposits were unevenly distributed on the augmented surface. Müller-Steinhagen (1988) carried out an experimental study using several externally threaded tubes. The results showed that the fouling resistance for a deeply threaded tube was lower than that for a bare tube under comparable flow conditions.

Several scaling experiments have been carried out (Watkinson *et al* (1974), Watkinson and Martinez (1975), Dreytser *et al* (1983), Sheikholeslami and Watkinson (1986)). The results seem to indicate that under certain conditions the augmented surface can have a higher overall heat transfer performance under fouled conditions than a plain surface.

Kornbau *et al* (1983) tested spirally-indented tubes for naval-vessel applications which might experience sea water biofouling. They concluded that the difference in fouling rate between an enhanced tube and a plain tube is insignificant. However they reported uneven distributions of biofilm between enhancement ridges. Panchal (1989) carried out an experimental investigation of sea water biofouling for

Table 1.6 Effects of augmented surfaces on fouling

Authors	Type of fouling	Type of augmented tube	Fluid	Experimental condition	Comparison with plain tube	Remarks
Patun et al (1981)	particulate fouling	spirally-ribbed tubes	water with iron rust	0.91m/s<Vm<3.7m/s	no comparison	
Muller-Steinhagen (1988)	particulate fouling	externally threaded ,knurled and grooved tubes	water with suspended particles	0.31m/s<Vm<0.43m/s	samller for deeply threaded tubes comparable for other tubes	uneven deposit distribution
Webb and Kim(1989) Kim and Webb(1991)	particulate fouling	internally-ribbed tubes	water with ferric oxide, aluminum oxide	14000<Re<30000	higher at low Re approximately the same at high Re (Re>26000)	uneven distribution of particles
Watkinson et al(1974)	scaling	inner finned and spirally-indented tubes	water with calcium carbonate	0.3m/s<Vm<1.8m/s 211C<Tsc<224C	higher for inner finned tubes lower for spirally indented tubes at Vm > 0.9m/s	
Watkinson and Martinez (1975)	scaling	spirally-indented tubes	water with calcium carbonate	0.5m/s<Vm<3.0m/s	comparable	
Dreytser et al (1983)	scaling	ring-type turbulance promoters	synthetic solution with high hardnes values	Vm=1.3m/s	lower	

Table 1.6 continued...

Table 1.6 continued...

Author	Type of fouling	Type of augmented tube	Fluid	Experimental condition	Comparison with plain tube	Remarks
Sheikholeslami and Watkinson (1986)	scaling	externally finned tubes	water with calcium carbonate	0.3m/s<Vm<0.8m/s	approximately comparable	on the fin thickness of scale decreases with distance from prime surface to top
Kornbau et al (1983)	biofouling	spirally-indented tubes	coastal sea water	comparison at same Vm and pressure drop	no significant difference	biofilm accumulates preferentially between ridges plant data
Panchal (1989)	biofouling	indented and fluted tues	sea water	Vm=1.8m/s	comparable	uneven biofilm growth plant data
Katz et al (1954)	hydrocarbon fouling	radial outer-finned tubes	fuel oil	comparative operating conditions	samller	plant data
Gough and Rogers (1989)	hydrocarbon fouling	HiTRAN insert fitted in tube	tar oil residue	similar operating conditions	much samller	plant data
Shalhi (1993)	hydrocarbon fouling	HiTRAN insert fitted in tube	crude oil	Vm=0.5m/s same heat flux	smaller	

indented tubes and fluted tubes and found that the rate of fouling for enhanced tubes was comparable to that of plain tubes.

Watkinson (1990) reanalysed the data of Katz *et al* (1954) for fuel oil fouling with radial outer fin tubes. The reanalysed results indicated that fouling for the finned tubes was less rapid than that for the plain tubes.

For hydrocarbon fouling, Gough and Rogers (1987) and Shalhi (1993) have reported that the HiTRAN insert is capable of dramatically reducing the fouling rate and the fouling resistance. These two studies, which are discussed in more detail in section 1.6.3, prompted the present study of HiTRAN inserts to control crude oil fouling.

In summary, previous studies with heat transfer enhancement devices have shown that fouling can sometimes be controlled under certain operating and geometric conditions.

1.6.3 Fouling of tubes fitted with HiTRAN inserts

Gough and Rogers (1987) have reported that the HiTRAN insert could significantly reduce a hydrocarbon fouling problem. A multi-tubular tar oil heater formerly required cleaning after every two months' operation due to the loss of performance resulting from the accumulation of deposits on the inside of the tubes through which tar oil was being heated. In order to improve the heat transfer performance, HiTRAN inserts were installed as a retrofit. After four months' operation, the

fouling resistance remained essentially zero. The performance of this exchanger continued to be monitored for several months and no deterioration in its performance was detected.

More recently Shalhi (1993) carried out a limited series of laboratory experiments with crude oil to compare the fouling rate for a tube fitted with a HiTRAN insert with that for a tube left bare. He found that under the same conditions of heat flux and fluid velocity the insert appeared to eliminate fouling.

These limited plant and pilot-scale experiments on hydrocarbon fouling show considerable promise. However the principal mechanism of such a reduction in fouling rate is not fully understood. A reduction in fouling could be attributable either to the increased turbulence generated by the HiTRAN insert in the vicinity of the inside tube surface or to the lower surface temperature which would occur when the insert is installed as a retrofit in situations where fouling is controlled by a chemical reaction mechanism.

1.7 Objectives of the current research

As stated before, the HiTRAN insert shows considerable promise as a novel and practical method by which hydrocarbon fouling can be overcome. However, the mechanism by which the insert reduces fouling is not clear. Elucidation of the mechanism(s) by which the insert reduces fouling could lead not only to the understanding of the full potential of such devices when applied in heat transfer

processes but also to a better understanding of hydrocarbon fouling in general. These are the prime objectives of this study.

Shalhi (1993) conducted preliminary experiments to check the effect of the HiTRAN insert on fouling from crude oil. However his experiments suffered from practical difficulties which related to methods of pressurising the apparatus to control vaporisation. Thus it was not possible for him to determine the fouling rate at a constant surface temperature, which is one of the most important parameters in chemical reaction fouling.

In the present study, a new measure is taken to maintain constant pressure during the period of each experiment which lasts up to a week. Experiments are then carried out to investigate the fouling characteristics for both the bare tube and the tube fitted with a HiTRAN insert.

From these experimental results, possible mechanisms by which the insert can reduce fouling are elucidated. A model is also developed to account for the dependency of initial fouling rate and asymptotic fouling resistance on velocity and on the film heat transfer coefficient. This model therefore takes into account the improvement in film heat transfer coefficient which occurs when a HiTRAN insert is installed. The model also takes into account the two heat transfer regimes of interest in crude preheat exchangers, namely purely convective flow heat transfer and subcooled nucleate boiling heat transfer.

2. EXPERIMENTAL APPARATUS AND PROCEDURE

2.1 Experimental apparatus

The apparatus is essentially that used by Shalhi (1993) but modified in a number of ways to overcome practical limitations. Schematic drawings of the apparatus, comprising a recycle flow loop, a pressure control system and a safety system are shown in Figures 2.1, 2.2 and 2.3 respectively. Photographs of the apparatus are provided as Figures 2.4(a) and 2.4(b). The recycle loop consisted of a feedstock reservoir (maximum capacity of 0.105 m^3), two identical horizontal tubular test sections in parallel, a variable speed centrifugal pump (Worthington-Simpson Ltd. 40/20 CMR 125), valves and flowmeters. The flow loop could be operated at temperatures up to 150°C and at pressures up to 20 bar above atmospheric.

Two identical test sections were used for comparative experiments to determine the effect of HiTRAN mechanical inserts and process variables such as flow rate and temperature on fouling. A photograph of the test section is provided as Figure 2.5. A schematic cross-section of a test section is shown in Figure 2.6. A thick-walled jacket (carbon steel) was fixed tightly around a commercial grade heat exchanger tube (14.83mm ID and 19.05mm OD) and electrical cable heaters were wound into grooves cut in the surface of the jacket. As shown in Figure 2.7, thermocouples were mounted inside the jacket. In order to calculate the local inside surface temperature of the test tube, the average total resistance (R_w) between these thermocouples and the inner surface of the tube (which includes the contact

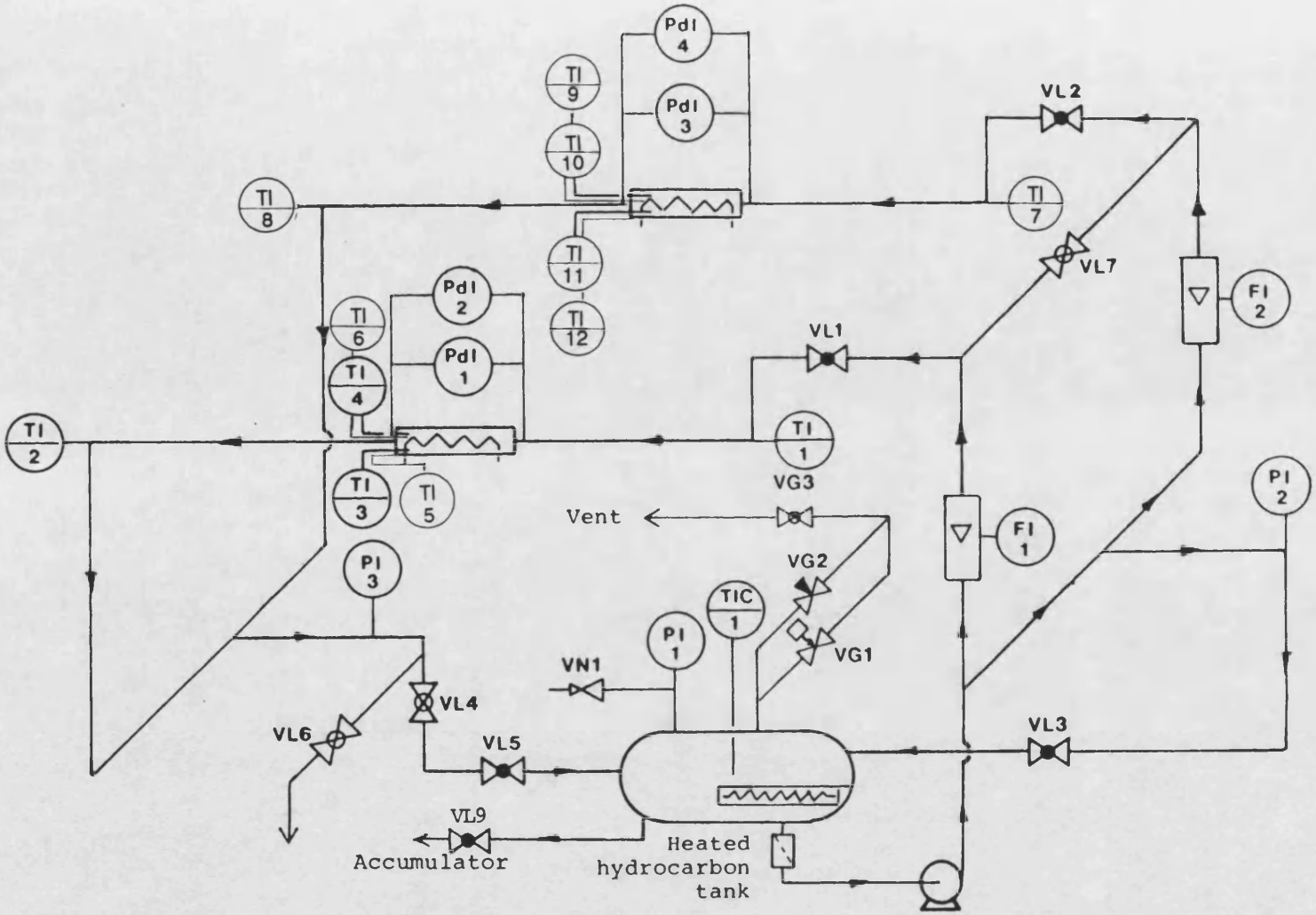

Figure 2.1 Schematic of hydrocarbon flow system

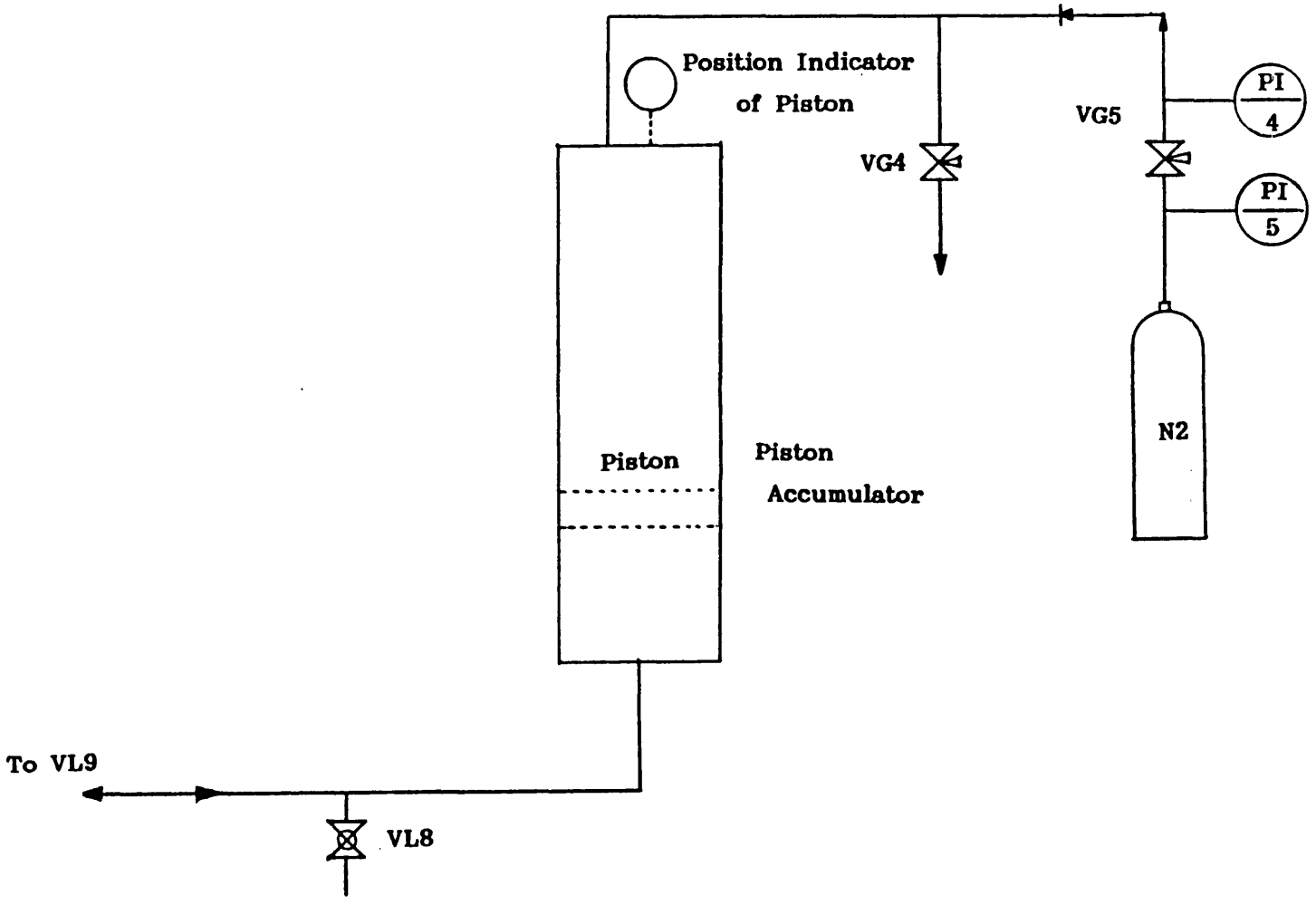

Figure 2.2 Schematic of pressure control system

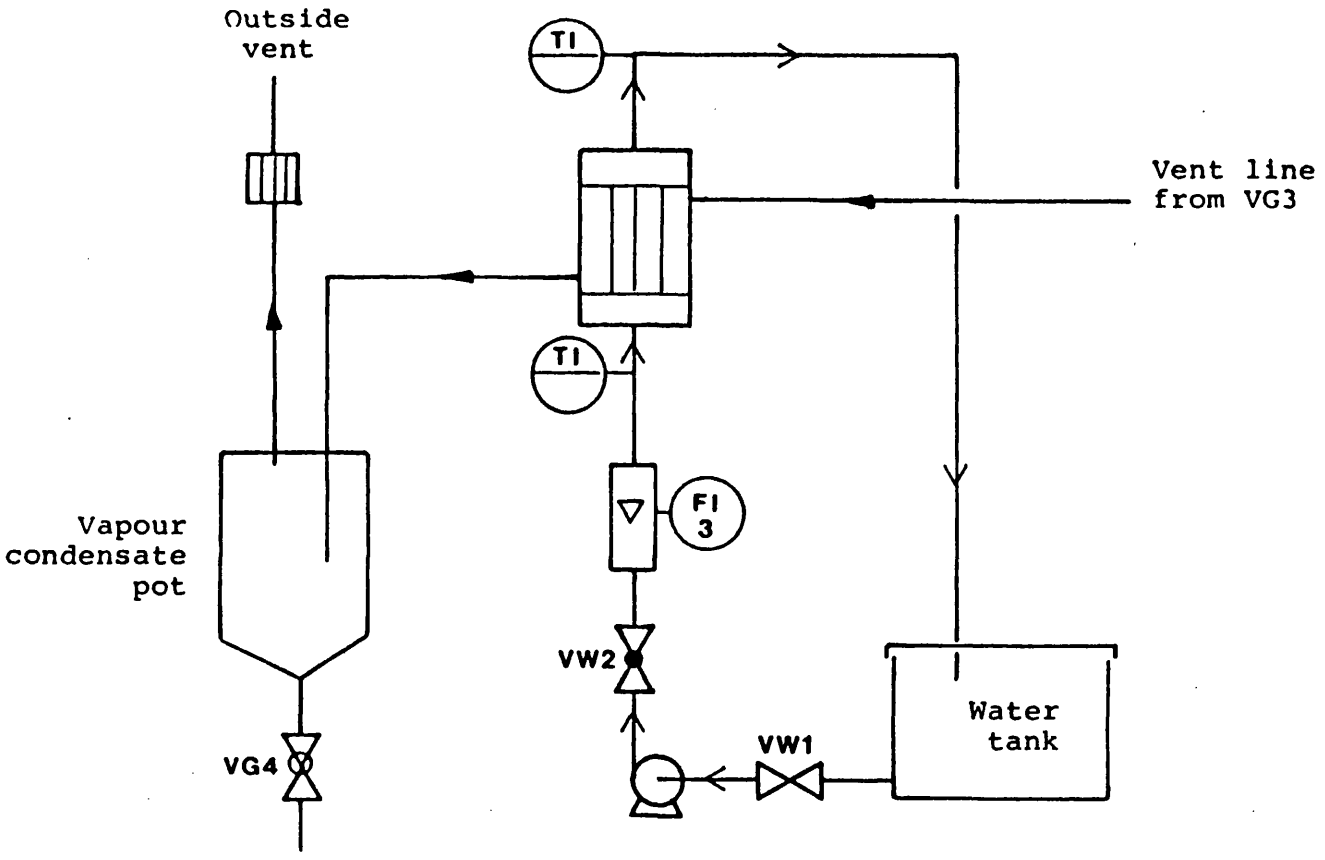

Figure 2.3 Schematic of vapour vent condensate system

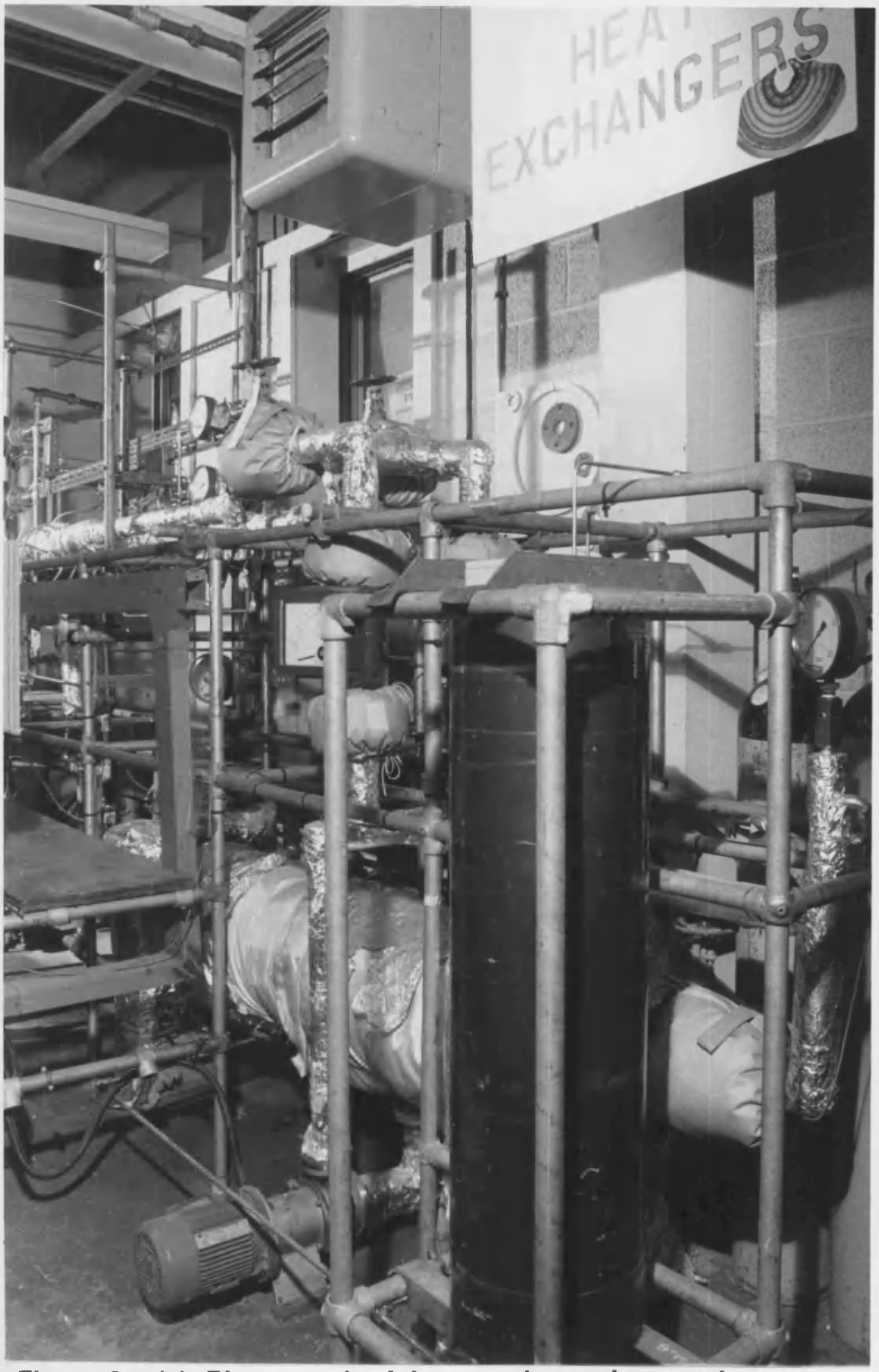

Figure 2.4 (a) Photograph of the experimental apparatus flow recycle loop and a pressure control system

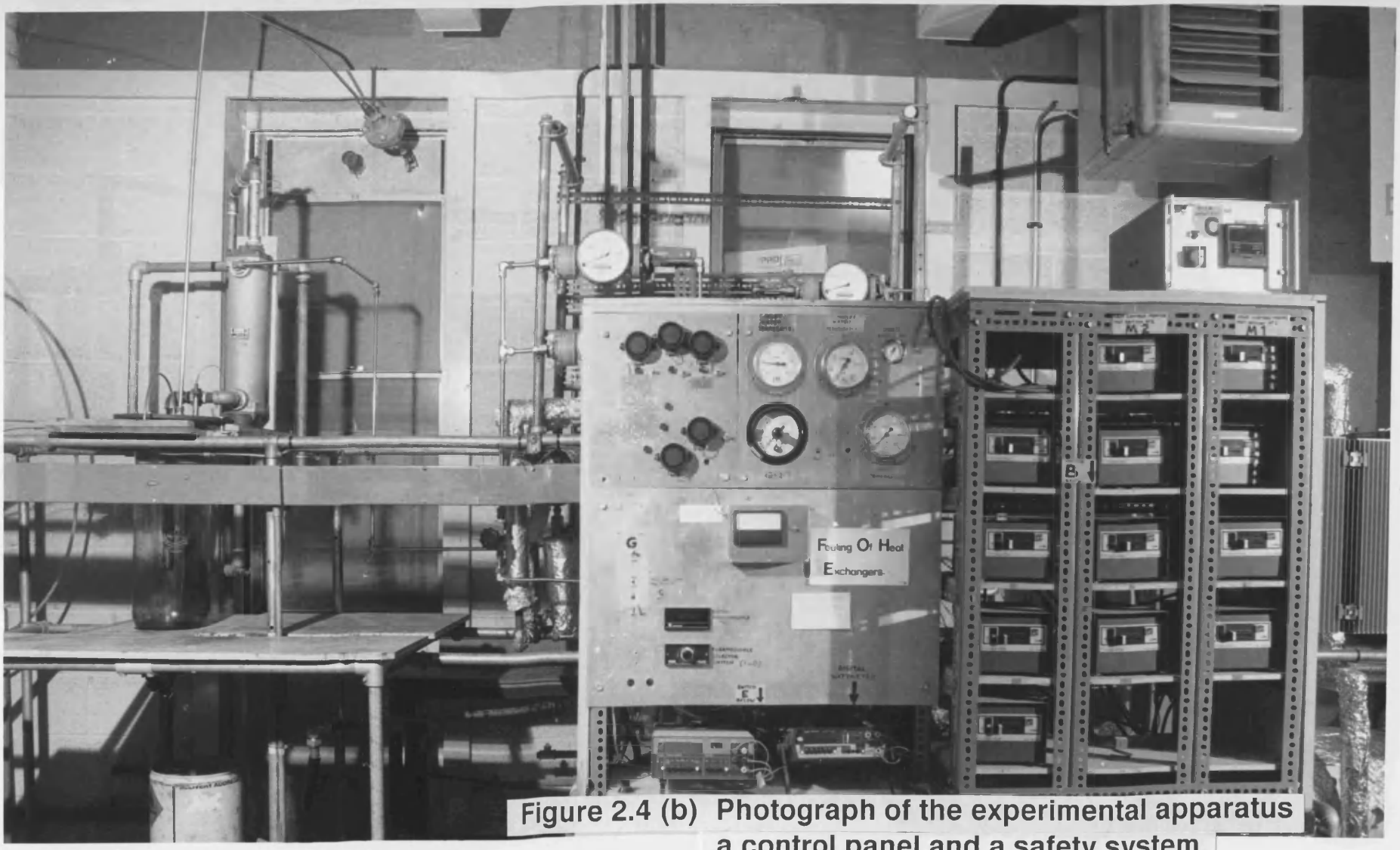

Figure 2.4 (b) Photograph of the experimental apparatus a control panel and a safety system

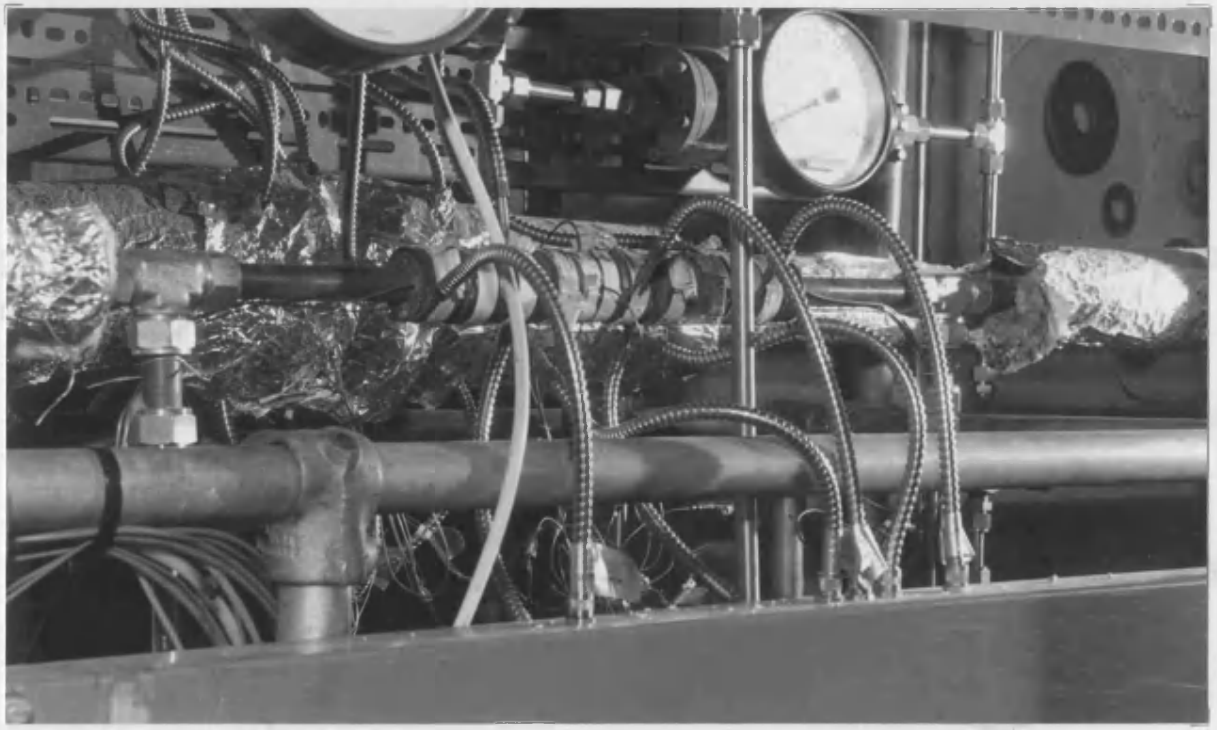

Figure 2.5 Photograph of the heated test section

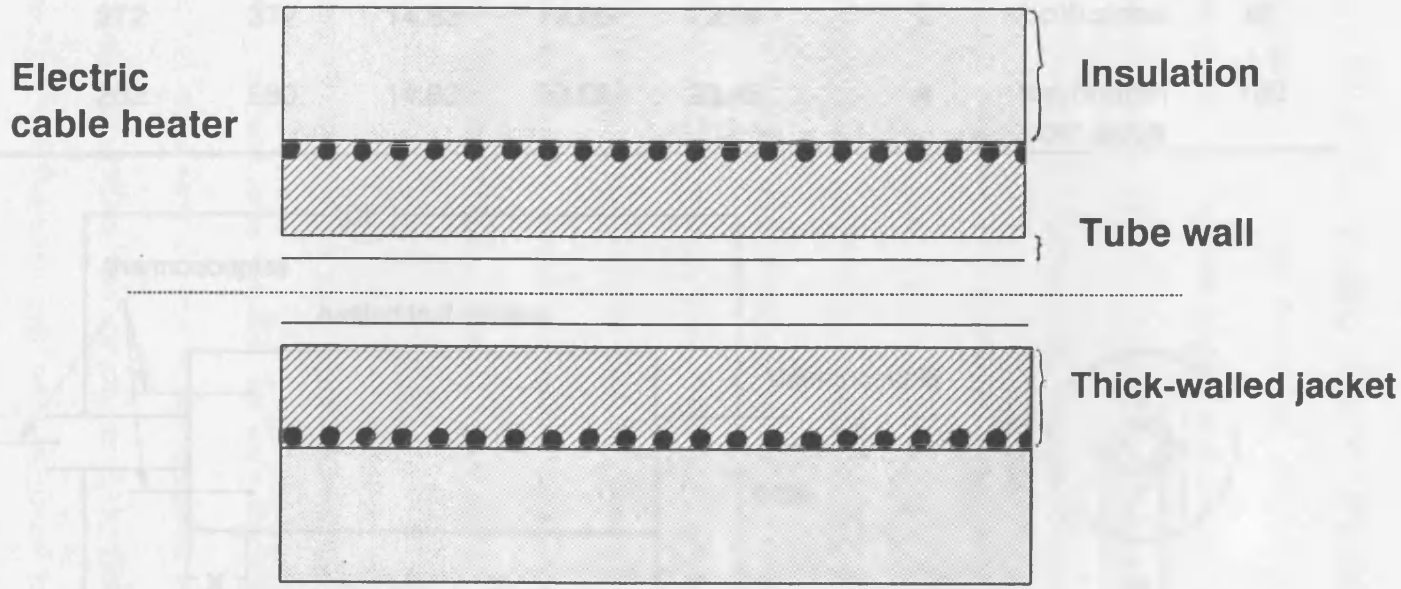

Figure 2.6 Schematic cross-section of a test section

	dimension (mm)						No. of thermocouple	location	maximum heat flux (kW/m2)
	x	y	z	di	do	dt			
old	32	272	372	14.83	19.05	23.05	2	both sides	80
new	20	262	580	14.83	19.05	23.45	4	top,bottom both sides	130

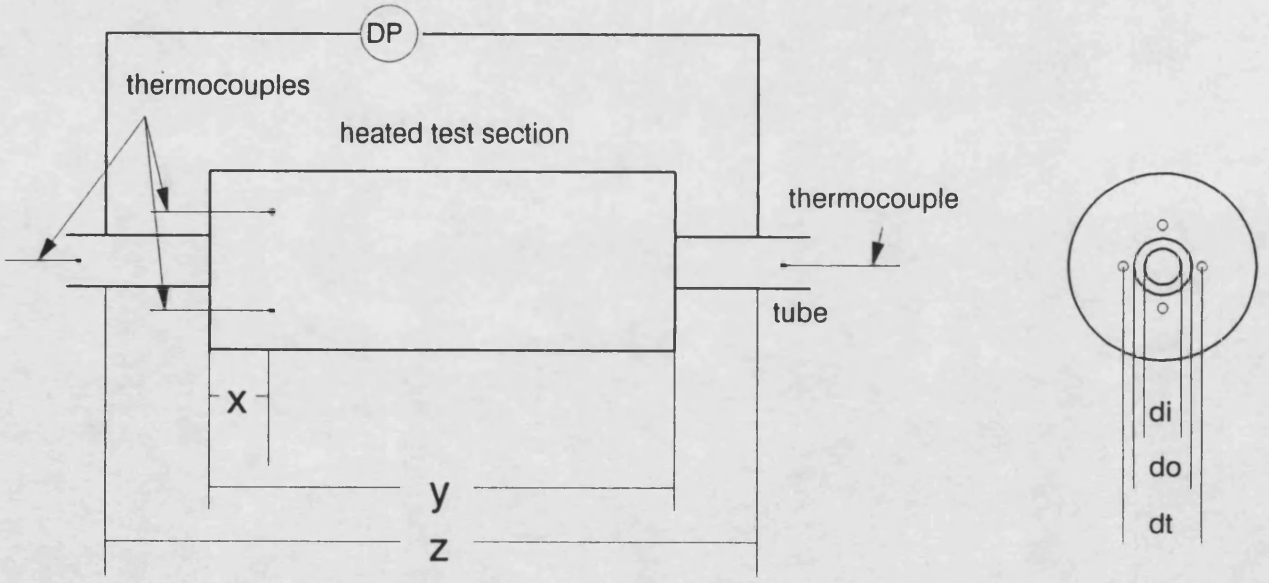

Figure 2.7 Dimensions of the old and new test sections

resistance between the jacket and the tube) was determined by conducting Wilson plot experiments (Wilson (1915)). Details are shown in Appendix 2. For this fouling study, two test sections of slightly different design, labelled "old" and "new", were used. Figure 2.7 shows the dimensions of the old and new test sections together with the number and location of their thermocouples and the location of the differential pressure gauges. The old test sections were used up to Run 6 described in Section 3.2 of Chapter 3. The new test sections were used from Run 7 to Run 19. The problem with the old test section design was that when a heat flux exceeded 80 kWm^{-2} the end part of the heater elements, which did not contact the jacket, were liable to burn out. Since higher heat fluxes were necessary to evaluate the fouling rate for a tube fitted with an insert, a pair of test sections to the new design were made, in which the ten heating elements had tail sections which were unheated thereby giving a maximum practical heat flux of about 130 kWm^{-2}. The power to the heating elements of each test section was controlled by triac regulators and measured by wattmeters (Tabor Electronics Ltd UDW 4501).

The chromel-alumel thermocouples were silver soldered into the thick-walled jacket around the tube at a fixed axial location for each test section. The feedstock temperature into and out of each test section was measured using sheathed chromel-alumel thermocouples protruding into the centre of the flow tube at the positions shown in Figure 2.7. All thermocouples were calibrated before use.

The crude oil feedstock was recycled through the test sections, to be returned to the reservoir. The flow rate for each test section was adjusted by a combination of the

speed controller (Danfoss VLT 101) of the motor driving the centrifugal pump and the setting of a control valve on each test section (VL1 and VL2, see Figure 2.1). The recycle loop around the pump was provided to maintain the minimum flow rate required by the pump. The flow rates of the fluid through each of the two test sections were measured by calibrated rotameters (KDG, 9300 series). The feedstock reservoir was fitted with an electrical heating element. During each experiment the bulk temperature was controlled by the power controller (Severn Science Ltd Type 810) connected to the electrical heating element.

In a previous study (Shalhi (1993)), pressurisation of the system to avoid boiling was carried out in one of two ways:

(1) by connecting the gas space above the liquid in the reservoir directly to a nitrogen cylinder fitted with a regulator.

(2) by filling as far as possible the whole apparatus with crude oil which was then pressurised with a hand pump.

The practical problems with respect to these methods of pressurisation are discussed by Shalhi (1993). In this study the pressure control system shown in Figure 2.2 was installed in order to maintain a constant pressure over long periods of time. The system consisted of a piston accumulator of which the inside was divided into gas and liquid sides by a rigid but movable piston. The crude oil pressure was controlled by maintaining the pressure of the gas side in the accumulator which was connected to a nitrogen cylinder via a pressure reducing valve. With the

accumulator the system pressure could be controlled to ± 0.1 bar at a pressure of 15 bar above atmospheric.

The safety system shown in Figure 2.3 was provided in the case of emergency. A relief valve was connected to the reservoir. If the relief valve were to open the vented gas and liquid would pass to a water-cooled heat exchanger. The liquid that would be condensed and cooled would then be collected in a condensate pot. The condensate pot was connected via a flame trap to the atmosphere outside the laboratory.

2.2 Experimental procedure

The heat transfer and fouling experiments were performed using two Arabian light crude oils, labelled A and B, provided by BP and Esso, respectively. The basic properties of the crude oils are given in Appendix 1. Crude A contained 10% waxy residue from a crude oil tank. Details of the composition change resulting from this addition are given in Appendix 1. For the reasons given in Section 1.5 of Chapter 1, the use of a closed recycle flow system was required for a laboratory study. Each experiment ran continuously for up to 100 hours and fouling Runs 1 to 18 were carried out without changing crude oil A because the supply of the feedstock was limited. The feedstock was changed to crude oil B for the last Run, Run 19. Recirculating systems for fouling studies may require the maintenance of something which takes part in the fouling process (Bryers and Characklis (1981), Hasson (1981), Wilson and Watkinson (1992)). However in the case of crude oil

as a feedstock, it is not straightforward to maintain a constant fluid composition because fouling precursors and/or reactants cannot be easily identified. The consequence of this will be discussed in Chapter 3.

In order to start an experiment, the whole system was filled up with about 115 litres of the crude oil and the gas side of the accumulator was pressurised via the pressure regulator set at 15 barg. Heating of the bulk fluid in the reservoir was then started with the temperature controller set at 150°C and the power controllers set for the chosen heat fluxes in the test sections. The crude oil was passed through the test sections at the maximum possible flow rates. The bulk fluid was heated up to 150°C within 5 hours, after which time the flow rates through the test sections were reduced to those selected for heat transfer measurements. By having high test section flow rates during the warm up phase, the above procedures ensured that the inside surface temperature of each test section was kept at a minimum, thereby minimising the formation of deposits during the start-up period.

Prior to each fouling Run, heat transfer measurements were made to ensure that reproducible heat transfer characteristics of the tubes (with or without inserts as required) were obtained. These heat transfer measurements were made for a range of flow velocities and heat fluxes and are reported in Section 3.1 of Chapter 3.
The fouling Run was then started at the desired flow rate. During each fouling experiment, the bulk temperature was held constant (148±2°C) by the temperature controller and the heat flux to each test section was kept constant by the power controllers. The wall and bulk thermocouple readings, together with the wattmeter

and pressure drop measurements were taken as often as needed, depending on the fouling rate, but usually every hour. At the end of most of the fouling experiments an attempt was made to evaluate the removal rate of the deposits due to the shearing action of the crude oil. The velocity of the crude oil through each test section was increased to 2.5ms^{-1} (Re$\simeq$ 32,000) for a chosen time and then the velocity was returned to that used in the fouling Run (0.5ms^{-1} to 1.1ms^{-1}). The new pseudo-steady state was achieved in 15 minutes, after which time the thermocouple readings, wattmeter and pressure drop measurements were noted.

After cooling the crude oil down at the end of the fouling run, the test sections were dismantled and the insides of the test tubes were inspected visually. Attempts to recover pieces of the deposits were made but proved successful only for Run 3. The inside of each test section was cleaned by the repetitive procedure of brushing and wiping with a piece of cloth. This was possible because the deposits were relatively soft and loosely adhering to the tube wall. After removal from a tube, an insert was cleaned in toluene. Experimental results showed that a tube could easily be cleaned to give good reproducibility in terms of its heat transfer characteristics. Evidence for this is provided in Section 3.1.2.1.1 of Chapter 3.

2.3 Data reduction

Table 2.1 provides a summary of the nomenclature used for temperatures in the following calculations.

Table 2.1 Summary of symbols used for temperature

Temperature	Definition
T_b	bulk temperature (general)
T_{bi}	inlet bulk temperature of the test section
T_{bo}	outlet bulk temperature of the test section
T_{bc}	bulk temperature in clean condition
T_{bd}	bulk temperature in fouled condition
T_{sc}	clean surface temperature
T_w	wall temperature (general)
T_{wc}	wall temperature in clean condition
T_{wd}	wall temperature in fouled condition

2.3.1 Heat transfer coefficients

For each wall thermocouple location shown in Figure 2.7, the local overall heat transfer coefficient (U) is calculated from equation (2.1).

$$U = \frac{Q/A_t}{(T_w - T_b)} \tag{2.1}$$

in which Q is the heat supplied and A_t is the area based on the distance between two diametrically opposed wall thermocouples, d_t. T_b is the bulk temperature at the wall

thermocouple axial location and T_w is the measured wall temperature.

Assuming that the heat capacity of the fluid is constant throughout the test section, the bulk temperature is determined from equation (2.2)

$$T_b = T_{bi} + \frac{Y - X}{Y} (T_{bo} - T_{bi}) \qquad (2.2)$$

in which T_{bi} and T_{bo} are the bulk temperatures at the inlet and the outlet of the test section respectively and X and Y are the dimensions shown in Figure 2.7

The local overall heat transfer coefficient (based on area A_t) may be expressed in terms of the local film heat transfer coefficient (h_i), wall resistance (R_w) and fouling resistance (R_f based on area A_t) by equation (2.3)

$$\frac{1}{U} = \frac{1}{h_i} \frac{d_t}{d_i} + R_w + R_f \qquad (2.3)$$

in which d_t and d_i are the diameters shown in Figure 2.7

In the case of the fouling resistance being zero, the in-tube film heat transfer coefficient is given by equation (2.4)

$$h_i = \frac{1}{\left(\frac{1}{U} - R_w\right) \frac{d_i}{d_t}} \qquad (2.4)$$

At any time the thermal coefficient H_i for the heat transfer film and the fouling layer combined is obtained from equation (2.5)

$$H_i = \frac{1}{\left(\frac{1}{h_i} + R_f \frac{d_i}{d_t}\right)} \tag{2.5}$$

The local wall resistances which correspond to each thermocouple location have been determined by the Wilson plot method (see Appendix 2).

2.3.2 Clean surface temperature

The temperature drop between the wall thermocouple location and the inner surface of the test section is subtracted from the wall temperature to obtain the clean surface temperature (T_{sc}):

$$T_{sc} = T_{wc} - R_w \left(\frac{Q}{A_t}\right) \tag{2.6}$$

in which T_{wc} is the initial value of the wall temperature.

2.3.3 Fouling resistance

The fouling resistance (based on area A_t) is defined by equation (2.7):

$$R_f = \frac{1}{U_d} - \frac{1}{U_c} \tag{2.7}$$

in which U_d and U_c are the dirty and clean overall heat transfer coefficients respectively (based on area A_t).

For each wall thermocouple location, the local heat flux is given by:

$$\frac{Q_d}{A_t} = U_d (T_{wd} - T_{bd}) \tag{2.8}$$

When the surface is in the clean condition:

$$\frac{Q_c}{A_t} = U_c (T_{wc} - T_{bc}) \tag{2.9}$$

in which T_{wd} and T_{wc} are the wall temperatures in the dirty and the clean conditions respectively. T_{bd} and T_{bc} are the bulk temperatures in the dirty and the clean conditions respectively. Hence,

$$R_f = \left(\frac{T_{wd} - T_{bd}}{Q_d / A_t}\right) - \left(\frac{T_{wc} - T_{bc}}{Q_c / A_t}\right) \tag{2.10}$$

2.3.4 Error assessment

A calibrated wattmeter was used to measure the power input to the heater elements for each test section. The heat loss to the environment through the outer insulation

of each test section has previously been estimated to be 2% of the total power input over the range of the heat fluxes tested (Shalhi, (1993)). Heat fluxes could be determined to ± 3kWm^{-2} at an average flux of 75 kWm^{-2}. All temperature readings from the thermocouples were deemed to be ± 0.5°C from calibration experiments. Using a maximum error analysis (Crittenden *et al* (1992)) the maximum error in the local bulk temperature calculated from equation (2.2) was estimated to be about ± 1.5°C. The average temperature difference between the wall and bulk was 90°C. Thus using equations (2.1), (2.4) and (2.10), the maximum errors in the computed in-tube film heat transfer coefficient and the calculated fouling resistance were estimated to be about ± 7% and ± 12% respectively for the average process conditions. Higher errors however could be expected at high flow rates, low heat fluxes and with the presence of an insert since a combination of such conditions results in a lower temperature difference between wall and bulk.

For each experiment, the heat transfer coefficient and the fouling resistance corresponding to each wall thermocouple location (shown in Figure 2.7) were computed. However little circumferential variations in the heat transfer coefficient and the fouling resistance were found (see Appendix 3). The values of the transfer coefficient and the fouling resistance shown in the figures and the tables of Chapter 3 are given as the mean value of the two or four circumferential measurements.

2.3.5 Example calculation

The calculation of the in-tube film heat transfer coefficient and the fouling resistance

from actual data is exemplified as follows:-

Run 14

	New test section	1 (bare tube)
	Flow velocity	0.5 ms^{-1}
	Power input	1400 W (set)
	Heat transfer area	0.0193 m^2 (A_t)
Wall resistance	R_w (average)	0.00016 ($m^2K\ W^{-1}$)
	R_w (top)	0.00017 ($m^2K\ W^{-1}$)
	R_w (side 1)	0.00015 ($m^2K\ W^{-1}$)
	R_w (bottom)	0.00016 ($m^2K\ W^{-1}$)
	R_w (side 2)	0.00017 ($m^2K\ W^{-1}$)

Run Data

time (hr)	power input (W)	T_{bi} (°C)	T_{bo} (°C)
0	1403	142.4	149.8
20	1407	141.3	149.2

time (hr)	T_w(top)	T_w(side 1)	T_w(bottom)	T_w(side 2)	T_w(average)
	(°C))	(°C)	(°C)	(°C)	(°C)
0	265.1	264.8	264.9	264.9	264.9
20	290.0	289.5	288.8	289.0	289.3

At time zero

equation (2.2):

$$T_{bc} = 142.4 + \frac{0.262 - 0.02}{0.262} (149.8 - 142.4) = 149.2\ ^{\circ}C$$

equation (2.1):

$$U_c = \frac{\frac{1403\ x\ 0.98}{0.0193}}{(264.9 - 149.2)} = 615.8\ (Wm^{-2}K^{-1})$$

equation (2.4):

$$h_i = \frac{1}{\left(\frac{1}{615.8} - 0.00016\right)\frac{0.01483}{0.02345}} = 1080.8\ (Wm^{-2}\ K^{-1})$$

equation (2.6):

$$T_{sc} = 264.9 - \frac{1403\ x\ 0.98}{0.0193}\ x\ 0.00016 = 253.5^{\circ}C$$

At 20 hours

equation (2.2):

$$T_{bd} = 141.3 + \frac{0.262 - 0.02}{0.0193} (149.2 - 141.3) = 148.6°C$$

equation (2.1):

$$U_d = \frac{\frac{1407 \; x \; 0.98}{0.0193}}{(289.3 - 148.6)} = 507.7 \; (Wm^{-2} \; K^{-1})$$

equation (2.10):

$$R_f = \frac{1}{507.7} - \frac{1}{615.8} = 3.46 \; x \; 10^{-4} \; (m^2K \; W^{-1})$$

3. RESULTS AND DISCUSSION

The experimental study consisted of pressure drop, heat transfer and fouling measurements with and without HiTRAN inserts fitted inside tubes. The programme of experiments was designed specifically to find out the following:

(1) Pressure drop and heat transfer characteristics, including:

- friction factor for the bare tube
- friction factor for the tube fitted with HiTRAN inserts
- heat transfer for the bare tube
- heat transfer for the tube fitted with HiTRAN inserts

(2) Fouling characteristics, including:

- reproducibility of fouling data
- effect of surface temperature
- effect of fluid velocity
- effect of the HiTRAN insert

The results are reported in two sections of this Chapter - pressure drop and heat transfer in Section 3.1 and fouling in Section 3.2.

A total of 19 fouling runs were performed in the current study. Each run is referenced as Run I - J. The integers I and J correspond to the fouling run number and the test section number, respectively. Fouling experiments were carried out in

Table 3.1 Summary of the experimental programme of fouling

programme	comparison between	condition			fouling run number
		heat flux	fluid velocity	surface temperature	
reproducibility of fouling data	bare tube vs bare tube	same	same	same	3
	low density insert vs low density insert	same	same	same	18
effect of surface temp.	bare tube vs bare tube	different	same	different	11, 14
	low density insert vs low density insert	different	same	different	12
effect of fluid velocity	bare tube vs bare tube	different	different	same	9, 15
	low density insert vs low density insert	different	different	same	10, 16
effect of insert	bare tube vs low density insert	same	same	different	1, 17
		different	same	same	2,8,13,19
	low density insert vs high density insert	same	same	different	5
		different	same	same	4, 6, 7

the order of the fouling run numbers (from 1 to 19 consecutively). A summary of the objectives of each Run in the experimental fouling programme is provided in Table 3.1.

Heat transfer experiments were carried out prior to each fouling run and are described as Exp I - J. The integer I corresponds to the number of the fouling run which follows the heat transfer experiment. The integer J is the test section number. Following tube cleaning at the end of Run 18, a heat transfer measurement was made. This is labelled Exp 18 (AF) - J.

3.1 Pressure drop and heat transfer.

Pressure drop and heat transfer measurements were carried out for a bare tube and a tube fitted with a HiTRAN insert. Two different densities of insert, labelled "low" and "high", were used. The density of the insert is defined by the number of loops per unit length as shown in Table 3.2.

Table 3.2 Loop density of inserts

insert	number of loops per insert	length of insert (cm)	loop density (loops/cm)
low density	86	27.5	3.13
high density	169	27.0	6.26

The operational data for the pressure drop and heat transfer measurements are given in Table 3.3.

3.1.1 Pressure drop

Pressure drops were measured at various flow velocities and at one of two heat fluxes, namely 21 or 41 kW m^{-2}. For the bare tube the pressure drop data were acquired when the heat transfer experiments of Exps 3 and 8-1 and the Wilson plot experiments were undertaken. At relatively low Reynolds numbers, the pressure drop for the bare tube was too small to be measured with the differential pressure gauges. Therefore, the data acquired when conducting the Wilson plot experiments were used to estimate friction factors for the bare tube. For the tube fitted with an insert, the pressure drop measurements were carried out in parallel with the heat transfer experiments of Exps 4, 7 and 8-2.

Example data with a constant heat flux of 21kWm^{-2} are shown in Figure 3.1. The Reynolds number was calculated from:

$$Re = \frac{\rho V_m d_i}{\mu_f} \qquad (3.1)$$

in which ρ is the density of the fluid at the bulk temperature T_b

d_i is the inside diameter of the tube

V_m is the mean velocity of the fluid based on d_i

μ_f is the viscosity at the film temperature (T_f) given by:

$$T_f = (T_b + T_{sc})/2 \qquad (3.2)$$

For the tube having an insert in place, the pressure drop is substantially higher than that for a bare tube at the same Reynolds number. It is believed that a substantial fraction of the pressure drop is due to form drag on the insert loops.

3.1.1.1 Friction coefficient

Figure 3.2 shows the friction coefficients for a bare tube and a tube fitted with an insert plotted against the Reynolds number. The experimental value of the friction coefficient, C_f, was calculated from:

$$C_f = \frac{\frac{\Delta p}{z} \cdot d_i}{2 \cdot \rho_a V_m^2} \qquad (3.3)$$

in which Δp is the pressure drop

z is the dimension shown in Figure 2.7

ρ_a is the density at the average bulk temperature of T_{bi} and T_{bo}

In the range of Reynolds numbers tested, approximately 12-fold and 60-fold increases in the friction coefficient above the bare tube case were obtained when the low and high density inserts, respectively, were installed.

Table 3.3 Operating data of pressure drop and heat transfer measurements

	test section		operation range		crude oil	heat transfer	pressure drop
			heat flux (based on dt)	fluid velocity			
	No.	condition	(kW/m2)	(m/s)			
Exp 1	1	Bare	41 - 66	0.50 - 2.51	A	yes	no
	2	Low					
Exp 2	1	Bare	41 - 81	0.50 - 0.88	A	yes	no
	2	Low					
Exp 3	1	Bare	41 - 76	0.50 - 0.88	A	yes	yes (41kW/m2 only)
	2	Bare					
Exp 4	1	High	41 - 96	0.50 - 1.69	A	yes	yes (41kW/m2 only)
	2	Low					
Exp 5	1	High	20 - 61	0.50 - 2.10	A	yes	no
	2	Low					
Exp 6	1	High	20 - 40	0.50 - 2.10	A	yes	no
	2	Low					
Exp 7	1	High	21, 42	0.50 - 2.10	A	yes	yes (21kW/m2 only)
	2	Low					
Exp 8	1	Bare	21, 42	0.50 - 2.51	A	yes	yes (21kW/m2 only)
	2	Low					
Exp 9	1	Bare	26	0.50 - 2.51	A	yes	no
	2	Bare					
Exp 10	1	Low	42	0.50 - 2.51	A	yes	no
	2	Low					

Table 3.3 continued.

Table 3.3 continued

	test section		operation range		crude oil	heat transfer	pressure drop
			heat flux (based on dt)	fluid velocity			
	No.	condition	(kW/m2)	(m/s)			
Exp 11	1	Bare	26 - 62	0.50 - 2.51	A	yes	no
	2	Bare					
Exp 12	1	Low	42 - 130	0.50 - 2.10	A	yes	no
	2	Low					
Exp 13	1	Bare	20 - 83	0.50 - 2.51	A	yes	no
	2	Low					
Exp 14	1	Bare	20 - 83	0.50 - 2.51	A	yes	no
	2	Bare					
Exp 15	1	Bare	20 - 83	0.50 - 2.51	A	yes	no
	2	Bare					
Exp 16	1	Low	41 - 104	0.50 - 2.51	A	yes	no
	2	Low					
Exp 17	1	Bare	31 - 104	0.50 - 2.51	A	yes	no
	2	Low					
Exp 18	1	Low	52 - 104	0.50 - 2.51	A	yes	no
	2	Low					
Exp18(AF)	1	Bare	20 - 104	0.50 - 2.51	A	yes	no
	2	Low					
Exp 19	1	Bare	31 - 130	0.50 - 1.69	B	yes	no
	2	Low					

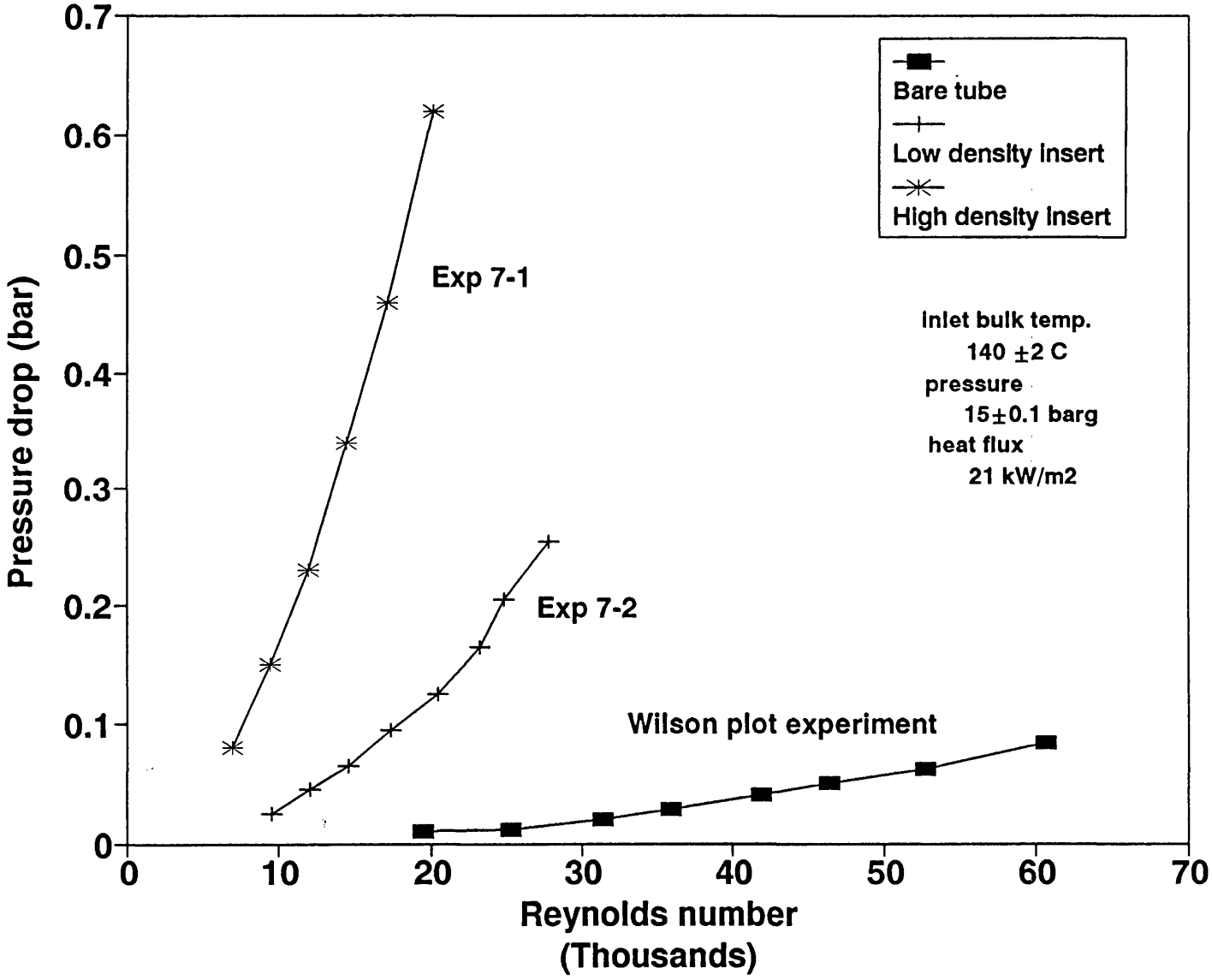

Figure 3.1 Pressure drop over the test section with and without inserts

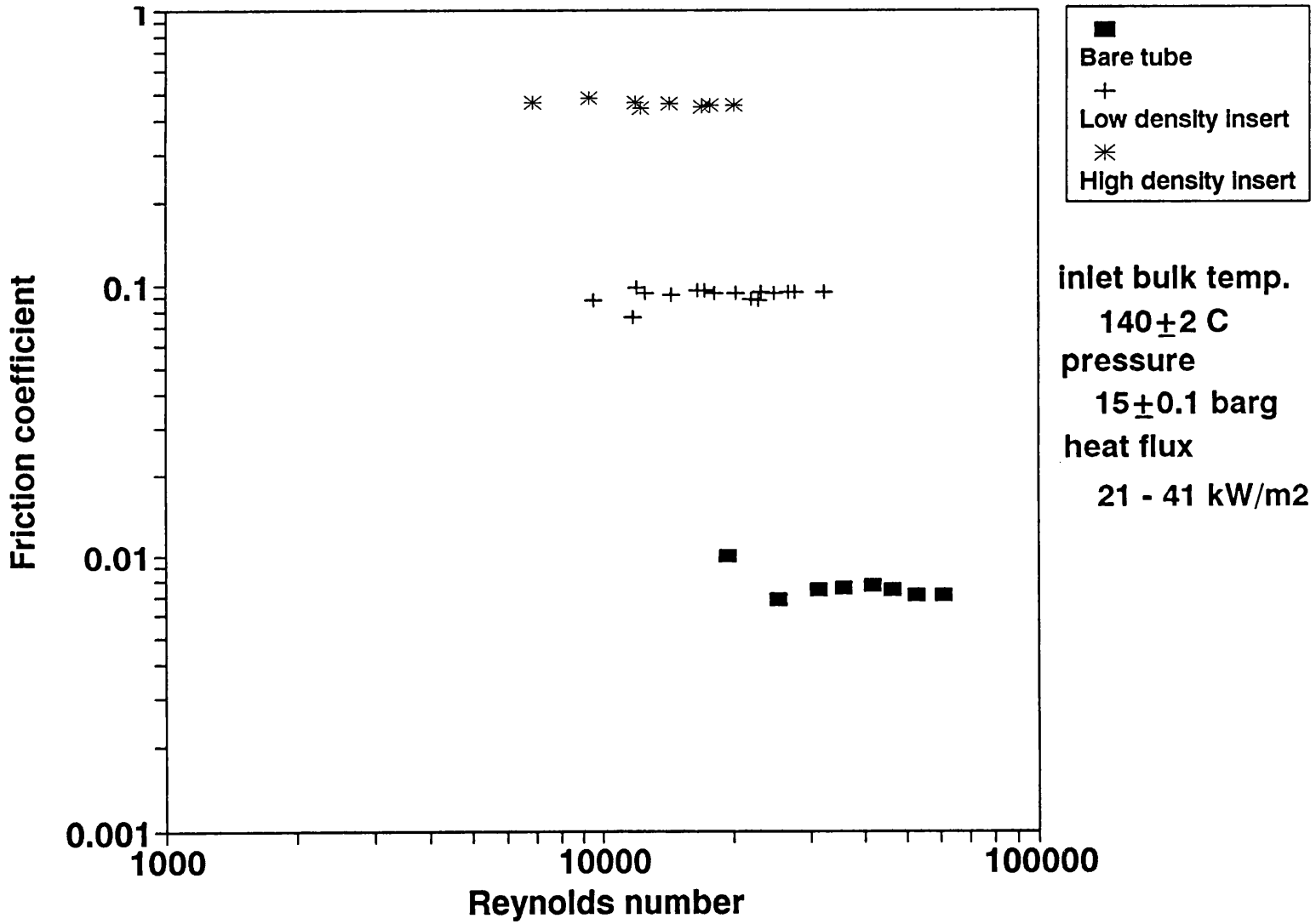

Figure 3.2 Friction coefficients for the bare tube and for the tube fitted with each insert

3.1.1.2 Roughness evaluation for the bare tube

A comparison of the experimental friction factor vs Reynolds number curves with an established diagram (Moody (1944)) for rough surfaces was conducted. The Moody fiction factor, f, is given by:

$$f = 4\ C_f \tag{3.4}$$

The comparison is shown in Figure 3.3 (reproduced from Moody (1944)), from which it may be concluded that the average relative roughness lies between 0.002 and 0.004, giving the average absolute roughness on the heat transfer surface between 0.03 and 0.06mm. This is as expected for commercial steel according to Figure 3.3.

3.1.2 Heat transfer

Heat transfer measurements were performed at various fluid velocities in the range 0.5 ms^{-1} to 2.5 ms^{-1} and heat fluxes in the range 20 kWm^{-2} to 130 kWm^{-2} with a constant inlet bulk temperature of 140 ± 2°C and a constant reservoir pressure of 15 ± 0.1 barg. Operational details for each experiment have been provided in Table 3.3.

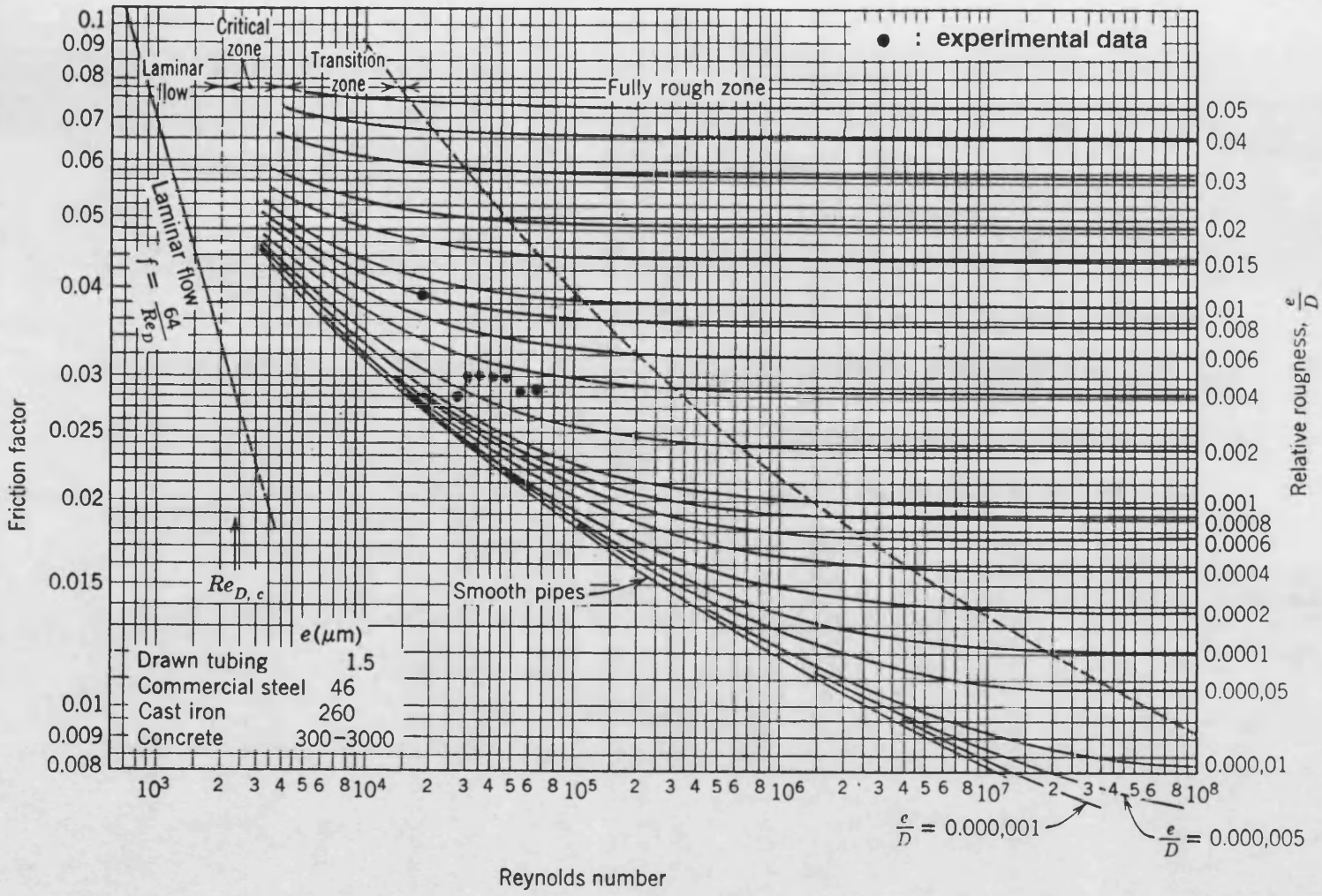

Figure 3.3 Friction factor for fully developed flow in a circular tube (Moody (1944))

3.1.2.1 Heat transfer for the bare tube

3.1.2.1.1 Reproducibility of heat transfer data after tube cleaning

Before and after most fouling experiments, heat transfer data were collected to ensure that reproducible heat transfer characteristics of the tube were obtained after cleaning. In order to avoid the possibility of nucleate boiling occurring, the reproducibility experiments were carried out at a relatively high velocity of 2.5 ms^{-1} and with a range of relatively low heat fluxes (26 - 52 kWm^{-2}). Shalhi (1993) had previously determined that repositioning an insert could lead to a change in heat transfer performance. Thus the reproducibility experiments were restricted to the bare tube only. The results are given in Table 3.4, from which it can be seen that heat transfer coefficients are well restored after the tubes are cleaned.

3.1.2.1.2 Effect of heat flux

Example data for Exp 13 - 1 are shown in Figure 3.4 to demonstrate the influence of heat flux on heat transfer coefficient for the bare tube. Two different types of trend exist. One is for the convective heat transfer regime in which the heat transfer coefficient is independent of heat flux but dependent on flow rate. The other is the nucleate boiling regime in which the heat transfer coefficient is also dependent on heat flux (as observed in the data for fluid velocities of 0.5 and 0.88 ms^{-1}). This result generally agrees with that obtained by Kreith and Summerfield (1949) who found that the heat transfer coefficient in the nucleate boiling regime for

Table 3.4 Heat transfer coefficients for the bare tube after cleaning

fluid velocity 2.5 ms^{-1} and heat flux 26 - 52 kW m^{-2}

Exp Number	heat transfer coefficient (W m^{-2} K^{-1})
1 - 1	2328
3 - 1	2870
3 - 2	2850
8 - 1	2830
9 - 1	2790
9 - 2	2706
11 - 1	2892
11 - 2	2759
13 - 1	2817
14 - 1	2691
14 - 2	2739
15 - 1	2890
15 - 2	2754
17 - 1	2943
Average	2776

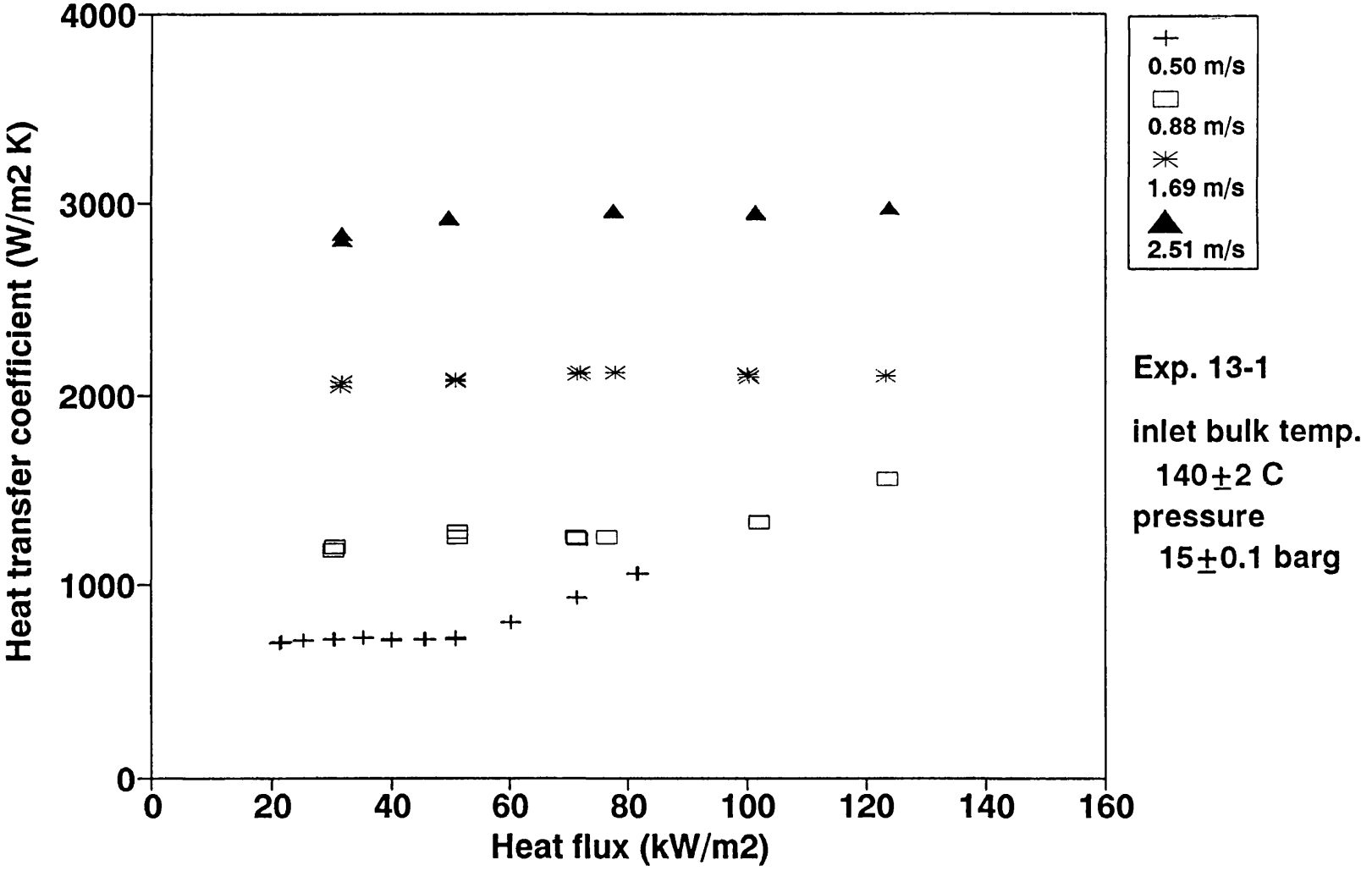

Figure 3.4 Effect of heat flux on heat transfer coefficient for the bare tube

water was dependent on heat flux but not on flow rate.

3.1.2.1.3 Effect of continued recirculation of feedstock

As stated previously, a series of experiments (with the exception of Run 19) was carried out without changing the crude oil. The onset of subcooled nucleate boiling (as indicated by the minimum heat flux at which the heat transfer coefficient started to increase with heat flux) varied from Run to Run (and hence with time) as shown in Figure 3.5. However, in the convective-only regime, the heat transfer coefficient for V_m = 0.5 ms^{-1} remained constant from Run to Run (Figure 3.5). Figure 3.6 shows the influence of surface temperature on heat transfer coefficient for V_m = 0.5 ms^{-1}, from which the minimum surface temperature at which nucleate boiling is believed to be taking place was estimated and plotted in Figure 3.7. It is clear that the minimum temperature for the onset of nucleate boiling increased as the series of fouling experiments was carried out.

Samples of crude oil A were taken before and after the whole series of experiments (Runs 1 to 18). The viscosity and specific gravity of each oil sample were measured by a viscometer (Brookfield Engineering Laboratory Inc. LVTDV-II) and by weighing a known volume, respectively. Data are shown in Table 3.5.

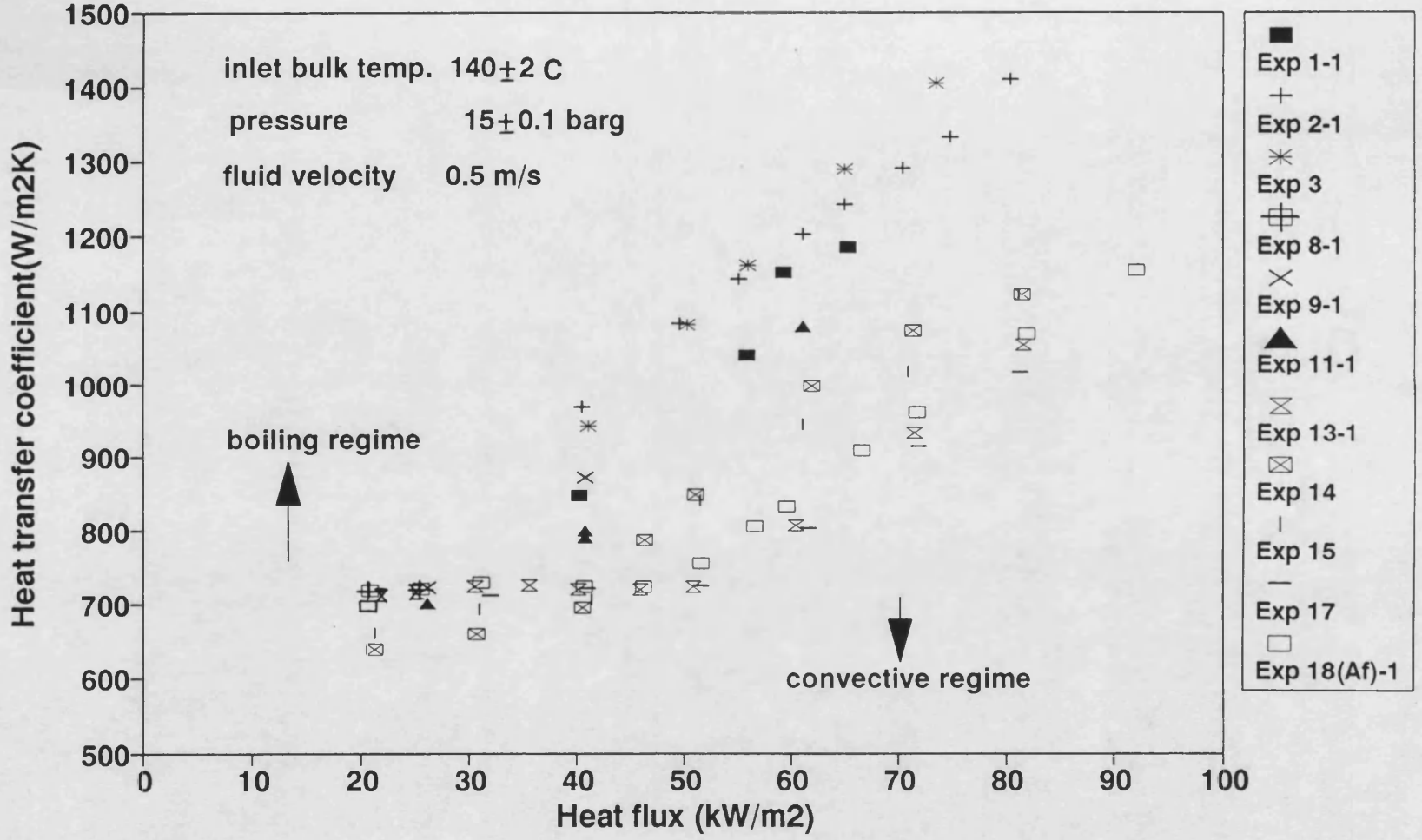

Figure 3.5 Influence of heat flux on heat transfer coefficient from Run to Run for the bare tube

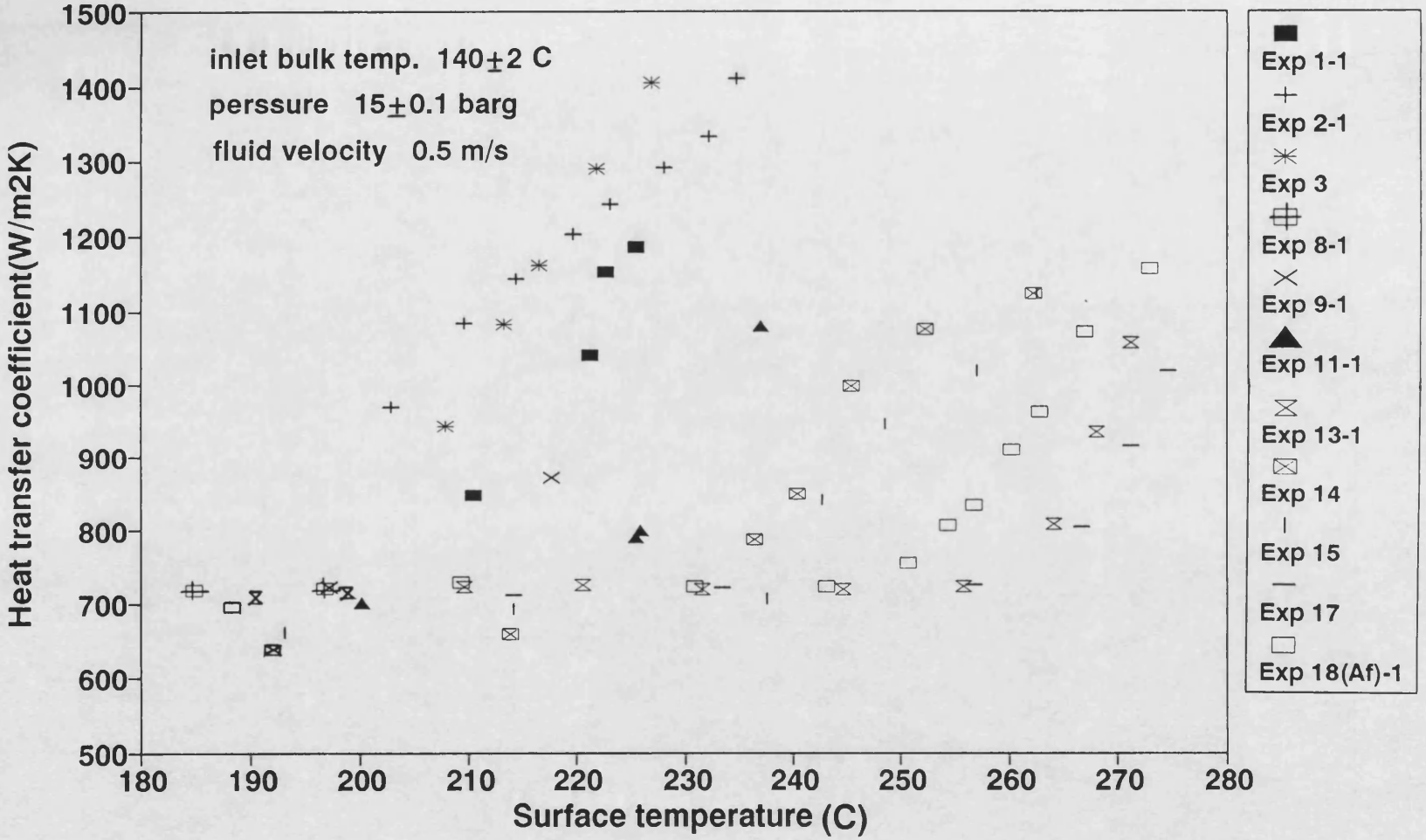

Figure 3.6 Influence of surface temperature on heat transfer coefficient from Run to Run for the bare tube

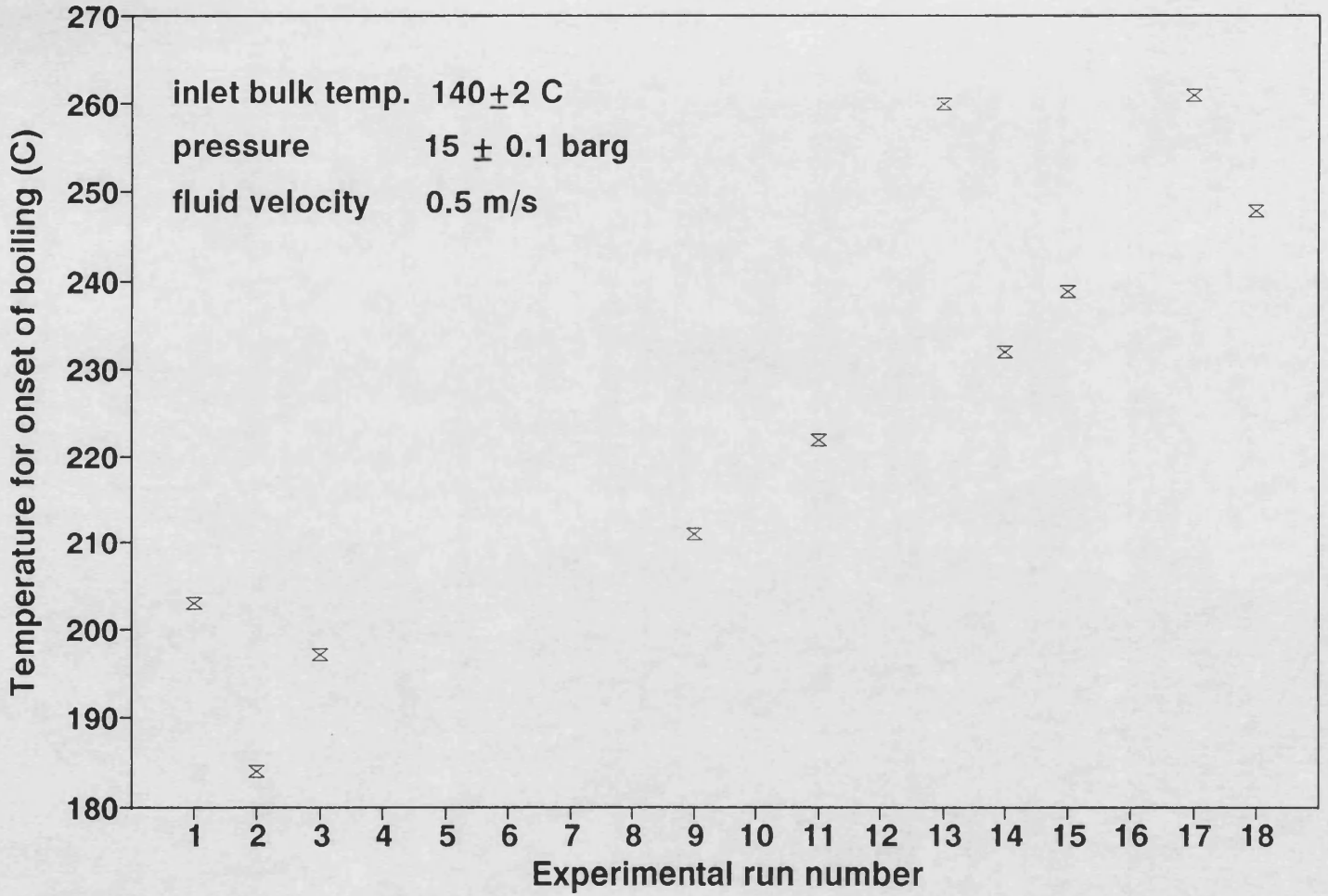

Figure 3.7 Minimum temperature for onset of subcooled nuleate boiling from Run to Run

Table 3.5 Properties of crude oil A

	kinematic viscosity (Pa s x 10^3)			specific gravity at 15/15°C
	41.0°C	60.1°C	79.0°C	
before use (prior to Run 1)	8.15	4.25	2.95	0.8619
after use (after Run 18)	8.20	not measured	2.90	0.8643

Little change was detected in the viscosity and only a small increase in the specific gravity of the oil was found over the whole series of experiments. It may be concluded therefore that the change in surface temperature at which subcooled nucleate boiling starts is probably due to a progressive degassing and a progressive loss of light components from crude oil A from Run to Run. A general chemical analysis of the oil prior to Run 1 and after Run 18 was undertaken by the University of Salford. Details are given in Table 3.6.

Table 3.6 Analyses of crude oil A (University of Salford)

	before Run 1	after Run 18
saturates	28.24%	28.72%
aromatics	48.96%	48.05%
resins	19.48%	19.39%
asphaltenes	3.32%	3.84%
Total	100%	100%

The analyses do not indicate any significant change in bulk composition.

For the subcooled nucleate boiling regime, no significant circumferential variation in local film heat transfer coefficient was observed. Evidence is provided in Appendix 3. A possible reason for this is as follows. The bubbles probably form uniformly around the heated tube and then condense in the colder bulk fluid away from the heating surface. As a result, no net vapour is produced in the bulk fluid to create a vapour flow along the top of the tube. Therefore, little circumferential variation of heat transfer coefficient should be expected. This is in marked contrast to saturated boiling for which Crittenden and Kolaczkowski (1978) reported that large circumferential variations in film heat transfer coefficients occurred with light hydrocarbons in a 0.02 m ID horizontal furnace tube. This is because in saturated boiling an insulating vapour blanket can form on the top surface of a tube.

From the heat transfer study with bare tubes, it was concluded that certain fouling Runs (Runs 1-1, 2-1, 3, 9, 11, 14-1 and 17-1) were carried out in the subcooled nucleate boiling regime.

3.1.2.1.4 Convective heat transfer

For the convective heat transfer regime only, all heat transfer data for the bare tube are plotted against the Reynolds number in Figure 3.8. Colburn's j factor, j_H (Colburn (1933)) is calculated from:

$$j_H = St \cdot Pr^{2/3} \qquad (3.5)$$

in which St is the Stanton number and Pr is the Prandtl number

The value of the viscosity is determined at the film temperature T_f and values of the other fluid properties are evaluated at the bulk temperature T_b.

For a smooth tube, the j_H factor (Colburn (1933)) is given by:

$$j_H = 0.023\ Re^{-0.2} \qquad (3.6)$$

From Figure 3.8 it can be seen that the experimental heat transfer coefficients are generally larger than those predicted by equation (3.6). Such an enhancement in heat transfer coefficient for a bare tube may be due to the roughness of the heat transfer surface.

3.1.2.2 Heat transfer for tubes with inserts

Example data are shown in Figures 3.9 and 3.10 to demonstrate the influence of heat flux on heat transfer coefficient for tubes fitted with the low density and high density inserts, respectively. With inserts the symptoms of subcooled nucleate boiling were not observed, *i.e.*, the coefficient was found to be virtually independent of heat flux. This is because the heat transfer coefficient is substantially higher than that for a bare tube, leading to a lower surface temperature for the tube fitted

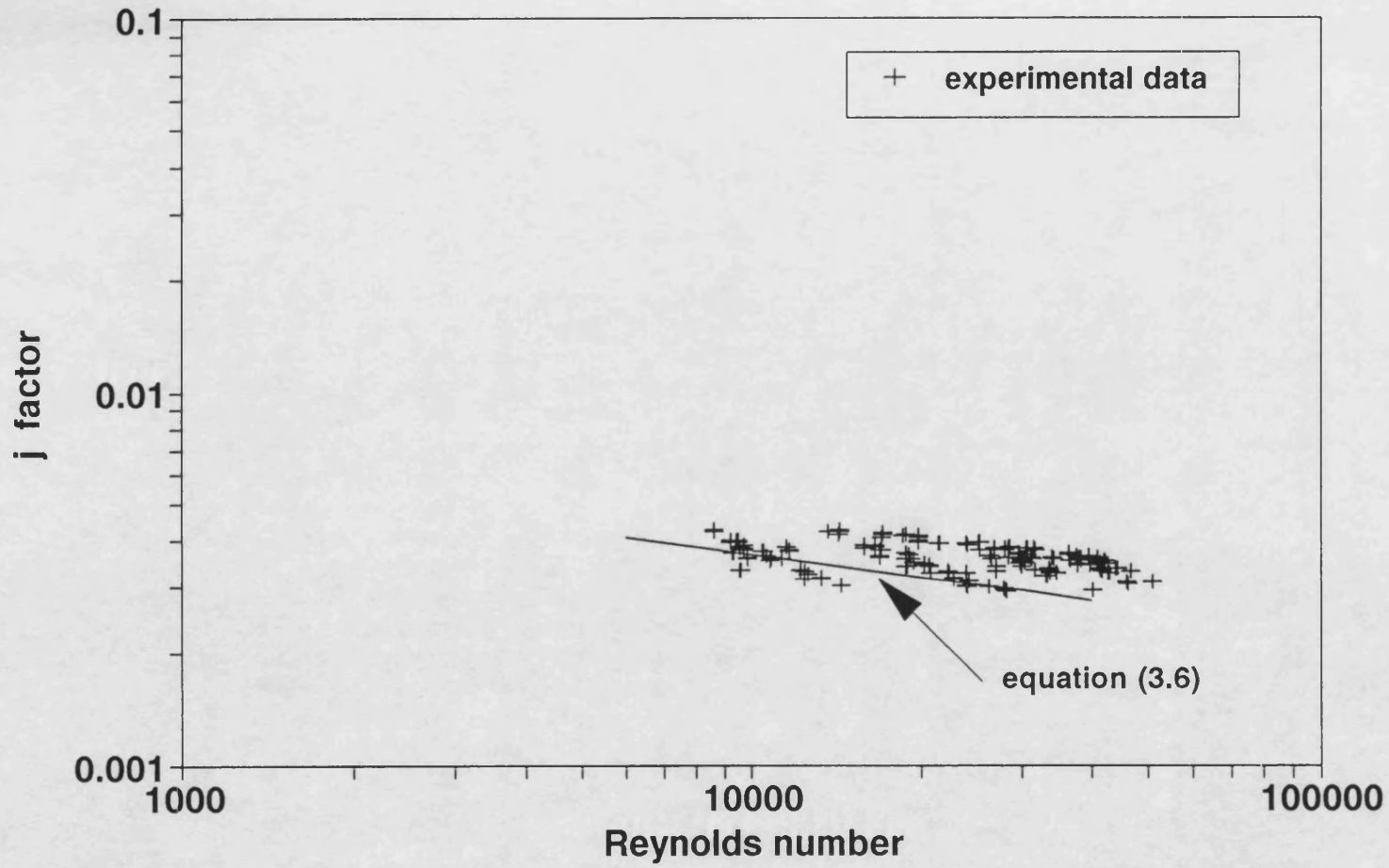

Figure 3.8 j factor for the bare tube

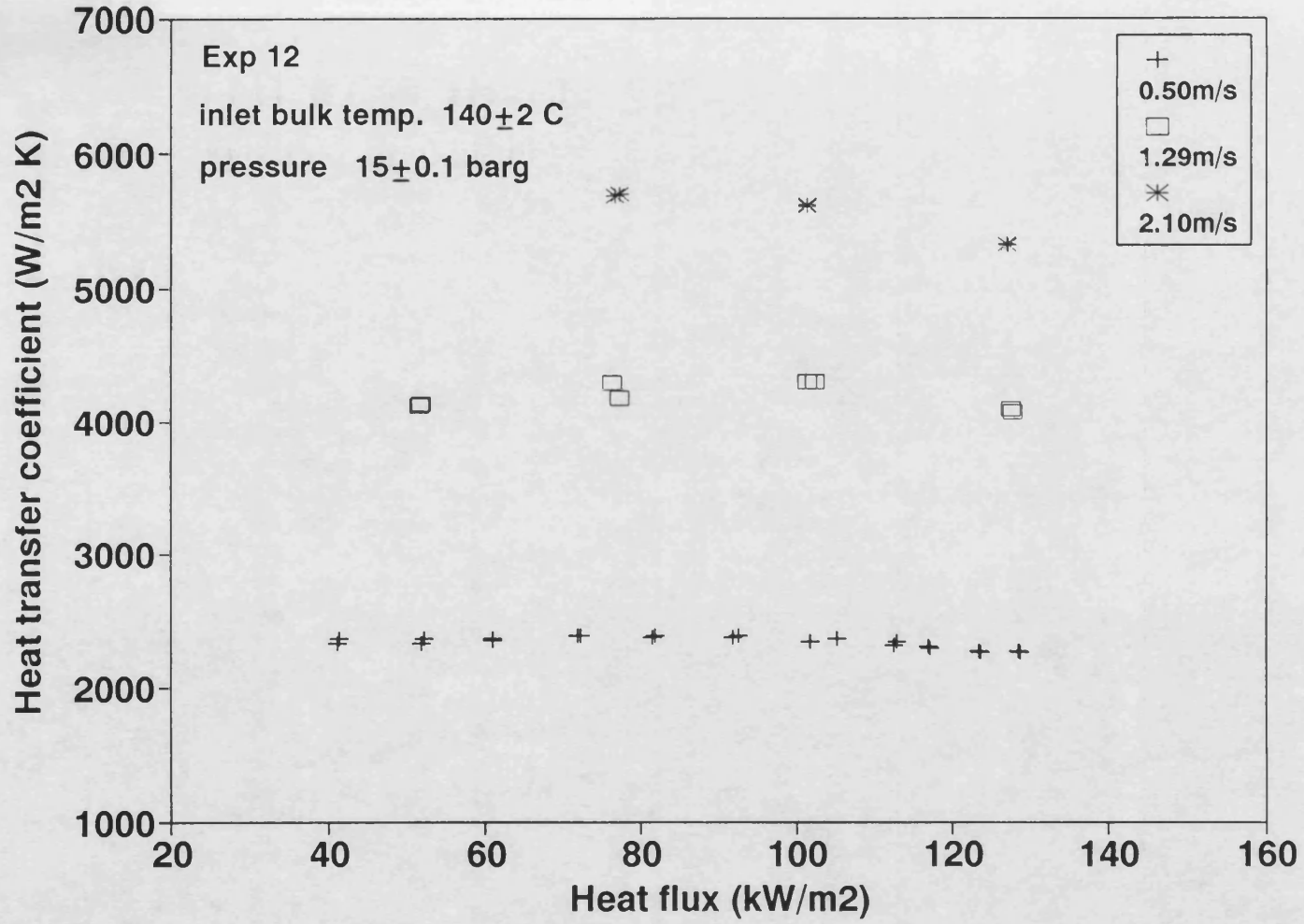

Figure 3.9 Influence of heat flux on heat transfer coefficient for the tube fitted with a low density insert

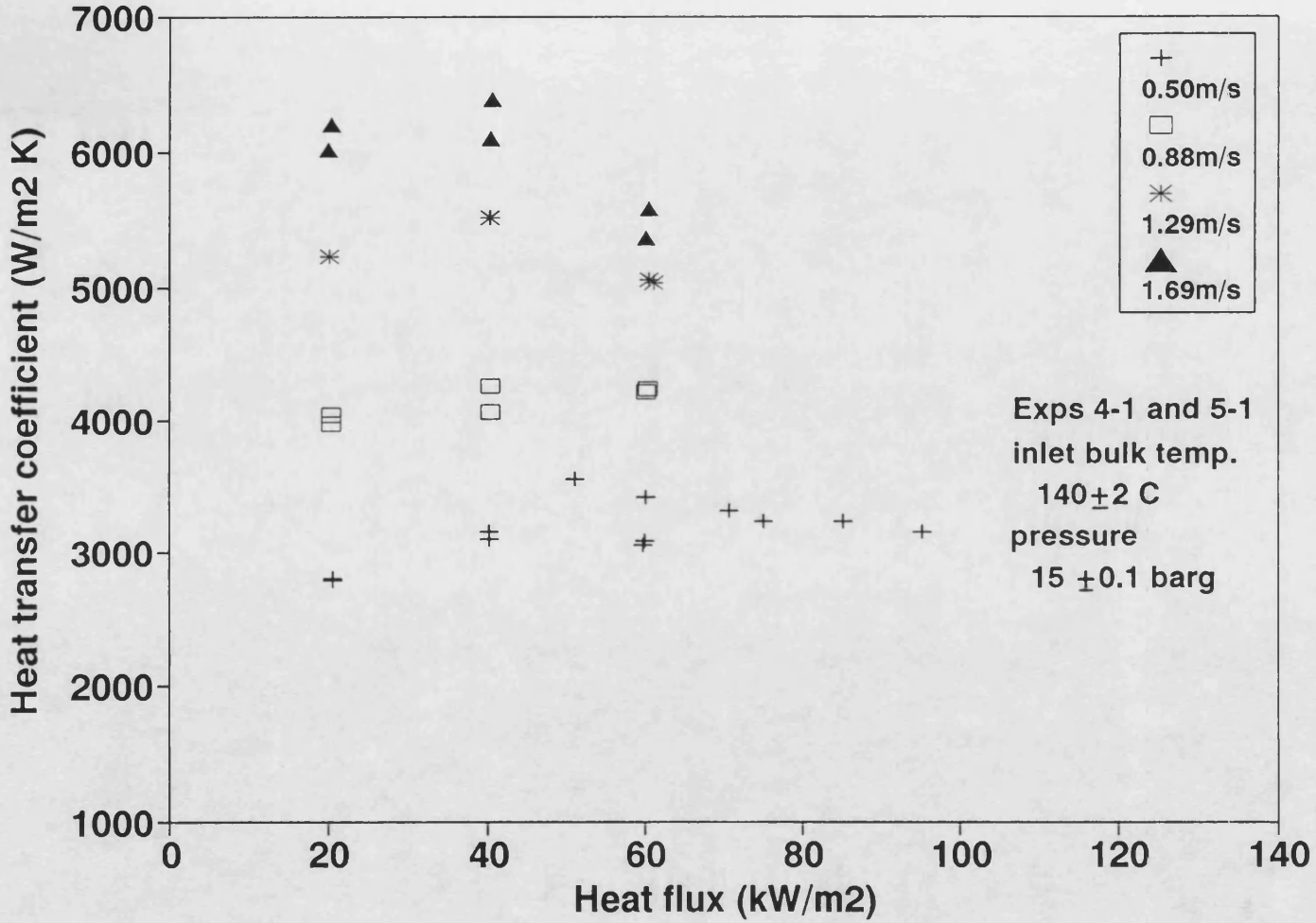

Figure 3.10 Influence of heat flux on heat transfer coefficient for the tube fitted with a high density insert

with an insert. The relatively high degree of scatter in the heat transfer data shown in Figures 3.9 and 3.10 is ascribed principally to errors due to the smaller temperature differences between the wall and the bulk fluid which arise when an insert is present. The scatter is not attributed to any other physical phenomenon. Thus, except for Run 2-2, all fouling experiments in which inserts were used (reported in section 3.2), were carried out with flow solely in the convective heat transfer regime.

Figure 3.11 compares the j_H factor data (plotted against the Reynolds number) for a bare tube and for a tube fitted with each insert. It can be seen that the heat transfer coefficient is profoundly increased by the presence of an insert. The j_H factors due to the presence of the low density and high density inserts are as much as 330 percent and 500 percent higher than those for the bare tube over the range of the Reynolds number tested.

For the tube fitted with each insert, an empirical correlation of the form given by equation (3.7) was fitted to the heat transfer data obtained from all the experiments, except for Exps 1-2 and 2-2 (omitted for reasons given below):

$$j_H = aRe^b \tag{3.7}$$

in which a and b are constants. The following relationship for each insert was obtained:

For the tube with the low density insert

$$j_H = 0.418\ Re^{-0.39}\ [7000 < Re < 40000 \text{ and } 6 < Pr < 17] \qquad (3.8)$$

For the tube fitted with the high density insert,

$$j_H = 0.832\ Re^{-0.41}\ [7000 < Re < 30000 \text{ and } 6 < Pr < 17] \qquad (3.9)$$

Correlation coefficients for equation (3.8) and (3.9) were calculated to be 0.869 and 0.852, respectively. All the experimental data were found to be correlated within standard deviations of ± 3.5% and ± 3.4% respectively.

The position of an insert inside a tube was found to affect the heat transfer coefficient. For the tube fitted with the low density insert in Runs 1-2 and 2-2, the insert was placed in the position shown in Figure 3.12 (a). For the remaining experiments, the insert was placed in the position shown in Figure 3.12 (b). The heat transfer coefficient measured with the insert at position (a) was found to be lower than that with the insert at position (b). Since the heat transfer coefficient is derived from local measurements this is as expected. Even so the heat transfer coefficient with the insert at position (a) was still enhanced owing to the additional turbulence generated by the insert in the boundary layer (Figure 3.13).

Finally, circumferential variations in heat transfer coefficient were found not to be significant with an insert installed. Evidence for this is provided in Appendix 3.

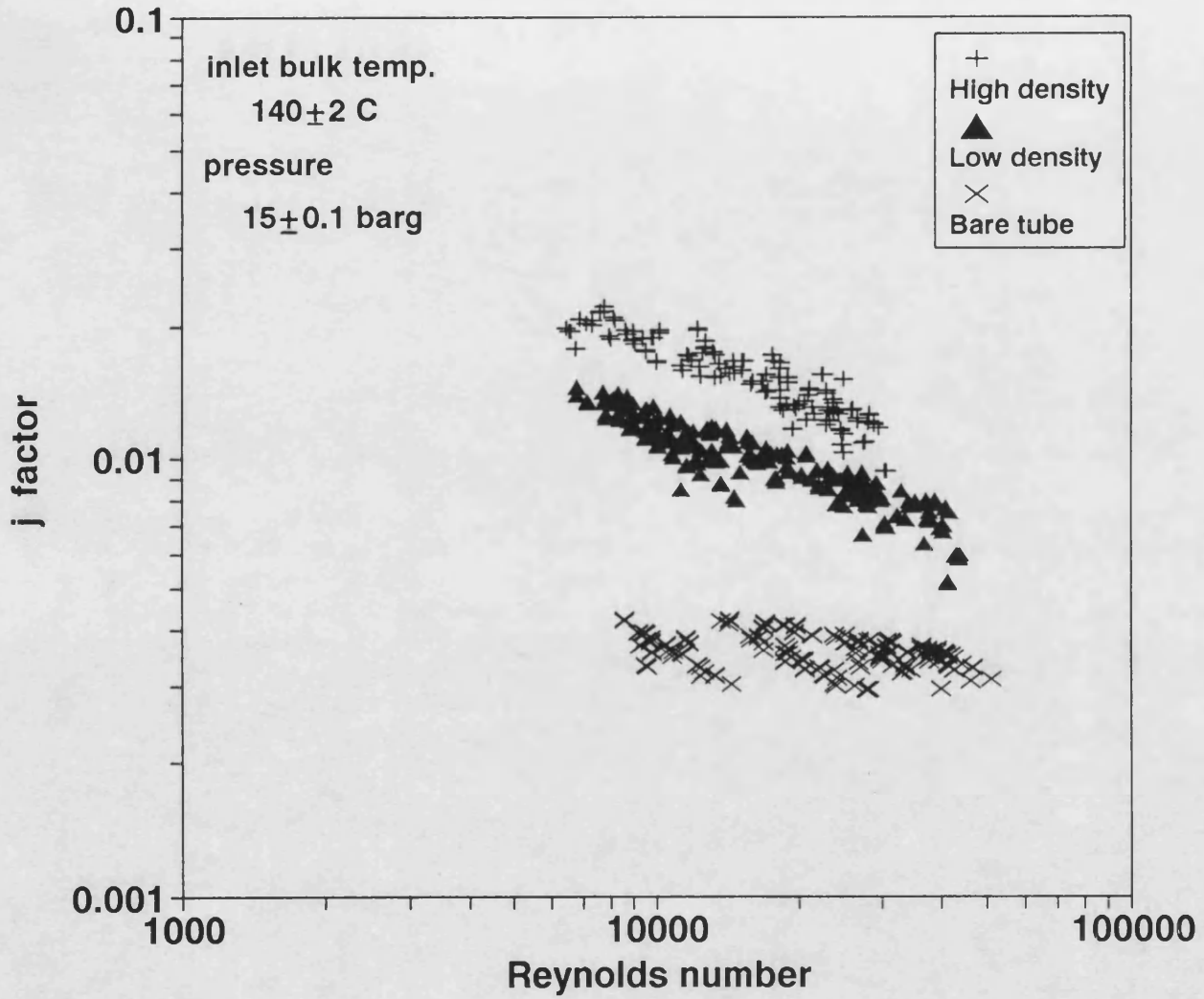

Figure 3.11 j factors for the bare tube and for the tube fitted with each insert

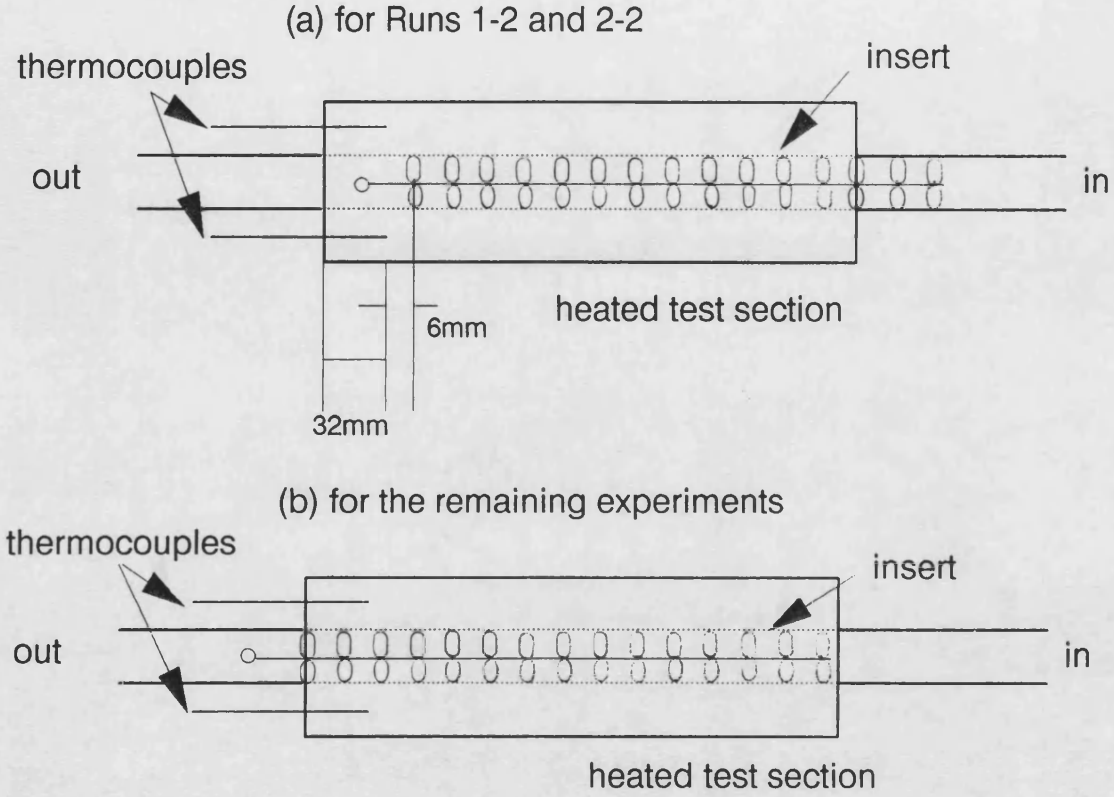

Figure 3.12 Position of the insert in the pipe

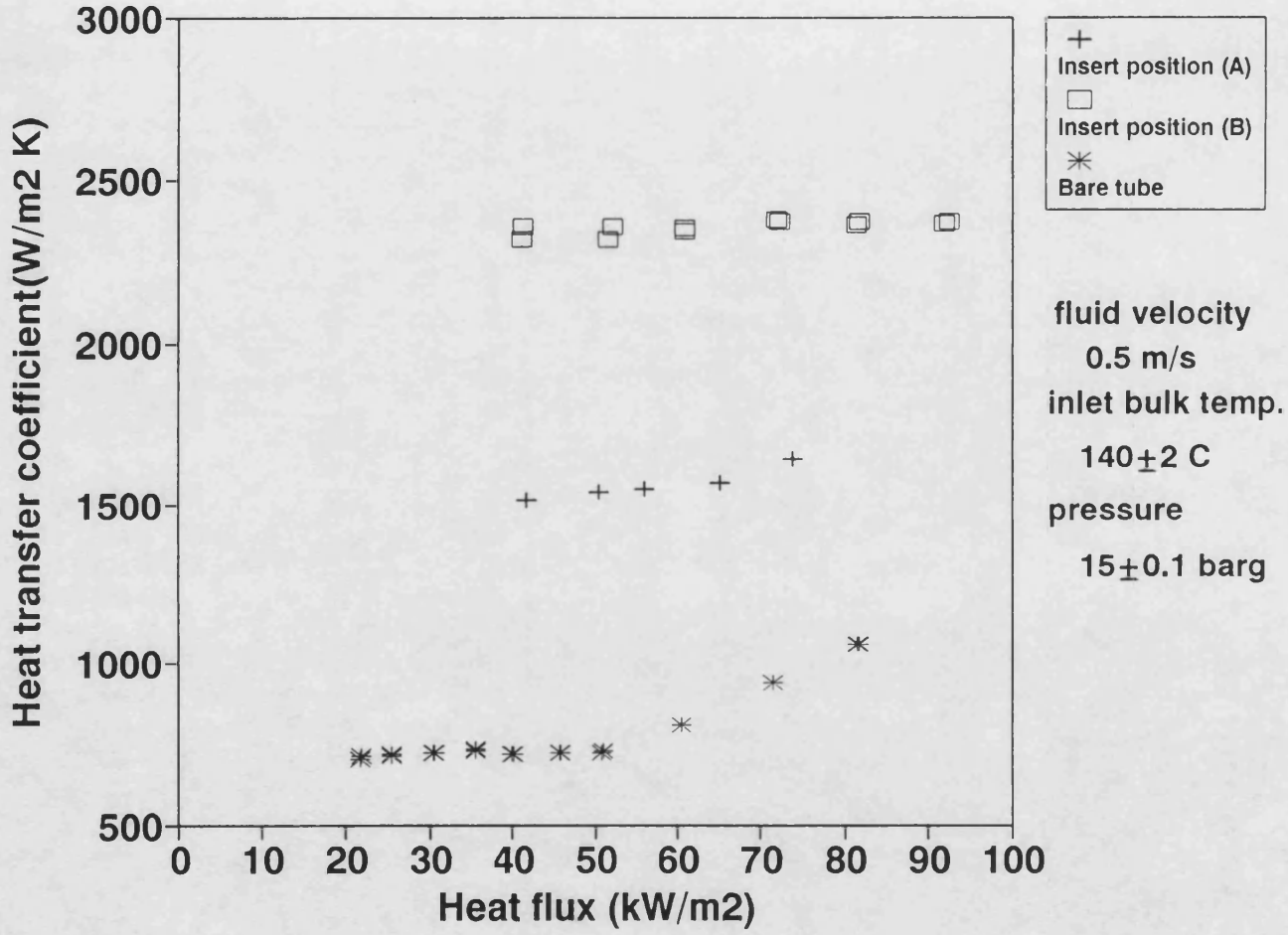

Figure 3.13 Effect of insert position in the tube on heat transfer coefficient

3.1.2.2.1 Comparison of j_H factors and friction coefficients

The ratio of j_H factor to friction coefficient ($2j_H$ / C_f) is a measure of the heat transfer obtainable per unit of pumping power. This ratio is important for engineering applications. Figure 3.14 shows the ratio plotted as a function of the Reynolds number. For the bare tube the ratio is almost equal to unity. However with the insert present the ratio is much less than unity. Therefore, it can be said that increases in j_H due to the presence of the insert are accompanied by larger increases in C_f over the range of the Reynolds number tested (7000 to 40000).

3.1.2.2.2 Effect of heat conduction

When an insert is placed in a tube, it is possible that some heat may be transferred by conduction along the insert wires as well as by forced convection. The contribution due to conduction has been estimated from a simple calculation, the details of which are provided in Appendix 4. The conclusion of this calculation is that conduction accounts for less than 1% of the total heat input. This is primarily because of the small contact area between the insert and the tube wall.

3.2 Fouling experiments

All fouling experiments were performed with a constant inlet bulk temperature of 140 ± 2°C and with a constant reservoir pressure of 15 ± 0.1 barg. At the end of most fouling runs, an attempt was made to check whether the deposits were

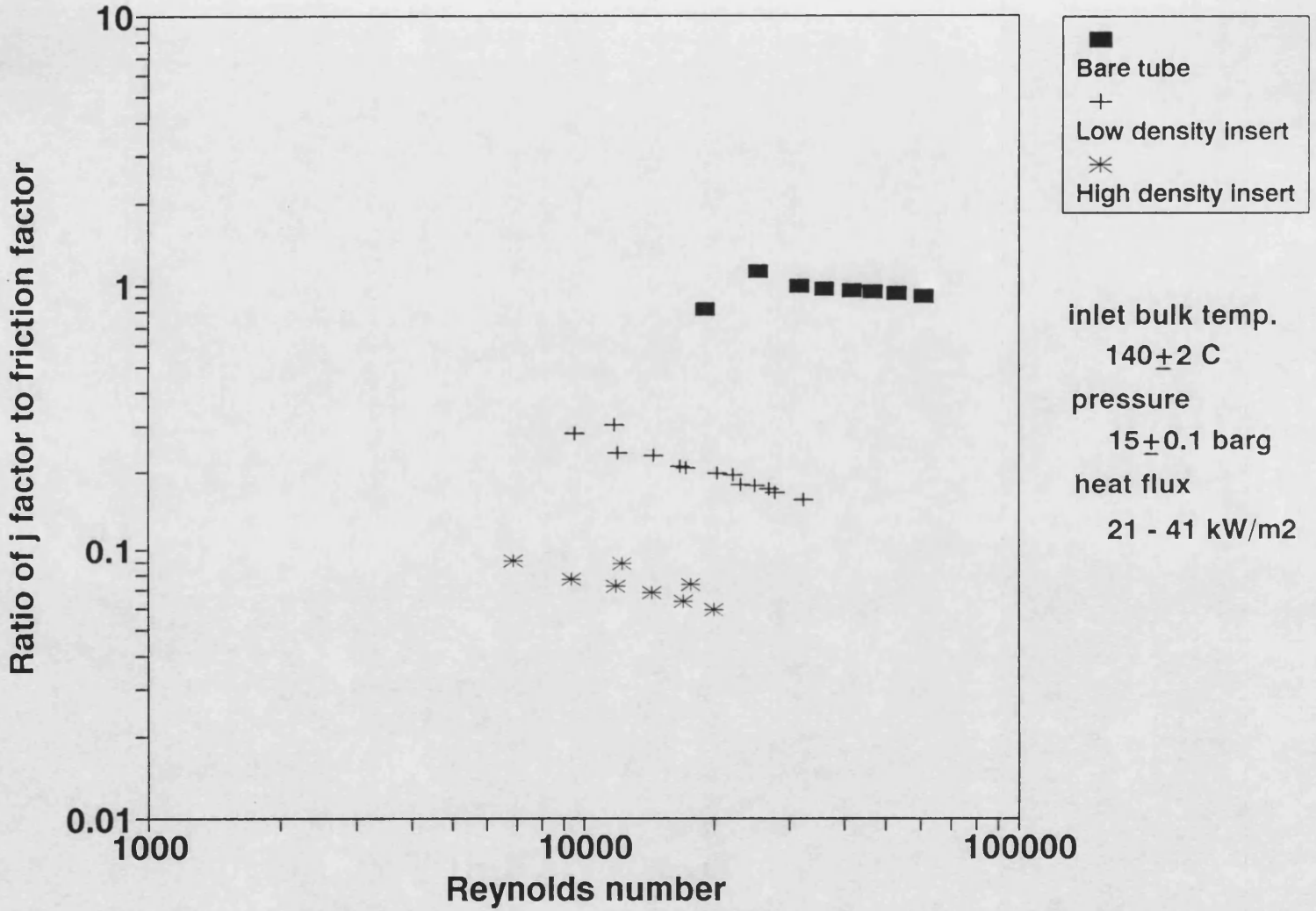

Figure 3.14 Ratio of j factor to friction factor for the bare tube and for the tube fitted with each insert

removable by increasing the velocity and hence the shearing action of the fluid. After cooling the crude oil down at the end of each fouling experiment the test sections were dismantled and then visually inspected. Attempts to recover pieces of the deposits were made but proved successful only for Run 3. In Section 3.2.1 each fouling Run is described in the chronological order in which the experiments were carried out. The basic results are then reported in three sub-sections, *i.e.* fouling data in Section 3.2.1.1, effect of velocity change in Section 3.2.1.2 and nature of deposits in Section 3.2.1.3. The results are then discussed more fully and modelled in Sections 3.2.2 to 3.2.11.

3.2.1 Chronology of fouling experiments

3.2.1.1 Fouling experiments

Table 3.1 presented at the beginning of this Chapter provides a summary of the objectives of each experiment. Operating data are summarised in detail in Table 3.7. Runs 1 to 18 were carried out chronologically with a single batch of crude oil A, which was not removed or added to during these experiments. Run 19 was made with fresh crude oil B. Runs 1, 2, 4 to 8, 13, 17 and 19 were carried out to evaluate the effect of inserts on fouling. Runs 4 and 6 were stopped at 26 hours and 19 hours, respectively, after the start of the Run because of the failure of the electrical heater elements. Runs 9 to 12 and 14 to 16 were carried out to determine the effect of process variables (flow velocity with Runs 9, 10, 15 and 16 and temperature with Runs 11, 12 and 14). Runs 3 and 18 were made to check the reproducibility of the

Table 3.7 Operating data of fouling experiments

	Test section		Heat flux*)	Fluid velocity	Surface temp.	Heat transfer	Period of	Induction period	Initial fouling rate*)	hi clean
	No.	condition	(kW/m2)	(m/s)	clean (C)	regime**)	run (h)	(h)	(m2K/Wh)	(W/m2K)
Run 1	1	Bare	55.9	0.5	216	B	82	14	2.10E-05	1030
	2	Low	55.9	0.5	198	C		14	0.41E-05	1380
Run 2	1	Bare	55.9	0.5	216	B	70	19	1.20E-05	1130
	2	Low	76.2	0.5	216	B		0	0.90E-05	1610
Run 3	1	Bare	55.9	0.5	216	B	82	14	1.00E-05	1130
	2	Bare	55.9	0.5	216	B		14	1.00E-05	1130
Run 4	1	High	91.4	0.5	197	C	26	?	no fouling	2800
	2	Low	76.2	0.5	197	C	(burnt)	?	no fouling	2320
Run 5	1	High	76.2	0.5	186	C	90	?	no fouling	2900
	2	Low	76.2	0.5	197	C		0	0.35E-05	2340
Run 6	1	High	91.4	0.5	197	C	19	?	no fouling	2720
	2	Low	76.2	0.5	197	C	(burnt)	0	0.24E-05	2270
Run 7	1	High	103.6	0.5	197	C	90	0	0.07E-05	3390
	2	Low	77.7	0.5	197	C		0	0.25E-05	2200
Run 8	1	Bare	25.9	0.5	197	C	100	0	0.30E-05	725
	2	Low	77.7	0.5	197	C		0	0.30E-05	2230
Run 9	1	Bare	41.5	0.5	217	B	96	0	3.72E-05	870
	2	Bare	67.4	1.1	217	B		0	0.85E-05	1430
Run 10	1	Low	129.5	1.1	203	C	94	0	0.08E-05	3600
	2	Low	77.7	0.5	203	C		0	0.49E-05	2230

Table 3.7 continued

Table 3.7 continued

	Test section		Heat flux*) (kW/m2)	Fluid velocity (m/s)	Surface temp. clean (C)	Heat transfer regime**)	Period of run (h)	Induction period (h)	Initial fouling rate*) (m2K/Wh)	hi clean (W/m2K)
	No.	condition								
Run 11	1	Bare	41.5	0.5	226	B	96	0	4.97E-05	800
	2	Bare	62.2	0.5	237	B		0	6.83E-05	1080
Run 12	1	Low	114.0	0.5	224	C	96	0	0.50E-05	2420
	2	Low	88.1	0.5	211	C		0	0.50E-05	2190
Run 13	1	Bare	44.0	0.5	239	C	97	0	0.55E-05	720
	2	Low	114.0	0.5	239	C		0	1.43E-05	2080
Run 14	1	Bare	72.5	0.5	254	B	86	0	2.58E-05	1080
	2	Bare	31.1	0.5	217	C		0	0.93E-05	690
Run 15	1	Bare	44.0	0.5	239	C	96	0	0.75E-05	740
	2	Bare	82.9	1.1	239	C		0	negative	1430
Run 16	1	Low	129.5	0.7	221	C	97	0	1.00E-05	2900
	2	Low	95.9	0.5	221	C		0	2.04E-05	2150
Run 17	1	Bare	62.2	0.5	264	B	97	0	4.68E-05	840
	2	Low	62.2	0.5	193	C		0	0.97E-05	2200
Run 18	1	Low	103.6	0.5	218	C	96	0	2.84E-05	2520
	2	Low	93.3	0.5	218	C		0	3.41E-05	2170
Run 19	1	Bare	36.3	0.5	216	C	78	0	0.87E-05	740
	2	Low	93.3	0.5	216	C		0	0.32E-05	2250

*) Based on At

**) B: subcooled nucleate boiling regime

C: convective heat transfer regime

fouling data for the two identical test sections.

For the remainder of Section 3.2.1.1 each Run is described on a new page which is followed by graphs showing the variations of thermal coefficient H_i and fouling resistance R_f with time.

Run 1 (Low density insert as a retrofit)

Initial evaluation of the effect of the mechanical insert on fouling was made with the same heat flux ($55.9 kWm^{-2}$) and the same flow rate ($0.5 ms^{-1}$) in each test section. The initial surface temperature of the tube containing the low density insert was lower at 198°C than that of the tube left bare at 216°C. Variation of the heat transfer coefficients with time is plotted in Figure 3.15. After an induction period of around 14 hours, during which the heat transfer coefficients remained more or less constant, the heat transfer coefficients then fell rapidly and then gradually levelled out. Figure 3.16 shows that the corresponding fouling resistances slowly levelled out although they did not completely reach asymptotic values. The initial fouling rates were estimated from the slopes of the initial linear portions of the fouling curves after the induction periods. Fluctuation in fouling resistance with time made this estimation difficult for some Runs. However for Run 1 a five-fold reduction in the initial fouling rate from that of the bare tube was found with the low density insert installed (Table 3.7).

Chenoweth (1990) has published information on the final report of the HTRI/TEMA Joint Committee to review the fouling section of the TEMA standards. Table 3.8 shows values for crude oil. The fouling resistance at 82 hours for test section 1 (bare tube) is about 0.63 $m^2K\ kW^{-1}$ based on d_t (0.40 $m^2K\ kW^{-1}$ based on d_i) and the fouling resistance vs time plot for the bare tube is only just beginning to tend towards an asymptotic shape after about 80 hours. It is expected therefore that the

test section in this study would reach the proposed TEMA design R_f (0.70 to 0.88 for 216°C) in a relatively short period of time. One possible reason for this high rate of fouling is the use of a relatively low velocity in this study (0.5 ms^{-1}) compared with that which would normally be used in a refinery heat exchanger (> 1ms^{-1}). Even so, previous comparisons with oil refinery plant data (Bott and Walker (1971), Crittenden et al (1992)) have shown that TEMA design resistances can be exceeded in very short operating periods.

Table 3.8 Proposed design fouling resistances for crude oil, desalted at ~ 120°C (selected from Chenoweth, 1990)

temperature	velocity	design R_f
°C	ms^{-1}	$m^2K\ kW^{-1}$
120	>1.22	0.35 to 0.70
120 - 177	>1.22	0.53 to 0.70
177 - 232	>1.22	0.70 to 0.88
>232	>1.22	0.88 to 1.06

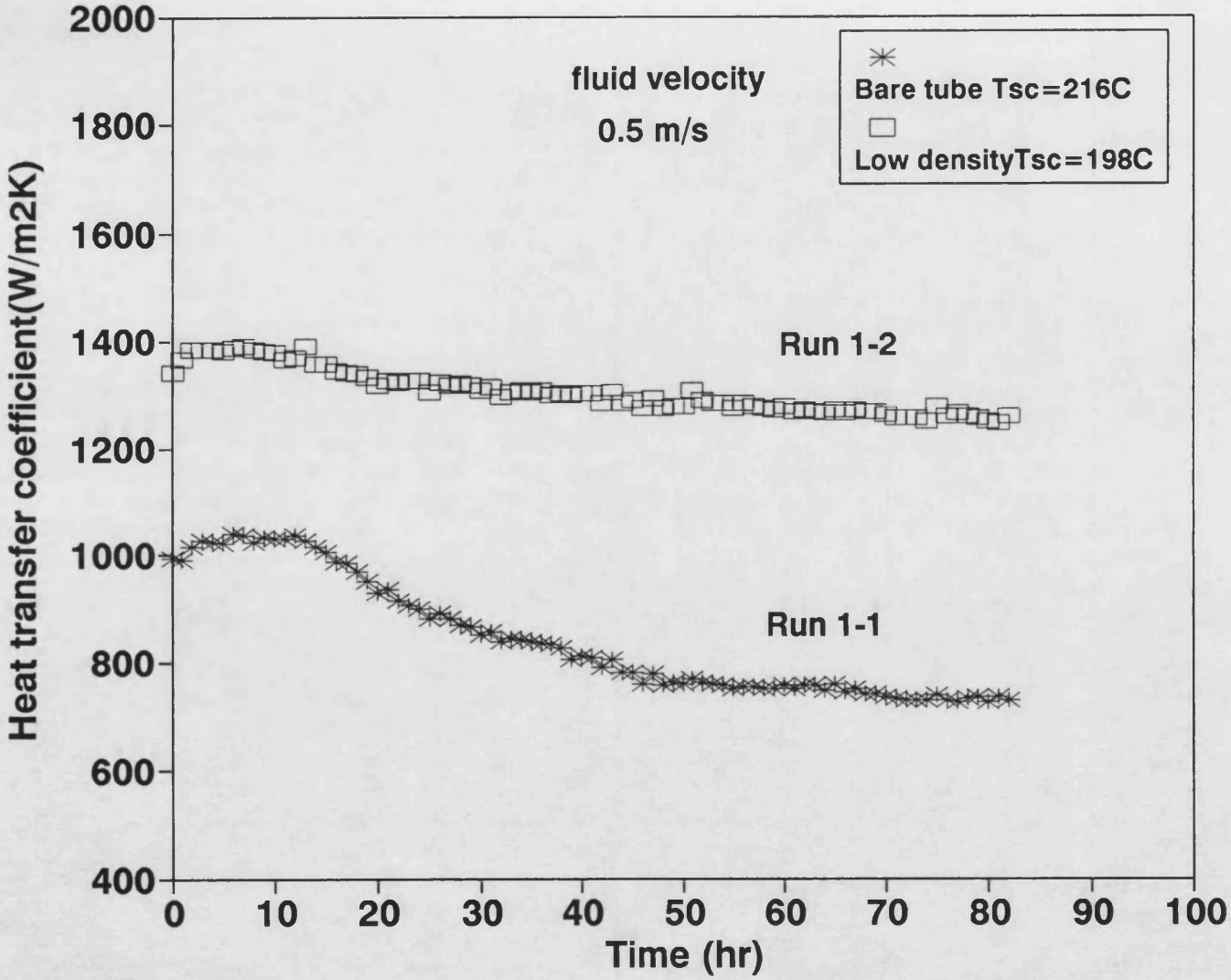

Figure 3.15 Thermal coefficient Hi for Run 1

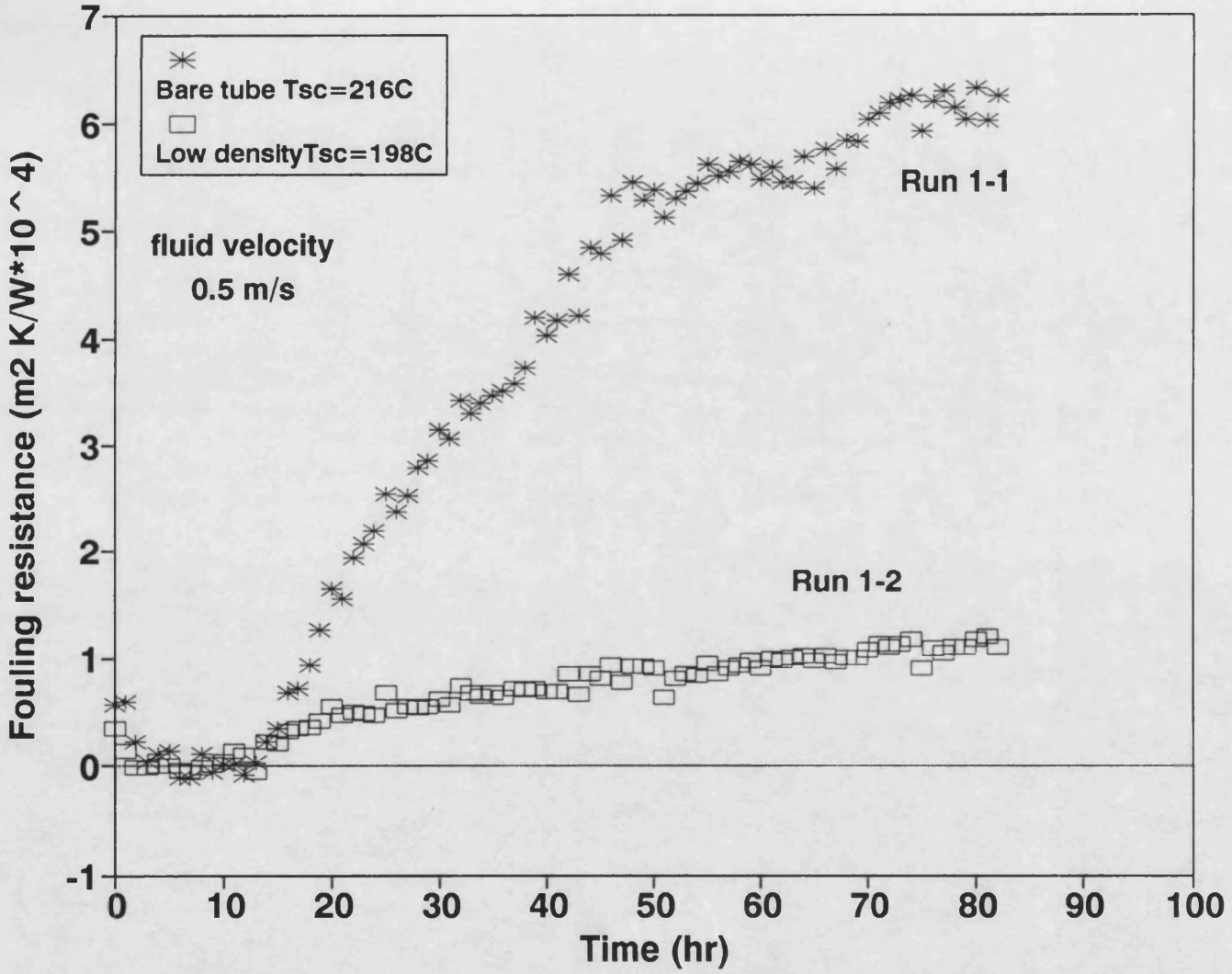

Figure 3.16 Fouling resistance - time data for Run 1

Run 2 (Effect of low density insert)

In this Run, the two test sections were operated at the same initial surface temperature of 216°C and the same flow rate of 0.5 ms^{-1}. To achieve the same surface temperature in this Run, the heat flux for the tube with the insert had to be set 36% higher than that for the bare tube. For the bare tube (Run 2-1) Figures 3.17 and 3.18 show a longer induction period than that for Run 1-1 (Figure 3.16). There appeared to be no induction period for the tube fitted with the insert in Run 2-2 (Figure 3.18). The initial fouling rate for the tube fitted with the insert (0.9 x 10^{-5} m^2K $W^{-1}h^{-1}$ based on d_i) was lower than that for the bare tube (1.2 x $10^{-5}m^2K$ $W^{-1}h^{-1}$ based on d_i) despite the initial surface temperatures being the same. In addition, the fouling resistance for the tube with the insert reached an asymptotic value at around 25 hours of operation. This asymptotic resistance was smaller than that which would ultimately have been obtained in the bare tube and at 0.2 m^2K kW^{-1} was between 23 and 28% of the TEMA design value (Table 3.8). Runs 1 and 2 demonstrated that the use of a HiTRAN insert could substantially reduce the magnitude of the fouling resistance and that the effect was possibly more than one of simply reducing the surface temperature. The mechanisms for this reduction will be explored in Sections 3.2.2 to 3.2.11.

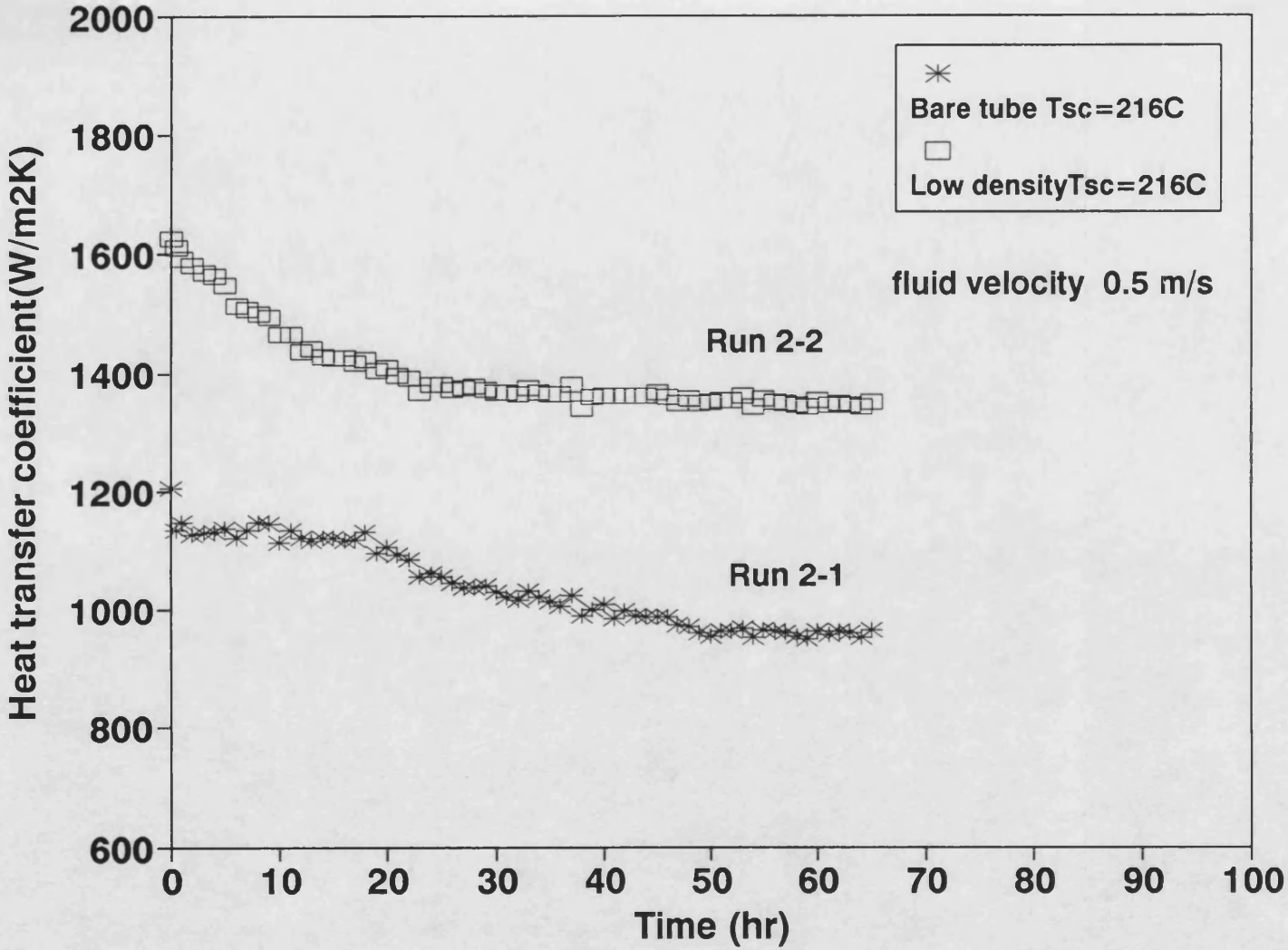

Figure 3.17 Thermal coefficient Hi for Run 2

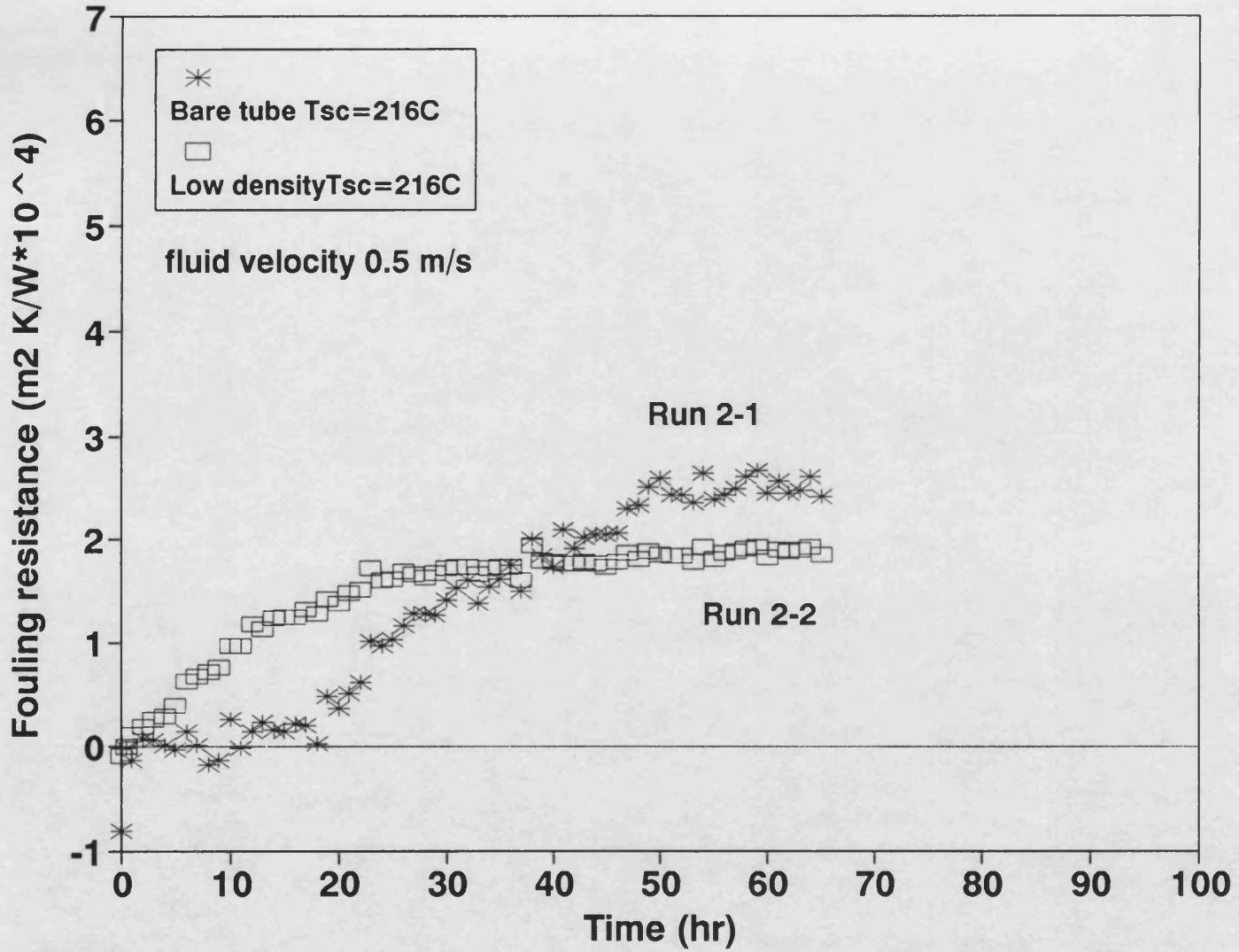

Figure 3.18 Fouling resistance - time data for Run 2

Run 3 (Reproducibility of data for bare tubes)

Run 3 was carried out to check the reproducibility of fouling data for the two identical bare tube test sections operating in parallel with the same feedstock. The operating conditions were identical for the two test sections (initial surface temperature = 216°C, flow velocity = 0.5 ms^{-1}, heat flux = 55.9 kW m^{-2}). As shown in Figures 3.19 and 3.20, excellent reproducibility in the heat transfer coefficients and the corresponding fouling resistances was obtained. These results created confidence that the two identical parallel test sections could be used for comparative experiments designed to evaluate accurately the effect of the HiTRAN insert and the effect of process variables. It was not anticipated that reproducibility from Run to Run could be achieved due to the recycle nature of the experiment and the continuous use of the same feedstock. Indeed comparison of the fouling data for bare tube Runs 1-1 and 1-2 (Figures 3.16 and 3.18) reveals differences in the fouling resistance vs time plots despite the identical operating conditions of flow velocity, initial surface temperature and heat flux.

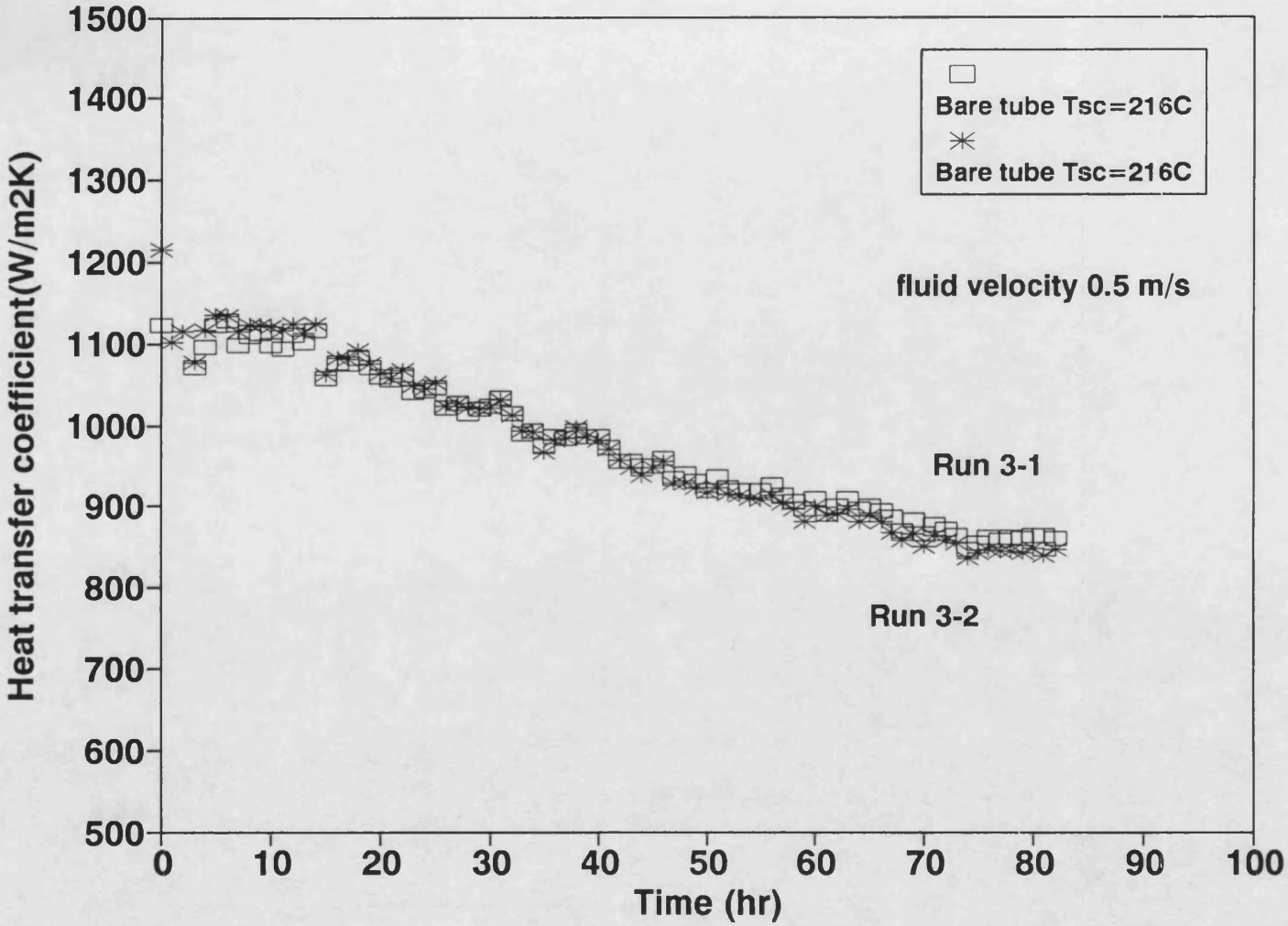

Figure 3.19 Thermal coefficient Hi for Run 3

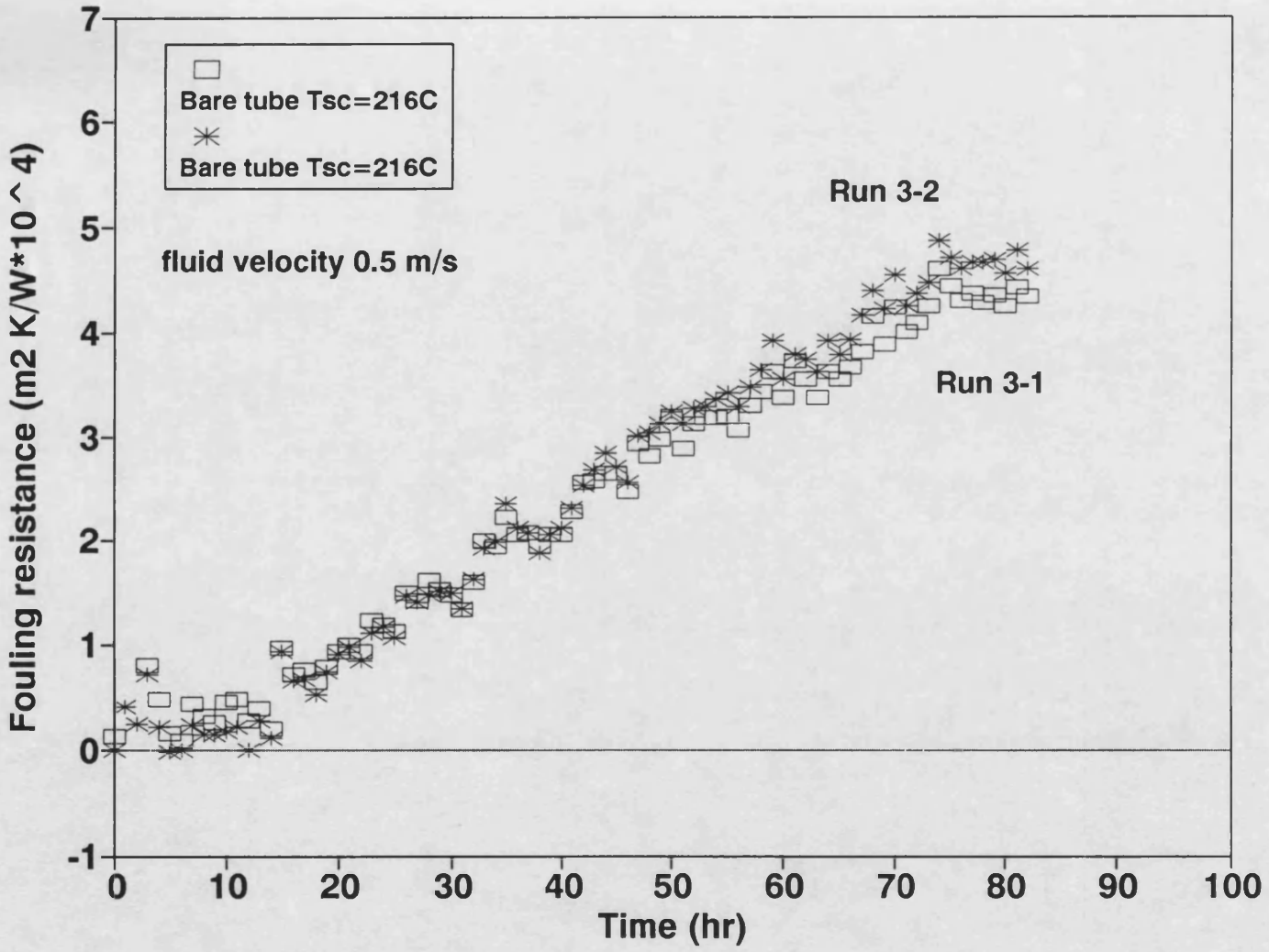

Figure 3.20 Fouling resistance - time data for Run 3

Run 4 (Effect of insert density)

The high density and low density elements were inserted into test sections 1 and 2 respectively. The experiment was carried out with the same initial surface temperature of 197°C and the same flow rate of 0.5 ms^{-1} in each test section. However the experiment had to be terminated after 26 hours due to the failure of the electrical heater elements. As seen in Figures 3.21 and 3.22, the data show some scatter but the tubes appeared not to have started fouling to any significant extent by 26 hours and this may have been the result of using a relatively low surface temperature.

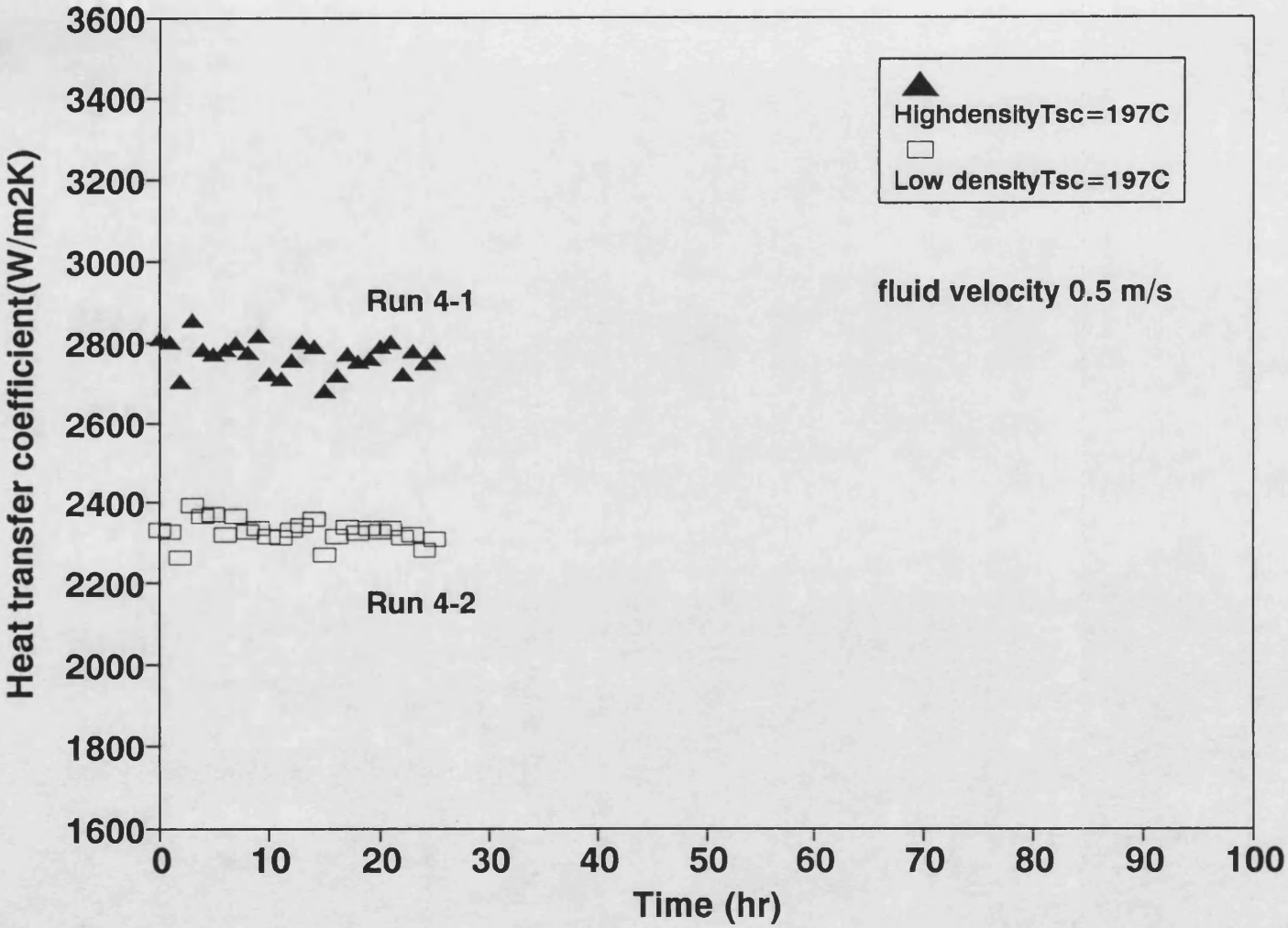

Figure 3.21 Thermal coefficient Hi for Run 4

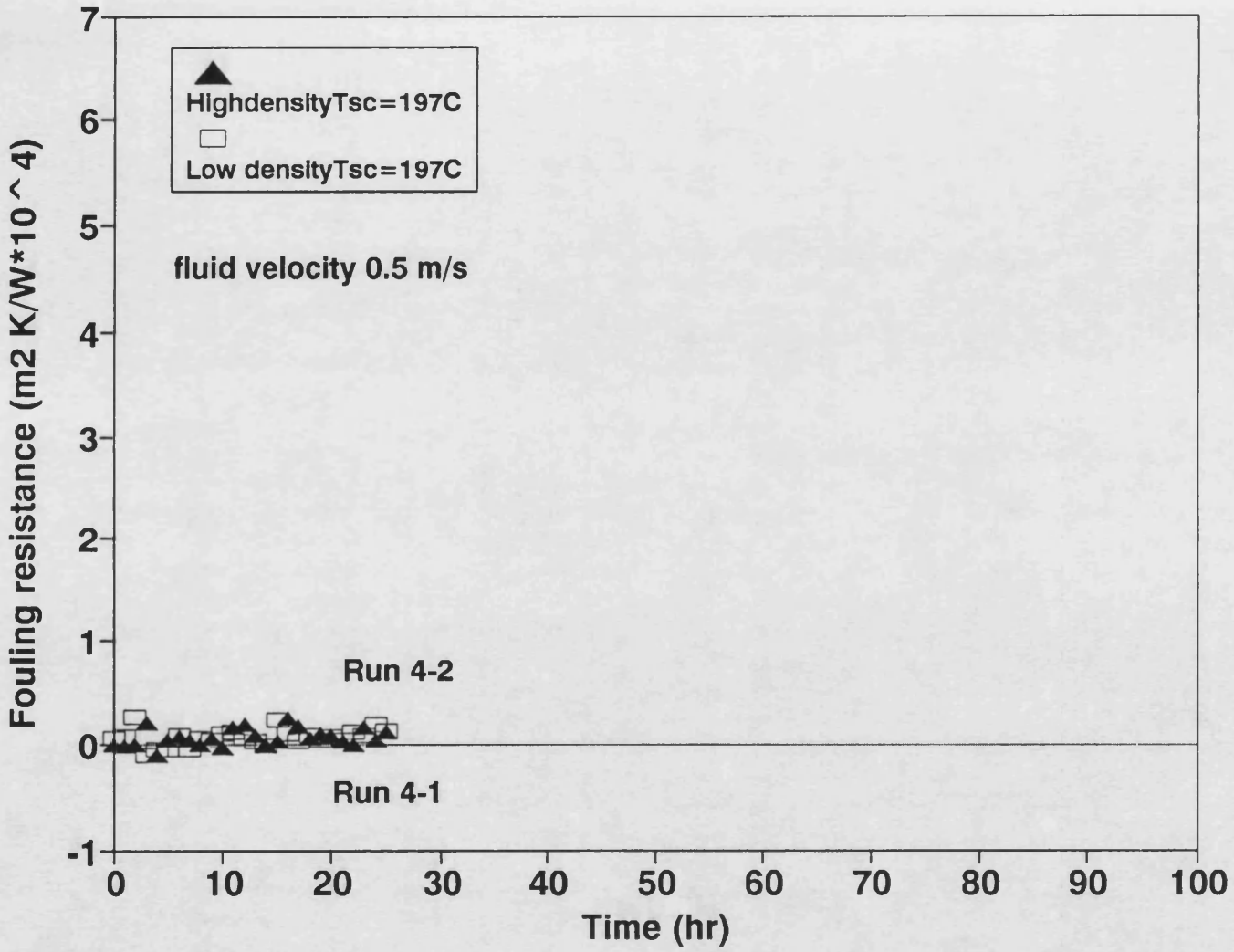

Figure 3.22 Fouling resistance - time data for Run 4

Run 5 (Effect of insert density)

Run 5 was carried out with the same heat flux of 76.2 kWm^{-2} and the same flow velocity of 0.5 ms^{-1} in the two test sections. Therefore, the initial surface temperature of the tube fitted with the high density insert (186°C) was lower than that with the low density insert (197°C). The results are shown in Figures 3.23 and 3.24. Unlike Run 4-2 (Figure 3.22), the tube with the low density insert (Run 5-2) started fouling almost immediately. The fouling resistance for the tube fitted with the high density insert was lower than that for the tube fitted with the lower density insert. Induction periods were not observed. Extrapolation of the data shown in Figure 3.24 suggests that the final R_f with an insert fitted would be considerably lower than the value recommended for design (Table 3.8) even with the low average velocity of 0.5 ms^{-1}.

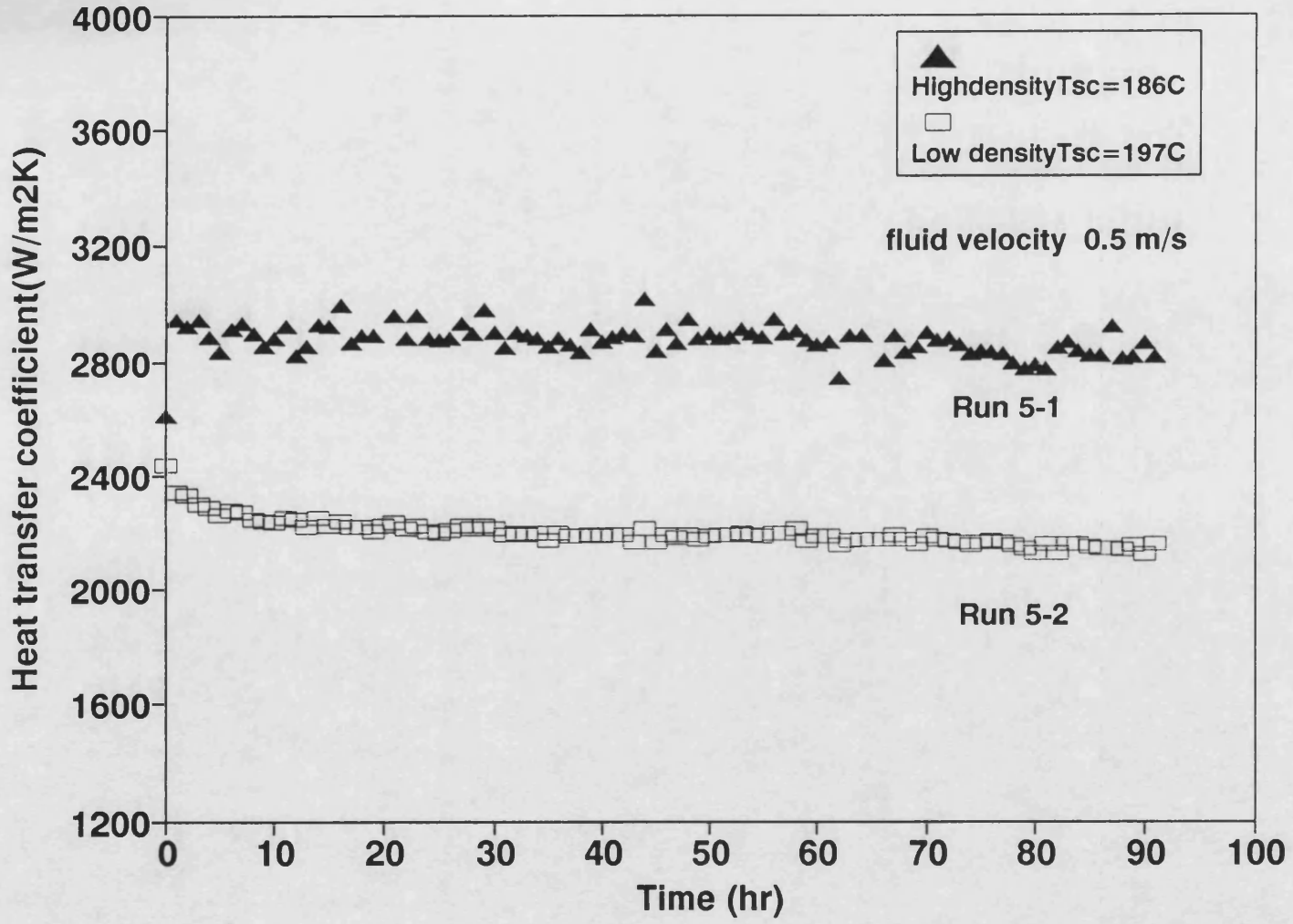

Figure 3.23 Thermal coefficient Hi for Run 5

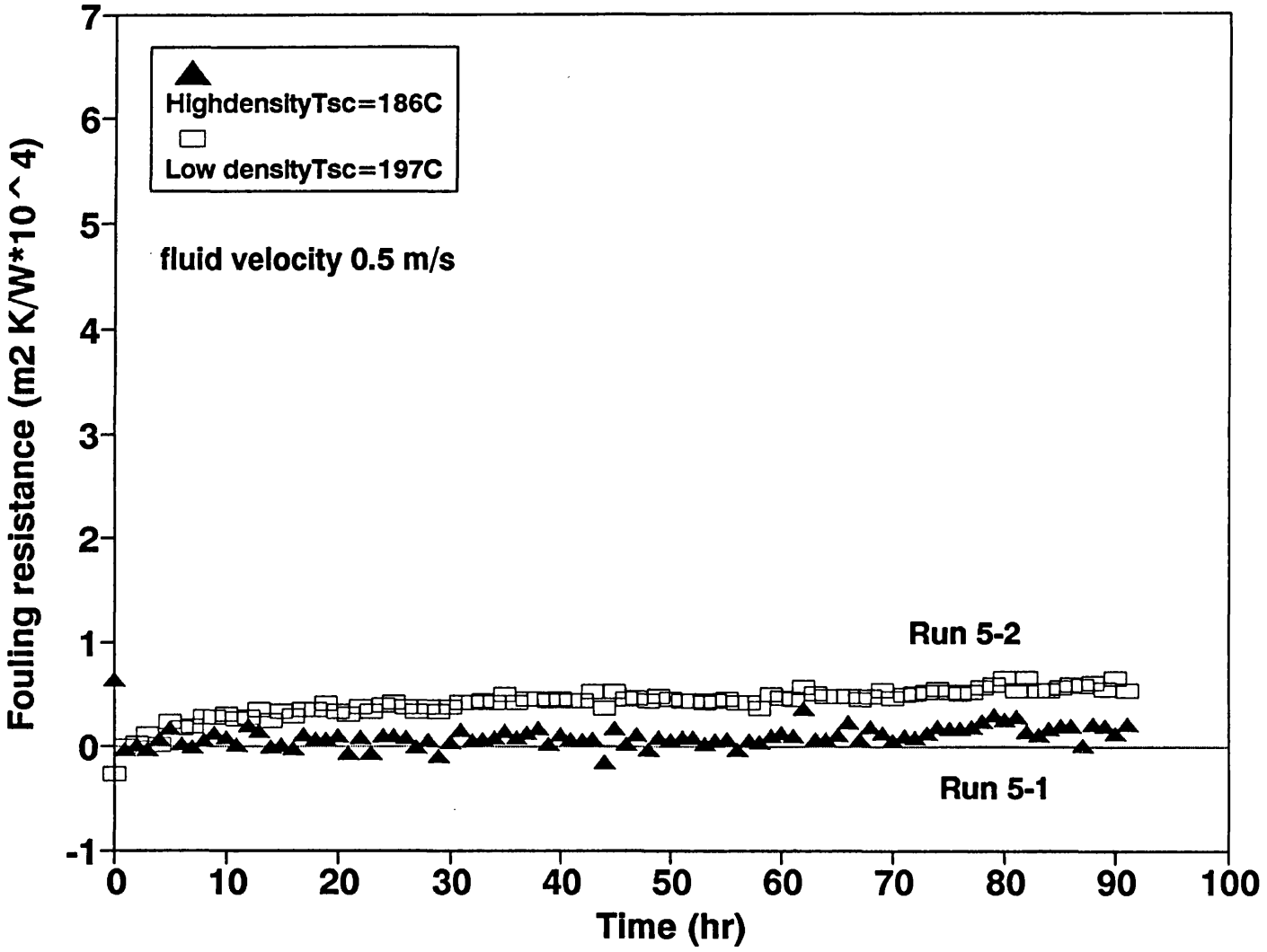

Figure 3.24 Fouling resistance - time data for Run 5

Run 6 (Effect of insert density)

Run 6 was an attempt to repeat Run 4 but with a temporary measure for ensuring a good heat sink for the cable heater elements. This measure proved to be unsuccessful and the experiment was stopped at 19 hours. Despite this difficulty Figures 3.25 and 3.26 show that fouling had commenced in the tube fitted with the low density insert but hardly at all in the tube fitted with the high density insert. Since the initial surface temperatures are equal, there is some evidence that the additional turbulence with the high density insert is capable of reducing the fouling rate. Comparison of Figures 3.24 and 3.26 for Runs 5-2 and 6-2 shows good reproducibility up to 19 hours for the test section fitted with the low density insert operated at identical conditions of flow velocity, initial surface temperature and heat flux.

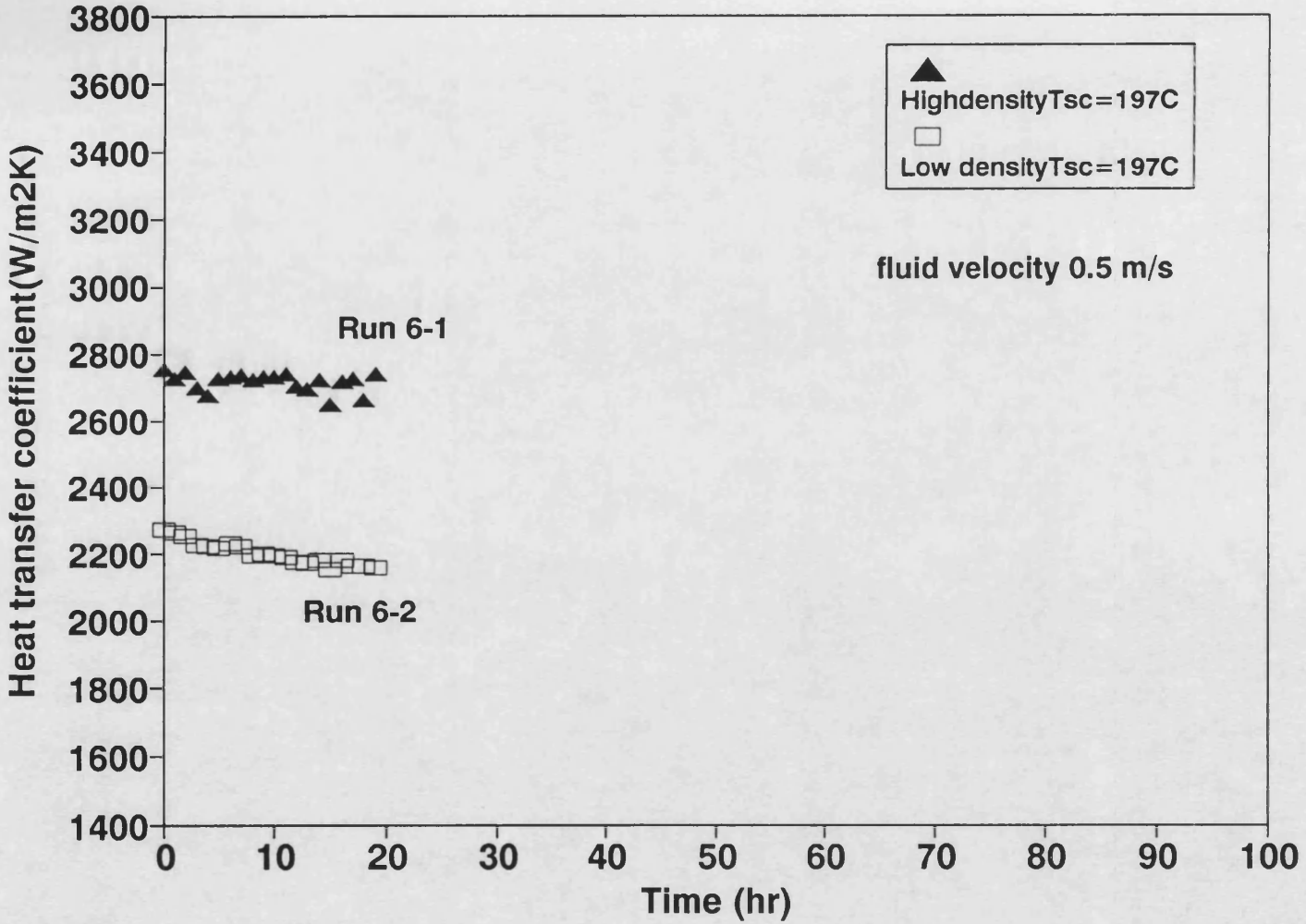

Figure 3.25 Thermal coefficient Hi for Run 6

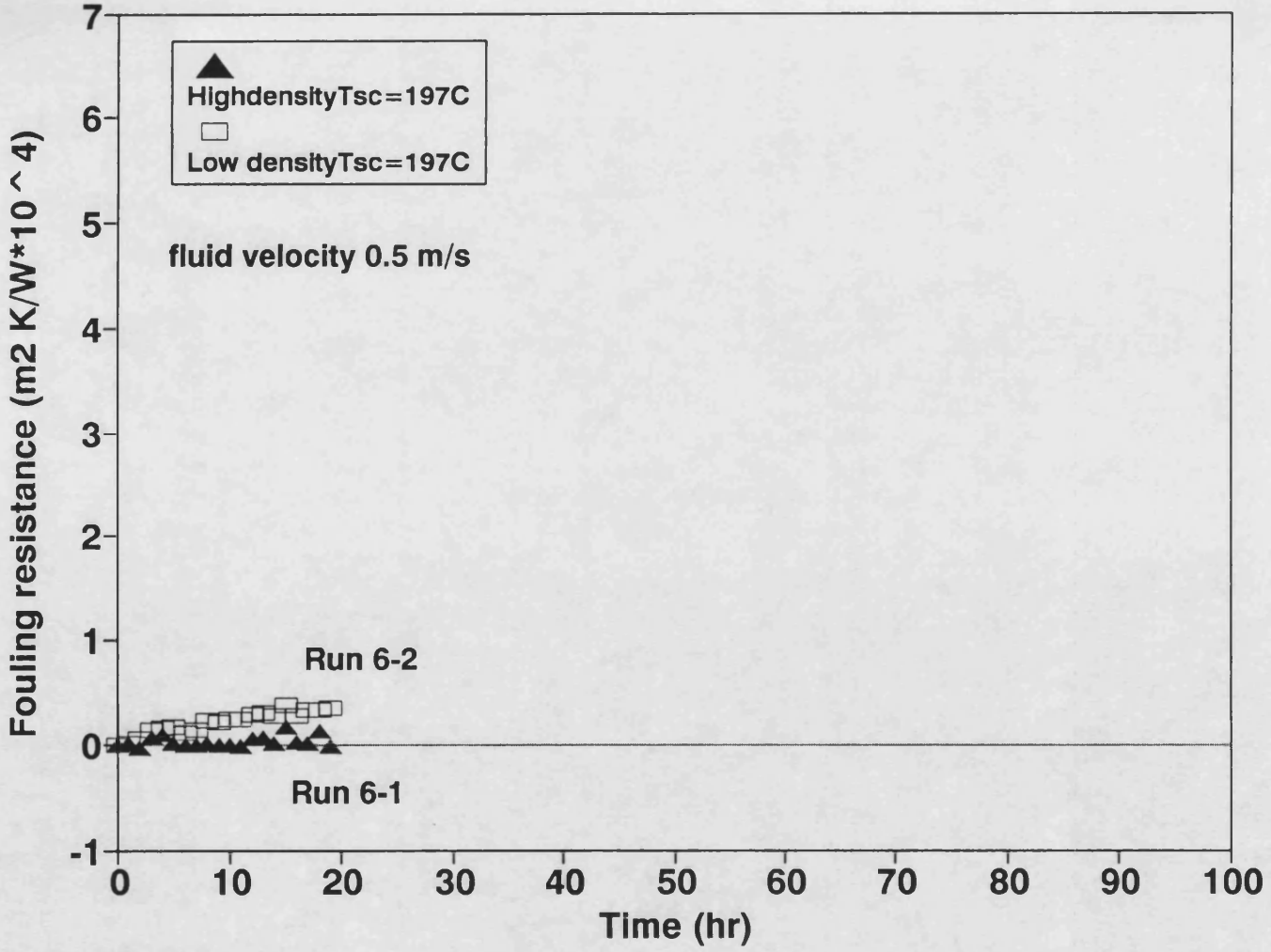

Figure 3.26 Fouling resistance - time data for Run 6

Run 7 (Effect of insert density)

Run 7 was a repeat of Runs 4 and 6 but with the new test sections. The results are shown in Figures 3.27 and 3.28. The experiment could now be carried out continuously for 90 hours. Induction periods were not found in spite of the first use of the new test sections. Although the initial surface temperatures (197°C) and the flow velocities (0.5 ms^{-1}) were the same, the initial fouling rate for the tube fitted with the high density insert was approximately 3.5 times lower than that for the tube fitted with the low density insert. In addition, the asymptotic fouling resistance for the tube fitted with the high density insert was about 25% of that for the tube fitted with the low density insert and about 2% of the TEMA design value (see Table 3.8).

Figures 3.26 and 3.28 show that the fouling resistance-time plot for Runs 6-1 and 6-2 compare well with the early portions of the curves for Runs 7-1 and 7-2. From this preliminary inspection of the results, it seems that, for otherwise identical operating conditions, the high density insert is more capable of reducing the fouling rate than the low density one. Possible mechanisms for this are discussed in Section 3.2.9.

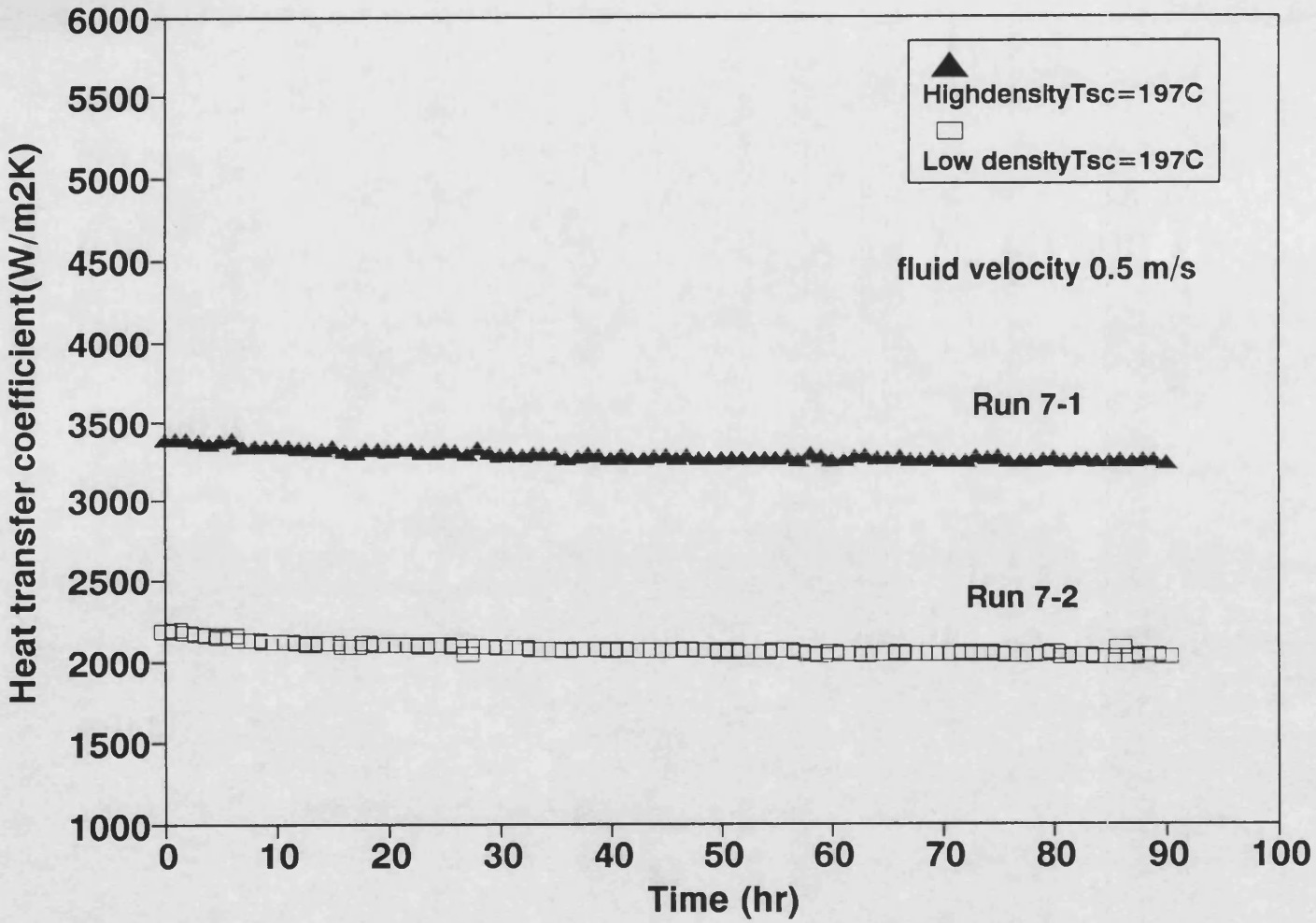

Figure 3.27 Thermal coefficient Hi for Run 7

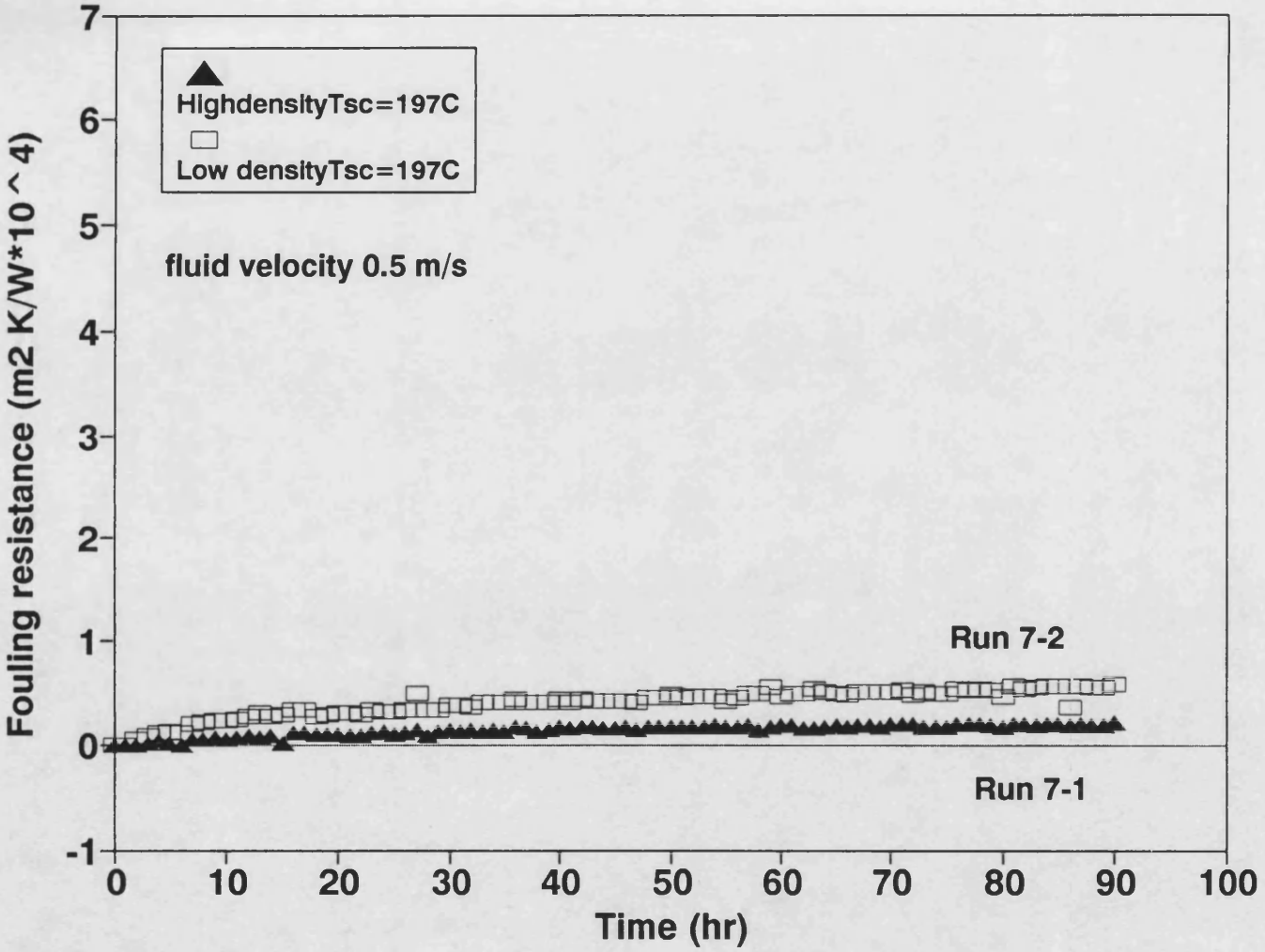

Figure 3.28 Fouling resistance - time data for Run 7

Run 8 (Effect of low density insert)

Run 8 was similar to Run 2 but with lower surface temperatures. The results are shown in Figures 3.29 and 3.30. There was little difference in fouling resistance between the two test sections and low asymptotic fouling resistances were obtained. These results may appear on first inspection to contradict those from Run 2 (Figures 3.17 and 3.18) However, it is important to note two differences. Firstly, the initial surface temperatures for Run 8 were 19°C lower at 197°C than those for Run 2 (216°C). Secondly, for reasons discussed in Section 3.1.2, the flow regime was believed to be convective in Run 8 rather than subcooled nucleate boiling in Run 2.

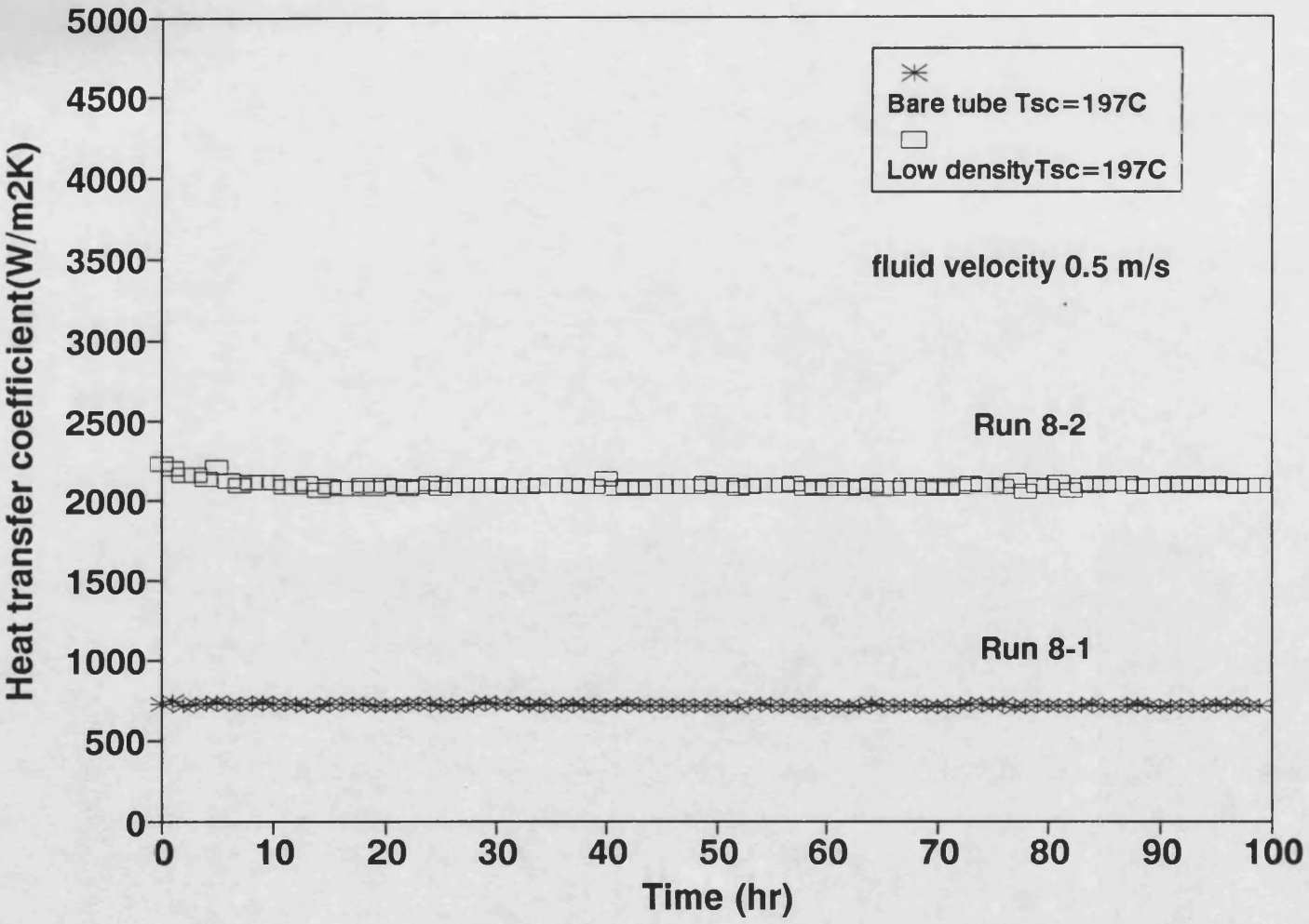

Figure 3.29 Thermal coefficient Hi for Run 8

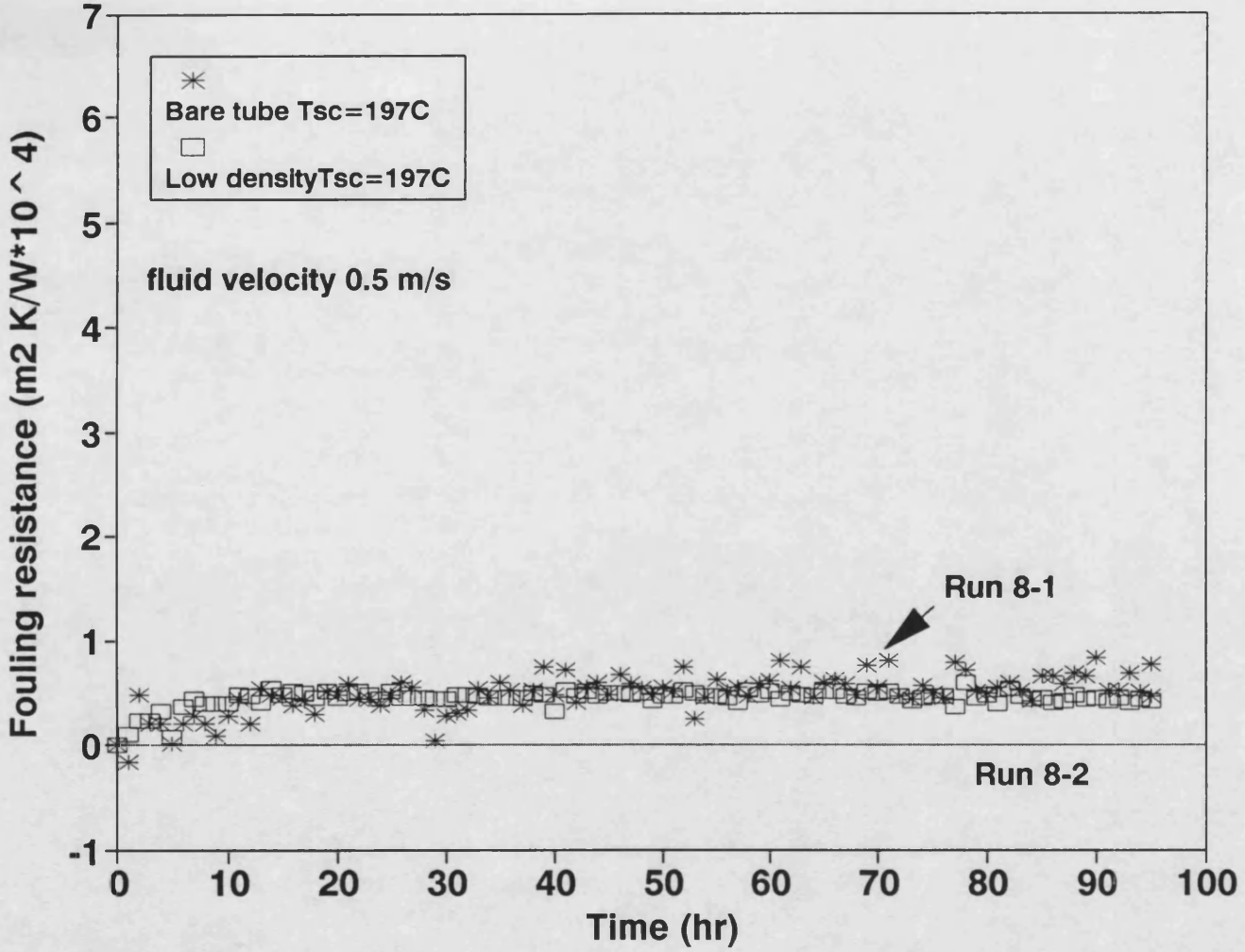

Figure 3.30 Fouling resistance - time data for Run 8

Run 9 (Effect of fluid velocity with bare tubes)

Run 9 was carried out to evaluate the effect of flow velocity in bare tubes. The results are shown in Figures 3.31 and 3.32. The flow velocities through test sections 1 and 2 were set at 0.5 ms^{-1} and 1.1 ms^{-1} respectively. The surface temperature in both cases was 217°C, this being believed to be high enough to cause subcooled nucleate boiling to occur (see section 3.1.2). However for the tube having the higher velocity (Run 9-2), the heat transfer coefficient was found to be only slightly higher than that with flow purely in the convective heat transfer regime. Thus to some extent nucleate boiling may have been suppressed by the higher flow velocity.

Figure 3.32 shows that asymptotic fouling resistances were obtained in both test sections and also shows that the use of the higher flow velocity substantially reduced the fouling rate and consequently the fouling resistance at any time. The effect of flow velocity on the initial fouling rate and the value of the asymptotic fouling resistance will be discussed in more detail in Section 3.2.7.

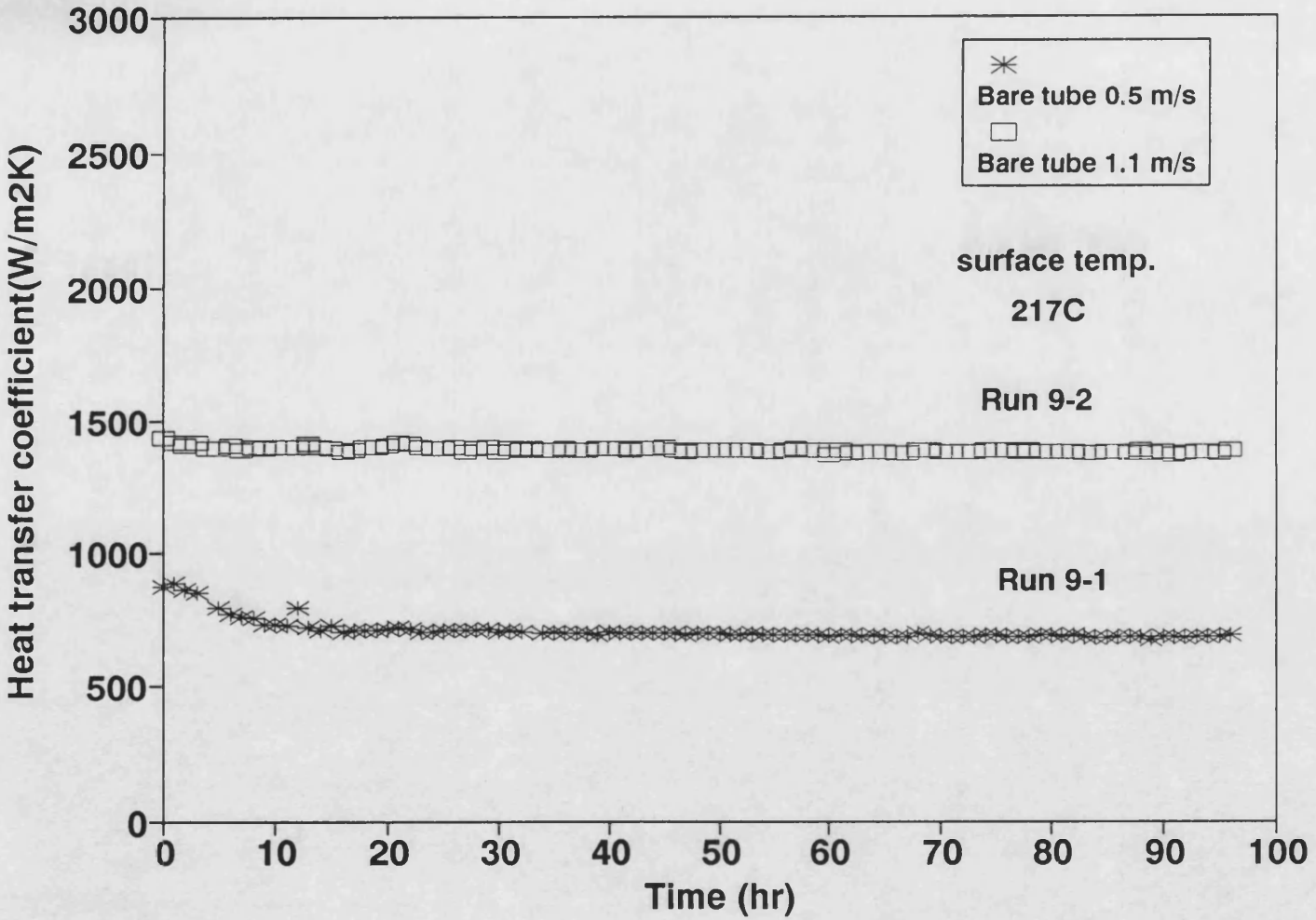

Figure 3.31 Thermal coefficient Hi for Run 9

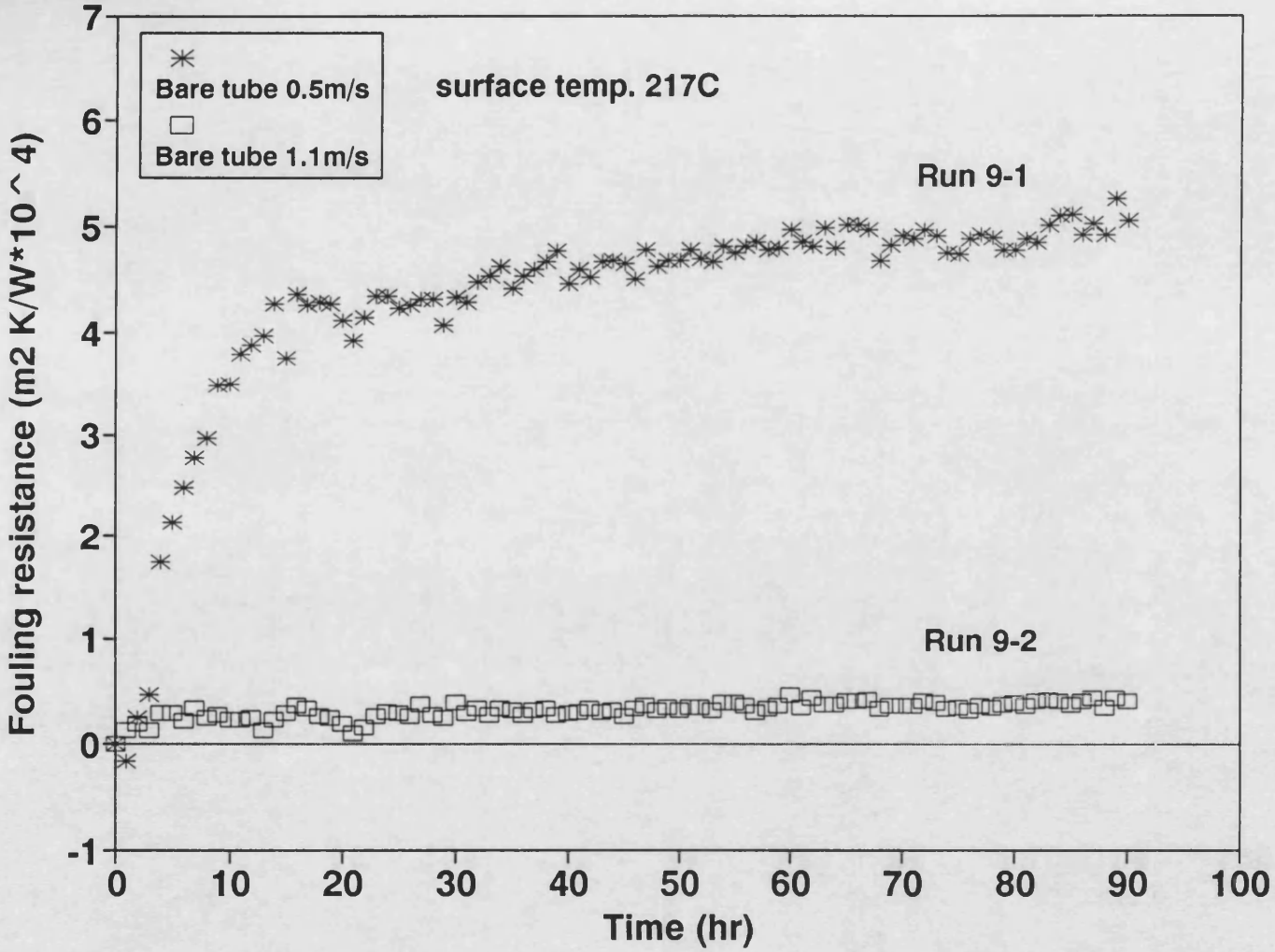

Figure 3.32 Fouling resistance - time data for Run 9

Run 10 (Effect of fluid velocity with low density inserts)

Run 10 was carried out to determine the effect of flow velocity when nominally identical low density inserts were present in the two test sections. The results are shown in Figures 3.33 and 3.34. The flow velocities through test sections 1 and 2 were set initially at 1.1 ms^{-1} and 0.5 ms^{-1} respectively. At 64 hours the flow velocities were exchanged, that is, the velocity of the fluid through test section 1 was decreased from 1.1 ms^{-1} to 0.5 ms^{-1} and the flow velocity through test section 2 was increased from 0.5 ms^{-1} to 1.1 ms^{-1}. After exchanging the velocities the experiment was continued for a further 30 hours.

For the tube having had the lower velocity (test section 2), fouling had commenced and reached an asymptotic value by about 40 hours. Thus after increasing the flow velocity to 1.1 ms^{-1}, the heat transfer coefficient (H_i which incorporates both the film coefficient h_i and the fouling resistance R_f) was lower than that of test section 1 having had the higher velocity (1.1 ms^{-1}). For test section 1, after decreasing the velocity, the heat transfer coefficient was almost equal to the initial heat transfer coefficient of test section 2 having had the lower flow velocity (0.5 ms^{-1}).

Figure 3.34 shows that a high flow velocity is beneficial in reducing the fouling resistance for tubes fitted with low density inserts as well as for the bare tubes (as shown for Run 9 in Figure 3.32). After exchanging the flow velocities, the fouling resistance for test section 2 gradually decreased as expected due to the imposition of the higher velocity. In addition, for test section 1 fouling began to take place

after the reduction in velocity but the rate of fouling seemed to be somewhat lower than that in the initial stages for test section 2 operated with a velocity of 0.5 ms^{-1}. This might indicate that some chemical which takes part in the fouling process could have become depleted during the fouling experiment. Perhaps under certain circumstances, the levelling-out of a fouling resistance could be due to the depletion of foulants and/or reactants in the closed recirculation system. This is discussed further in section 3.2.2.

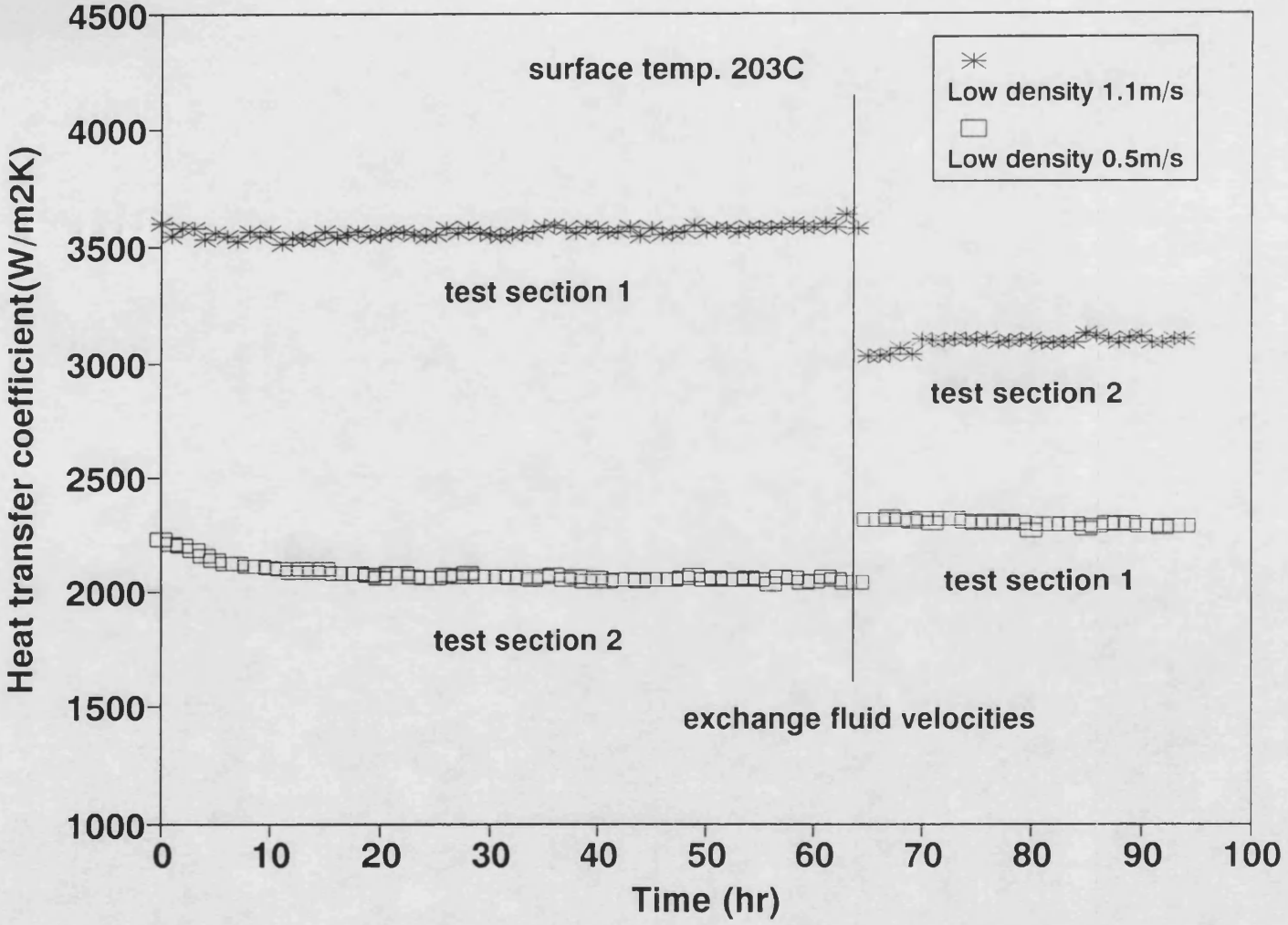

Figure 3.33 Thermal coefficient Hi for Run 10

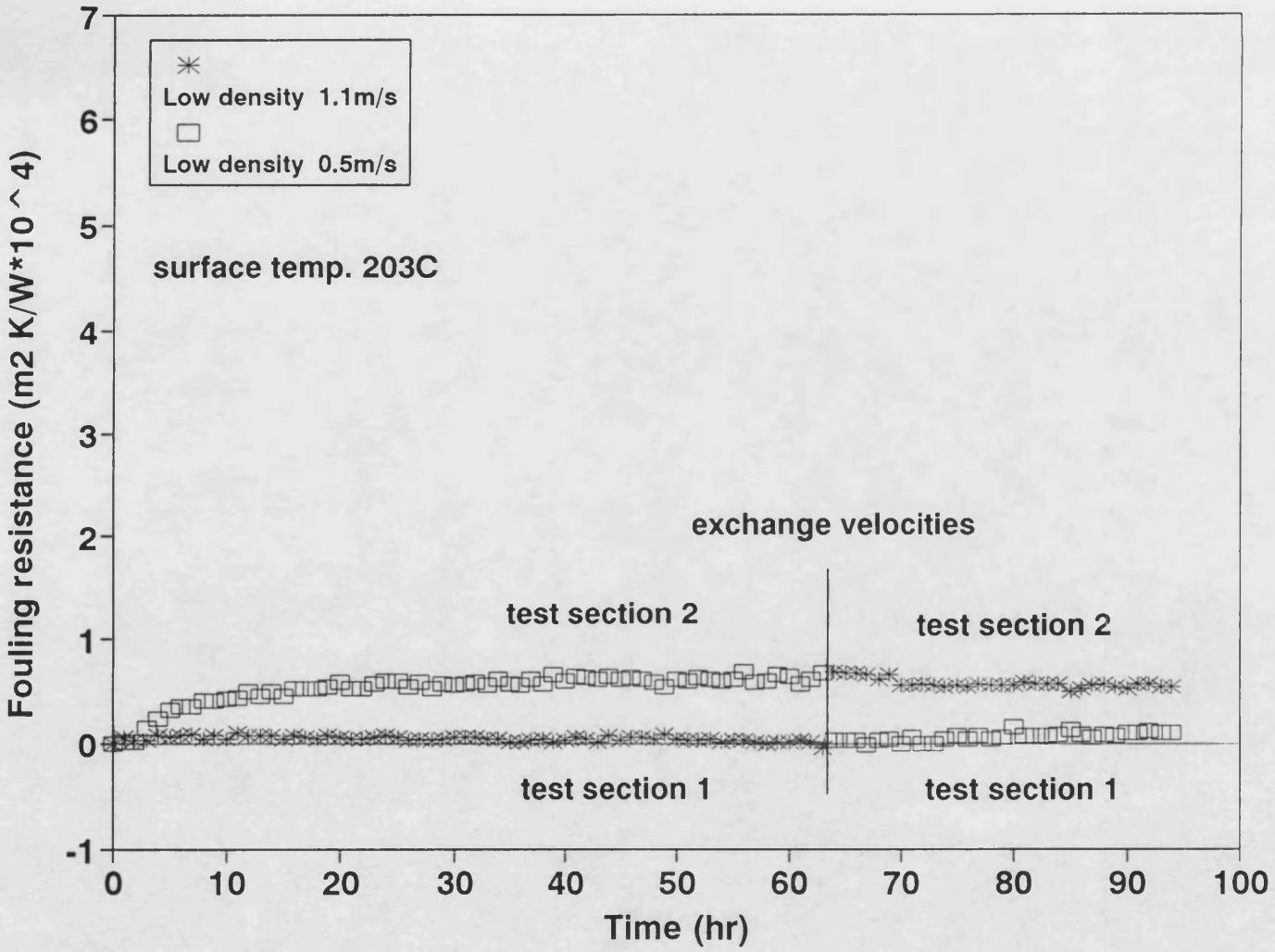

Figure 3.34 Fouling resistance - time data for Run 10

Run 11 (Effect of surface temperature with bare tubes)

Run 11 was carried out to evaluate the dependency of fouling in bare tubes on the surface temperature. The results are shown in Figures 3.35 and 3.36. The velocity in both test sections was 0.5 ms^{-1}. The initial surface temperatures for test sections 1 and 2 were set at 226°C and 237°C respectively. These initial temperatures were high enough to cause nucleate boiling to occur. As shown in Figure 3.36, substantial fouling occurred and the higher surface temperature in test section 2 led to greater fouling as expected. The fouling resistance in test section 1 reached an asymptotic value.

The effect of surface temperature is explored further in Section 3.2.6.

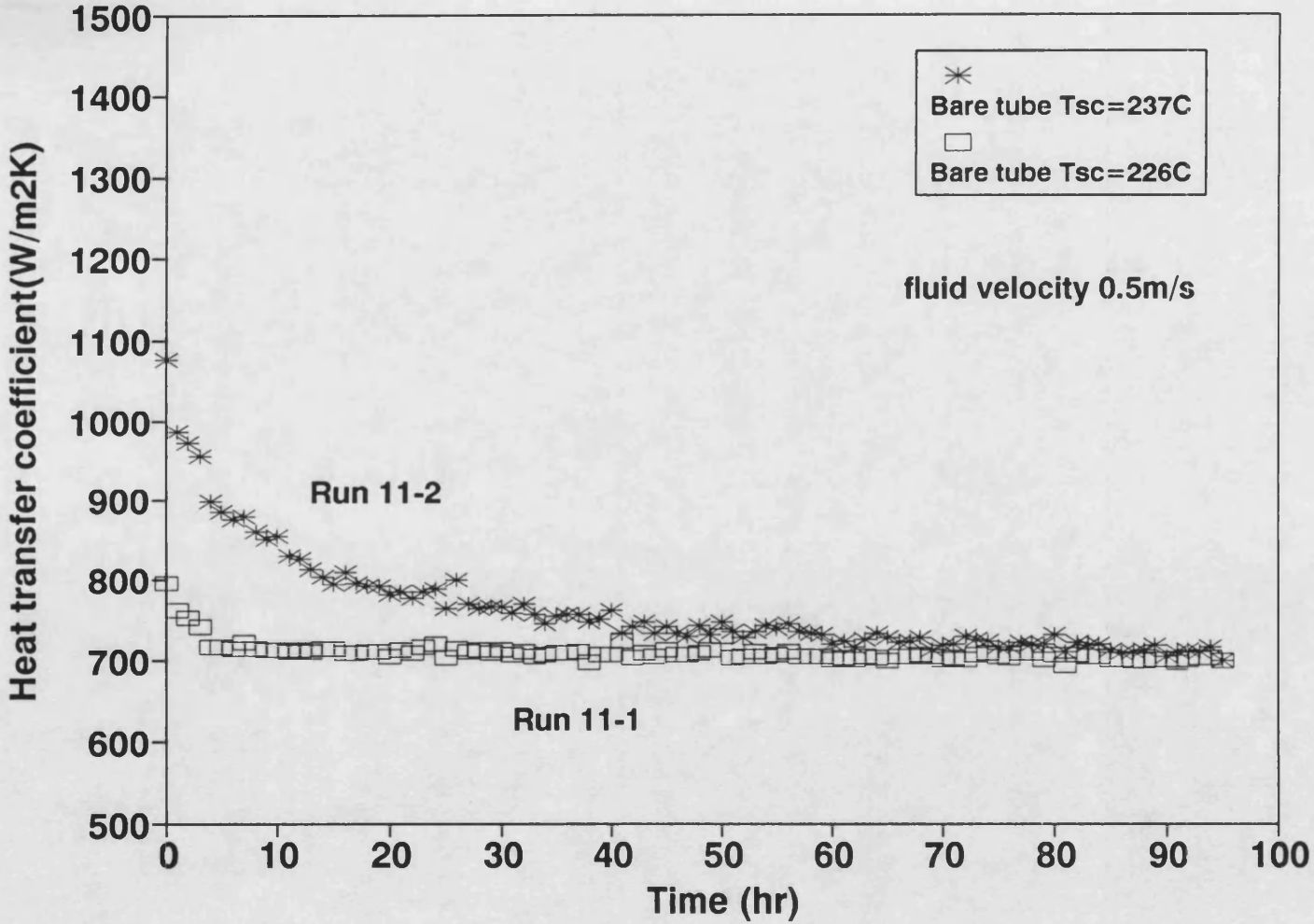

Figure 3.35 Thermal coefficient Hi for Run 11

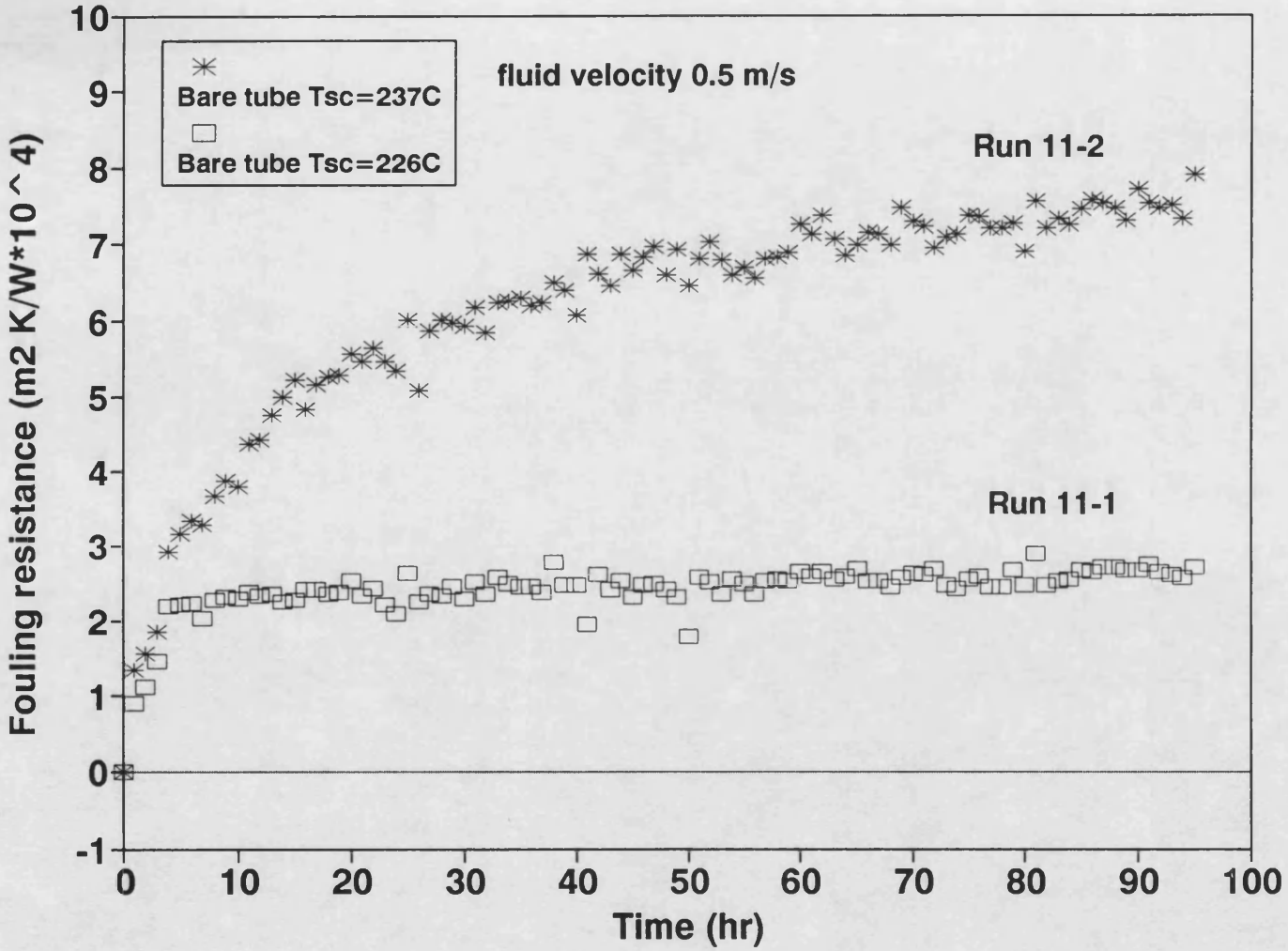

Figure 3.36 Fouling resistance - time data for Run 11

Run 12 (Effect of surface temperature with low density inserts)

Run 12 was carried out to determine the effect of surface temperature for tubes fitted with low density inserts. The velocity in both test sections was 0.5 ms^{-1}. The initial surface temperatures for test sections 1 and 2 were set at 224°C and 211°C respectively. Figure 3.37 shows that despite the same velocity, the initial heat transfer coefficient for test section 1 having the higher surface temperature (224°C) was about 11 percent higher than that for test section 2 having the lower surface temperature (211°C). Figure 3.38 shows that fouling resistances for both test sections were very low and reached asymptotic values within about 20 hours. In addition the fouling resistance for test section 1(having the higher surface temperature and the higher heat transfer coefficient) was lower at any time than that for test section 2 (having the lower surface temperature and the lower heat transfer coefficient).

Possible reasons for these seemingly anomalous results are as follows:-

(1) The exact position of the insert in each test section is likely to be different. As found by Shalhi (1993), the position of an insert can affect the local heat transfer coefficient. Thus local positioning could conceivably also affect the local fouling rate.

(2) Since the values of the fouling resistance in the two test sections are very small and the difference between them is also very small, it is possible that the anomalous result is due in part to errors involved in calculating the

fouling resistances.

Whatever the reason, it seems for this Run at least, that surface temperature has little effect when an insert is present. The effect of surface temperature is discussed more fully in Section 3.2.6

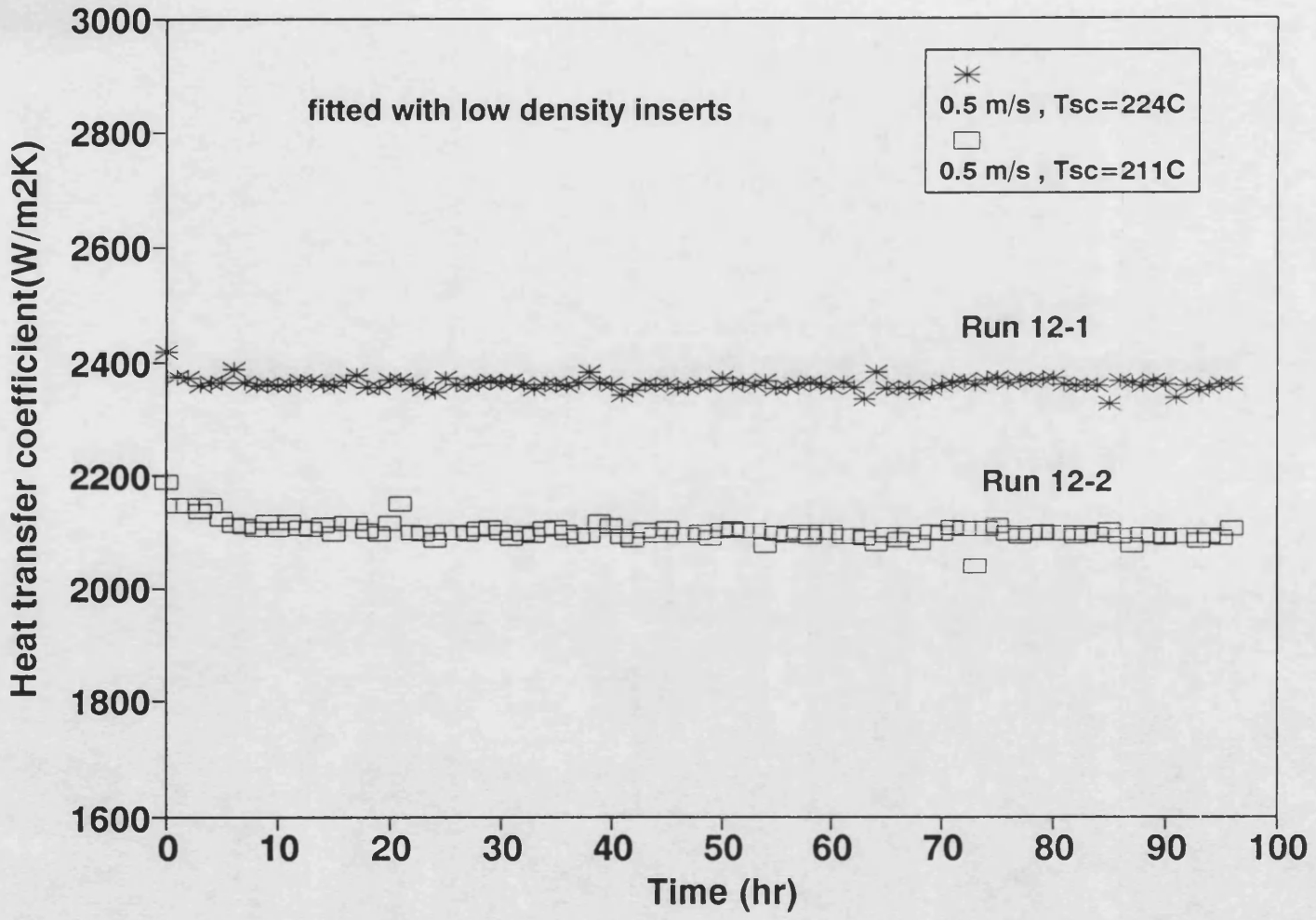

Figure 3.37 Thermal coefficient Hi for Run 12

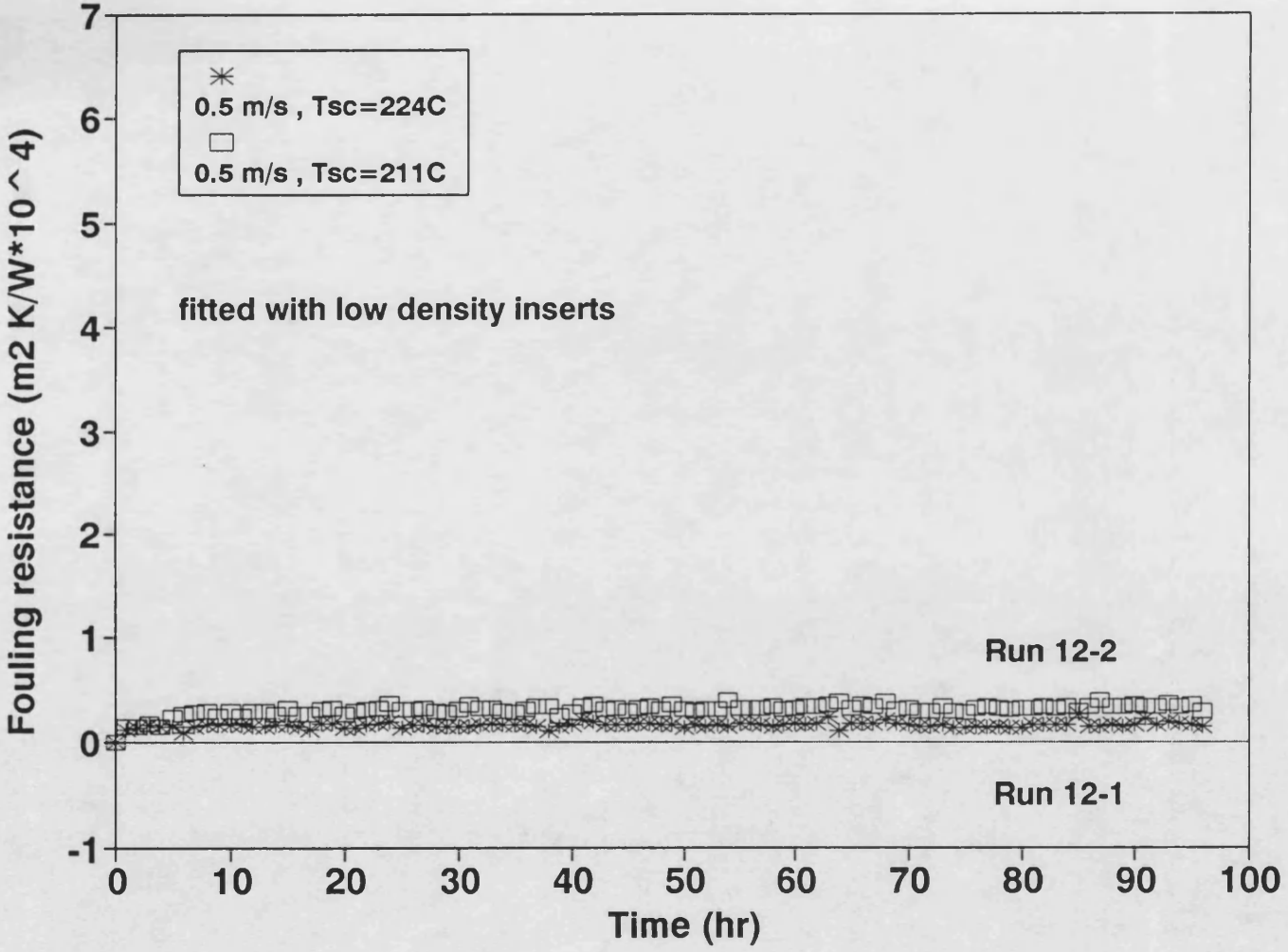

Figure 3.38 Fouling resistance - time data for Run 12

Run 13 (Effect of low density insert)

Run 13 was a further comparison of bare tube against that containing a low density insert with a velocity of 0.5 ms^{-1} (see Runs 2 and 8) but with a higher surface temperature of 239°C. The shapes of the heat transfer coefficient and the fouling curve for Run 13-2 (with the insert) shown in Figures 3.39 and 3.40 respectively are quite different from those for Runs 2-2 and 8-2 and indeed for any Runs described previously. For Run 13-2 the fouling resistance initially increased rapidly, reached a maximum and then decreased slowly and eventually levelled out. One important difference between Runs 13-2 and 2-2 was the occurrence of subcooled nucleate boiling in the latter. This matter is discussed further in Section 3.2.5.

For Run 13 the initial fouling rate with the insert in place was about 2.6 times higher than that for the bare tube. Compared with previous results, this is somewhat anomalous. Since the HiTRAN insert is capable of promoting rates of mass transfer as well as heat transfer, thought was given initially to whether the rate of the deposition process had become controlled by the mass transfer of species to the surface at the relatively high temperature of 239°C. Using the analogy between heat transfer and mass transfer and assuming that heat transfer by conduction along insert wire loops is negligible (see Appendix 4), then the ratio of foulant precursor transfer to the wall with the insert to that without the insert was estimated to be about 2.9, lending some support to the hypothesis that perhaps the fouling process had become governed by mass transfer of foulants. This aspect is discussed further in Section 3.2.8.2.

A more likely explanation of the fouling curve for Run 13-2 is that some particulate material present in the flow system was deposited very early in the Run and removed gradually by the turbulent flow created by the presence of the insert. Thus the initial fouling was perhaps not caused by a chemical reaction mechanism but purely by a purely physical mechanism. The gradual reduction in fouling to a low, probably asymptotic, value is a particularly useful finding in terms of the value of the insert in reducing fouling.

In the testing of the model which is developed in Section 3.2.10, special consideration is given to the data from Run 13 in Section 3.2.11.

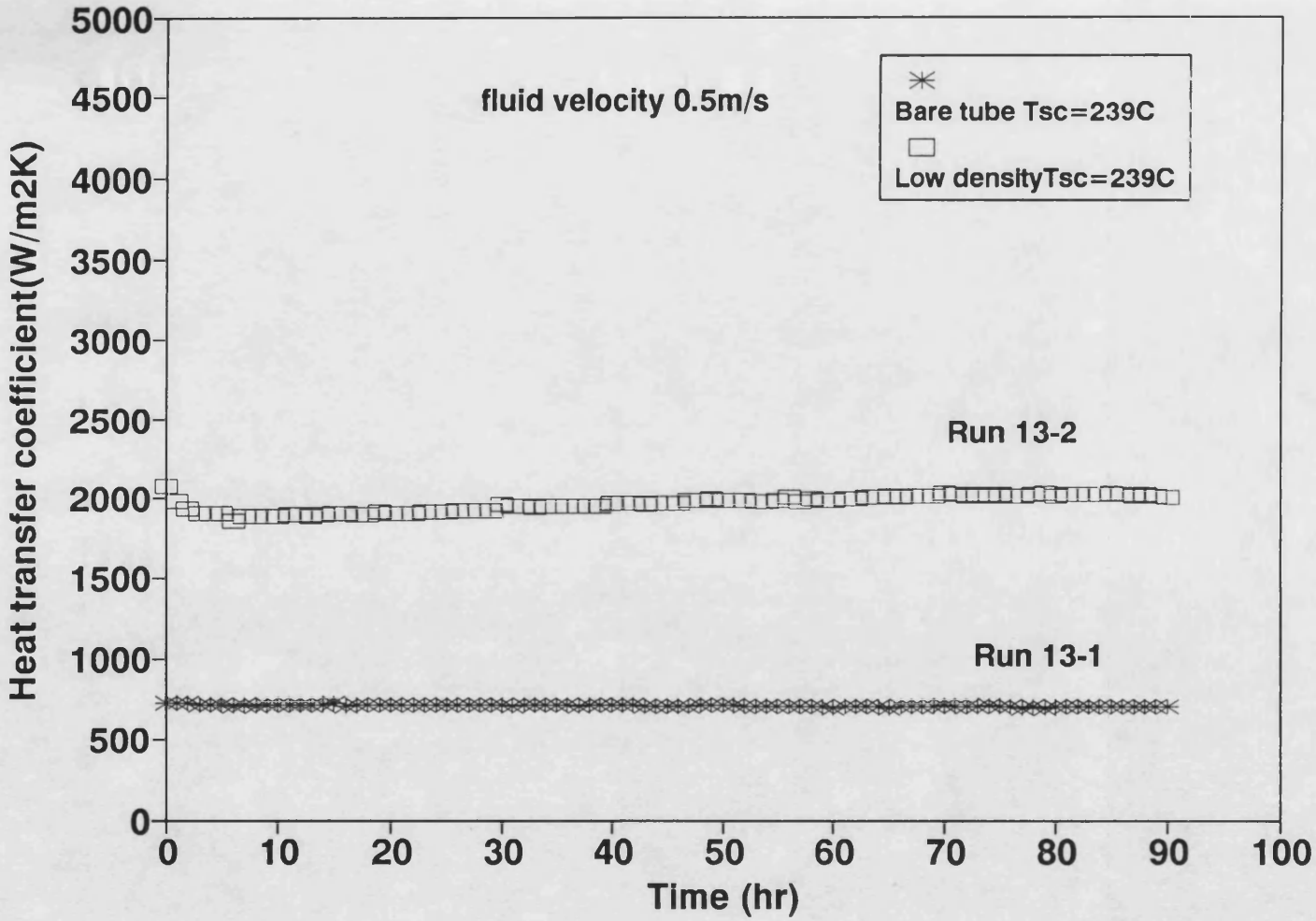

Figure 3.39 Thermal coefficient Hi for Run 13

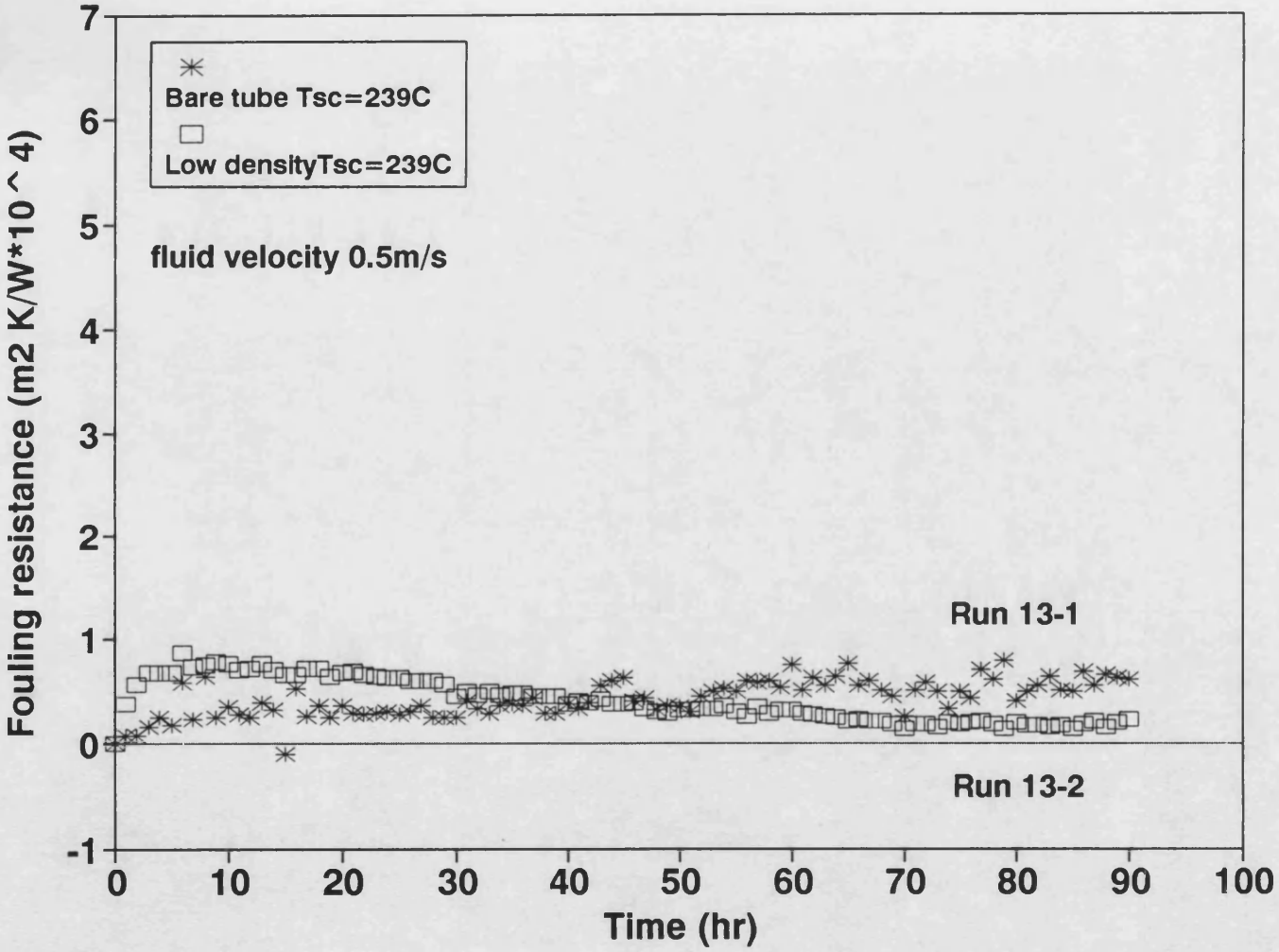

Figure 3.40 Fouling resistance - time data for Run 13

Run 14 (Effect of surface temperature with bare tubes)

Run 14 was similar to Run 11 but with a larger difference in initial surface temperature between the two test sections. The results are shown in Figures 3.41 and 3.42. Subcooled nucleate boiling is caused to occur at the higher surface temperature, set to be 254°C, in test section 1, but not at the lower surface temperature, set to be 217°C, in test section 2. Figure 3.42 shows that, as for Run 11, the higher surface temperature results in a higher fouling rate and a higher fouling resistance at any time.

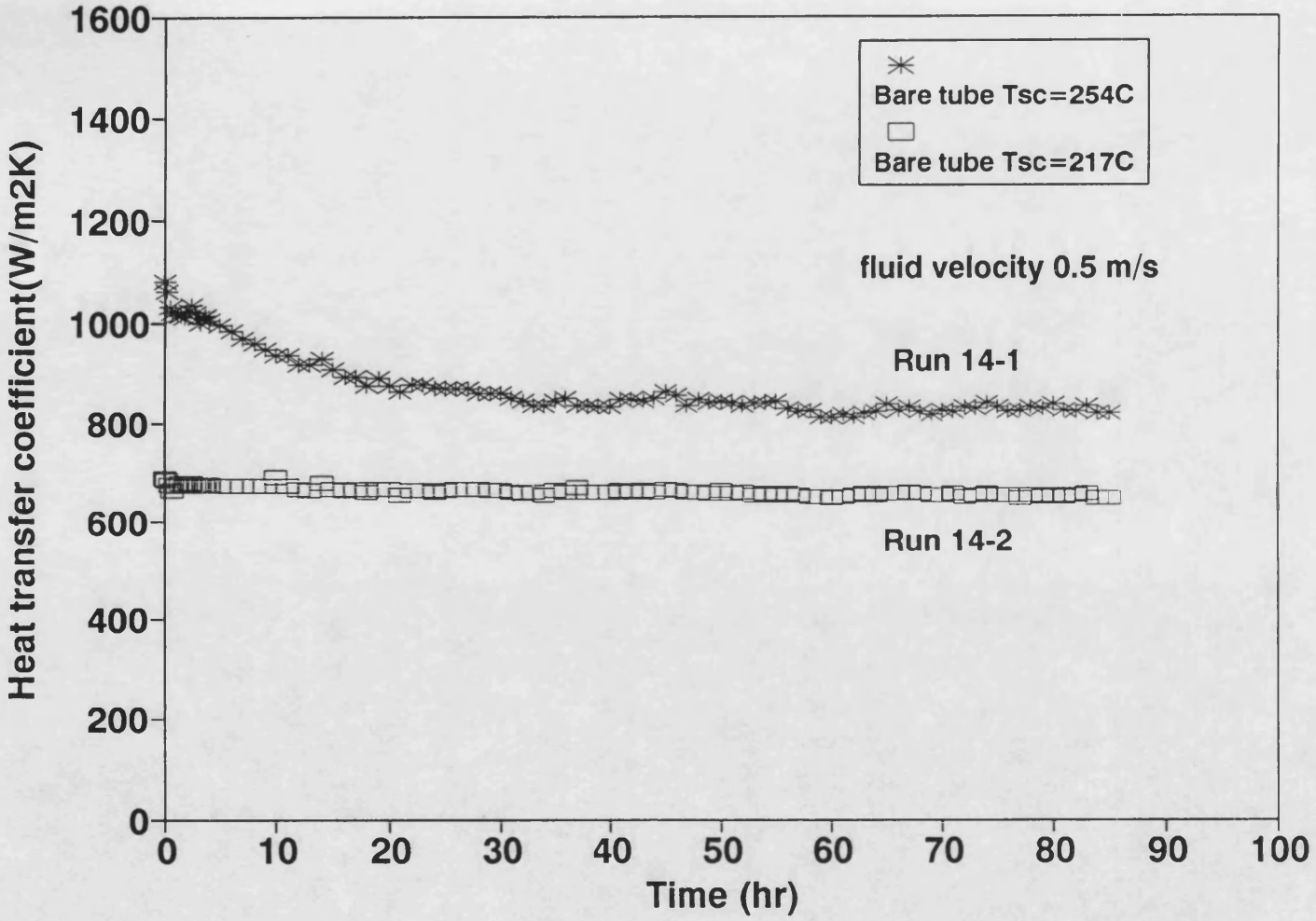

Figure 3.41 Thermal coefficient Hi for Run 14

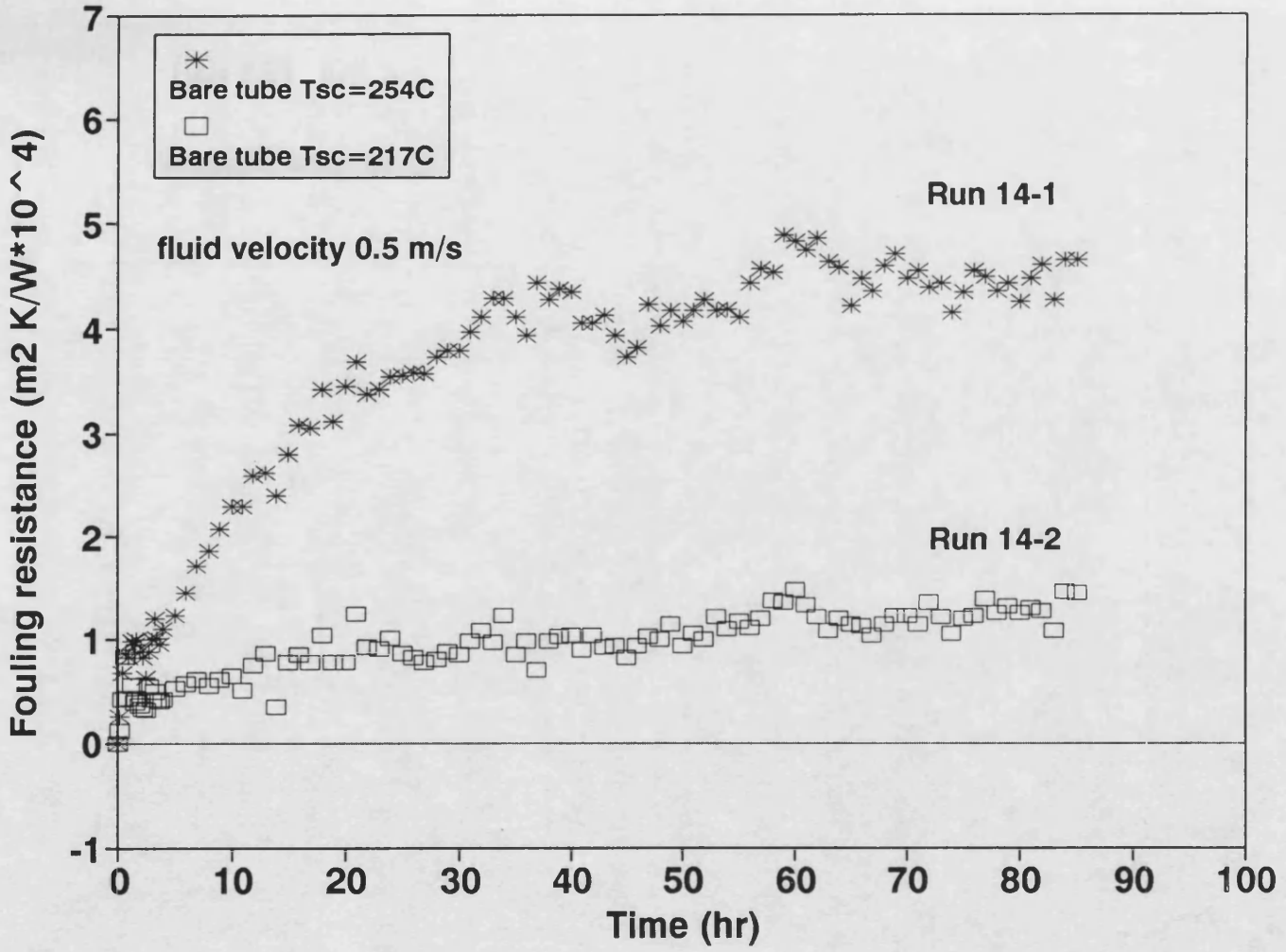

Figure 3.42 Fouling resistance - time data for Run 14

Run 15 (Effect of fluid velocity with bare tubes)

Run 15 was similar to Run 9 but with higher initial surface temperatures (239°C) in both test sections. As shown in Figure 3.43 for test section 2 having the higher fluid velocity (1.1 ms^{-1}) the heat transfer coefficient initially increased rapidly, reached a maximum and then gradually decreased. Corresponding fouling resistances are shown in Figure 3.44. For test section 2 (1.1 ms^{-1}), apparently negative fouling resistances were obtained. On the other hand positive values of fouling resistance were obtained for test section 1 (0.5 ms^{-1}).

Negative values of fouling resistance during the initial stages of fouling are not unusual and have been reported previously by several investigators (Bott and Gudmundsson (1978), Epstein (1981), Crittenden and Khater (1987), Shalhi (1993)). This event is generally thought to be caused by a small amount of deposit creating a rough surface in the early stages of a fouling process and thereby increasing the in-tube heat transfer coefficient to an extent sufficient to counteract the additional thermal resistance due to the deposit itself. The increase in in-tube film heat transfer coefficient also causes a reduction in the interfacial temperature between the deposit and the fluid, resulting in the probable decrease in the rates of chemical reactions which could be responsible for the fouling process.

Another possible mechanism for the negative values of fouling resistance is the occurrence of nucleation caused by dissolved gases leaving solution at the hot surface (Shalhi (1993)). Degassing on the heat transfer surface may cause

nucleation, resulting in an increase in the in-tube heat transfer coefficient. This can also cause a decrease in the interfacial temperature between the deposit and the fluid, leading to a probable reduction in the rate of fouling formed through chemical reactions. The negative fouling resistances seen for Run 15-2 could be due to one or both of these mechanisms.

For Run 9 (Figure 3.32) with the tube having the higher flow velocity (test section 2) negative values of fouling resistance were not observed. One important difference between Runs 9 and 15 was the presence of subcooled nucleate boiling in the former. This matter is discussed further in Section 3.2.5.

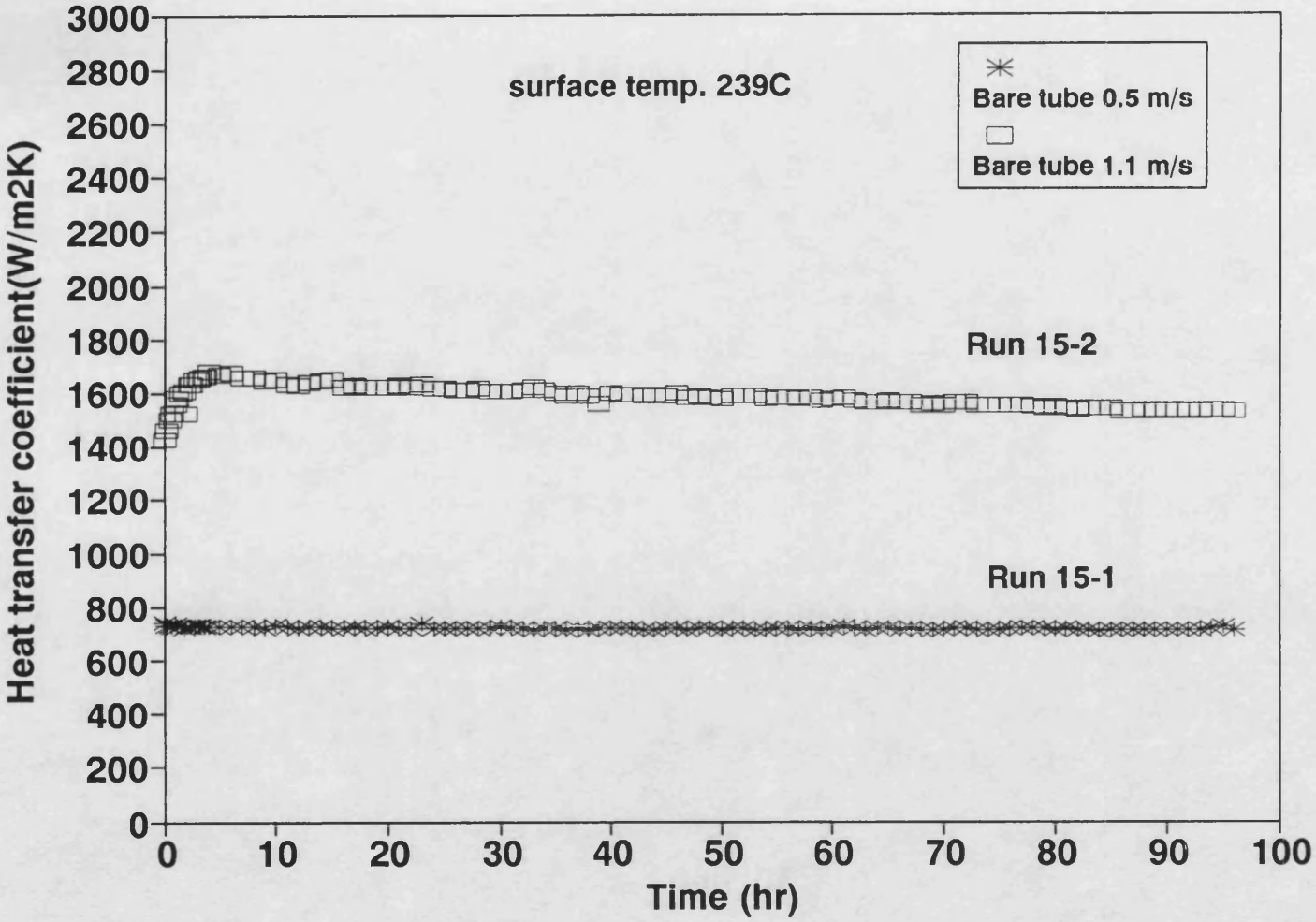

Figure 3.43 Thermal coefficient Hi for Run 15

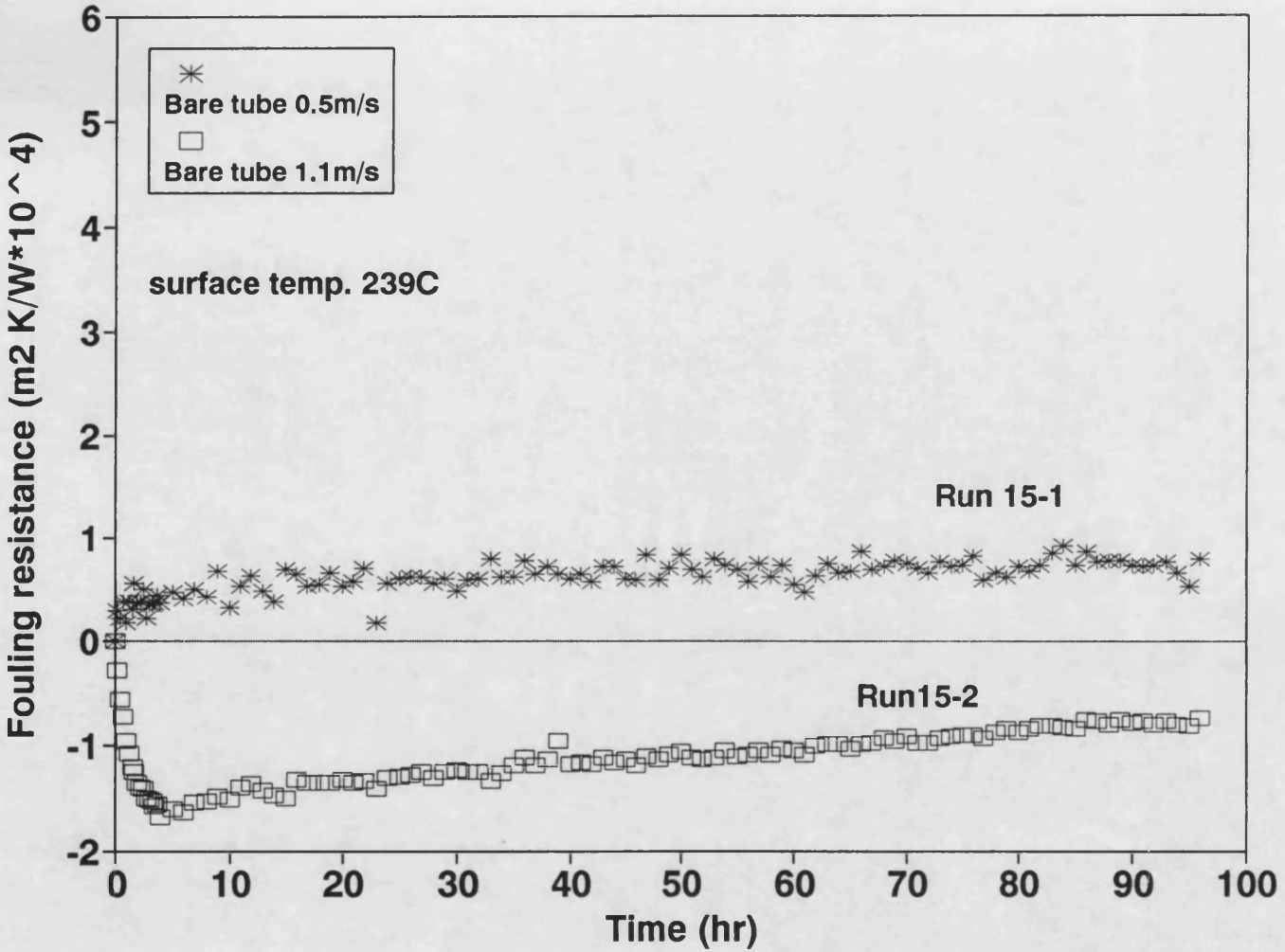

Figure 3.44 Fouling resistance -time data for Run 15

Run 16 (Effect of fluid velocity with low density inserts)

Run 16 was carried out to evaluate the effect of fluid velocity with low density inserts installed. The fluid velocities through test sections 1 and 2 were set at 0.7 ms^{-1} and 0.5 ms^{-1} respectively. The results are shown in Figures 3.45 and 3.46. Figure 3.46 shows the advantage of the higher flow velocity in reducing the fouling resistance, an aspect which is discussed more fully in Section 3.2.7.

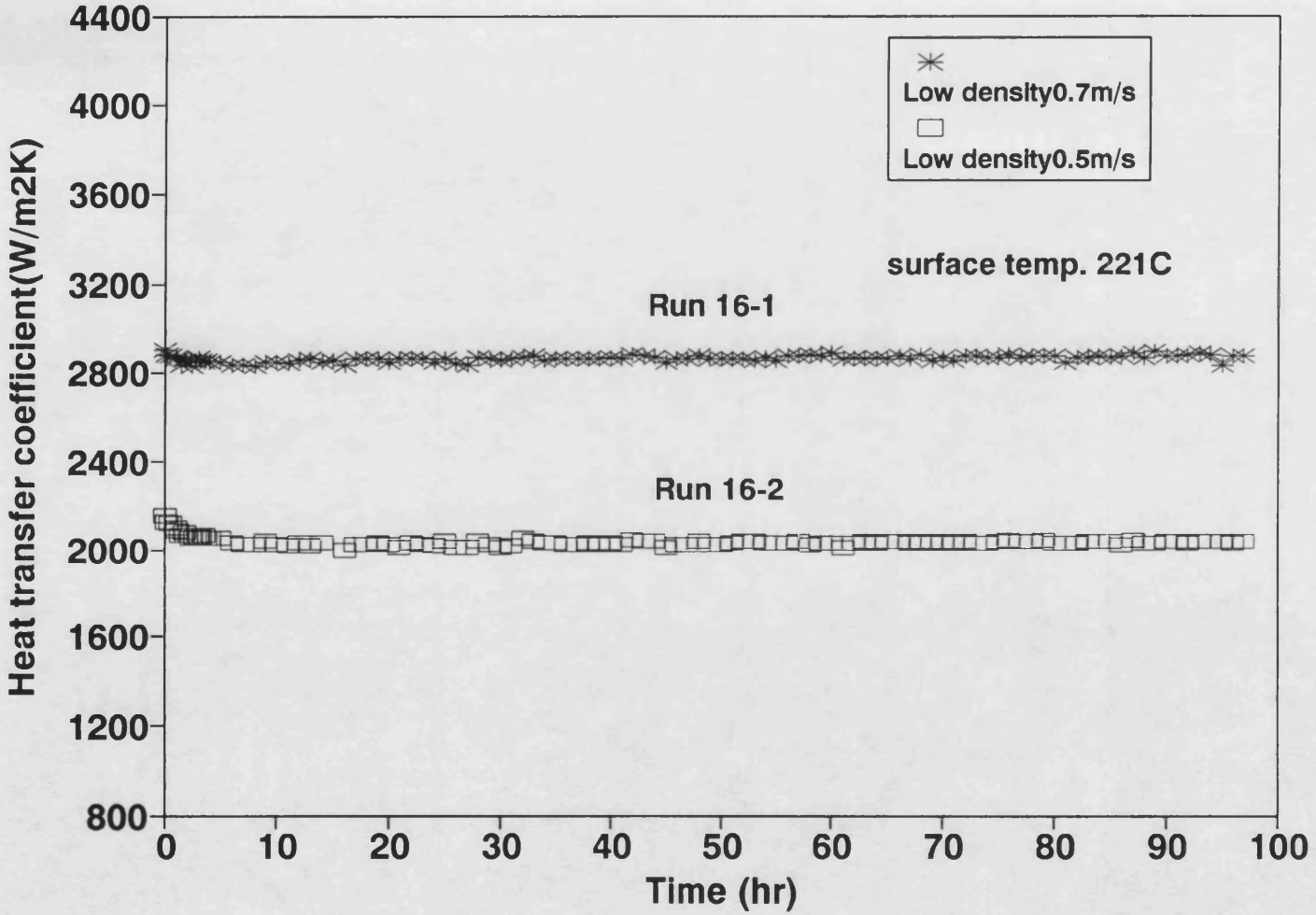

Figure 3.45 Thermal coefficient Hi for Run 16

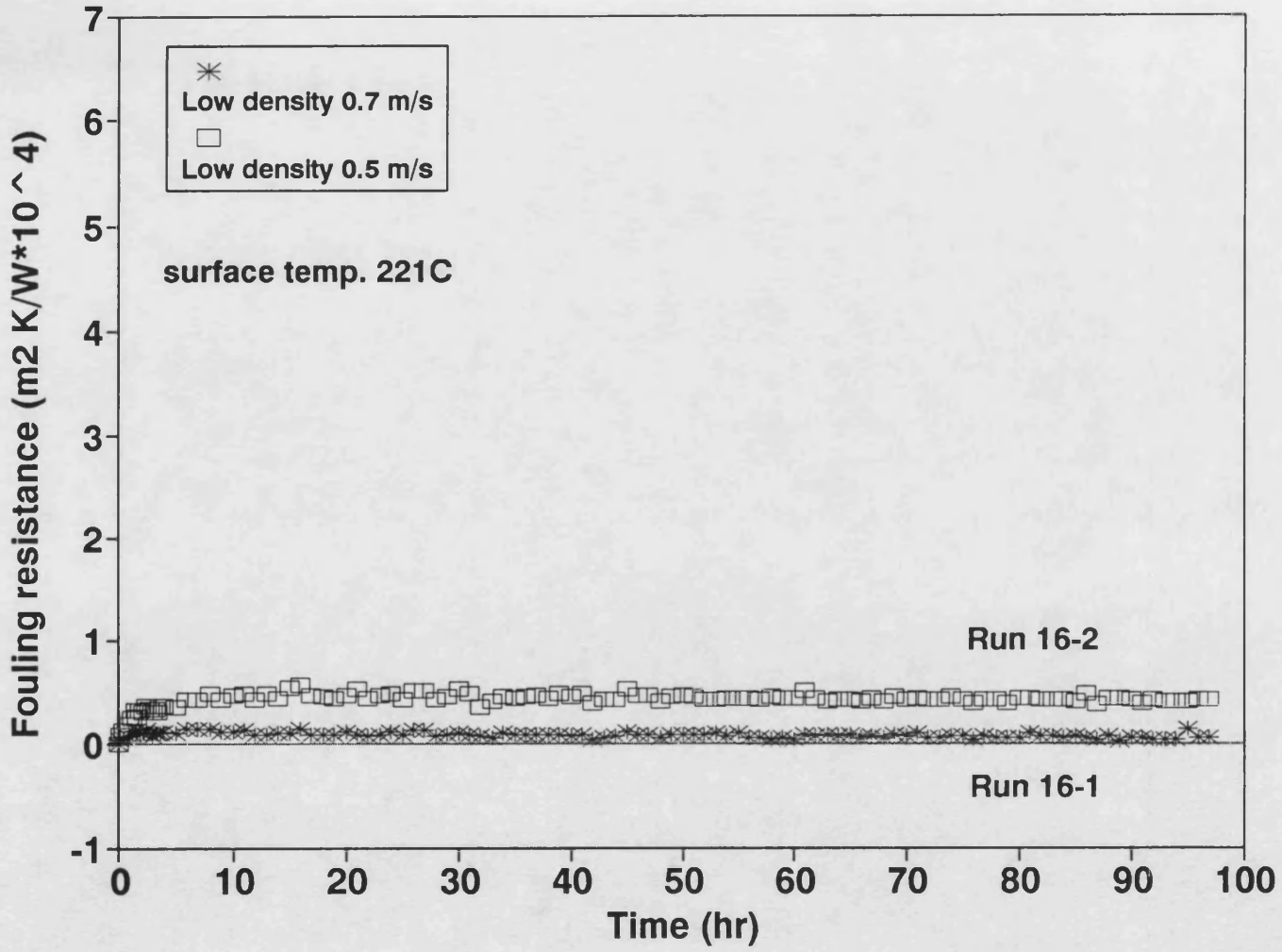

Figure 3.46 Fouling resistance -time data for Run 16

Run 17 (Effect of low density insert)

Run 17 was carried out to confirm the effect of a mechanical insert at the same heat flux (62.2 kW m^{-2}) and the same flow velocity (0.5 ms^{-1}). The objective of Run 17 was therefore similar to that of Run 1. The bare tube surface temperature was initially hotter at 264°C than that for test section 2 fitted with the insert (193°C). The temperature of 264°C was hot enough to cause subcooled nucleate boiling to occur in test section 1 but 193°C was too low for subcooled nucleate boiling to occur in test section 2 fitted with the insert. The results are shown in Figures 3.47 and 3.48. Figure 3.48 confirms that for a given heat flux and flow velocity the presence of an insert leads to a reduction in the fouling resistance.

The fouling resistances for the bare tube (Run 17-1) were seemingly relatively modest when it is considered that this Run had the highest initial surface temperature (264°C) in the whole series of experiments. However, it is important to note that the initial fouling rate for Run 17-1 (T_{sc} = 264°C) was about 2.2 times that for Run 1-1 (T_{sc} = 216°C). The asymptotic resistance of around 2.3 x 10^{-4} m^2K W^{-1} for Run 17-1 was surpassed in Run 1-1 after a total time of about 25 hours (or 11 hours after the end of the induction period).

One factor of importance is the possible exhaustion of precursors and/or reactants in crude oil A which had not been changed during the whole series if experiments. Similar findings were reported by Watkinson and Epstein (1969) and this matter is discussed further in Section 3.2.2. A second factor of concern, introduced in

Section 3.1.2, is the progressive loss of light ends from the feedstock as manifested by a progressive increase in the minimum temperature at which subcooled nucleate boiling could commence. This matter is discussed further in Section 3.2.5.

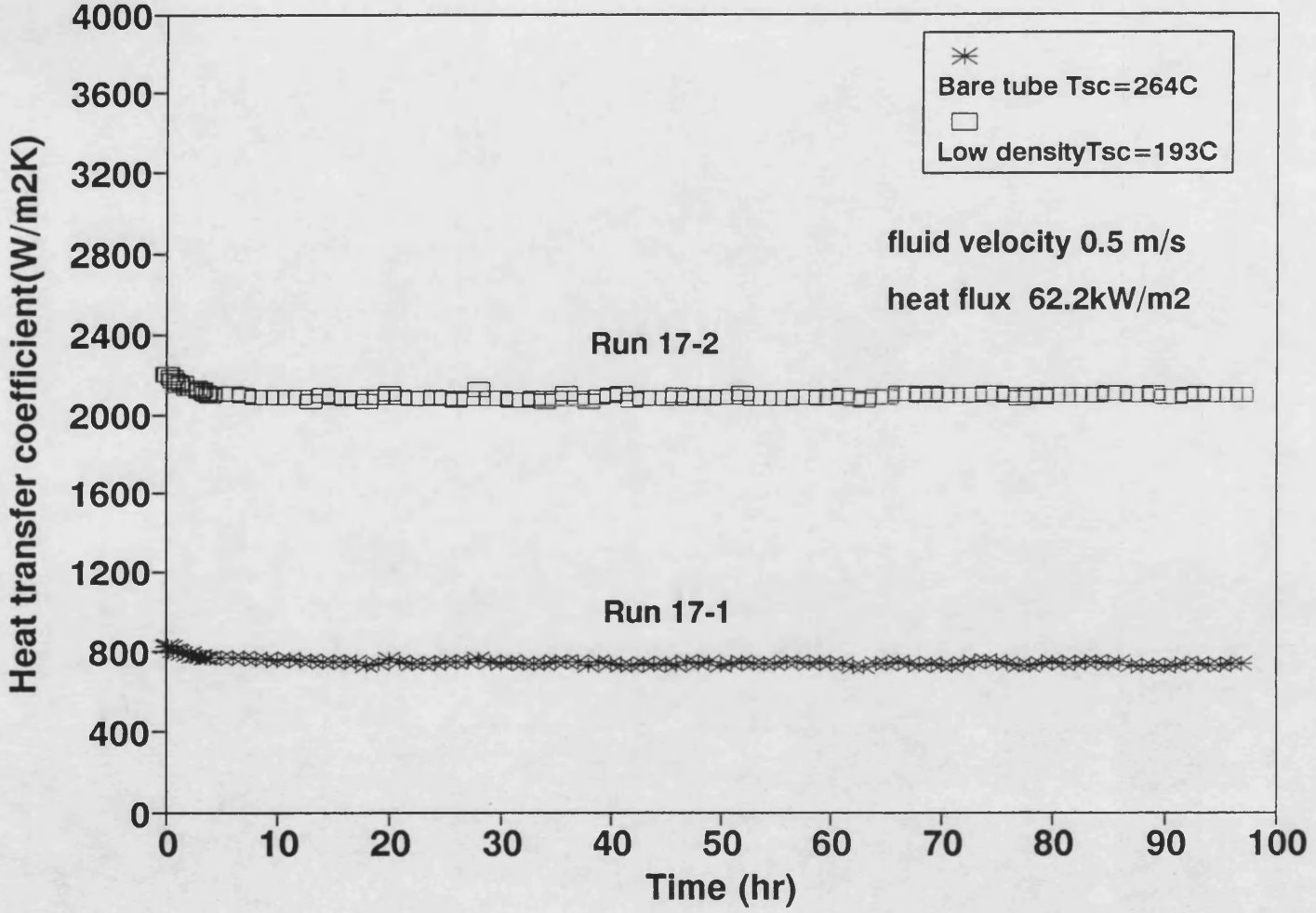

Figure 3.47 Thermal coefficient Hi for Run 17

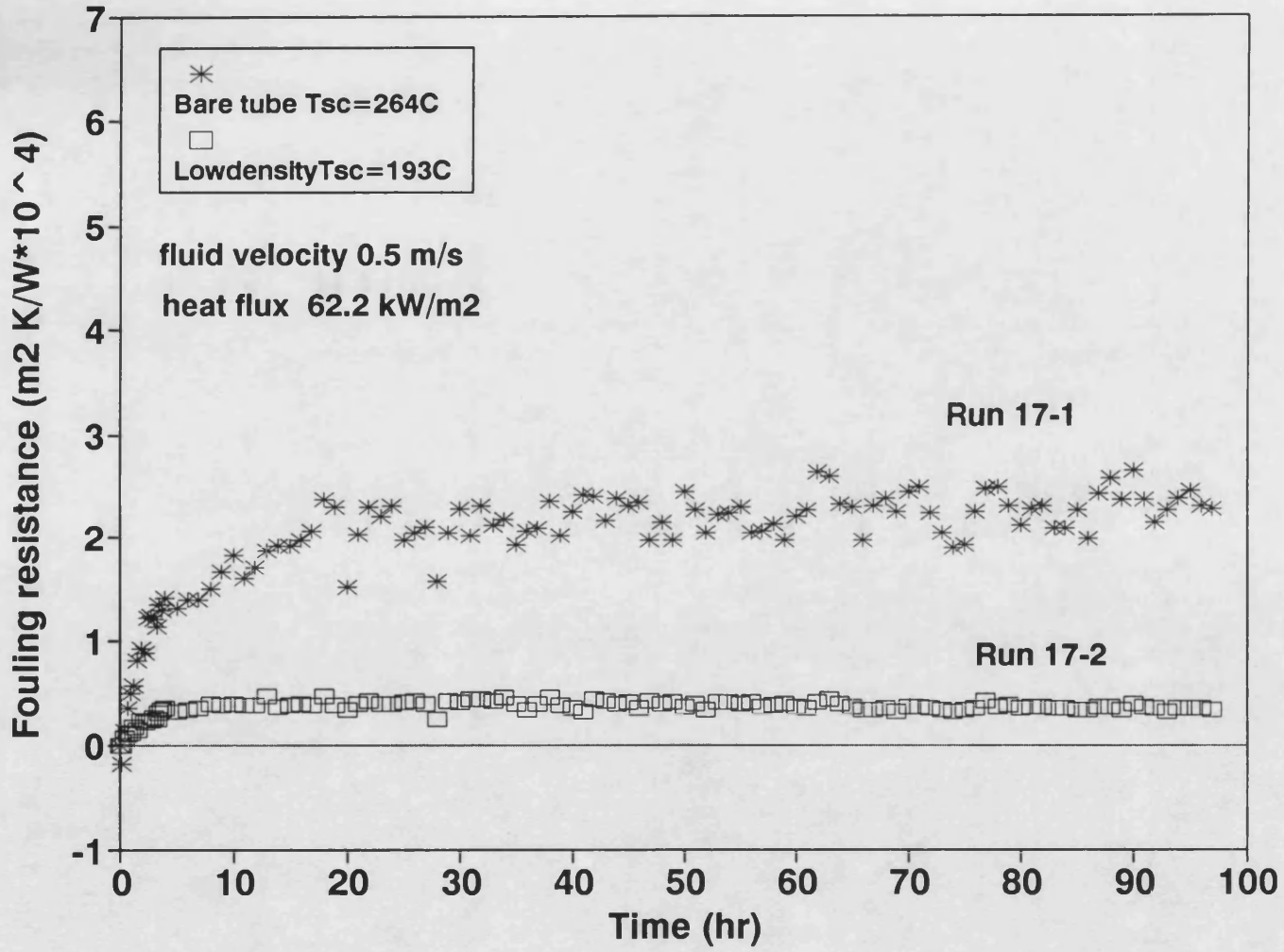

Figure 3.48 Fouling resistance - time data for Run 17

Run 18 (Reproducibility of data for nominally identical inserts)

Run 18 was carried out to check the reproducibility of fouling data with the presence of two nominally identical low density inserts for the two identical test sections in parallel. Figure 3.49 shows that, despite the use of two nominally identical low density inserts, the initial heat transfer coefficients were found to differ by about 15 percent. Thus in order to obtain the same initial surface temperatures, different heat fluxes (103.6 kW m^{-2} and 93.3 kW m^{-2}) were supplied to test sections 1 and 2 respectively. As shown in Figure 3.50, the tube having the higher heat transfer coefficient (test section 1) yielded the lower values of fouling resistance at any time.

Possible reasons for the differences are as follows:-

(1) Heat transfer coefficient measurements are made at local axial positions. It has been found that the position of an insert can affect substantially the local coefficient (Shalhi (1993)).

(2) Fouling was correspondingly determined at axial-specific locations. The local characteristics of fouling may vary with the local positioning of insert wires. It is therefore possible, when using an insert, that fouling substances may be deposited unevenly around and along the tube. However the circumferential variation in the fouling resistance with a low density insert present was found to be no more than ± 8% (see Appendix 3).

(3) The values of fouling resistance were rather small and the build up of fouling was found to occur rather quickly at the beginning of the Run so that the error in the calculated heat transfer coefficient at time zero could affect the computed fouling resistances to some extent.

Whatever the reason for the observation that, for otherwise identical conditions, the tube with the higher initial film heat transfer coefficient suffers from less fouling is very significant and is accounted for in the model developed in Section 3.2.10 and tested in Section 3.2.11.

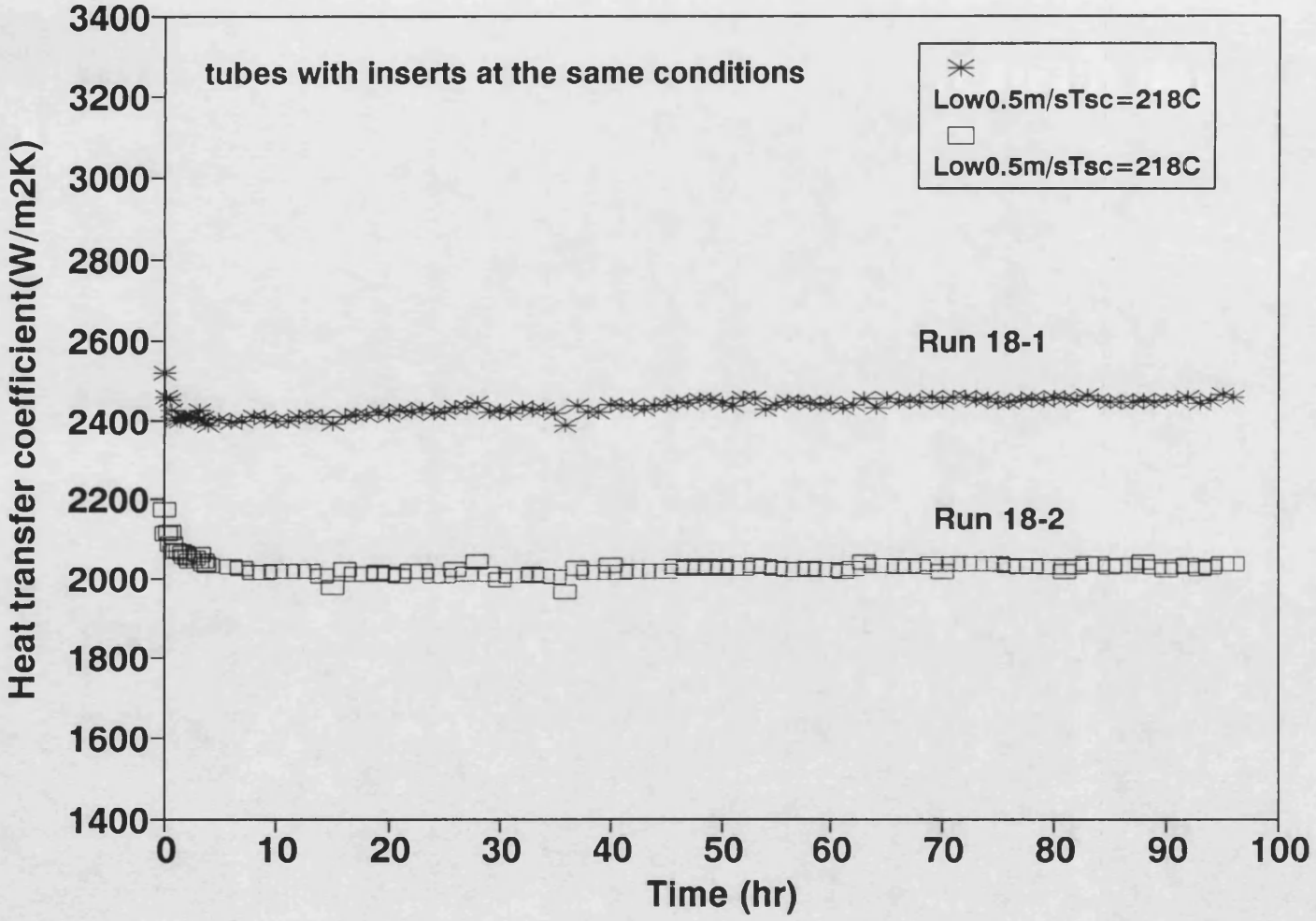

Figure 3.49 Thermal coefficient Hi for Run 18

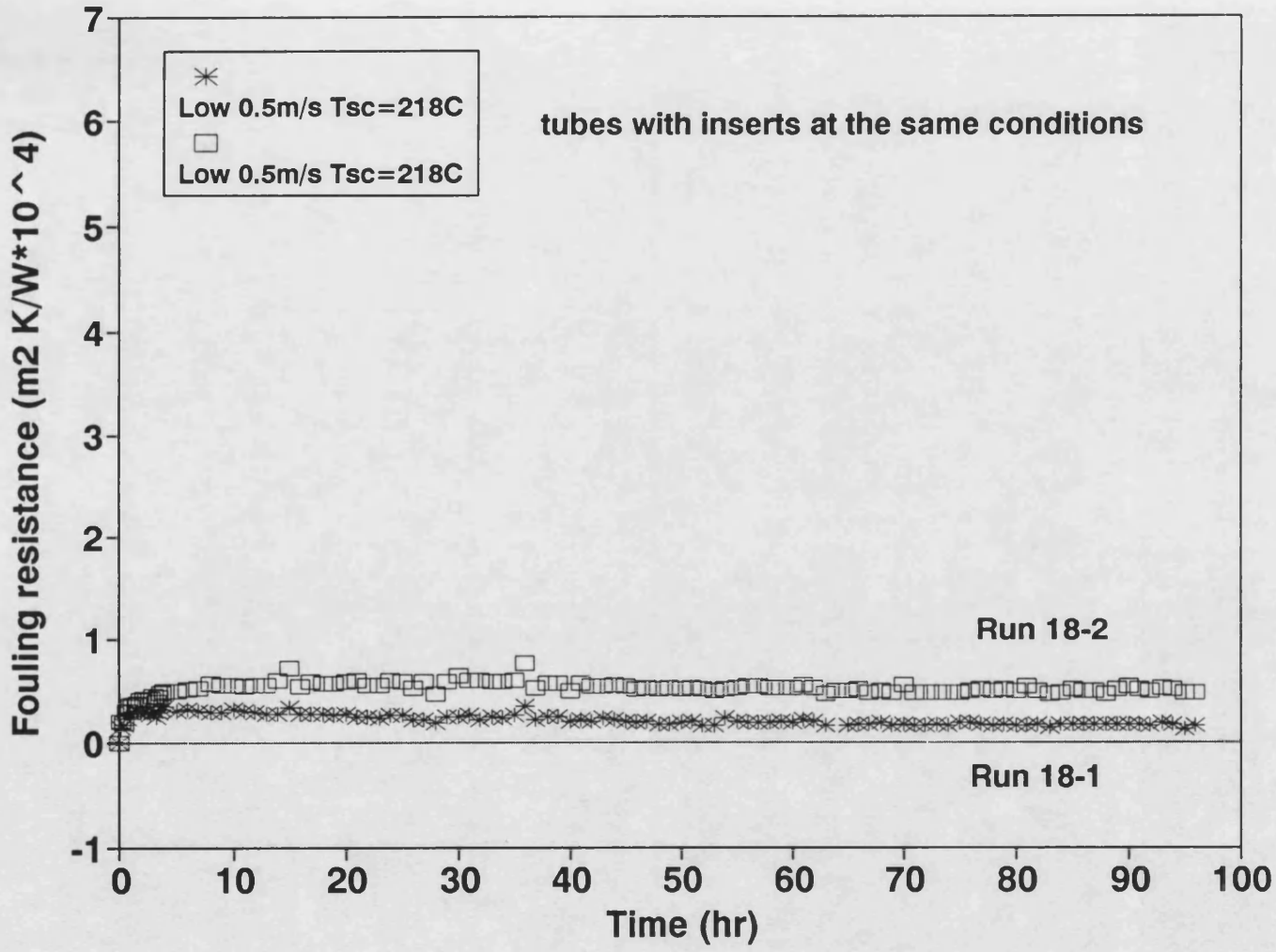

Figure 3.50 Fouling resistance - time data for Run 18

Run 19 (Effect of low density insert with fresh crude oil)

Run 19 was similar to Run 2 but with the insert at the position shown in Figure 3.12(b) and with fresh crude oil B. The results are shown in Figures 3.51 and 3.52. Despite the use of fresh oil, the values of the fouling resistances are lower than those for Run 2. This is probably due to the absence from crude oil B of sludge containing asphaltene. Another important difference between Runs 2 and 19 is the presence of subcooled nucleate boiling in the former.

Despite these differences, Figure 3.52 shows that the effect of the HiTRAN insert is similar to that for Run 2 in that it reduces fouling.

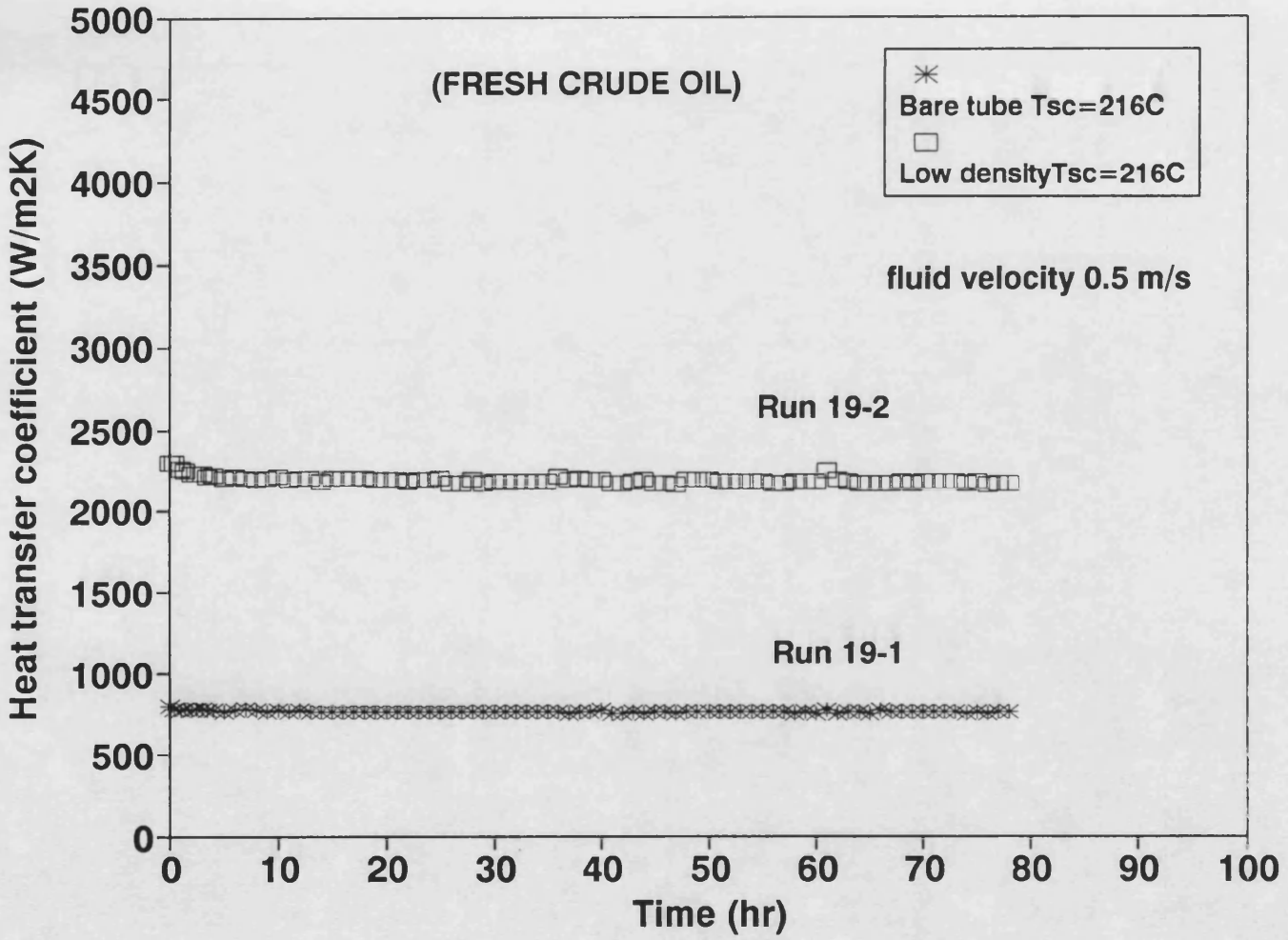

Figure 3.51 Thermal coefficient HI for Run 19

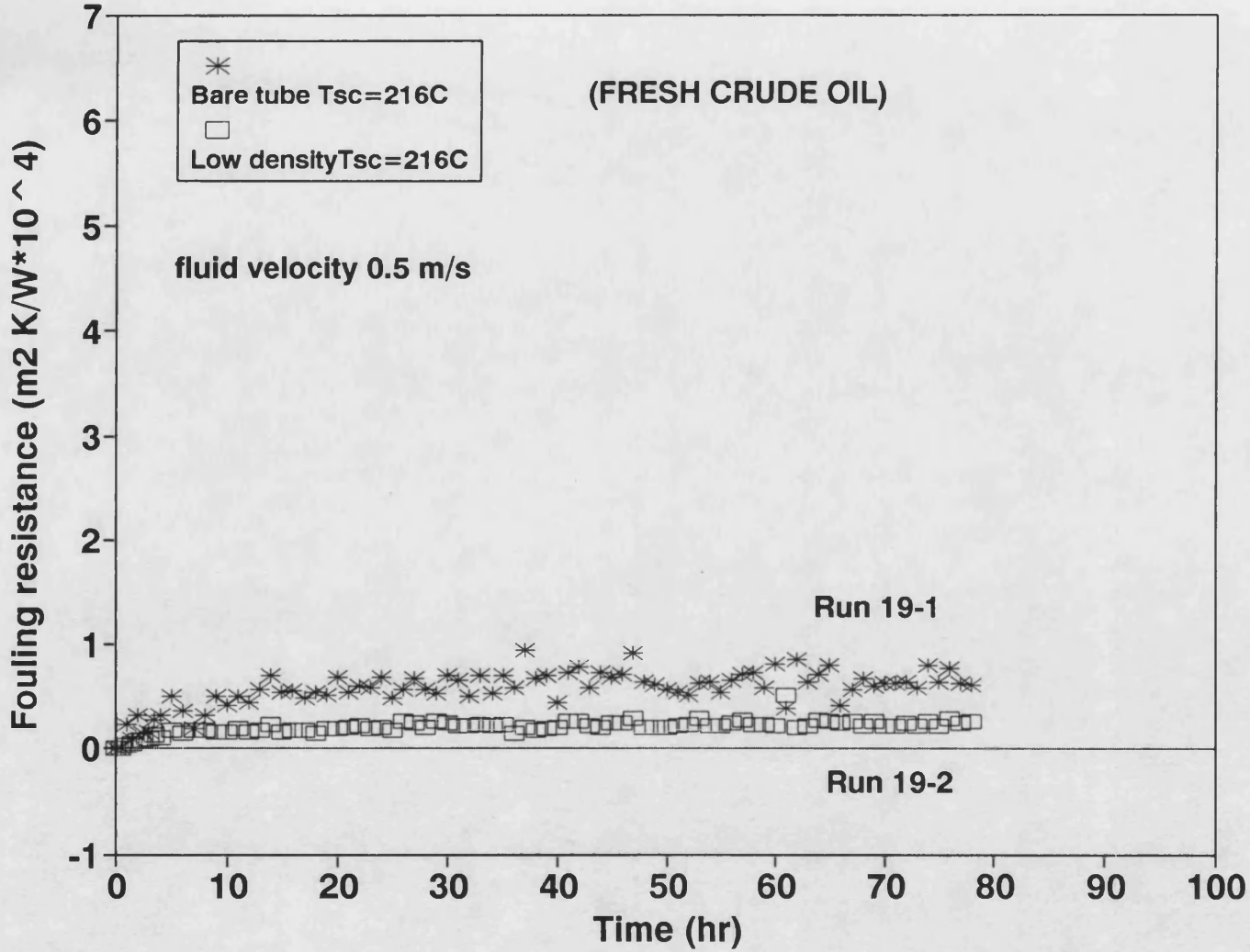

Figure 3.52 Fouling resistance - time data for Run 19

3.2.1.2 Effect of change of fluid velocity

At the end of most experiments the fluid velocity through each test section was increased to check whether or not the deposit was removable by the higher shearing action of the fluid. Operating data are summarised in Table 3.9.

After a chosen period in which the fluid velocity was at the elevated value, the velocity was returned to that used in the fouling Run. The new pseudo-steady state was achieved within 15 minutes and then thermocouple readings, wattmeter and pressure drop measurements were taken. For Runs 5, 9 and 14, this procedure was repeated once. For Run 3 it was carried out four times.

The change of fouling resistance (ΔR_f) due to the higher shearing action of the fluid was calculated as follows:

$$\Delta R_f = \left(\frac{R_f(1) - R_f(2)}{R_f(1)} \right) x\ 100 \qquad (3.10)$$

in which $R_f(1)$ is the fouling resistance at the end of the fouling Run and $R_f(2)$ is the fouling resistance measured after the increase in flow velocity.

In the case of ΔR_f being equal to zero, the fouling resistance would have remained unchanged and the deposit would seemingly not have been removed by the higher shearing action of the fluid. In the case of ΔR_f being 100%, the heat transfer

Table 3.9 Operating data of change of fluid velocity

	Test section		Rf at end of Run (m2K/W)	Increase flow velocity				final Rf**) (m2K/W)	Reduction in Rf**) (%)
				yes or no	velocity (m/s)	test tube heater	operating period(min)		
Run 1	1	Bare	6.26E-04	yes	2.5	on	30	5.88E-04	6
	2	Low	1.11E-04		2.5	on	30	1.13E-04	-2
Run 2	1	Bare	2.41E-04	yes	2.5	off	240	1.72E-04	29
	2	Low	1.86E-04		2.5	off	240	1.08E-04	42
Run 3	1	Bare	4.35E-04	no	(0.5)	off	240	3.84E-04	12
							240	3.85E-04	11
							240	3.52E-04	19
							240	4.98E-04	-15
	2	Bare	4.62E-04	no	(0.5)	off	240	6.95E-04	-50
							240	3.15E-04	32
							240	5.24E-04	-13
							240	4.64E-04	0
Run 4	1	High	0	no	-	-	-	n/a	n/a
	2	Low	0		-	-	-	n/a	n/a
Run 5	1	High	0	yes	1.3	on	120	n/m	n/m
							120	n/m	n/m
	2	Low	0.52E-04		2.5	on	120	0.27E-04	48
							120	-0.01E-04	102
Run 6	1	High	0	no	-	-	-	n/a	n/a
	2	Low	0.35E-04		-	-	-	n/a	n/a

(continued)

Table 3.9 continued

	Test section		Rf at end of Run (m2K/W)	Increase flow velocity				final Rf**) (m2K/W)	Reduction in Rf**) (%)
				yes or no	velocity (m/s)	test tube heater	operating period(min)		
Run 7	1	High	0.22E-04	yes	1.6	on	60	0.01E-04	95
	2	Low	0.59E-04		2.1	on	60	0.06E-04	90
Run 8	1	Bare	0.33E-04	yes	2.5	on	15	-0.05E-04	115
	2	Low	0.44E-04		2.5	on	15	0.03E-04	94
Run 9	1	Bare	4.87E-04	yes	2.5	on	15	3.83E-04	21
							15	3.39E-04	30
	2	Bare	0.34E-04		2.5	on	15	0.27E-04	21
							15	0.23E-04	48
Run 10	1	Low	0	no	-	-	-	n/a	n/a
	2	Low	0.68E-04		-	-	-	n/a	n/a
Run 11	1	Bare	2.73E-04	no	-	-	-	n/a	n/a
	2	Bare	7.91E-04		-	-	-	n/a	n/a
Run 12	1	Low	0.15E-04	yes	2.5	on	15	0.04E-04	73
	2	Low	0.29E-04		2.5	on	15	0.02E-04	93
Run 13	1	Bare	0.56E-04	yes	2.5	on	15	-0.04E-04	107
	2	Low	0.12E-04		2.5	on	15	-0.02E-04	117

(continued)

Table 3.9 continued

	Test section		Rf at end of Run (m2K/W)	Increase flow velocity				final Rf**) (m2K/W)	Reduction in Rf**) (%)
				yes or no	velocity (m/s)	test tube heater	operating period(min)		
Run 14	1	Bare	4.65E-04	yes	2.5	on	15	4.01E-04	14
							15	3.73E-04	20
	2	Bare	1.46E-04		2.5	on	15	0.73E-04	50
							15	0.38E-04	74
Run 15	1	Bare	0.80E-04	yes	2.5	on	15	0.49E-04	39
	2	Bare	-0.74E-04		2.5	on	15	-0.72E-04	0
Run 16	1	Low	0.05E-04	yes	2.5	on	15	-0.01E-04	120
	2	Low	0.42E-04		2.5	on	15	-0.03E-04	107
Run 17	1	Bare	2.28E-04	yes	2.5	on	15	1.87E-04	18
	2	Low	0.34E-04		2.5	on	15	0.02E-04	94
Run 18	1	Low	0.15E-04	yes	2.5	on	15	0.11E-04	27
	2	Low	0.48E-04		2.5	on	15	0.20E-04	58
Run 19	1	Bare	0.61E-04	yes	2.5	on	15	0	100
	2	Low	0.26E-04		2.5	on	15	0.08E-04	69

**) n/a : not applicable
n/m : not measured

coefficient (H_i which includes R_f) measured after the increase in velocity, would have returned to the initial value and the deposit would seemingly have been relatively easily removed by the higher fluid shear. Negative values of ΔR_f would mean that the fouling resistance increased as a result of the increased flow velocity.

For Run 2, the test sections were not heated during the period in which the flow velocity was increased. For Run 3 the fouled test sections were left for a selected time without heating but with the fluid velocity through each test section at the values used in the fouling Run. Further details of these two Runs are given below.

For Runs 4, 6, 10 and 11 an increase in the fluid velocity was not made at the end of the fouling Run. The reasons for this are as follows:

Runs 4 and 6:	the failure of the heater elements
Run 10:	the effect of a change of velocity was studied during the fouling run.
Run 11:	an attempt was made to recover the deposit at the end of the fouling run.

In the following Sections the effect of velocity change is described in the chronological order of the fouling runs.

Run 1 (1: bare tube; 2: low density insert)

The velocity of the crude oil through each test section was increased to 2.5 ms^{-1} for 30 minutes and then returned to 0.5 ms^{-1}. Table 3.9 shows that the fouling resistances for test sections 1 (bare) and 2 (insert) showed little change, *i.e.* ΔR_f = 6 and -2% respectively. Thus it is assumed that the deposit adhered firmly to the wall.

Run 2 (1: bare tube; 2: low density insert)

The velocity of the fluid was increased to 2.5 ms^{-1} for four hours, during which time the test sections were not heated but the bulk temperature was kept constant. Then the velocity was returned to that used in the Run (0.5 ms^{-1}) and the test sections were again heated at the fluxes used in the fouling run. At the new pseudo-steady state Table 3.9 shows that the values of fouling resistance for test sections 1 (bare) and 2 (insert) decreased by 29% and 42% respectively. An importance difference between the velocity increase experiment for Runs 1 and 2 was that for Run 2 the change in surface temperature introduced by switching the heater off and on may have made the deposits more susceptible to breakage due to thermal stress. Weakened deposits may then have been more likely to be removed by the higher shearing action of the fluid.

Run 3 (1: bare tube; 2: bare tube)

At the end of the fouling Run, the fouled test sections were left for four hours without heating but with the velocity through each test section remaining constant at 0.5 ms^{-1} and the bulk temperature being kept constant. The test sections were then heated with the heat flux used in the fouling run and thermocouple readings were taken. This whole procedure was carried out four times. Table 3.9 shows that there was no clear pattern of increase or decrease in fouling resistance. One possible reason for this is as follows. Local voids between the deposit and the surface of the tube could have been formed leading to the deposit being more susceptible to breakage by the repetitive procedure of thermal shocking and shear stressing described above. If the local voids were then to become filled with the bulk fluid, the measured fouling resistance would rise because the newly formed thin liquid layer would give an additional thermal resistance to that caused by the deposit itself. In such circumstances, the deposit might not adhere firmly to the surface of the tube and pieces could move along the tube wall. If these events were to occur simultaneously then the fouling resistances could either increase or fall as shown in Table 3.9. The repetitive experiment described above seems to show that the deposits are not readily soluble in the bulk fluid.

Run 5 (1: high density insert; 2: low density insert)

For test section 2 (low density insert), the velocity of the fluid was increased to 2.5 ms^{-1} for two hours, during which time the test section was kept heated at the same

heat flux as that used in the fouling Run. Then the velocity was returned to 0.5 ms^{-1}. This procedure was repeated. After these changes Table 3.9 shows that the fouling resistance became equal to zero. Thus the deposit formed in Run 5 seems to have been more readily removed by the higher shearing action than for the three Runs described previously.

Run 7 (1: high density insert; 2: low density insert)

The velocities of the fluid through test sections 1 and 2 were increased to 1.6 ms^{-1} and 2.1 ms^{-1} respectively for 60 minutes and the test sections remained heated at the same heat fluxes as used in the fouling Run. It was not possible to increase the velocity through test section 1 up to 2.5 ms^{-1} due to the higher pressure drop exerted by the high density insert. Table 3.9 shows that the fouling resistances for both test sections were reduced almost to zero by the increase in fluid velocity. Thus the deposits from Run 7-2 seem to have been more quickly removed by the shearing action of the fluid than those from Run 5-2.

Run 8 (1:bare tube; 2: low density insert)

The velocity through each test section was increased to 2.5 ms^{-1} for 15 minutes. Despite the short period of operation at increased velocity, Table 3.9 shows that the fouling resistances for both test sections became equal to zero. The small negative value of fouling resistance for test section 1 measured after increasing the velocity is probably due to measurement error and should not be interpreted as being due to

any particular physical phenomenon.

Fouling Runs 5-2, 7-2 and 8-2 with the low density insert installed were carried out at the same operating conditions (initial surface temperature 197°C, flow velocity 0.5 ms^{-1} and heat flux around 77 kW m^{-2}). Table 3.9 shows that the deposits laid down under these conditions seem to have been easily removed by the shearing action of the fluid.

Run 9 (1: bare tube; 2: bare tube)

The velocity of the fluid through each test section was increased to 2.5 ms^{-1} for 15 minutes and then reduced to 0.5 ms^{-1} and 1.1 ms^{-1} as shown in Table 3.9. This procedure was carried out twice. The fouling resistances for test sections 1 (0.5 ms^{-1}) and 2 (1.1 ms^{-1}) were reduced by 30% and 48% respectively. Clearly some of the deposits seem to have been removed by the shearing action of the fluid. Thus the deposits seem to have adhered more weakly than those in Run 1.

Run 12 (1: low density insert; 2: low density insert)

The velocity through each test section was increased to 2.5 ms^{-1} and then returned to 0.5 ms^{-1}. Table 3.9 shows that the fouling resistances for test sections 1 and 2 were reduced by 73% and 93%, respectively. Most of the deposits therefore seem to have been removed by the shearing action of the fluid. Comparing Runs 8-2 and 12, the lower surface temperature for Run 8-2 (T_{sc} = 197°C) seems to have yielded

a weaker deposit than the higher temperature used in Runs 12-1 and 12-2 (T_{sc} = 224°C and 211°C, respectively).

Run 13 (1: bare tube; 2: low density insert)

The velocity of the fluid through each test section was increased to 2.5 ms^{-1} for 15 minutes and then returned to 0.5 ms^{-1}. Despite the relatively high initial surface temperatures, Table 3.9 shows that the fouling resistances for both test sections returned almost to zero. Therefore the deposits seem to have adhered weakly to the wall.

Run 14 (1: bare tube; 2: bare tube)

The velocity through each test section was increased to 2.5 ms^{-1} for 15 minutes and then returned to 0.5 ms^{-1}. This procedure was repeated once. Table 3.9 shows that after the whole operation, the fouling resistances for test section 1 (254°C) and 2 (217°C) were reduced by 20 percent and 74 percent respectively. The deposits formed in the tube having the higher surface temperature seem to have adhered more firmly to the wall.

For the bare tube, fouling Runs 1-1, 2-1, 3-1, 3-2, 9-1 and 14-2 were carried out at similar operating conditions (T_{sc} = 216 - 217°C, V_m = 0.5 ms^{-1}). Comparing the results when the velocity is increased at the end of a fouling run, it seems that the deposits become more easily removed by the shearing action of the fluid when

repeated increases in velocity are used.

Run 15 (1: bare tube; 2: bare tube)

The velocity of the fluid through each test section was increased to 2.5 ms^{-1} for 15 minutes and then returned to 0.5 ms^{-1} and 1.1 ms^{-1} for test sections 1 and 2, respectively. Table 3.9 shows that the fouling resistance for test section 1 (V_m = 0.5 ms^{-1}) was reduced by 39%. However for test section 2 (V_m = 1.1 ms^{-1}), the fouling resistance was not altered. Comparing Runs 15-1 and 13-1 (bare tube, T_{sc} = 239°C and V_m = 0.5 ms^{-1}), the deposits from Run 15-1 seem to have adhered more firmly to the wall.

Run 16 (1: low density insert; 2: low density insert)

The velocity through each test section was increased to 2.5 ms^{-1} for 15 minutes and then returned to 0.7 ms^{-1} and 0.5 ms^{-1} for test sections 1 and 2 respectively. Table 3.9 shows that the fouling resistances for both test sections returned to zero.

Run 17 (1: bare tube; 2: low density insert)

The velocity through each test section was increased to 2.5 ms^{-1} for 15 minutes. As shown in Table 3.9 the fouling resistances for test sections 1 (bare tube, T_{sc} = 264°C) and 2 (insert, T_{sc} = 193°C) were reduced by 18% and 94%, respectively. The higher surface temperature is likely to create a deposit with a greater bond

strength. However despite the highest initial surface temperature in the whole series of experiments, the deposits for Run 17-1 seem to have adhered less firmly to the wall than those from Runs at the beginning of the series of experiments (Runs 1-1 and 2-1).

Run 18 (1: low density insert; 2: low density insert)

The velocity through each test section was increased to 2.5 ms^{-1} for 15 minutes and then returned to 0.5 ms^{-1}. Table 3.9 shows that the fouling resistances for test sections 1 and 2 were reduced by 27% and 58% respectively.

Run 19 (1: bare tube; 2: low density insert)

The velocity through each test section was increased to 2.5 ms^{-1} for 15 minutes and then returned to 0.5 ms^{-1}. Table 3.9 shows that the fouling resistances for test sections 1 and 2 were reduced by 100% and 69% respectively. The difference between Runs 1 and 19 is possibly attributable to the difference in composition of the crude oil and/or the absence of subcooled nucleate boiling in Run 19.

Summary of effects of velocity change

The effects of the velocity change experiments are summarised in Figure 3.53. It appears that, in general, the greater the fouling resistance at the end of a fouling run, the smaller is the value of ΔR_f calculated from equation (3.10). Another important

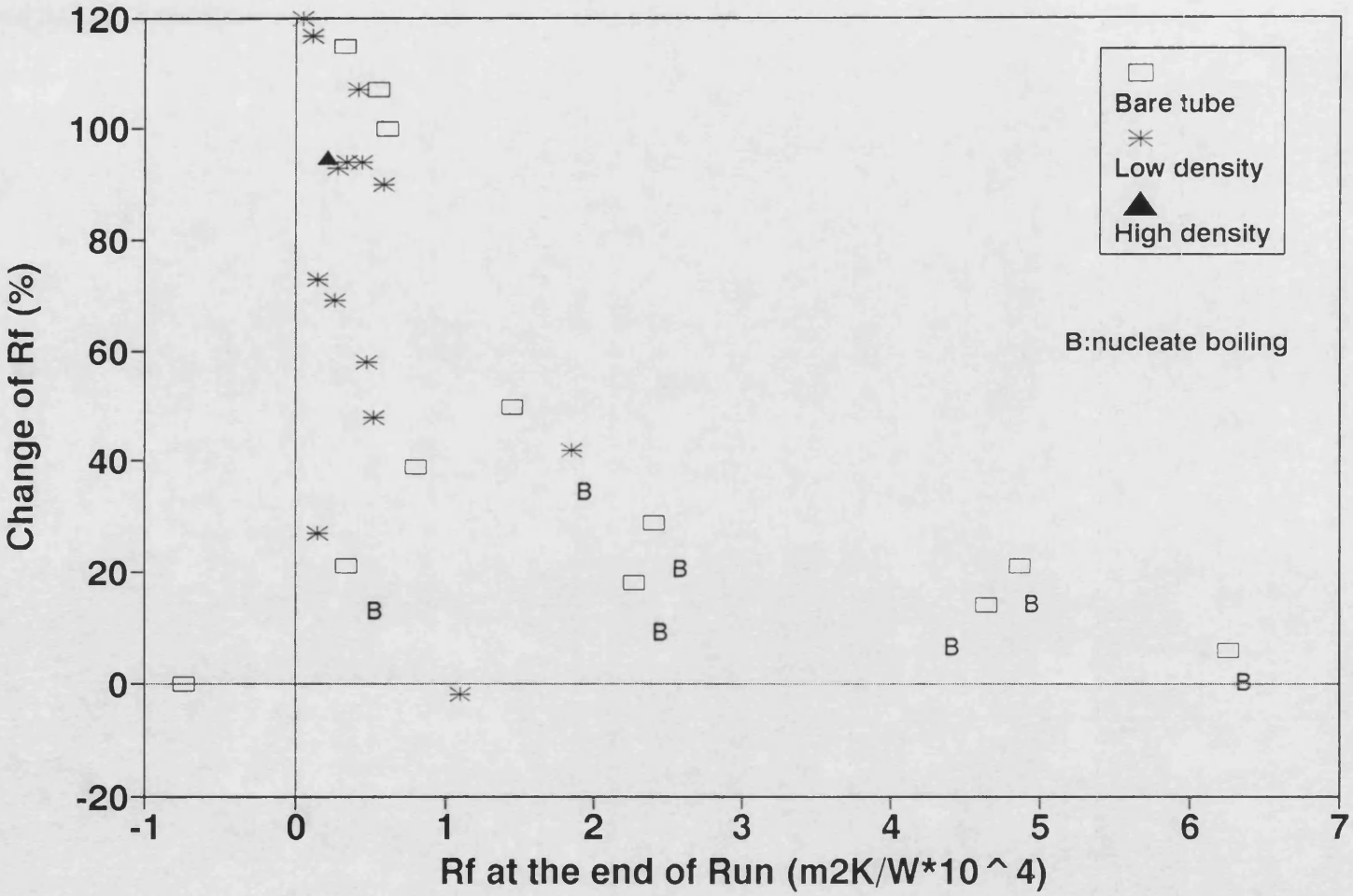

Figure 3.53 Reducion in fouling resistance by the increased fluid velocity

aspect to note from Figure 3.53 is that, in the case of deposits formed with flow in subcooled nucleate boiling, the values of ΔR_f are relatively small and hence the deposits formed with such flow seem to have greater bond strengths.

Most of the fouling runs with the insert present were carried out with flow solely in the convective regime and yielded relatively small fouling resistances. Figure 3.53 shows that a large reduction in fouling resistance with the insert in place can occur with this flow regime.

3.2.1.3 Nature of deposits

After shut-down, each test section was dismantled. Clearly it was not possible to see the inside of a tube fitted with an insert. Therefore visual inspection was restricted to the bare tube. Attempts were also made to recover deposits. For Runs 1 and 2, small amounts of deposit were recovered. For Run 3 relatively large pieces of deposit were collected and examined by the scanning electron microscope (SEM) and analysed for the inorganic content. For other Runs, attempts were made to recover substantial pieces of deposit but proved unsuccessful. It is important to note that the visual inspections and recovery of deposits were made following Runs at the end of which the flow velocity had sometimes been increased as previously described in Section 3.2.1.2. What was observed therefore was not always representative of conditions at the end of the fouling Run.

Run 1-1

The deposits seemed to be formed evenly around the hottest end of the heated tube. Small amounts of deposit were recovered and were found to be black and soft.

Run 2-1

Visual inspection revealed deposits which were similar to those seen in Run 1-1. Small amounts of deposit were recovered and were black and soft, similar to those from Run 1-1.

Run 3-1, 2

From the visual inspection, the deposits were seen to be evenly distributed around the hottest end of the heated tube. Several relatively large pieces of deposit, shown in Figure 3.54, were recovered and examined by SEM. Photographs are shown in Figure 3.55. The deposits had a fine porous structure of near-hemispherical particles, similar in nature to the deposits obtained from air saturated kerosene at relatively low furnace temperature by Khater (1983).

The thermal conductivity of the deposit was estimated by dividing the deposit thickness (0.07 - 0.1 mm, measured by SEM) by the final fouling resistance. The thermal conductivity was found to be in the range of 0.15 to 0.23 $Wm^{-1} K^{-1}$, similar to that obtained in other crude oil studies (0.29 to 0.86 $W m^{-1} K^{-1}$, by Scarborough

(a) Run 3-1 (b) Run 3-2

Figure 3.54 Photograph of deposits from Runs 3-1 and 3-2

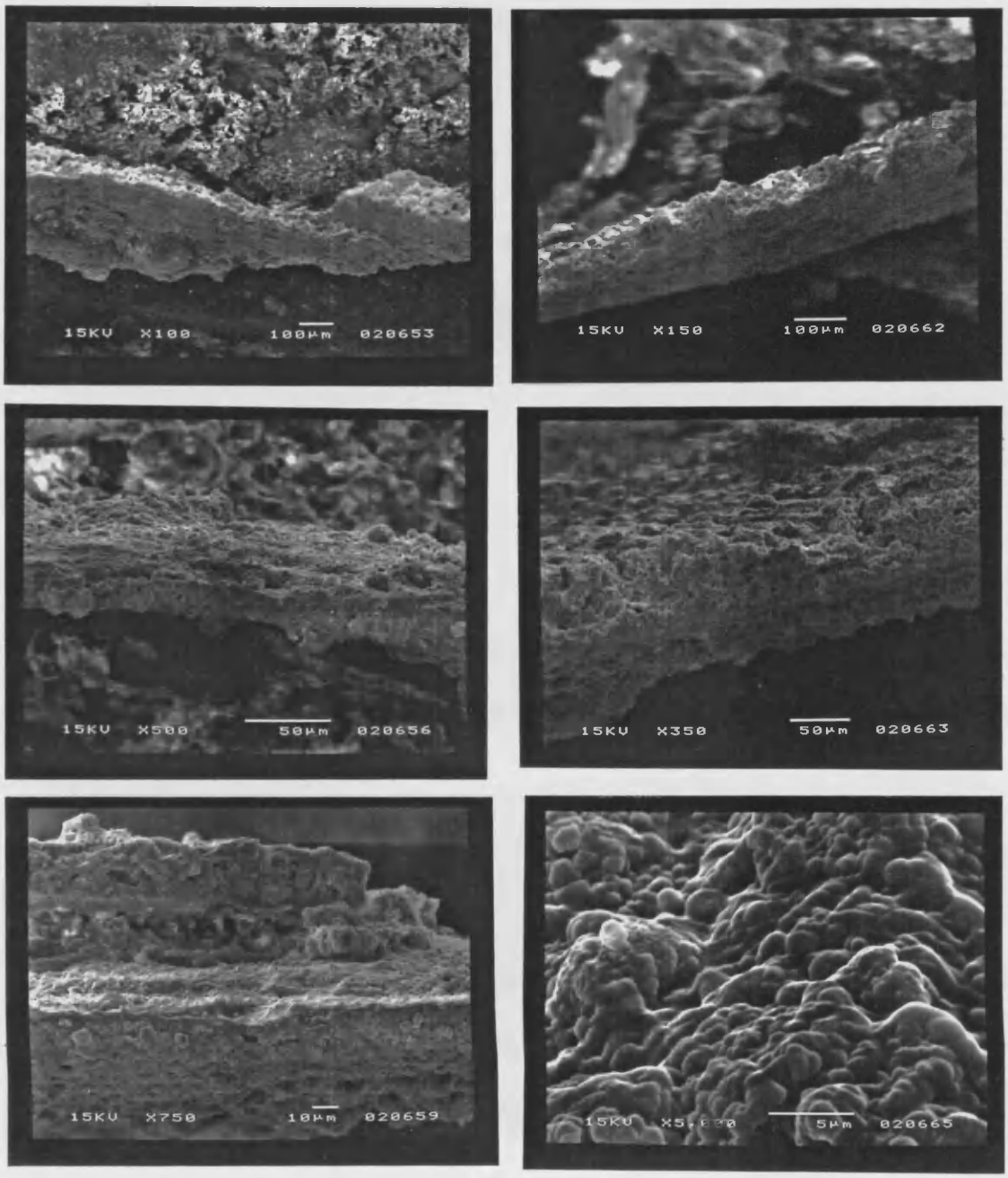

(a) Run 3-1 (b) Run 3-2

Figure 3.55 Electron micrographs of deposits

et al (1979) and 0.204 W m^{-1} K^{-1}, by Eaton and Lux (1984)). The deposit was found to contain 18% ash by weight.

Run 8-1

The visual inspection revealed that the tube seemed to be clean. This was as expected since the fouling resistance returned almost to zero after the flow velocity had been increased at the end of the fouling Run.

Run 9-1, 2

For both tubes, the deposits were seen to be evenly distributed around the hottest end. In addition the amount of deposit from Run 9-1 (final $R_f = 3.39 \times 10^{-4}$ m^2K W^{-1}) appeared to be more than that from Run 9-2 (final $R_f = 0.23 \times 10^{-4}$ m^2K W^{-1}).

Run 11-1, 2

The visual inspection was made before attempting to recover the deposits. The tube having had the higher surface temperature (test section 2) seemed to have more deposit on the wall than that having the lower surface temperature (test section 1). From the appearance of the reflection of light on the deposit the surface was judged to be rougher than that for Runs 1-1, 2-1 3-1 and 3-2.

An attempt was made to recover the deposits from this experiment. Since the

fouling resistances were high, it was anticipated that substantial amounts of deposit could be recoverable. However, the deposits were very soft and less in quantity than expected. Therefore it was not possible to collect them as reasonably sized pieces for SEM examination.

Runs 13-1

The tube was seen to be clean. This was expected because of the return of R_f almost to zero after increasing the velocity at the end of the fouling run.

Run 14-1, 2

For both tubes, the deposits seemed to be mainly accumulated at the hottest end of the heated tube and evenly distributed around the tube.

Runs 15-1, 2

The deposits were seen at the hottest end of the tubes and evenly distributed for both tubes. The amount of deposit for test section 2 yielding the negative fouling values (final $R_f = -0.72 \times 10^{-4}$ $m^K K\ W^{-1}$) appeared to be less than that for test section 1 (final $R_f = 0.49 \times 10^{-4}$ $m^2K\ W^{-1}$). The surface of the deposits for both test sections seemed to be rough, similar to that for Run 11.

Run 17-1

Visual inspection revealed that the deposits were similar to those for Runs 14 and 15.

Run 19-1

The visual inspection was not made.

3.2.2 Effect of continued recirculation of feedstock on fouling

Virtually the whole series of experiments (Runs 1 to 18) was carried out using the same batch of crude oil A with no fresh oil added. Such continued recirculation could possibly affect fouling from Run to Run, a matter which is explored further in this Section.

3.2.2.1 Reproducibility of fouling data from Run to Run (bare tubes)

Figure 3.56 shows fouling curves for the bare tubes obtained from five Runs which were carried out at more or less the same initial surface temperature (216 - 217°C) and at the same fluid velocity (0.5 ms^{-1}). As shown in Table 3.7, Runs 1-1, 2-1, 3-1 and 3-2 were carried out consecutively under identical conditions of initial surface temperature (216°C), fluid velocity (0.5 ms^{-1}) and heat flux (55.9 kW m^{-2}). Nucleation was believed to have occurred in all these Runs. Figure 3.56 seems to

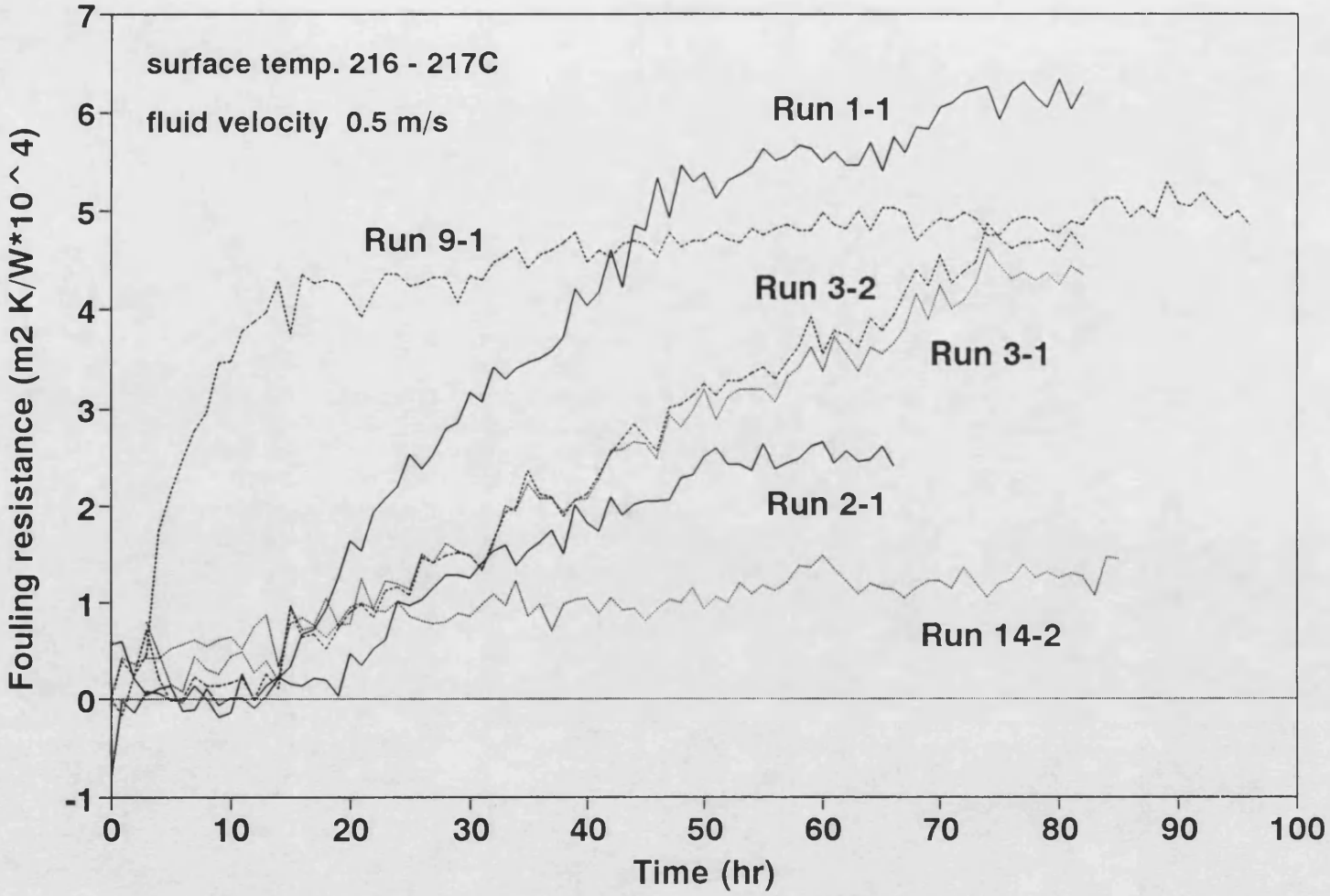

Figure 3.56 Effect of continued recirculation on fouling from Run to Run for the bare tube

show that good reproducibility of fouling data from Run to Run does not occur. In addition no particular trend seems to exist. Possible reasons for this are as follows:

(1) Continued recirculation of feedstock is likely to deplete fouling precursors, a situation which might result in a reduction in fouling rate particularly in the absence of oxygen and/or oxygen-containing compounds (Eaton and Lux (1983), Wilson and Watkinson (1992)).

(2) The test sections were opened to clean the tubes after every Run. Hence a certain, but unknown and possibly variable, amount of air could enter the system. The presence of air or oxygen is known to have a profound effect on fouling rates from hydrocarbons (Crittenden and Khater (1987), Eaton and Lux (1983), Wilson and Watkinson (1992)).

These two possibilities can work against each other and could therefore explain why there could be either an increase or decrease in fouling rate from Run to Run.

Another possible factor is the progressive loss of light ends from the crude oil from Run to Run (see Section 3.1.2.1.3). This also appears to give rise to a complex effect on fouling. Runs 9-1 and 14-2 were carried out at the same clean surface temperature and at the same velocity as Runs 1-1, 2-1, 3-1 and 3-2 but with different heat fluxes (Run 9-1: 41.5 kW m^{-2}; Run 14-2: 31.1 kW m^{-2}) from the first three Runs (55.9 kW m^{-2}). In Run 9-1, a higher initial fouling rate and a lower

asymptotic fouling resistance were obtained compared with those in Run 1-1. Run 14-2 was carried out with flow solely in the convective regime and the fouling resistance was the lowest of all the Runs which were carried out at T_{sc} = 216°C and V_m = 0.5 ms^{-1}. The combination of the loss of, or further formation of, fouling precursors and the progressive loss of light ends from the crude oil which result from its continued recirculation seems to yield a complex effect on fouling from Run to Run. Therefore comparison of data from Run to Run needs to be made with extreme care.

One important observation which can be made from the data shown in Figure 3.56 is that the fouling rate for Run 14-2, in which flow was solely convective in nature, was lower than that obtained from the other Runs in which nucleation was occurring. The effect of nucleation is discussed further in section 3.2.5.

3.2.2.2 Reproducibility of fouling data from Run to Run (with inserts present)

Figure 3.57 shows the fouling curves for the tubes fitted with a low density insert for three Runs (5-2, 7-2 and 8-2) which were carried out with flow in the convective regime and under the same conditions of initial surface temperature (197°C), fluid velocity (0.5 ms^{-1}) and heat flux (76.2 - 77.7 kW m^{-2}). Compared with the fouling curves for the bare tubes (Figure 3.56), the fouling resistances with inserts present are relatively low but better reproducibility of fouling data from Run to Run is obtained. This suggests that it is something unique to the bare tube case which

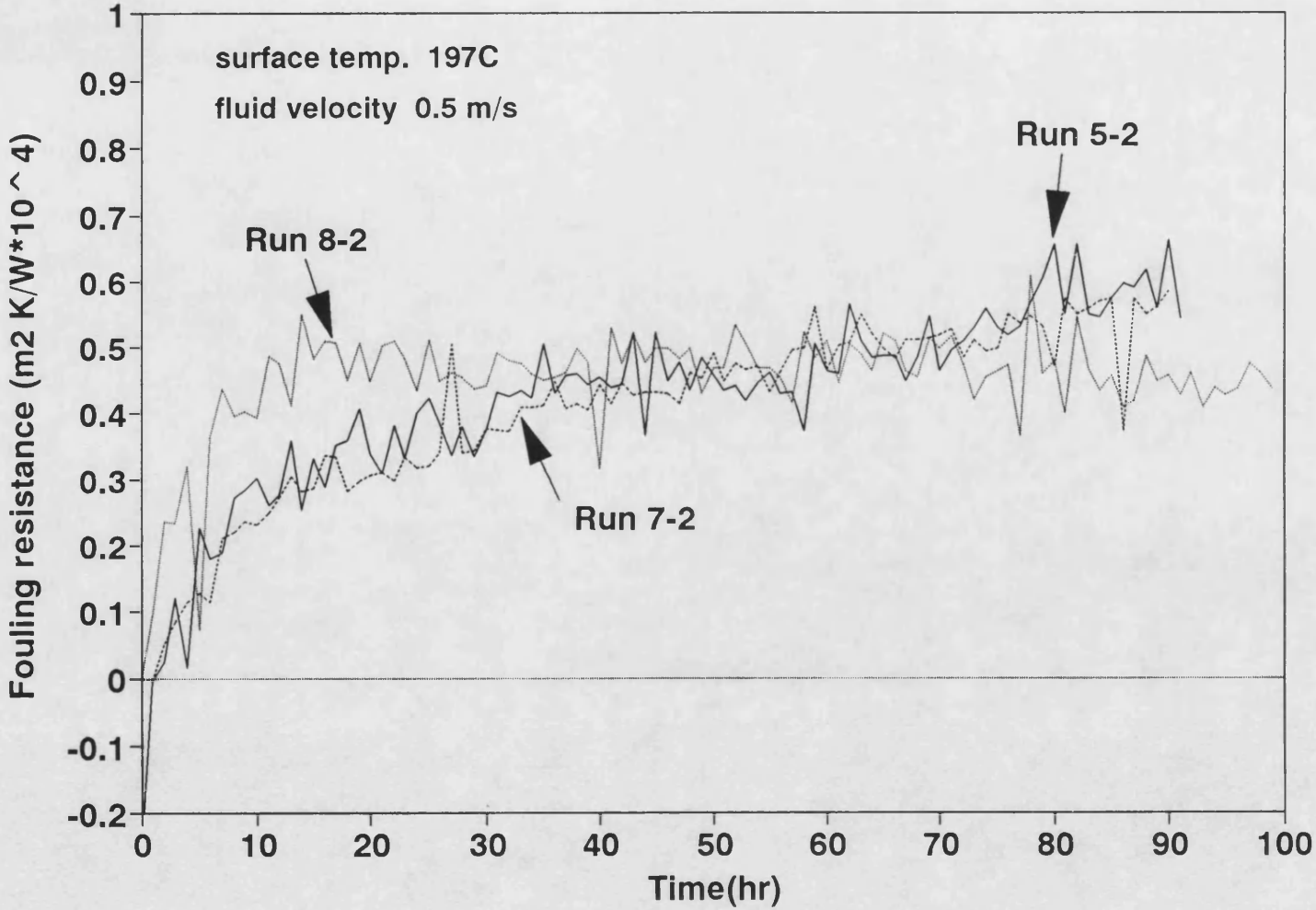

Figure 3.57 Effect of continued recirculation on fouling from Run to Run for the tube fitted with the low density insert

causes the poor reproducibility shown in Figure 3.56. That is, it is nothing to do with the chemical properties of the crude oil or constituents in it. The major difference can only be the presence of subcooled nucleate boiling in most of the bare tube Runs.

3.2.3 Reproducibility of fouling data for two identical test sections in the same Run

As explained before, good reproducibility of fouling data from Run to Run could not be anticipated due to the recycle nature of the experiments and to the continued use of the same feedstock. Therefore a check was made to ensure good reproducibility of fouling data between the two identical test sections in the same Run.

3.2.3.1 Reproducibility between two identical bare test sections

Run 3 was carried out to confirm the reproducibility between two bare tube test sections. Details have been described in Section 3.2.1.1. Figure 3.19 shows that the heat transfer coefficients , H_i, decreased identically with time and Figure 3.20 shows that the corresponding fouling resistances increased identically with time. This excellent degree of reproducibility between two identical test sections confirms that results obtained from the two parallel test sections in the same Run can be compared with confidence. This is especially encouraging in view of the apparent variability from Run to Run shown in Figure 3.56.

3.2.3.2 Reproducibility between tubes fitted with nominally identical HiTRAN inserts

The two identical test sections fitted with nominally identical HiTRAN inserts were operated under the same conditions of initial surface temperature and fluid velocity in Run 18. Details have been provided in Section 3.2.1.1. The heat transfer coefficients, H_i, and the corresponding fouling resistances are shown in Figures 3.49 and 3.50 respectively, from which some noteworthy features can be seen. Firstly, the clean heat transfer coefficients differ by about 350 W m^{-2} K^{-1}. Since wall temperature measurements were made at fixed axial locations for each test section, the heat transfer coefficients are local values rather than values averaged over the test section. Therefore, the reason for the differences shown in Figure 3.49 are believed to be due to the differences in the exact positioning of an insert in the two otherwise identical test sections.

Secondly, despite the use of the same initial surface temperature, the same velocity and nominally the same inserts, Figure 3.50 shows that the fouling resistance-time curves are not identical. The tube fitted with the insert having the higher heat transfer coefficient yields the lower fouling resistance at any time. According to the heat transfer film model, the film heat transfer coefficient is inversely proportional to the heat transfer film thickness. Thus it may be that the fouling is related in some way to the volume of fluid which is exposed to a temperature higher than that of the bulk, a simple model of hydrocarbon fouling suggested originally by Nelson (1934). This idea is developed further in Section 3.2.10 which considers

the modelling of fouling data.

3.2.4 Induction period

For Runs 1-1, 1-2, 2-2, 3-1 and 3-2, induction periods in the range of 14 to 19 hours were observed as shown in Figures 3.16, 3.18 and 3.20. However induction periods were not observed for any subsequent Runs, not even with the first use of the new test sections for Run 7 and with the use of fresh crude oil B in Run 19. Several plausible reasons for the existence of induction periods are as follows:

(1) The tube surface may require conditioning before a deposit can form or adhere.

(2) A certain amount of time may be required for foulant precursors to be formed in the bulk fluid.

(3) Roughening of a heat transfer surface by deposition may increase the film heat transfer coefficient to an extent sufficient to counteract the additional thermal resistance of the deposit itself (Crittenden and Alderman (1987)).

(4) Nucleation on the heat transfer surface may increase the film heat transfer coefficient to an extent sufficient to counteract the additional thermal resistance of the deposit itself (Shalhi (1993)).

If the first two reasons are responsible for the existence of induction periods, then after continued recirculation of feedstock for several Runs, induction periods should not be expected to occur.

It has not been possible in this study to determine which of the above mechanisms was responsible for the occurrence of induction periods. It is possible that all were involved.

3.2.5 Effect of subcooled nucleate boiling

As shown in Figure 3.56, Run 14-2, in which flow was convective, yielded a lower fouling resistance at any time than those from Runs in which subcooled nucleate boiling was occurring. The presence of subcooled nucleate boiling appears to give rise to a higher fouling resistance at any time.

Further evidence for this hypothesis exists. Runs 11-2, 13-1 and 15-1 were carried out at similar initial surface temperatures (237°C - 239°C) and the same fluid velocity (0.5 ms^{-1}) but with flows in different heat transfer regimes (Run 11-2 in the subcooled nucleate boiling regime and Runs 13-1 and 15-1 in the convective regime). Fouling resistances for these three Runs are plotted against time in Figure 3.58, from which it can be seen that a higher initial fouling rate and a higher ultimate fouling resistance seem to arise for the tube operated under the conditions of subcooled nucleate boiling. This large difference in fouling resistance is not believed to be simply due to the possible variability from Run to Run which might be caused by the reasons given in Section 3.2.2.1. The presence of subcooled nucleate boiling certainly seems to increase the fouling rate and the fouling resistance. Possible reasons are as follows:-

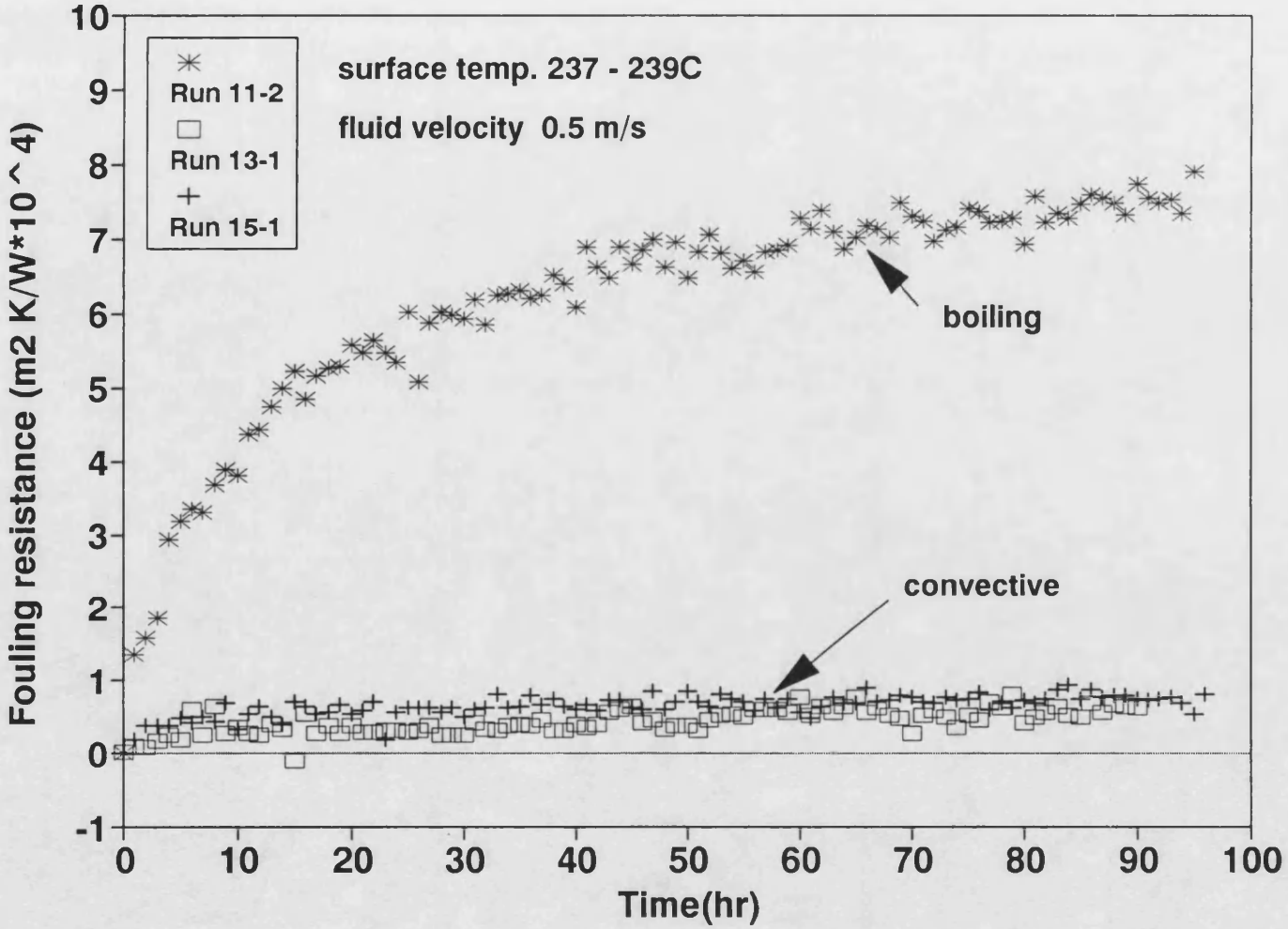

Figure 3.58 Effect of nucleate boiling on fouling for the bare tube

(1) Boiling, in general, gives rise to a higher heat flux. The heat flux for Run 11-2 (62.2 kW m^{-2}) was greater than that for Runs 13-1 and 15-1 (44.0 kW m^{-2}). In the subcooled nucleate boiling regime, therefore, the fouling rate may be increased (for otherwise similar conditions of initial surface temperature and fluid velocity) because of the higher heat flux. The cause could be the greater flow of heat through the heat transfer film.

(2) In the subcooled nucleate boiling regime, a more porous deposit (which would have a lower effective thermal conductivity and a lower density) could possibly result from the formation of bubbles close to or at the heat transfer surface. The formation of a more porous deposit would manifest itself as a higher fouling resistance for the following reason. The effective thermal conductivity of deposits may be estimated as a function of porosity using the Maxwell model:

$$k_{eff} = k_b \frac{1 + 2X - 2\psi_d (X - 1)}{1 + 2X + \psi_d (X - 1)} \qquad (3.11)$$

in which k_{eff} is the effective thermal conductivity of the deposit

k_b is the thermal conductivity of the fluid

X is the ratio of thermal conductivity of the fluid to that of the deposit (k_d), *i e* k_b/k_d

ψ_d is the fractional volume of the deposit

$$\psi_d = \frac{V_d}{V_b + V_d} \qquad (3.12)$$

in which V_d and V_b are the volumes of deposit and fluid respectively. Equation (3.11) is plotted in Figure 3.59, from which it can be seen that the effective thermal conductivity of a deposit is strongly dependent on the porosity of the deposit.

3.2.6 Effect of surface temperature

For the bare tube, Figures 3.36 and 3.42 (Runs 11 and 14, respectively, operated with the same velocity) show that the fouling rate and the initial fouling resistance increase as the initial surface temperature increases. The Arrhenius-type plot is shown in Figure 3.60 from which the activation energy for initial fouling has been computed to be about 60 kJ mol^{-1}. Values over 40 kJ mol^{-1} indicate the predominance of a chemical mechanism in the fouling process. It is important to note that Runs 14-1 and 14-2 were carried out with flow in different heat transfer regimes (Run 14-1 in the subcooled nucleate boiling regime and Run 14-2 in the convective heat transfer regime). Runs 11-1 and 11-2 were carried out with flow in the subcooled nucleate boiling regime but, due to the difference in temperatures, the degree of nucleate boiling may well have been different. As discussed in the previous Section, the presence of subcooled nucleate boiling appears to cause a higher fouling rate and a correspondingly higher fouling resistance at any time. Thus if a higher degree of nucleate boiling leads to a higher fouling rate, then the values of activation energy obtained from Runs 11 and 14 could be overestimates of those which would occur for single phase convective flow. It is important to

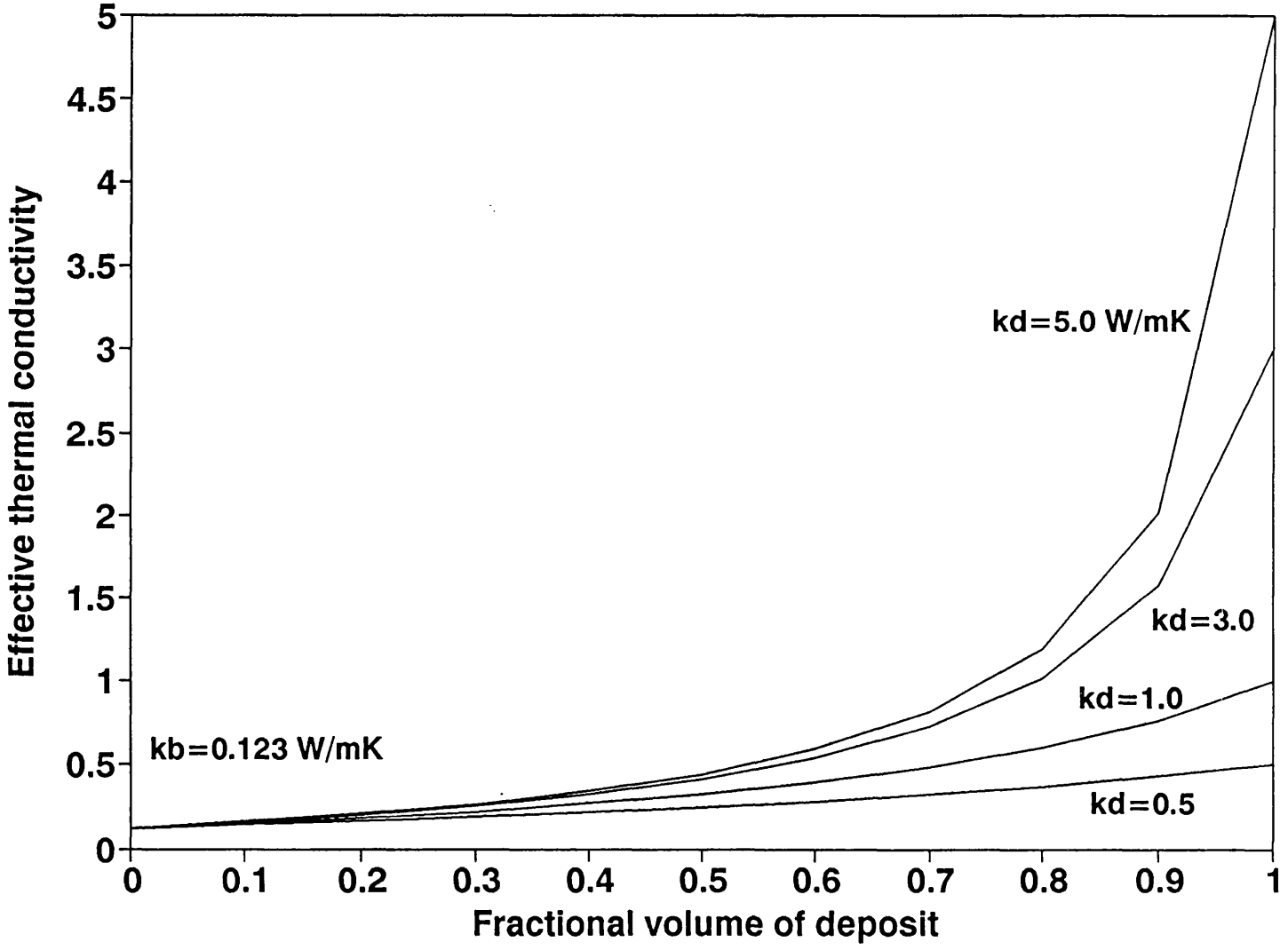

Figure 3.59 Effect of porosity of a depositon effective thermal conductivity

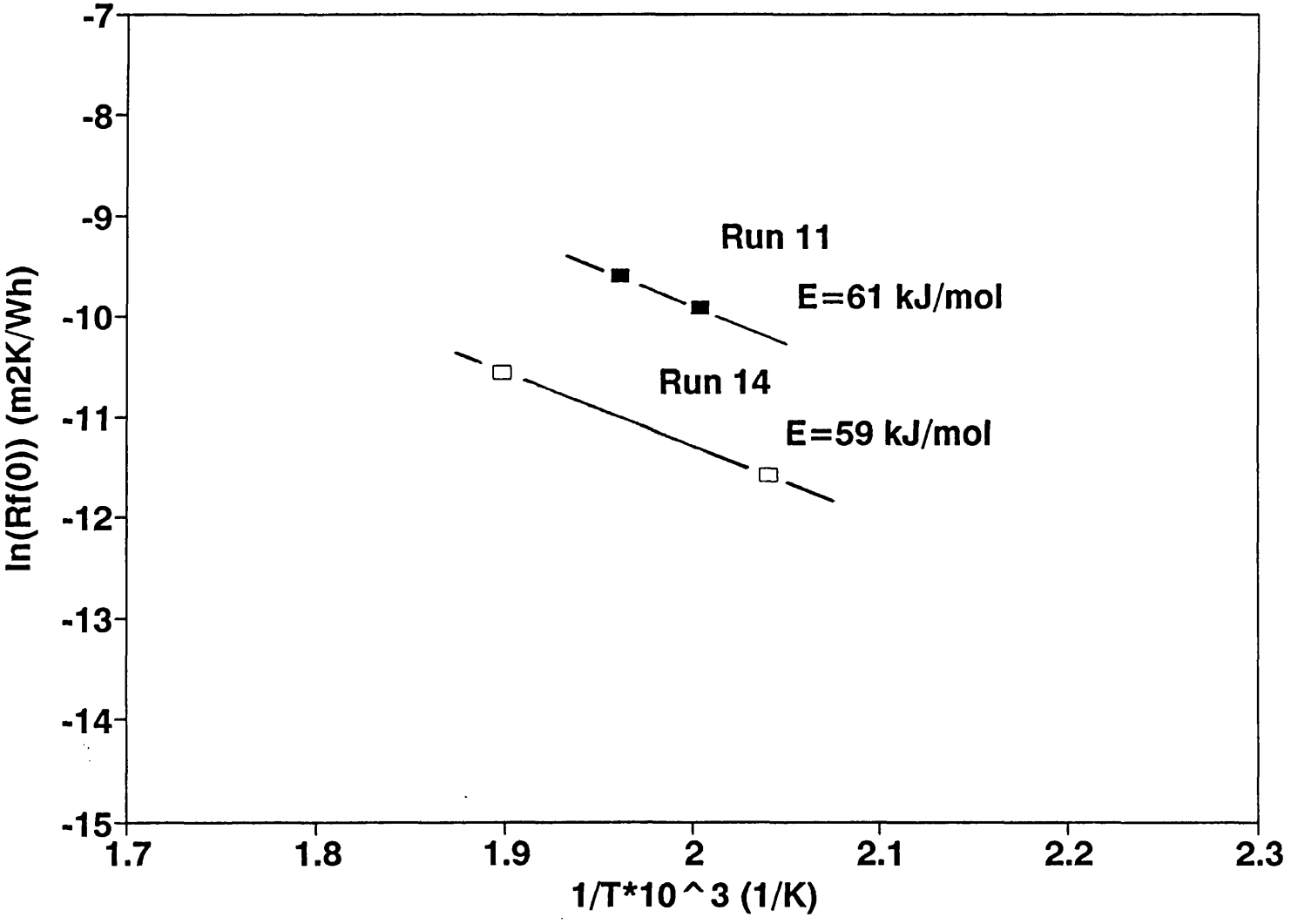

Figure 3.60 Arrhenius plot for Runs 11 and 14

note however that activation energies from other hydrocarbon fouling studies, listed in Table 3.10, are comparable with those obtained in the current study.

Table 3.10 Activation energies for chemical reaction fouling

fluid	activation energy kJ mol $^{-1}$	surface temperature range, °C	reference
sour gas oil	120	146 - 204	Watkinson and Epstein (1969)
styrene polymerisation	39	22 - 98	Crittenden *et al* (1987a)
pure n-paraffins	40	93 - 260	Taylor (1969)
liquid jet fuel	42	149 - 260	Vranos *et al* (1981)
'light' crude oil	33	160 - 280	Crittenden *et al* (1992)
'heavy' crude oil	21	160 - 280	Crittenden *et al* (1992)
light crude oil + 10% sludge	60	216 - 254	this study

In Run 12 the test sections, fitted with nominally the same inserts, were operated with flow solely in the convective regime. The data shown earlier in Figure 3.38 have been expanded and the initial stages of the experimental data are shown again in Figure 3.61. Despite the difference in the initial surface temperatures of the two test sections (224°C for Run 12-1 and 211°C for Run 12-2), the initial fouling rates seem to be similar. This seems to indicate that the activation energy is small when the inserts are present in the tubes. Lower fouling resistances (for any time) are yielded in the tube which has the higher heat transfer coefficient, despite having the higher initial surface temperature (for this Run 12-1). This result is somewhat similar to that in Run 18 and again suggests that the fouling rate may be related strongly to the heat transfer film thickness. If such a physical aspect was predominant, then a low activation energy might

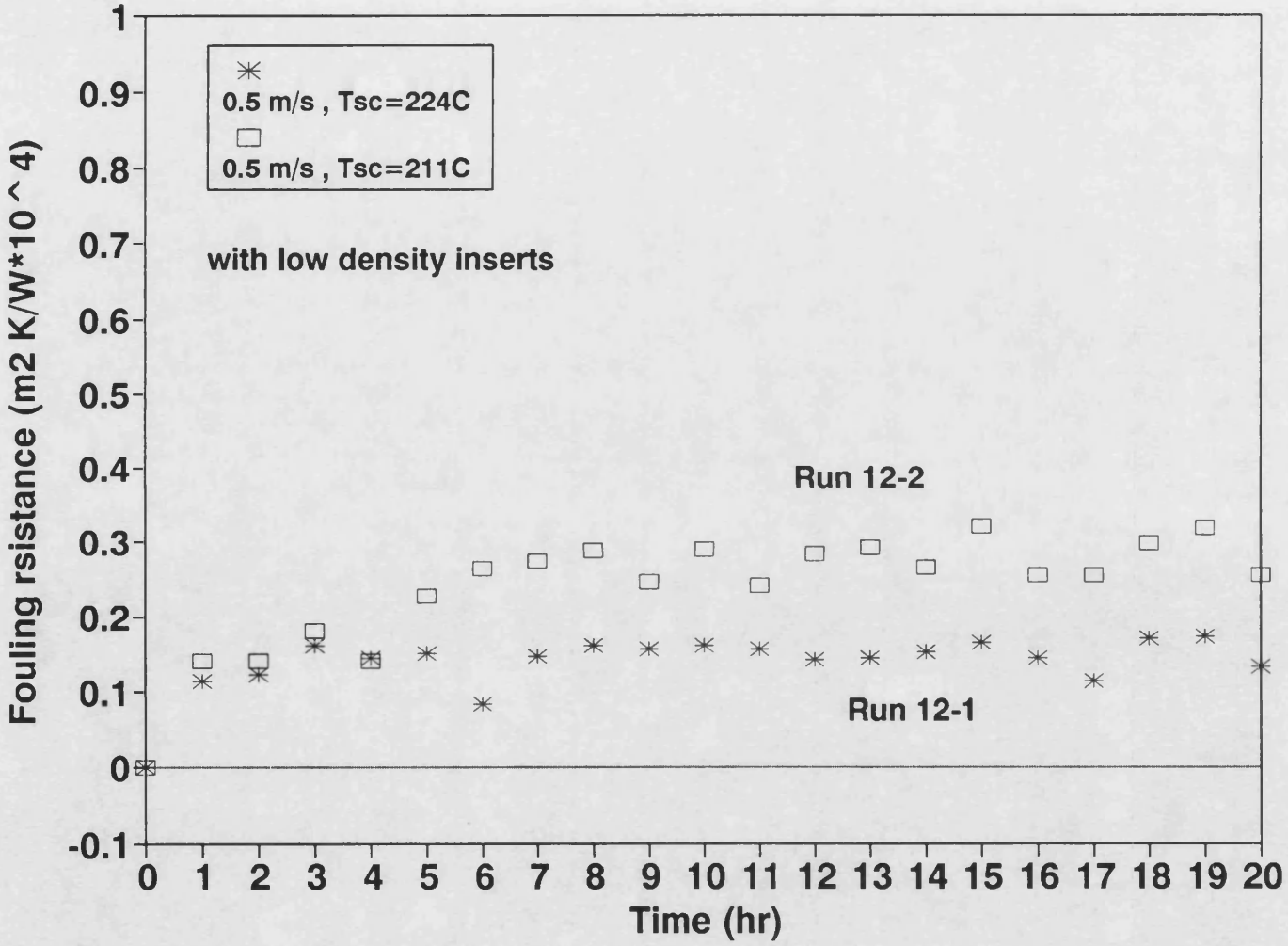

Figure 3.61 Expanded fouling resistance - time data for Run 12

indeed be expected.

3.2.7 Effect of flow velocity

The results for Runs 9, 10 and 16 (Figures 3.32, 3.34 and 3.46, respectively) revealed that the use of a higher fluid velocity is beneficial in reducing the magnitude of fouling resistance for both the bare tube (Run 9) and the tube fitted with an insert (Runs 10 and 16). In Run 10 the test section operating at the higher fluid velocity of 1.1 ms^{-1} was seemingly not fouled over the period of operation. In Run 15 for the bare tube, negative values of fouling resistance were found for the higher velocity (1.1 ms^{-1}) over the period of operation.

Data from all these runs confirm the widely held belief that fouling from hydrocarbons can be reduced by operation at increased velocity.

In Run 16 the fouling resistances were found to be small when low density inserts were present. Therefore the data are expanded and the initial stages of fouling are shown again in Figure 3.62 to confirm the effect of velocity. In both Runs 9 and 16 the fouling resistances reached asymptotic values. The operating conditions and the values of asymptotic fouling resistance and initial fouling rate are summarised in Table 3.11.

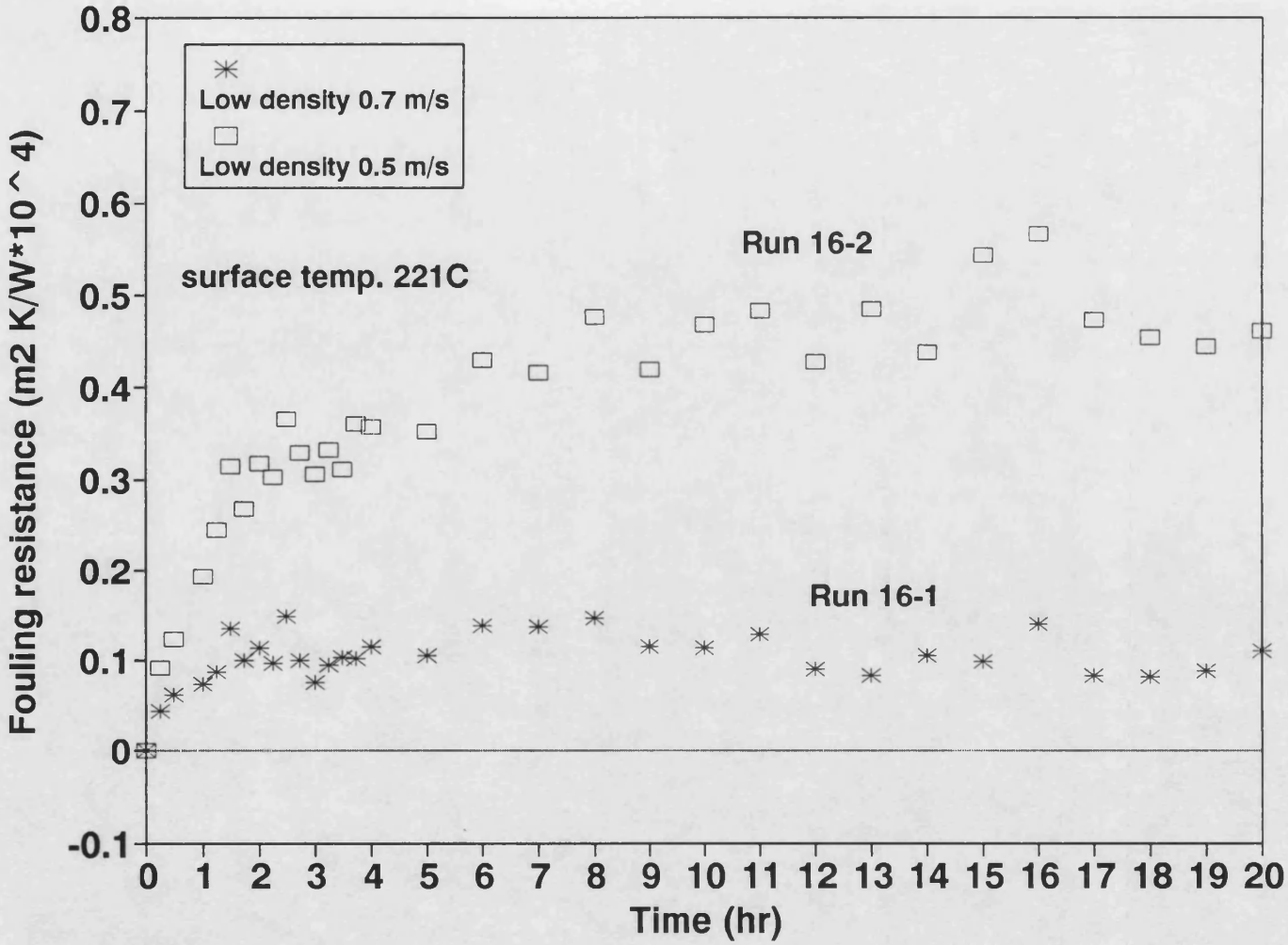

Figure 3.62 Expanded fouling resistance - time data for Run 16

Table 3.11 Effect of velocity

Run	fluid velocity (ms^{-1})	R_f* ($m^2K\ W^{-1} \times 10^4$)	initial fouling rate ($m^2K\ W^{-1}\ h^{-1} \times 10^5$)
9 - 1 (bare)	0.5	4.79	3.72
9 - 2	1.1	0.33	0.85
16 - 1 (low density)	0.7	0.11	1.00
16 - 2 (insert)	0.5	0.45	2.04

The effect of velocity on the asymptotic fouling resistance and on the initial fouling rate are shown in Figures 3.63 and 3.64 respectively, from which the values of the velocity exponent for the log-log plots have been calculated. The results are summarised in Table 3.12 and compared with data from previous studies.

Table 3.12 Velocity exponent

fluid	flow system		$R_f^{\bullet}$	initial fouling rate	reference
light crude oil with 10% waxy residue	recycle	(bare)	-3.5	- 1.9	this study
		(low density insert)	-4.2	- 2.1	
sour gas oil	recycle		-2	- 1.07	Watkinson and Epstein (1969)
crude oil	once-through		not determined	-1.77	Scarborough *et al* (1979)

In the current study, fouling in the bare tube and in the tube fitted with the low density insert seem to have reasonably similar relationships with fluid velocity. However the relationships in this study do not agree particularly well with those

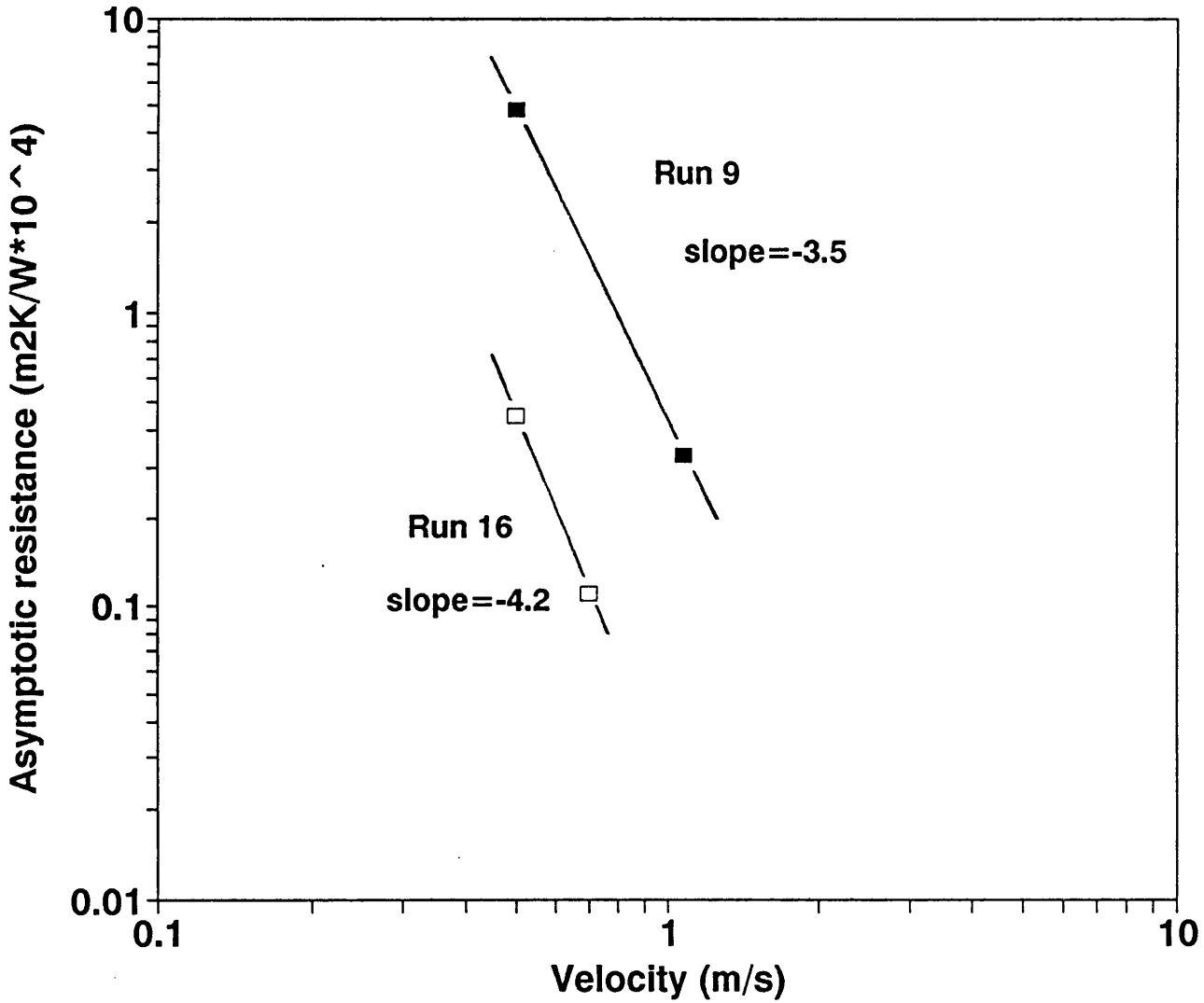

Figure 3.63 Effect of velocity on asymptotic resistance for the bare tube and for the tube fitted with the low density insert

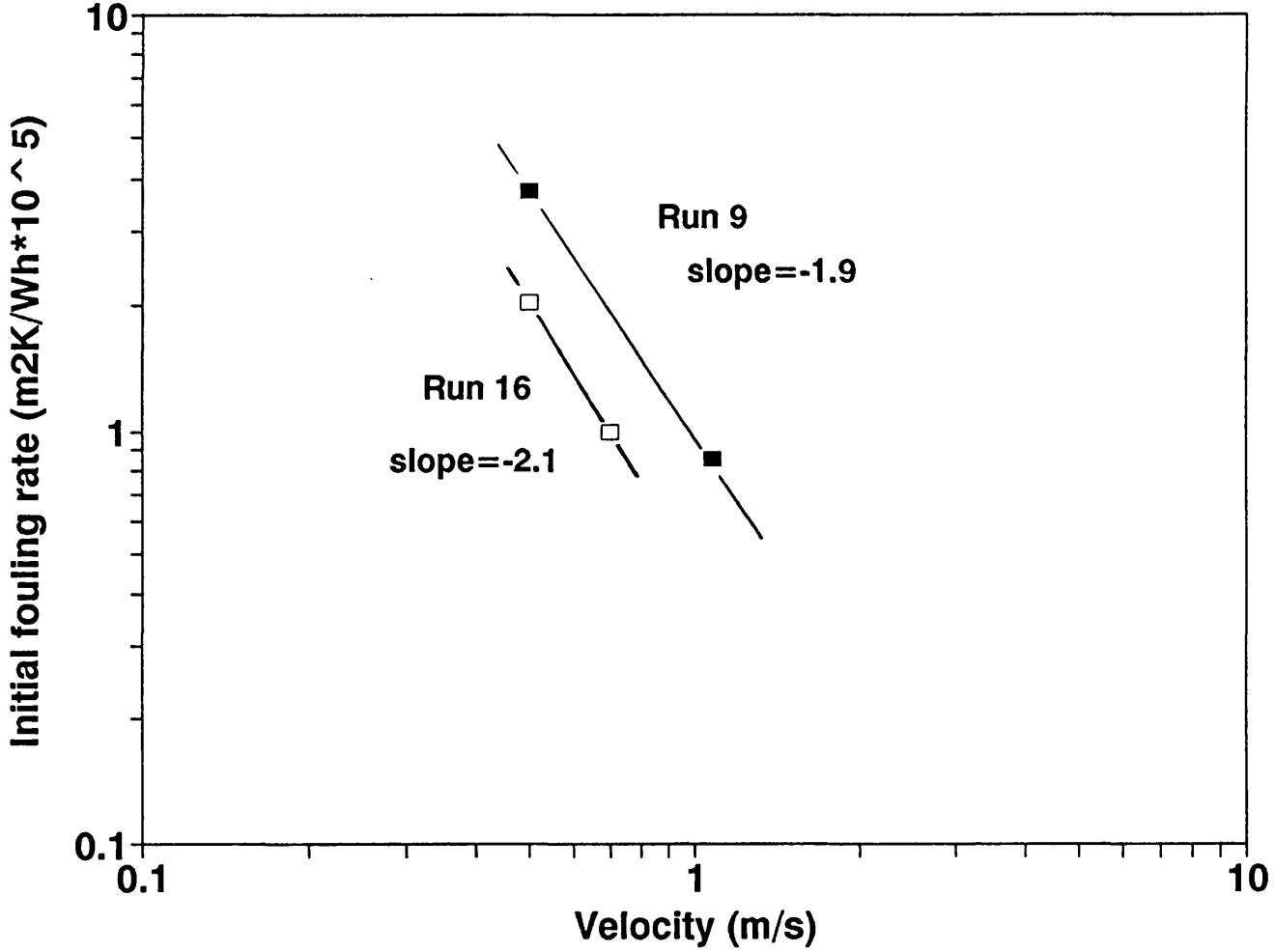

Figure 3.64 Effect of velocity on initial fouling rate for the bare tube and for the tube fitted with the low density insert

obtained by Watkinson and Epstein (1969) who worked with gas oils. Watkinson (1988) correlated the data of Scarborough *et al* (1979) who investigated the effect of velocity on crude oil coking. The correlation is shown in Table 3.12. The exponent for the initial fouling rate (-1.77) is broadly similar to that obtained for crude oil in the current study (- 1.9 to - 2.1).

3.2.8 Effect of inserts

3.2.8.1 Effect of insert as a retrofit (bare tube vs. low density insert)

For both Runs 1 and 17 the two test sections were operated under the same conditions of fluid velocity and heat flux. Figures 3.16 and 3.48 both reveal that use of the low density insert can significantly reduce the magnitude of the fouling resistance at any time. Use of the insert provides two important advantages:

(1) Since the presence of an insert increases the film heat transfer coefficient, the initial surface temperature can be reduced with the insert in place (see Table 3.7 for Runs 1 and 17). Reducing the initial surface temperature simply leads to lower chemical reaction rates which thereby decreases the fouling rate.

(2) In the presence of the insert, flow in subcooled nucleate boiling can be avoided through the reduction in the initial surface temperature (compare Run 1-1 with 1-2 and Run 17-1 with 17-2 in Table 3.7). It has been noted

before (see Section 3.2.5) that the presence of subcooled nucleate boiling seems to give rise to an increased fouling rate.

3.2.8.2 Comparison under the same conditions of surface temperature and fluid velocity (bare tube vs. low density insert)

For Runs 2, 8, 13 and 19 the two test sections were operated at the same conditions of initial surface temperature and fluid velocity. In Runs 2 and 8 the test section fitted with the insert was ultimately less fouled than that left bare (Figures 3.18 and 3.30). In Run 13 the presence of the insert seems to have increased the initial fouling rate (see Table 3.5 and 3.40). However the probable explanation for this has been give in Section 3.2.1.1. Ultimately, the tube fitted with the insert in Run 13 provided the lower fouling resistance.

It could be argued that the ability of the insert to reduce fouling was relatively poor for Runs 8 and 13 and that perhaps the insert was promoting the rates of mass transfer of foulant precursors to the hot surface. Runs 8 and 13 were carried out with flow solely in the convective regime and at the relatively low flow velocity (0.5 ms^{-1}), the corresponding Reynolds number was about 6800. For the bare tube under such conditions, the rate controlling step in deposition could perhaps be governed to some extent by the mass flux of precursors to the wall. Under such circumstances the presence of an insert (and perhaps even the presence of subcooled nucleate boiling for a bare tube) might increase the mass flux of precursors to the hot wall. In Runs 8 and 13 the initial fouling rate for

the bare tube with its lower degree of turbulence would accordingly be less rapid than that for the tube fitted with the insert. Run 13 was carried out at a higher initial surface temperature (239°C) than Run 8 (197°C). Since a mass transfer rate is less sensitive to temperature than a chemical reaction rate, the difference in the initial fouling rates between Runs 13-1 and 13-2 should be larger than that between Runs 8-1 and 8-2. This was indeed the case (see Table 3.7).

Whether this argument is valid or not, it should be borne in mind that the fouling resistances found for both Runs 8 and 13 were low, whether the insert were installed or not. This provides further evidence of fouling control by the avoidance of subcooled nucleate boiling.

In contrast, Run 2 was carried out with flow in the subcooled nucleate boiling regime and perhaps the initial fouling rates for both test sections were being controlled by the chemical kinetics. In this case, it would be expected that the initial fouling rate for the tube fitted with the insert would be lower, as confirmed in Table 3.7 and Figure 3.18. If the hypothesis is correct, one of the reasons for the large increase in the initial fouling rate when flow is in the subcooled nucleate boiling regime (for otherwise the same conditions of initial surface temperature and fluid velocity) could be the difference in the rate controlling step. The experiments in the current study were conducted at Reynolds numbers which are somewhat lower than those which are typically used in the hydrocarbon processing industries. Therefore for convective flow in a bare tube at Reynolds numbers well in excess of 10000, mass transfer of precursors may not become the rate

controlling step in the deposition process. This would be the case if the surface temperature were not too high and the chemical reaction rate were relatively low at moderate temperatures.

Run 19, in which fresh crude oil B was used, was carried out with flow in the convective regime. The results (Table 3.7 and Figure 3.52) show that the fouling rate with the insert in place is lower than that for the bare tube. Enhanced mass transfer of precursors seems not to have occurred with the insert and reaction kinetics therefore seem to control the rate determining step in deposition. This effect may be due to a difference in composition of precursors which participate in the fouling process. It is possible that when sludge is present in the crude oil (as for Runs 1 to 18), relatively large molecules such as waxes and asphaltenes could act as important precursors and their transport to the hot surface may be responsible for the deposition process.

3.2.8.3 Effect of insert loop density (low vs. high)

A greater reduction in fouling rate with a higher loop density insert has been found. The results for Run 7 (Table 3.7 and Figure 3.28) which was carried out under the same conditions of initial surface temperature (197°C) and fluid velocity (0.5 ms^{-1}) indicate that the higher turbulence created by the higher loop density insert seems to be more beneficial in reducing the fouling rate. The insert with the higher film coefficient has yielded the lower fouling resistance, an aspect of great significance in the model developed in Section 3.2.10. Further

evidence is provided by Run 6 (the same clean surface temperature and fluid velocity) and by Run 5, although in this latter case the heat fluxes and velocities were the same, *ie* the surface temperature for the tube fitted with the high density insert was lower at 186°C than that for the tube fitted with the low density insert at 197°C.

3.2.9 Mechanism(s) for reducing the fouling rate

The effect of an insert is not simply one of reducing the surface temperature. It appears that the presence of an insert can alter the hydrodynamics in the tube in a beneficial manner, possibly in a manner similar to that caused by the use of a higher velocity. A greater reduction in fouling appears to occur with an insert of higher loop density and a tube with a higher film heat transfer coefficient provides a lower fouling resistance for the same initial surface temperature. These observations indicate that the fouling rate could be related to the film heat transfer coefficient and thereby to the thickness of the thermal boundary layer.

Another important mechanism for the reduction in fouling rate appears to be the avoidance of subcooled nucleate boiling.

The additional turbulence close to the heat transfer surface generated either by the presence of an insert or by the use of a high velocity could provide four advantageous effects:

(i) A reduction in the volume of the fluid which is heated to a temperature higher than that of the bulk fluid.

(ii) A reduction in the residence time of fouling precursors in the fluid which is exposed to a hot surface.

(iii) An increase in the rate of removal or release of deposits at or close to the wall.

(iv) A suppression of nucleation.

3.2.10 Fouling model for the bare tube and the tube fitted with an insert

For the sake of simplicity the following assumptions are made:

(i) The fouling reaction is assumed to occur only throughout the region of the fluid which is exposed to a temperature higher than that of the bulk fluid, *i.e* in the region of the thermal boundary layer.

(ii) The production rate of foulant materials is proportional to the residence time of the fluid in the thermal boundary layer.

(iii) Fouling occurs through a single reaction mechanism and the reaction is of first order.

(iv) The concentration of fouling precursors in the bulk fluid remains constant with time.

(v) Properties of the deposit do not change as fouling proceeds

3.2.10.1 Deposition

The initial rate of fouling is expressed in terms of a mass production rate and the properties of the deposit.

$$\frac{dR_f}{dt} = \frac{1}{\rho_d k_d} N_f \quad (m^2K\ W^{-1}s^{-1}) \tag{3.13}$$

in which N_f is the mass flux of foulant (kg m^{-2} s^{-1})

ρ_d is the density of the deposit (kg m^{-3})

k_d is the thermal conductivity of the deposit ($Wm^{-1}K^{-1}$)

Under the above assumptions it is proposed that N_f may be expressed as:

$$N_f = A\int_o^{\delta_T} \theta\ (x)\ C_p\ (x)\ \exp\left(-\frac{E}{RT\ (x)}\right) dx \tag{3.14}$$

in which C_p (x) is the concentration of precursors at the position x from the wall (kg m^{-3})

θ (x) is the residence time at the position x from the wall (s)

E is the activation energy (kJ mol^{-1})

R is the gas constant (kJ mol^{-1} K^{-1})

T (x) is the temperature at the position x from the wall (K)

A is a constant (s^{-2})

δ_T is the thickness of the thermal boundary layer (m)

The concentration profile of fouling precursors in the diffusion boundary layer may be expressed in a similar manner to that for the absorption of gases with simultaneous chemical reaction.

$$D_p \frac{\partial^2 C_p(x)}{\partial x^2} = A\theta(x)\ C_p\ (x)\ \exp\left(-\frac{E}{RT\ (x)}\right) \qquad (3.15)$$

in which D_p is the diffusivity of precursors ($m^2\ s^{-1}$)

Boundary conditions are as follows:

At the fluid-wall interface (x= 0)

$$\left(\frac{d\ C_p(x)}{dx}\right)_{x\ -\ 0} = 0 \qquad (3.16)$$

At the diffusion boundary thickness, δ_m

$$C_p = C_{pb} \qquad (3.17)$$

in which C_{pb} is the concentration of precursors in the bulk fluid ($kg\ m^{-3}$)

The thickness of the thermal boundary layer δ_T can be related to the film heat transfer coefficient, h_i by the film model:

$$\delta_T = \frac{k_f}{h_i} \quad (m) \tag{3.18}$$

in which k_f is the thermal conductivity of the fluid ($Wm^{-1}\ K^{-1}$)

The thickness of the diffusion boundary layer may be estimated from a simple heat and mass transfer analogy:

$$\delta_m = \delta_T \left(\frac{Pr}{Sc}\right)^{1/3} \quad (m) \tag{3.19}$$

The residence time of precursors in the thermal boundary layer may be taken to be inversely proportional to be velocity of the fluid in the layer.

$$\theta\ (x) = \frac{\beta_1}{V(x)} \quad (s) \tag{3.20}$$

in which V(x) is the velocity of the fluid at the position x from the wall (ms^{-1}) and β_1 is a constant (m).

Using equations (3.13), (3.14) and (3.20), the initial rate of fouling is given by:

$$\frac{dR_f}{dt} = \frac{\beta_1 A}{\rho_d k_d} \int_0^{\delta_T} \frac{C_p(x)}{V(x)} \exp\left(- \frac{E}{RT(x)} \right) dx \qquad (3.21)$$

If the velocity and temperature profiles in the layer and the reaction kinetic data are known, then the initial rate of fouling may be solved numerically using equation (3.21). C_p (x) would need to be obtained from equation (3.15).

Since the reaction rate can be considered to be very slow for fouling from crude oil and therefore kinetically controlled, the concentration of precursors in the thermal boundary layer can be assumed to be constant (Finlayson, (1980)). In this case equation (3.15) need not be incorporated and equation (3.21) becomes

$$\frac{dR_f}{dt} = \frac{\beta_1 A\, C_{pb}}{\rho_f k_f} \int_0^{\delta_T} \frac{1}{V(x)} \exp\left(- \frac{E}{RT(x)} \right) dx \qquad (3.22)$$

Unfortunately the velocity profile for a tube fitted with an insert is not available. Thus the following assumptions with respect to the velocity profile are made:

(i) The thickness of the momentum boundary layer is equal to the thickness of the thermal boundary layer.

(ii) The velocity of the fluid decreases to zero at the wall.

(iii) The velocity profile is linear in the thermal boundary layer.

With the above assumptions, the velocity profile in the thermal boundary layer is then given by:

$$V(x) = \frac{x}{\delta_T} V_m \qquad (3.23)$$

in which V_m is the mean velocity of the fluid based on d_i (ms^{-1})

Equation (3.22) is normalised in terms of the distance x, starting from y = 0 at the surface and proceeding to y = 1 at the edge of the thermal boundary layer. Then:

$$\frac{dR_f}{dt} = \frac{\beta_1 A\, C_{pb}}{\rho_d\, k_d} \cdot \frac{\delta_T}{V_m} \int_0^1 \frac{1}{y} \exp\left(- \frac{E}{RT(y)} \right) dy \qquad (3.24)$$

where

$$x = \delta_T\, y \qquad (3.25)$$

Using equation (3.18), equation (3.24) is expressed as:

$$\frac{dR_f}{dt} = \pi_1 = \frac{\beta_1 A\, C_{pb}\, k_f}{\rho_d\, k_d} \frac{1}{h_i V_m} \int_0^1 \frac{1}{y} \exp\left(-\frac{E}{RT(y)} \right) dy \qquad (3.26)$$

Equation (3.26) shows that the initial fouling rate is inversely proportional to both the film heat transfer coefficient and the mean velocity of the fluid. Assuming that for a bare tube the film heat transfer coefficient depends on velocity raised

to the power 0.8, equation (3.26) shows that the dependency of the initial fouling rate on bulk velocity is expected to be to the power -1.8. This is in good agreement with the experimental value of -1.9 reported in Table 3.12 (Section 3.2.7)

3.2.10.2 Deposit removal

Kern and Seaton (1959) originally proposed that a deposit may be removed from a wall by the shearing action of the fluid. In such a mechanism the removal rate was assumed to be proportional to both the shear stress at the wall and the thickness of the deposit. Thus,

$$removal\ rate = -\frac{\tau x_d}{\psi k_d} \qquad (3.27)$$

in which x_d is the deposit thickness (m)

τ is the shear stress at the wall (Nm^{-2})

ψ is a function of deposit structure introduced by Taborek *et al* (1972)

Assuming that within the momentum boundary layer transport is by molecular processes only, the shear stress at the wall is given by equation (3.28) in which μ_f is the viscosity of the fluid based on the film temperature.

$$\tau = \mu_f \left(\frac{\partial V(x)}{dx} \right)_{x=0} \tag{3.28}$$

Applying the same assumptions in terms of velocity profile in the boundary layer, as made in Section 3.2.10.1,to equation (3.28), the shear stress at the wall may be expressed as:

$$\tau = \frac{\mu_f V_m}{\delta_T} \quad (Nm^{-2}) \tag{3.29}$$

Using equations (3.18) and (3.29), the removal rate may be written as:

$$removal\ rate = -\beta_2 h_i V_m R_f = -\pi_2 R_f \tag{3.30}$$

in which

$$\beta_2 = \frac{\mu_f}{\psi k_d k_f} \tag{3.31}$$

3.2.10.3 Overall deposition rate

The net deposition rate of foulant may be expressed as the difference between the deposition rate and the removal rate

$$\frac{dR_f}{dt} = \pi_1 - \pi_2 R_f \tag{3.32}$$

Integration of equation (3.32) gives:

$$R_f = \frac{\pi_1}{\pi_2}\left(1 - \exp\left(-\pi_2 t\right)\right) \tag{3.33}$$

The asymptotic fouling resistance, R_f^*, is given by:

$$R_f^* = \frac{\pi_1}{\pi_2} \tag{3.34}$$

Using equations (3.26) and (3.30), it follows that:

$$R_f^* = \beta_3 \frac{1}{(h_i * V_m)^2} \int_0^1 \frac{1}{y} \exp\left(-\frac{E}{RT(y)}\right) dy \tag{3.35}$$

in which

$$\beta_3 = \frac{\psi \beta_1 A C_{pb} k_f^2}{\mu_f \rho_d} \tag{3.36}$$

Assuming that for a bare tube the film heat transfer coefficient depends on velocity raised to the power 0.8,equation (3.35) shows that the dependency of the asymptotic fouling resistance on bulk velocity is expected to be to the power -3.6. This is in good agreement with the experimental value of -3.5 reported in Table 3.12 (Section 3.2.7)

3.2.11 Testing the fouling model

The experimental results are now compared with the model equations.

3.2.11.1 Initial fouling rate

From equation (3.26) the ratio of the initial fouling rates for two test sections in the same Run is given by equation (3.37):

$$\frac{\left(\frac{dR_f}{dt}\right)_1}{\left(\frac{dR_f}{dt}\right)_2} = \frac{\frac{1}{h_{i1}V_{m1}}\int_0^1 \frac{1}{y}\exp\left(-\frac{E}{RT_1(y)}\right)dy}{\frac{1}{h_{i2}V_{m2}}\int_0^1 \frac{1}{y}\exp\left(-\frac{E}{RT_2(y)}\right)dy} \qquad (3.37)$$

For the same bulk temperature and the same initial surface temperature for the two test sections, equation (3.37) is reduced to:

$$\frac{\left(\frac{dR_f}{dt}\right)_1}{\left(\frac{dR_f}{dt}\right)_2} = \frac{\frac{1}{h_{i1}V_{m1}}}{\frac{1}{h_{i2}V_{m2}}} \qquad (3.38)$$

Rearranging, it follows that:

$$\frac{\left(\frac{dR_f}{dt}\right)_1}{\left(\frac{dR_f}{dt}\right)_2} * \frac{(h_{i1} * V_{m1})}{(h_{i2} * V_{m2})} = 1 \qquad (3.39)$$

In Figure 3.65 the ratio of the experimental initial fouling rates is plotted against the ratio of (h_i * V_m). The relationship predicted by equation (3.39) is also shown on Figure 3.65. Although there are few exceptions (notably Runs 8 and 13), in general, the results are in good agreement with those predicted by equation (3.39). The anomalous nature of the fouling resistance-time data for Run 13 has been accounted for in Sections 3.2.1.1and 3.2.8.2. The data point for Run 13 shown in Figure 3.65 should not be considered.

3.2.11.2 Asymptotic fouling resistance

The ratio of asymptotic fouling resistances for two parallel test sections in the same Run is obtained from equation (3.35). Thus

$$\frac{R_{f1}^*}{R_{f2}^*} = \frac{\beta_3 \frac{1}{(h_{i1} * V_{m1})^2} \int_0^1 \frac{1}{y} \exp\left(- \frac{E}{RT}(y) \right) dy}{\beta_3 \frac{1}{(h_{i2} * V_{m2})^2} \int_0^1 \frac{1}{y} \exp\left(- \frac{E}{RT(y)} \right) dy} \qquad (3.40)$$

For the same bulk temperature and the same initial surface temperature for the two test sections equation (3.40) reduces to:

$$\frac{R_{f1}^*}{R_{f2}^*} = \frac{(h_{i2} V_{m2})^2}{(h_{i1} V_{m1})^2} \qquad (3.41)$$

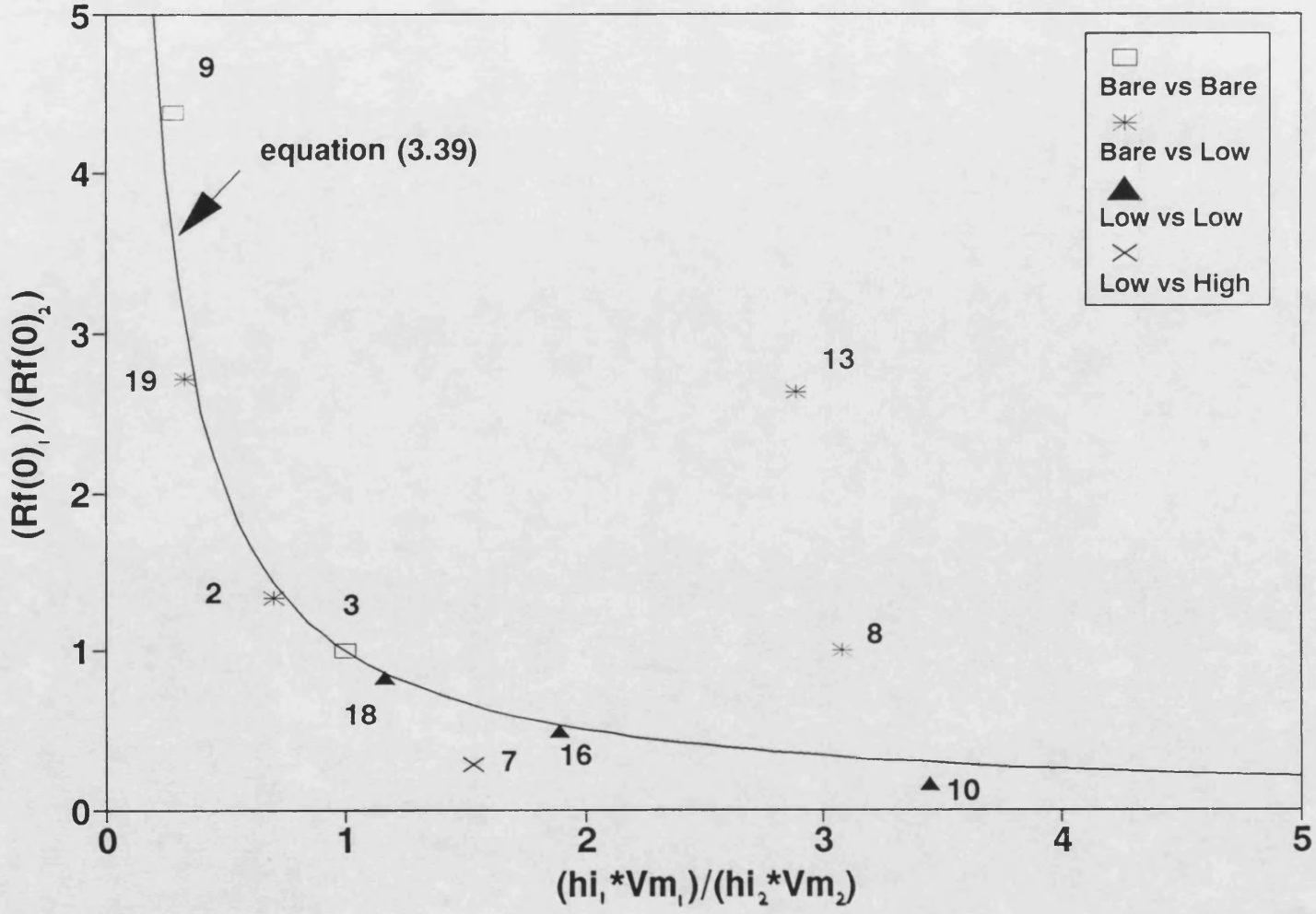

Figure 3.65 Relationship of the ratio of initial fouling rate with the ratio of product of heat transfer coefficient and mean fluid velocity

Rearranging equation (3.41) gives

$$\frac{R_{f1}^*}{R_{f2}^*} * \left(\frac{h_{i1} * V_{m1}}{h_{i2} * V_{m2}}\right)^2 = 1 \qquad (3.42)$$

Values of the asymptotic fouling resistance for Runs in which the two parallel test sections were operated at the same initial surface temperature are summarised in Table 3.13. In the cases where the fouling resistances seemed not to have reached asymptotic values, the fouling resistances at the end of Run are given in the Table.

The ratio of experimental asymptotic fouling resistances is plotted against the experimental ratio of $(h_i * V_m)^2$ in Figure 3.66. The relationship predicted by equation (3.42) is also shown in Figure 3.66. The experimental results agree well with those predicted by equation (3.42).

Equation (3.42) shows the dependency of the asymptotic fouling resistance on the important process variables of velocity and film heat transfer coefficient. Reducing the asymptotic fouling resistance can be achieved in one or both of two ways for a given surface temperature:

(1) increasing the bulk flow velocity (which increases both h_i and V_m)

(2) installing an insert (which increases h_i)

Table 3.13 Asymptotic fouling resistances

Run no	test section		surface temp.(C)	velocity (m/s)	clean hi (W/m2K)	Rf* (m2K/W)
2	1	Bare	217	0.5	1130	2.49E-04*)
	2	Low	217	0.5	1380	1.92E-04
3	1	Bare	217	0.5	1130	4.35E-04*)
	2	Bare	217	0.5	1130	4.62E-04*)
7	1	High	197	0.5	3390	0.20E-04
	2	Low	197	0.5	2200	0.57E-04
8	1	Bare	197	0.5	725	0.50E-04
	2	Low	197	0.5	2230	0.43E-04
9	1	Bare	217	0.5	870	4.79E-04
	2	Bare	217	1.1	1430	0.33E-04
10	1	Low	203	1.1	3600	0.02E-04
	2	Low	203	0.5	2230	0.62E-04
13	1	Bare	239	0.5	720	0.65E-04
	2	Low	239	0.5	2080	0.18E-04
16	1	Low	221	0.7	2900	0.11E-04
	2	Low	221	0.5	2150	0.45E-04
18	1	Low	218	0.5	2520	0.17E-04
	2	Low	218	0.5	2170	0.50E-04
19	1	Bare	217	0.5	740	0.62E-04
	2	Low	217	0.5	2250	0.22E-04

*) not asymptotic value

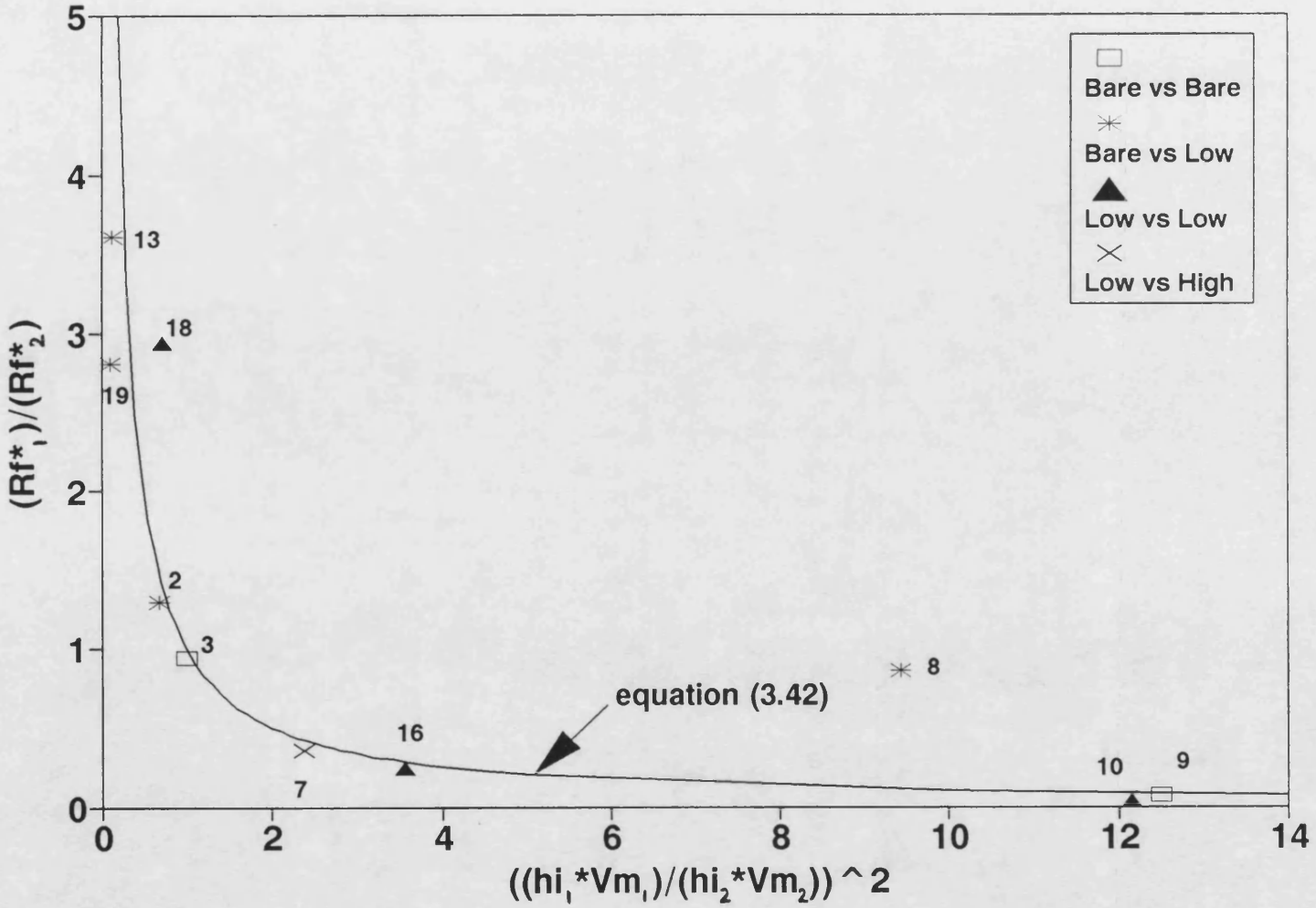

Figure 3.66 Relationship of the ratio of asymptotic fouling resistance with the ratio of (hi*Vm) ^ 2

Equation (3.42) therefore allows the designer or process engineer to explore alternative combinations of fluid velocity and insert configuration which provide an acceptable level of ultimate fouling. Factors such as pressure drop and the cost of installing inserts need to be taken into account in such a process optimisation.

Regrettably it has not been possible to test the model against the effect of a change in surface temperature. Nonetheless it appears that without an insert present the activation energy of the initial fouling process is around 60 kJ mol^{-1}. Since installation of an insert can reduce the surface temperature when crude oil is being heated, an additional reduction in fouling rate must be expected.

The successful testing of the model described above demonstrates its versatility. The data shown in Figures 3.65 and 3.66 have been derived from experiments in which

(1) flow has been purely convective or subcooled nucleate boiling

(2) inserts have not been used, or

(3) inserts of two different densities have been fitted

(4) bulk velocities have ranged from 0.5 ms^{-1} to 1.1 ms^{-1}

(5) initial surface temperatures have ranged from 197°C to 239°C

(6) two different crude oils, one containing 10% by weight of crude storage tank sludge, have been used.

Success with such a wide range of operating parameters augurs well for the success of the model for more general application, at least with crude oil heating. Clearly much more testing is required. To give credit, the original concept developed by Nelson in 1934 deserves much more attention for hydrocarbon fouling than has been paid in the past two decades.

4. CONCLUSIONS

The principal conclusions of this study are as follows:

1. Low density and high density HiTRAN inserts can increase the film heat transfer to crude oil over that of the bare tube case by 3.3 and 5.0 times respectively at a Reynolds number of about 7000. The concomitant increase in the pressure drop is 12 times and 60 times that of the bare tube, respectively. Increases in the heat transfer factor due to the presence of the insert are accompanied by larger percentage increases in the friction factor over the range of the Reynolds number tested ($7000 < Re < 40000$).

2. A higher surface temperature causes a higher fouling rate and fouling resistance with the crude oil tested. The activation energy is estimated to be around 60 kJ mol $^{-1}$ for the bare tube. However such a value relates to fouling in the presence of nucleation on the surface and may well be an overestimate for a purely convective flow regime.

3. Use of a higher velocity is beneficial in reducing the fouling rate with the crude oil tested. The initial fouling rates for both the bare tube and the tube fitted with the low density insert are found to vary inversely with the velocity of the fluid raised to the power of about two.

4. The presence of surface nucleation certainly seems to increase the fouling

rate and the fouling resistance for a given surface temperature. The increased fouling rate may be due to the higher heat flux, the formation of a more porous deposit (which would manifest itself as a higher fouling resistance) and/or the degassing of oxygen on the hot surface. Avoidance of nucleation results in a reduced fouling rate.

5. For a given heat flux, bulk temperature and flowrate, the HiTRAN insert increases the film heat transfer coefficient and thereby reduces the initial surface temperature. This leads to lower chemical reaction rates and hence to decreases in the fouling rate. Also, through the reduction in surface temperature, nucleation can be suppressed, which in itself can lead to a lowering of the fouling rate. Even for a given initial surface temperature and flowrate, the fouling rate with an insert present appears to be lower than that for the tube left bare. Thus it appears that the presence of an insert alters the hydrodynamics in a beneficial manner.

6. For a given surface temperature and flowrate, a lower fouling rate has been found to occur with an insert of higher loop density. This effect is presumably caused by a greater degree of turbulence close to the heat transfer surface with the higher density insert.

7. Possible mechanisms for the reduction in the fouling rate caused either by the presence of an insert or by the use of a higher velocity include:

(i) A reduction in the volume of the fluid which is heated to a temperature higher than that of the bulk fluid.

(ii) A reduction in the residence time of fouling precursors in the fluid which is exposed to a hot surface.

(iii) An increase in the rate of removal or release of deposits at or close to the wall due to increased fluid shear.

(iv) A suppression of nucleation

8 The following equation, applicable equally to the bare tube and to the tube fitted with an insert, is proposed to account for the initial rate of fouling from the crude oil:

$$\left(\frac{dR_f}{dt}\right)_{t-o} = \frac{\beta_1 A C_{pb} k_f}{\rho_d k_d} \frac{1}{h_i V_m} \int_0^1 \frac{1}{y} \exp\left(-\frac{E}{RT(y)}\right) dy$$

This equation indicates that the initial fouling rate is inversely proportional to both the film heat transfer coefficient and the mean velocity of the fluid. The ratio of the initial experimental fouling rates for the two parallel test sections (when operated with the same bulk temperature and the same initial surface temperature) correlates well with the ratio of the products of h_i and V_m in accordance with the model equation given above. This good correlation is supportive of one of the earliest film-based models of hydrocarbon fouling proposed by Nelson (1934), the principles of which have been recently been embodied in a reaction fouling model to account for

milk fouling (Patterson and Fryer, (1988)).

9. Incorporation of the equation given above into the Kern and Seaton model of fouling followed by integration provides an expression for the variation of fouling resistance with time. The asymptotic fouling resistance is given by

$$R_f^* = \frac{\beta_3}{(h_i^* V_m)^2} \int_0^1 \frac{1}{y} \exp\left(- \frac{E}{RT(y)} \right) dy$$

The ratio of the asymptotic fouling resistances for the two parallel test sections (when operated with the same bulk temperature and the same initial surface temperature) correlates well with the ratio of the square of the product of h_i and V_m in accordance with the model equation given above. This good correlation further supports the vision of Nelson (1934).

10. Assuming that for a bare tube the film heat transfer coefficient depends on velocity raised to the power 0.8, the equations in conclusions 8 and 9 show that the dependencies of the initial fouling rate and the asymptotic fouling resistance on velocity are to the powers -1.8 and -3.6, respectively. These values correspond very well with those found experimentally, albeit from limited data.

11. The model shows that the asymptotic fouling resistance can be reduced in

one or both of two ways for a given surface temperature. Firstly, increasing the bulk flow velocity increases both h_i and V_m. Secondly, installing an insert increases h_i. The model therefore allows the design or process engineer to explore alternative combinations of fluid velocity and insert configuration which provide an acceptable level of ultimate fouling, whilst maintaining an acceptable pressure drop and capital investment.

12. It has not been possible in the time available to test the model against the effect of surface and bulk temperatures. Nonetheless it appears that without an insert present the activation energy for the initial fouling process is about 60 kJ mol^{-1}. Since installation of an insert can reduce the surface temperature when crude oil is being heated, an additional reduction in fouling rate must be expected.

13. The model has been applied to a range of experiments in which

(i) flow has been purely convective or subcooled nucleate boiling

(ii) inserts have not been used, or

(iii) inserts of two different densities have been fitted

(iv) bulk velocities have ranged from 0.5 to 1.1 ms^{-1}

(v) initial surface temperatures have ranged from 197 to 239°c

(vi) two different crude oils, one containing 10% by weight of crude storage tank sludge, have been used.

Success with such a wide range of operating parameters augurs well for the success of the model for more general application, at least with crude oil heating. However, much more testing, especially with other crude oils is required.

5. RECOMMENDATIONS FOR FURTHER WORK

It is recommended that the following studies on heat transfer and fouling from hydrocarbons should be carried out:

1. The fouling apparatus should be modified to allow operation at higher bulk temperatures and higher pressures to more fully cover the ranges found in crude oil preheat trains. Higher bulk temperatures would give higher surface temperatures for a given heat flux and thus could also lead to a shortening in the duration of each experiment. Adaptation of the apparatus to operate at higher pressures would also lead to the ability to avoid subcooled nucleate boiling at higher surface temperatures.

2. Experiments should be carried out with a broad range of crude oils.

3. Continued recirculation and continued use of the feedstock can yield a poor repeatability of fouling data from Run to Run. Thus, more parallel test sections should be installed to enable the trends of velocity, surface temperature, heat flux and insert density to be better established for each Run.

4. For the single-phase heat transfer regime, the effect of velocity, surface and bulk temperature and heat flux on fouling for both the bare tube and the tube fitted with an insert should be examined further.

5. The nucleation phenomenon is likely to occur in crude oil preheat exchangers. Since subcooled nucleate boiling appears to increase substantially the fouling rate it is important to examine further its effect on fouling and thereby elucidate the mechanism.

6. The fouling rate in the region where the thermal boundary layer is developing should be studied in order to determine further the influence of the thermal boundary layer thickness on fouling.

7. The optimum insert geometry, *e g* loop density, should be explored not only to obtain the minimum fouling rate but also to obtain the best combination of film heat transfer coefficient, fouling resistance and pressure drop.

8. HiTRAN inserts should be studied in service in refinery crude oil preheat exchangers and/or in side streams off them.

6 REFERENCES

API Technical Data Book - Petroleum Refining, vol. I, II (1988)

Atkins, GT (1962) What to do about high coking rates, *Petrol Chem Eng*, 34 (4), 20-25

Bergles, AE (1985) Techniques to Augment Heat Transfer, In Handbook of Heat Transfer Applications, eds. Rohsenow, WM, Hartnett, JP and Ganic, NE, McGraw-Hill, New York, Chapter 3

Bergles, AE (1988) Some Perspectives on Enhanced Heat Transfer - Second Generation Heat Transfer Technology, *J. Heat Transfer,* 110, 1082-1096

Bohnet, M (1987) Fouling of Heat Transfer Surface, *Chem Eng. Technol,* 10, 113-125

Bott, TR and Walker RA (1971) Fouling in heat transfer equipment, *The Chemical Engineer* (London), No. 255, 391-395

Bott, TR and Gudmundssen, JS (1978) Rippled silica deposits in heat exchanger tubes, *Proc. 6th Int. Conf. on Heat Transfer,* vol. 4, Hemisphere, Washington, pp 373-378

Bott, TR (1990) Fouling Notebook, IChemE, Rugby, England

Braun, R (1977) The nature of petroleum process fouling - results with a practical instrument, *Material Performance,* 16, (11), 35-41

Brooks, BT (1926) The chemistry of gasolines particularly with respect to gum formation and discoloration, *Ind. Engng. Chem.* 18, 1198-1203

Bryers, JD and Characklis, WG (1981) Kinetics of Initial Biofilm Formation within a Turbulent Flow System, In Fouling of Heat Transfer Equipment, eds. Somerscales, EFC and Knudsen, JG, Hemisphere, Washington, pp 313-333

Butler, RC, McCurdy, WN and Linden, NJ (1949) Fouling rates and cleaning methods in refinery heat exchangers, *Trans ASME,* 71, 843-847

Canapary, RC (1961) How to Control Refinery Fouling, *Oil & Gas Journal,* Oct. 9, 114-118

Chantry, WA and Church, DM (1958) Design of high velocity forced circulation reboilers for fouling service, *Chem Eng Prog,* 54 (10). 64-67

Chen, J and Maddock, MJ (1973) How much spare heater for ethylene plants?, *Hydrocarbon Process,* 52 (5), 147-150

Chenoweth, JM and Impagliazzo, M eds. (1981) Fouling in Heat Exchange Equipment, HTD-17, ASME, New York

Chenoweth, JM (1988) Liquid Fouling Monitoring Equipment, In Fouling Science and Technology, eds. Melo, LF, Bott, TR and Bernardo, CA, Kluwer Academic Publishers, Dordrecht, pp 49-65

Chenoweth, JM (1990) Final report of the HTRI/TEMA Joint Committee to review the fouling section of the TEMA standard, *Heat Transfer Eng.*, 11, 73-107

Colburn, AP (1933) A Method of Correlating Forced Convective Heat Transfer Data and a Comparison with Fluid Heat Transfer Data and a Comparison with Fluid Friction, *Trans ASME,* 29, 174-210; reprinted in *Int. J. Heat Mass Transfer,* 7, 1359-1384 (1964)

Crittenden, BD and Kolaczkowski, ST (1978) Forced convective heat transfer coefficients to hydrocarbons vaporising in a horizontal furnace tube, *Proc. Annual Research Meeting,* Birmingham University, IChemE, London, pp 25-27

Crittenden, BD and Kolaczkowski, ST (1979a) Mass transfer and chemical kinetics in hydrocarbons fouling, *Proc. Conf. on Fouling, Science or Art?,* I Corr Sci and Techn/IChemE, London, pp 169-187

Crittenden, BD and Kolaczkowski, ST (1979b) Energy savings through the accurate prediction of heat transfer fouling resistance, In Energy for Industry, ed. O'Callaghan, PW, Pergamon, Oxford, pp 257-266

Crittenden, BD and Khater, EMH (1984) Fouling in a hydrocarbon vaporiser, *IChemE Symp. Ser,* 86, 401-414

Crittenden, BD Hout, SA and Alderman, NJ (1987a) Model experiments of chemical reaction fouling, *Chem Eng Res Des,* 65, 165-170

Crittenden, BD, Kolaczkowski, ST and Hout, SA, (1987b) Modelling hydrocarbon fouling, *Chem Eng Res Des,* 65, 171-179

Crittenden, BD and Khater, EMH (1987) Fouling from vaporising kerosine, *J. Heat Transfer,* 109, 583-589

Crittenden, BD (1988a) Basic Science and Models of Reaction Fouling, In Fouling Science and Technology, eds. Melo, LF, Bott, TR and Bernardo, CA, Kluwer Academic Publishers, Dorchrecht, pp 293-313

Crittenden, BD (1988b) Chemical Reaction Fouling of Heat Exchanger, In Fouling Science and Technology, eds. Melo, LF, Bott, TR and Bernardo, CA, Kluwer Academic Publishers, Dorchrecht, pp 315-332

Crittenden, BD and Alderman, NJ (1988) Negative fouling resistance: the effect of surface roughness, *Chem Eng Sci,* 43, 829-838

Crittenden, BD, Downey, IL and Kolaczkowski, ST (1988) Acquisition and interpretation of oil refinery plant data for fouling studies, *Int. Conf. Fouling in Process Plant,* I Corr Sci and Techn/IChemE, Oxford, pp 32-51

Crittenden, BD and Alderman, NJ (1992) Mechanisms by Which Fouling Can Increase Overall Heat Transfer Coefficient, *Heat Transfer Eng,* 13 (4), 32-41

Crittenden, BD, Kolaczkowski, ST and Downey, IL (1992) Fouling of crude oil preheater exchangers, *Trans. IChemE,* 70A, 547-557

Crittenden, BD, Kolaczkowski, ST and Takemoto, T (1993) Use of in-tube inserts to reduce fouling, *29th AIChE Heat Transfer Conf,* Atlanta, 8-11 August

Dickakian, G and Seay, S (1988) Asphaltene precipitation primary crude exchanger fouling mechanism, *Oil & Gas Journal,* Mar. 7, 47-50

Dickakian, G (1989) Crude oil fouling control by a fouling analyzer, In Heat Transfer Equipment Fundamentals, Design, Application and Operating Problems, ed. Shah, RK, HTD - 108, pp 331-336

Dittus. FW and Boelter, LMK (1930) University of California, Berkeley, *Publications on Engineering,* vol. 2, p443

Dreytser, GA, Gomon, VI and Aronov, IZ, (1983) Comparison of fouling in tubes and annular turbulence promoters and in tubes of smooth shell-and-tube heat exchangers, *Heat Transfer,* Sov. Res., 15 (1), 87-93

Eaton, P and Lux, R (1984) Laboratory fouling test apparatus for hydrocarbon feedstocks, ASME, HTD-35, pp 33-42

Emanuel, NM, Denisov, EV and Maizus, ZK (1967) Liquid phase oxidation of hydrocarbons, Plenum, New York

Epstein, N (1981a) Fouling of heat exchangers, *Proc. 6th Int. Conf. on Heat Transfer,* Vol 6, Hemisphere, Washington, pp 235-253

Epstein, N (1981b) Fouling: Technical Aspects (Afterword to Fouling in Heat Exchangers, In Fouling of Heat Transfer Equipment, eds. Somerscales, EFC and Knudsen, JK, Hemisphere, Washington, pp 31-52

Epstein, N (1983) Thinking About Heat Transfer Fouling: A 5 x 5 Matrix, *Heat Transfer Eng.* 4 (1), 43-56

Epstein, N (1988) General Thermal Fouling Models, In Fouling Science and Technology, eds. Melo, LF, Bott, TR and Bernardo, CA, Kluwer Academic Publishers, Dorchrecht, pp 15-30

Fernandez-Baujin, JM and Solomon, SM (1976), An industrial application of pyrolysis technology: Lummus SRT III Module, In Industrial and Laboratory Pyrolyses, eds. Albright, LF and Crynes, BL, *ACS Symp. Ser.* No. 32, Washington, pp 345-372

Finlayson, BA (1980) Nonlinear Analysis in Chemical Engineering, McGraw-Hill, New York, Chapter 4-5

Fitzer, E, Mueller, K and Schaeffer, W (1971) The chemistry of the pyrolytic conversion of organic compounds to carbon, In Chemistry and Physics of Carbon, vol 7, ed. Walker, PL jnr, Marcel Dekker, New York, pp 237-383

Garrett-Price, BA, Smith BA, Watt, RL, Knudsen, JG, Marner, WJ and Suitor, JW (1985) Fouling of Heat Exchangers, Characteristics, Costs, Prevention, Control and Removal, Noyes Publications, Park Ridge

Gough, MJ and Rogers, JV (1982) UK Patent Application, GB 2097910A

Gough, MJ and Rogers, JV (1987) Reduced fouling by enhanced heat transfer using wire matrix radial mixing elements, *AIChE Symp. Ser.*, 83 (257), 16-21

Gough, MJ and Rogers, JV (1991) Getting more performance from heat transfer, *Processing,* July, 15-16

Hasson, D (1981) Precipitation Fouling, In Fouling of Heat Transfer Equipment, eds. Somerscales, EFC, and Knudsen, JG, Hemisphere, Washington, pp 527-568

Jackman, A and Aris, R (1971) Optimal control for pyrolytic reactors, *Proc. 4th Euro Symp on Chemical Reaction Engineering,* Pergamon, Oxford, pp 411-419

Katz, DL, Knudsen, JG, Balekjian, G and Grover, SS (1954) Fouling of Heat Exchangers, *Petroleum Refiner,* 33 (8), 123-125

Kern, DQ and Seaton, RE (1959) A theoretical analysis of thermal surface fouling, *Brit. Chem. Eng.*, 4 (5), 258-262

Khater, EMH (1983) Fouling in a hydrocarbon vaporiser, PhD Thesis, University of Bath

Kim, N-H and Webb, RL (1991) Particulate fouling of water in tubes having a two-dimensional roughness geometry, *Int. J. Heat Mass Transfer,* 34 (11), 2727-2738

Knudsen, JG (1981) Apparatus and Techniques for Measurement of Fouling of Heat Transfer Surface, In Fouling of Heat Transfer Equipment, eds. Somerscales, EFC and Knudsen, JG, Hemisphere, Washington pp 57-81

Kolaczkowski, ST, Crittenden, BD and Varley, R (1988) Operability of crude oil preheat exchangers: computer software to manage the problem, *Proc Int. Conf. on Fouling in Process Plant*, I Corr Sci and Techn/IChemE, London, pp 52-67

Kornbau, RW, Richard, CC and Lewis, RO (1983) Seawater Biofouling Countermeasures for Spirally Enhanced Condenser Tubes, *IChemE Symp. Ser.*, 75, 200-212

Kreith, F and Summerfield, M (1949) Heat Transfer to water at high flux densities with and without surface boiling, *Trans. ASME,* 71, 805-815

Lambourn, GA and Durrieu, M (1983) Fouling in Crude Oil Preheat Trains, In Heat Exchangers - Theory and Practice, eds. Taborek, J, Hewitt, GF and Afgan, N, Hemisphere, Washington pp 841-852

Lawer, D (1979) Fouling by Crude Oil in Refinery Heat Exchangers, In Fouling-Science or Art? I Corr Sci and Techn/IChemE, London, pp 155-168

Lenz, RW (1982) Polymerisation mechanisms and processes, In Kirk-Othmer Encyclopedia of Chemical Technology, vol. 18. Wiley, New York, pp 720-744

Melo, LF, Bott, TR and Bernardo, CA eds. (1988) Fouling Science and Technology, Kluwer Academic Publishers, The Netherlands

Moody, LF (1944) Friction factor for pipe flow, *Trans. ASME,* 66, 671-684

Muller-Steinhagen, H (1988) Particulate Fouling for Low Finned Tubes and for Plate Heat Exchangers, *Int. Conf on Fouling in Process Plant,* Oxford, pp 113-130

Nelson, WL, (1934) Fouling of heat exchangers, *Refiner and Nat Gas Man,* 13 (7), 271 - 276

Nelson, WL (1958) Petroleum Refinery Engineering, 4th Ed, McGraw-Hill, New York, p549

Nijsing, R (1964) Diffusional and Kinetic phenomena associated with fouling, Euratom Report EUR 543e

Oliver, DR and Aldington, RWJ (1988) Heat Transfer Enhancement in Round Tubes Using Wire Matric Turbulators: Newtonian and Non-Newtonian Liquids, *Chem Eng Res. Dev,* 66, 555-565

Panchal, CB (1989) Experimental investigation of seawater biofouling for enhanced surfaces, In Heat Transfer Equipment Fundamentals, Design, Applications and Operating Problems ed. Shah, RK, HTD - 108, pp 231-238

Panchal, CB and Watkinson, AP (1993) Chemical Reaction Fouling Model for Single-Phase Heat Transfer, *29th Heat Transfer Conf.*, Atlanta, 8 - 11 August

Patterson, WR and Fryer, PJ (1988) A reaction engineering approach to the analysis of fouling *Chem Eng Sci.*, 43, 1714-1717

Patun, RJ, Krueger, RH and Starner, K (1981) Fouling studies and heat transfer test stand real time data acquisition system, In Fouling of Heat Transfer Equipment, eds. Somerscales, EFC and Knudsen, JG, Hemisphere, Washington, pp 111-131

Pritchard, AM (1988) The Economics of Fouling, In Fouling Science and Technology, eds. Melo, LF, Bott, TR and Bernardo, CA, Kluwer Academic Publishers, Dordrecht, pp 31-45

Rawson, MW, O'Neill, BK and Agnew, JB (1991), Thermal fouling of crude oil heat exchangers, 9th Australasian Chemical Engineering Conf. Newcastle, pp 850-855

Rebello, WJ, Richlen, SL and Childs, F (1988) The cost of heat exchanger fouling in the US industries, Report EGG M 39187

Reich, L and Stivala, SS (1969) Autoxidation of hydrocarbons and polyolefins: Kinetics and Mechanisms, Marcel Dekker, New York

Ritter, RB (1984) Crystalline Fouling Studies, In Fouling in Heat Exchange equipment, eds. Chenoweth, JM and Impagliazzo, M, HTD - 17, pp 67-72

Rogers, JV, Bowen, JE and Gough, MJ (1989) Demonstration of improving heat transfer in a high viscosity, low Reynolds number application, *AIChE Symp. Ser,* 85 (269), 160-165

Saunders, EAD (1988) Heat Exchangers, Selection, Design and Construction, Longman Scientific & Technical, England

Scarborough, CE, Cherrington, DC, Diener, R and Golan, LP (1979) Coking of crude oil at high heat flux levels, *CEP,* 75 (7), 41-46

Shah, YT, Stuart, EB and Sheth, KD (1976) Coke formation during thermal cracking of n- octane, *Ind Engng Chem Proc Des Dev,* 15 518-524

Shalhi, AM (1993) Use of HiTRAN inserts to enhance heat transfer and control fouling from hydrocarbon, Ph.D. thesis, University of Bath, UK

Sheikholeslami, R and Watkinson, AP (1986) Scaling of Plain and Externally Finned Heat Exchanger Tubes, *J Heat Transfer,* 108, 147-152

Smith, JD (1969) Fuel for the supersonic transport: effects of deposition on heat transfer to aviation kerosine, *Ind Engng Chem Proc Des Dev,* 8, 299-308

Somerscales, EFC and Knudsen, JG, eds. (1981) Fouling of Heat Transfer Equipment, Hemisphere, Washington

Somerscales, EFC (1988) Fouling of heat transfer surface: An historical review , essays in honour of 50th anniversary of the ASME heat transfer division; Layto, ET and Lienhard, JH eds. ASME

Speight, JG (1980) The Chemistry and Technology of Petroleum, Marcel Dekker, New York

Suitor, JW and Prichard, AM, eds. (1984) Fouling in Heat Exchange Equipment, HTD - 35, ASME, New York

Sundaram, KM and Froment, GF (1979) Kinetics of coke deposition in the thermal cracking of propane, *Chem Eng Sci,* 34, 635-644

Taborek, J, Aoki, T, Ritter, RB, Palen, JW and Knudsen, JG (1972a) Fouling: The Major Unsolved Problems in Heat Transfer, *Chem Eng Prog.*, 68 (2), 59-68

Taborek, J, Aoki, T, Ritter, RB, Palen, JW and Knudsen,m JG (1972b) Predictive Methods for Fouling Behaviour, *Chem Eng. Prog.*, 68 (2), 69-78

Taylor, WF, and Wallace, TJ (1968) Kinetics of deposit formation from hydrocarbons: effect of trace sulphur compounds, *Ind Engng Chem Prod Res Dev,* 7, 198-202

Taylor, WF (1969) Kinetics of deposit formation from hydrocarbons, *Ind. Engng Chem Prod Res Dev,* 8, 375-380

Taylor, WF (1974) Deposit formation from deoxygenated hydrocarbons 1. General features, *Ind Engng Chem Prod Res Dev,* 13, 133-138

Taylor, WF (1976) Deposit formation from deoxygenated hydrocarbons 2. Effect of trace sulphur compounds, *Ind Engng Chem Prod Res Dev,* 15, 64-68

Taylor, WF and Frankenfeld, JW (1978) Deposit formation from deoxygenated hydrocarbons 3. Effect of trace nitrogen and oxygen compounds, *Ind Engng Chem Prod Res Dev,* 17, 86-90

TEMA (1968), Tubular Exchangers Manufacturers' Association, 1968 Standards, New York, 138-142

Thackery, P (1979) The Cost of Fouling in Heat Exchange Plant, *Proc. Conf on Fouling, Science or Art?* I Corr Sci and Techn/IChemE, London, pp 1-9

Touloukian YS and Ho, CY, (eds) (1972), Thermophysical Properties of Matter, Plenum Press, New York, vol 1, Thermal conductivity of Metallic Solids

Van Nostrand, WL, Leach, SH and Haluska, JL (1981) Economic Penalties Associated with the Fouling of Refinery Heat Transfer Equipment. In Fouling of Heat Transfer Equipment, eds. Somerscales, EFC and Knudsen, JG, Hemisphere, Washington, pp 619-643

Vranos, A (1981) Influence of Film Boiling on the Thermal Decomposition of Vaporising n- Hexadecane, *Ind Engng Chem Prod Res Dev*, 20, 167-169

Vranos, A, Martenery, PJ and Knight, BA (1981) Determination of coking rate in jet fuel, In Fouling of Heat Transfer Equipment, eds. Somerscales, EFC and Knudsen, JG, Hemisphere, Washington, pp 489-499

Watkinson, AP and Epstein, N (1969) Gas oil fouling in a sensible heat exchanger, *Chem Engng Prog Symp Ser,* 65 (92), 84-90

Watkinson, AP and Epstein, N (1970) Particulate fouling of sensible heat exchangers, *Proc 4th Int. heat Transfer Conf.* Paris, vol. 1. Paper HE 1.6, Elsevier, Amsterdam

Watkinson, AP, Louis, L and Brent, R (1974) Scaling of Enhanced Heat Exchanger Tubes, *Can J. Chem Eng,* 52, 558-562

Watkinson, AP and Martinez, O (1975) Scaling of Spirally Indented Heat Exchanger Tubes, *J Heat Transfer,* 97, 490-492

Watkinson, AP (1988) Critical review of organic-fluid fouling. Argonne National Laboratory Report, ANL/CNSV - TM - 208

Watkinson, AP (1990) Fouling of Augmented Heat Transfer Tubes, *Heat Transfer Eng,* 11 (3), 57-65

Webb, RL (1987) Enhancement of Single-phase heat transfer, In Handbook of Single-Phase Convective Heat Transfer, eds. Kakac, S, Shah, RK and Aung, W, John Wiley & Sons, New York, Chapter 17

Webb, RL and Kim N-H (1989) Particulate fouling of internally ribbed tubes, In Heat Transfer Equipment Fundamentals, Design, Applications and Operating Problems, ed. Shah, RK, HTD - 108, pp 315-324

Weiland, JH, McCay, RC and Barnes, JE (1949) Rates of fouling and cleaning of unfired heat transfer equipment, *Trans ASME,* 71, 849-853

Wilson, DI and Watkinson, AP (1992) Mechanism and solvent effects in chemical reaction fouling, *IChemE Symp Ser,* 129, 987-994

Wilson, EE (1915) A basis for rational design of heat transfer apparatus, *Trans ASME,* 37, 47-89

APPENDIX 1 CHARACTERISTICS OF CRUDE OIL

The physical properties and TBP distillation curve provided by BP for Arabian light crude oil are shown in Table A1.1 and Figure A1.1 respectively.

The density and viscosity of crude oil A (Arabian light crude oil to which 10% by weight waxy residue from a crude oil tank has been added) were measured, the data being shown in Table 3.5 in Section 3.1.2.1.3. The effect of the addition of the waxy residue on the overall composition of the crude oil was determined at the University of Salford and is shown below:

	before addition	after addition
saturates	36%	28%
aromatics	43%	49%
resins	19%	19.5%
asphaltenes	2%	3.5%
total	100%	100%

Using Figure 11A4.1 in the API Technical Data Book, the Watson K value of crude oil A was estimated to be 12.0 based on the measured density and viscosity.

The following correlations are used for extrapolating the physical properties of crude oil.

Table A1.1

Generic Data for Arabian Light Crude

Density at 15°C	0.8575 gm/ml
Gravity (°API)	33.4
Distillation test data	see attached sheet
Sulphur content	1.78% mass
H_2S (dissolved	n/a
Viscosity:	
Kinematic at 20°C	9.67 cs
at 30°C	7.30 cs
Pour point	-57°C
Wax content	n/a
Carbon residue	4.0% mass
Asphaltenes	1.0% wt.
Water	< 0.05% vol.
Water and sediment	n/a
Salt content (as NaCl)	2.7 lb/1000 bbl
Metallic elements:	
nickel	4 ppm
vanadium	15 ppm

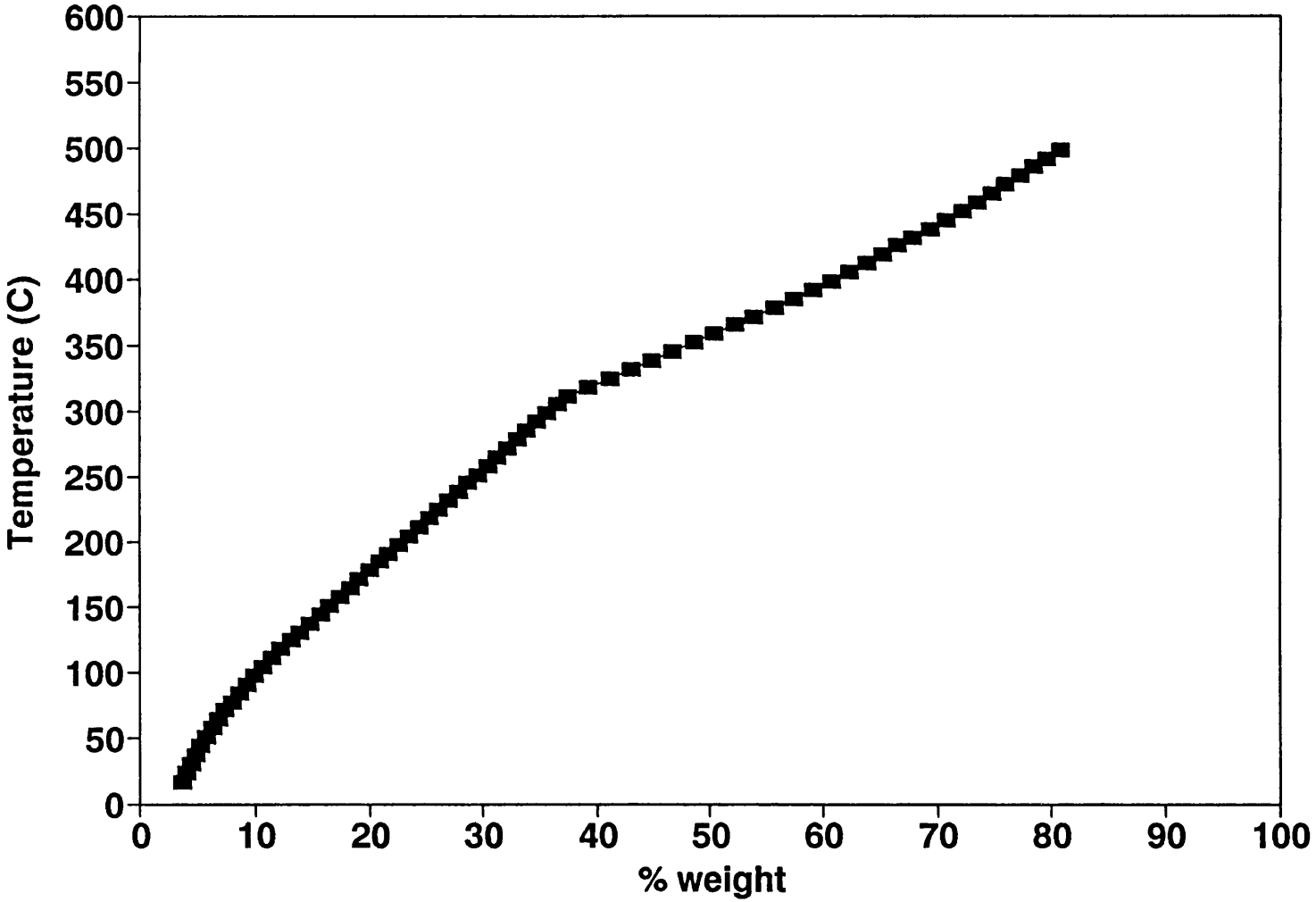

Figure A1.1 TBP distillation curve of Arabian light crude oil supplied by BP

Density, ρ, from:

$$\rho = m_1 T + C_1 \qquad (kg\ m^{-3}) \qquad \text{(A1.1)}$$

in which T is temperature (°C) and m_1 and C_1 are constants

Viscosity, μ, from:

$$\ln \mu = \frac{m_2}{(492 + 1.8T)} + C_2 \qquad (Pa.s) \qquad \text{(A1.2)}$$

in which m_2 and C_2 are constants

Specific gravity, sg, from:

$$sg = \frac{\rho_{15C}}{998.4} \qquad \text{(A1.3)}$$

in which ρ_{15C} is the density at 15°C

Specific heat, C_p, from:

$$C_p = [0.681 - 0.308sg + (1.8T + 32)(0.000815 - 0.000306sg)] * [230.45\ WK + 1466.5] \qquad (J\ kg^{-1}\ °C^{-1}) \qquad \text{(A1.4)}$$

in which WK is the Watson K value.

Thermal conductivity, k, from:

$$k = \frac{1.4065\ (1\ -\ 0.0054T)}{12\ x\ sg} \qquad (Wm^{-1}{}^{\circ}C^{-1}) \qquad \text{(A1.5)}$$

The constants m_1, m_2, C_1 and C_2 were determined from measurements at two temperatures, as follows:

$$\rho_1 = m_1 T_1 + C_1 \qquad \text{(A1.6)}$$

$$\rho_2 = m_1 T_2 + C_1 \qquad \text{(A1.7)}$$

Thus

$$m_1 = \frac{\rho_1 - \rho_2}{T_1 - T_2} \qquad \text{(A1.8)}$$

$$C_1 = \frac{\rho_2 T_1 - \rho_1 T_2}{T_1 - T_2} \qquad \text{(A1.9)}$$

For viscosity

$$ln\ \mu_1 = \frac{m_2}{(492 + 1.8\ T_1)} + C_2 \qquad \text{(A1.10)}$$

$$ln\ \mu_2 = \frac{m_2}{(492 + 1.8T_2)} + C_2 \qquad \text{(A1.11)}$$

Thus

$$m_2 = ln\left(\frac{\mu_1}{\mu_2}\right) * \frac{(492 + 1.8T_1)\ (492 + 1.8T_2)}{1.8\ (T_2 - T_1)} \qquad \text{(A1.12)}$$

$$C_2 = ln\mu_1 - ln\left(\frac{\mu_1}{\mu_2}\right) * \frac{(492 + 1.8T_2)}{1.8(T_2 - T_1)} \qquad \text{(A1.13)}$$

For example, for crude oil A, the constants m_1, m_2, C_1 and C_2 are calculated to be as follows:

Density: From Figure 6A 3.5 in API Technical Data Book. $\rho_1 = 810$ kg m^{-3} at 100°C and $\rho_2 = 702$ kg m^{-3} at 250°C Thus $m_1 = -0.72$ and $C_1 = 882$.

Viscosity: From Figures 6A 3.5 and 11A 4.1 in API Technical Data Book, $\mu_1 = 1.95 \times 10^{-3}$ Pa.s at 98.9°C and $\mu_2 = 8.29 \times 10^{-3}$ Pa.s at 37.8°C. Thus $m_2 = 4945.5$ and $C_2 = -13.623$.

APPENDIX 2 DETERMINATION OF WALL RESISTANCE (Rw) BY WILSON PLOT METHOD

The local thermal resistance between the sleeve thermocouple and the inner surface of the tube have been determined by a graphical technique developed by Wilson (1915). For the test sections used for this study, the overall heat transfer coefficient, U_t, is expressed as:

$$\frac{1}{U_t} = \left(\frac{d_t}{d_i}\right)\frac{1}{h_i} + R_w \qquad \text{(A2.1)}$$

For turbulent flow the heat transfer coefficient may be given by the Dittus-Boelter equation (1930):

$$Nu = 0.023 Re^{0.8} Pr^{0.4} \qquad \text{(A2.2)}$$

Assuming constant physical properties, the heat transfer coefficient is proportional to the velocity of the fluid raised to the power 0.8. Thus equation (A2.1) may be rewritten as:

$$\frac{1}{U_t} = C\left(\frac{1}{V_m}\right)^{0.8} + R_w \qquad \text{(A2.3)}$$

in which V_m is the average velocity of the fluid and C is a constant

Hence a plot of $1/U_t$ versus $V_m^{-0.8}$ should be a straight line, from which an intercept at $Vm^{-0.8} = 0$ gives the local wall resistance R_w.The Wilson plots (average thermal resistances of four thermocouple locations) for both test sections are shown in Figure A2.1, from which the average values of R_w for test sections 1 and 2 are shown to be 0.000161 $m^2K\ W^{-1}$ and 0.00021 $m^2K\ W^{-1}$ respectively. Using the same procedure, the local wall resistance for each thermocouple is given as follows:

	Thermal resistance ($m^2K\ W^{-1}$)	
location	test section 1	test section 2
top	0.00017	0.00018
side (1)	0.00015	0.00017
bottom	0.00016	0.00021
side (2)	0.00017	0.00028

Relatively little circumferential variation in resistance is observed. Also Figure A2.1 shows that the data are well correlated by straight lines even though the physical properties were assumed to be constant. It may be concluded therefore that a changing wall temperature has little effect on R_w.

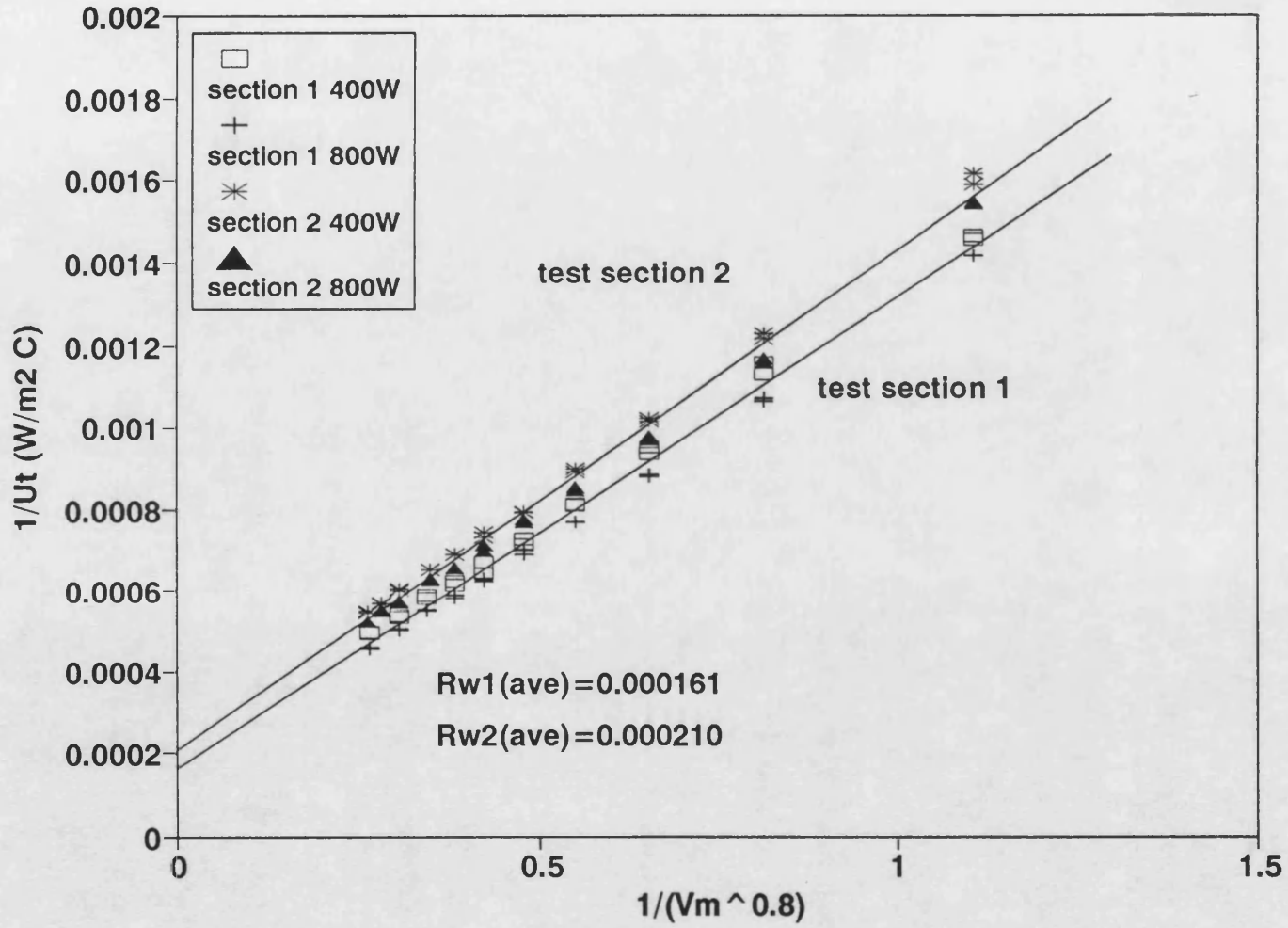

Figure A2.1 Wilson plot for thermal resistance calculation for both test sections

APPENDIX 3 CIRCUMFERENTIAL VARIATIONS OF HEAT TRANSFER COEFFICIENT AND FOULING RESISTANCE

Circumferential variations of both the heat transfer coefficient and the fouling resistance for the bare tube and the tubes fitted with inserts were found to be relatively small over the range of conditions tested.

A.1. Circumferential variations of heat transfer coefficient

For the convective flow regime, example data are shown in Figures A3.1 and A3.2 to illustrate the circumferential variations of heat transfer coefficient for the bare tube and the tube fitted with a low density insert respectively. The variation of heat transfer coefficient around the tube appears to be small.

In order to evaluate the degree of circumferential variation, the variation of the heat transfer coefficient at each circumferential position is plotted against the average heat transfer coefficient in Figure A3.3. All data were measured at a heat flux of 41.5 kW m^{-2}. The variation is calculated from equation (A3.1):

$$Variation(\%) = \frac{difference\ in\ h_i\ between\ the\ highest\ and\ the\ lowest}{h_i\ (average)} x\ 100 \qquad (A3.1)$$

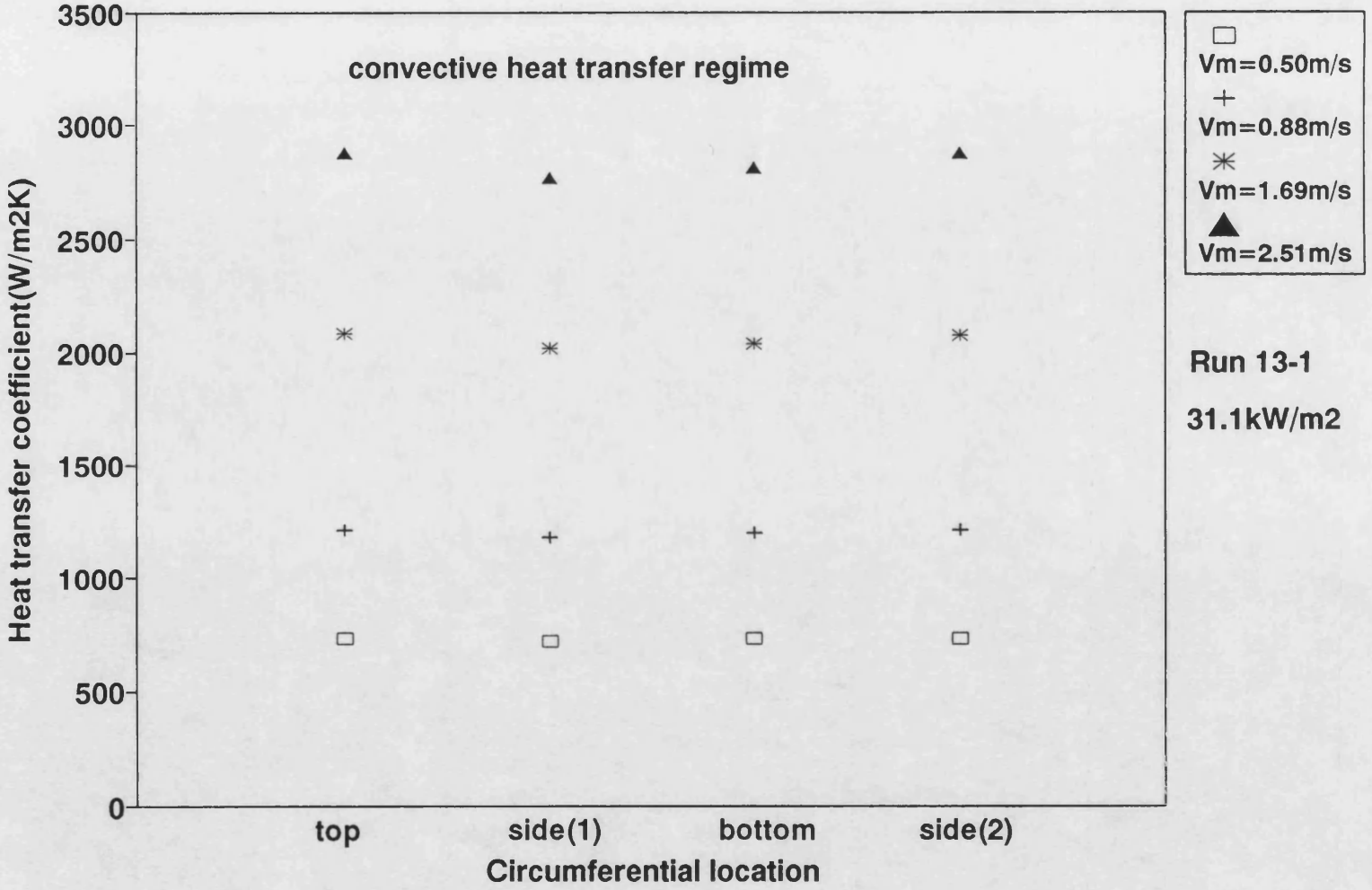

Figure A3.1 Circumferential variation of heat transfer coefficient for the bare tube with flow in convective regime

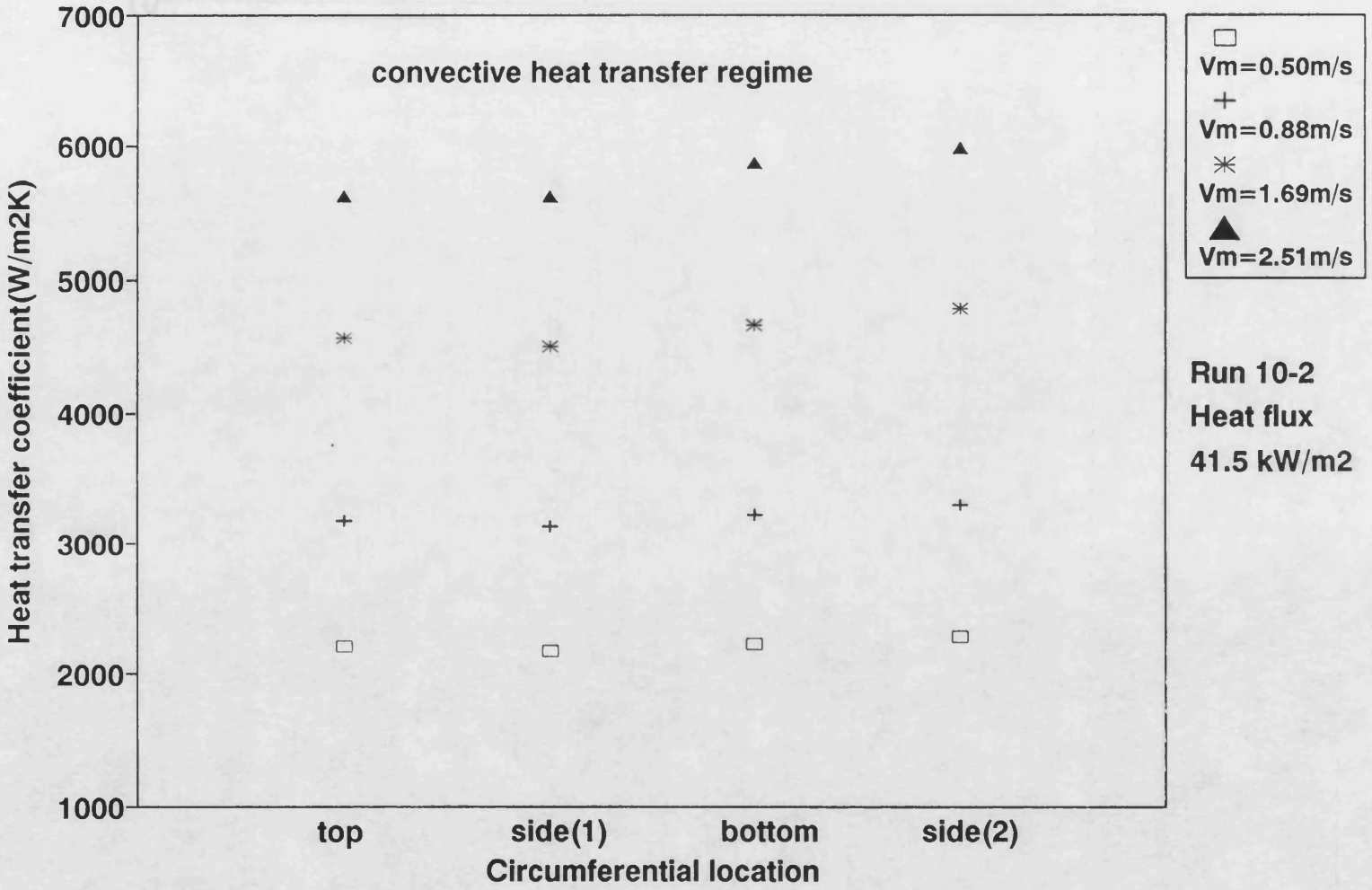

Figure A3.2 Circumferential variation of heat transfer coefficient with the low density insert present with flow in convective regime

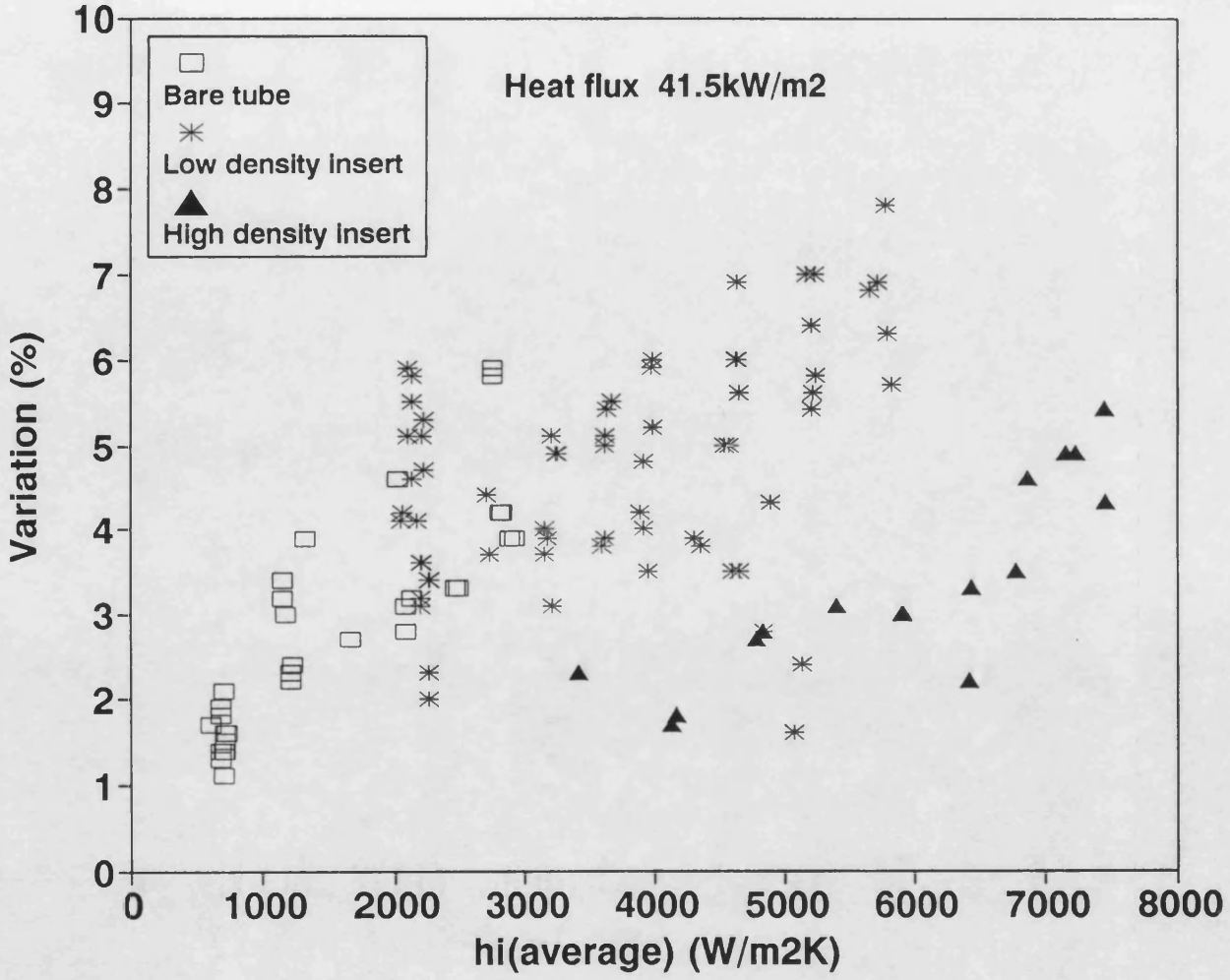

Figure A3.3 Circumfrerntial variation of heat transfer coefficient for the bare tube and for the tube fitted with each insert

In general, the variation appears to increase as the average heat transfer coefficient increases. This is probably due to the increase in the error in the calculated heat transfer coefficient which is caused by the smaller temperature difference between the sleeve thermocouple and the bulk fluid. Figure A3.3 shows that, in general, variation (%) with the heat transfer coefficient decreases slightly from bare tube through low density insert to high density insert.

For the subcooled nucleate boiling regime, the local heat transfer coefficients for the bare tube are shown in Figure A3.4. It can be seen that the circumferential variation with flow in the subcooled nucleate boiling regime seems to remain at about the same level as that for the convective regime over the range of conditions tested.

A.2. **Circumferential variation of fouling resistance**

Table A3.1 summarises the local fouling resistances at the end of the Runs in which the new test sections were used (Run 7 onwards) and the relative magnitude of local fouling resistance (calculated in the same way as shown in Section 2.3). The circumferential variation seems to be less than ± 8% with the exception of the cases in which the fouling resistances are rather small (Runs 7-1, 10-1, 12-1 and 16-1). Examples of local fouling resistance versus time plots for each thermocouple location in a Run are shown in Figures A3.5, A3.6 and A3.7 for Runs 14-2, 14-1 and 16-2, respectively.

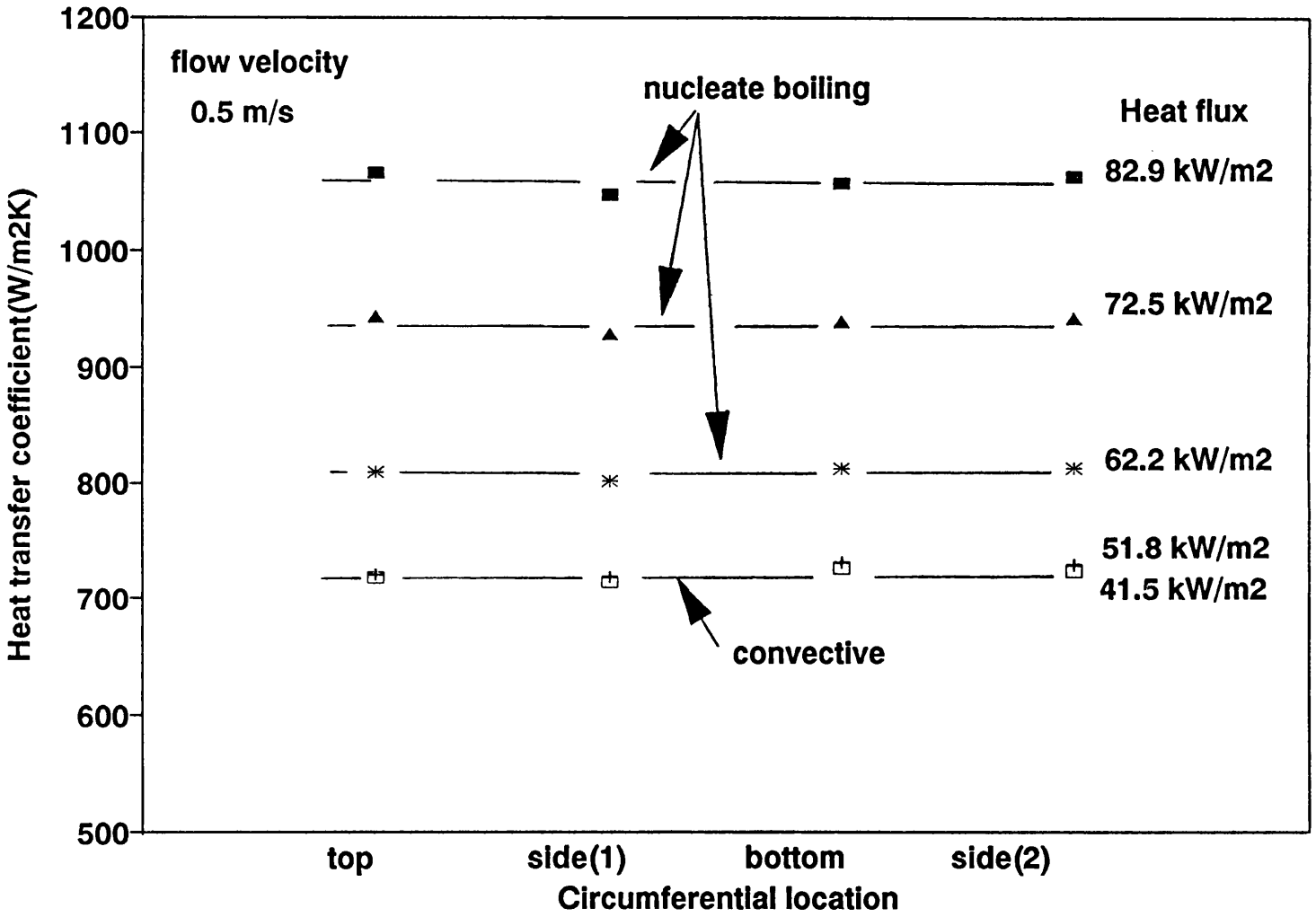

Figure A3.4 Circumferential variation of heat transfer coefficient for the bare tube with flow in subcooled nucleate boiling regime

Table A3.1 Circumferential variation on fouling resistance

Run no	test section	Rf at the end of Run (m2K/W*10^4) Relative magnitude of Rf (%) top	side 1	bottom	side 2	average
Run 7	1 high	0.221 (101)	0.24 (110)	0.191 (88)	0.221 (101)	0.218 (100)
	2 low	0.573 (98)	0.572 (98)	0.603 (103)	0.593 (101)	0.585 (100)
Run 8	1 bare	0.334 (102)	0.333 (102)	0.341 (104)	0.303 (92)	0.328 (100)
	2 low	0.446 (102)	0.434 (100)	0.43 (99)	0.433 (99)	0.436 (100)
Run 9	1 bare	5.05 (104)	5.08 (104)	4.65 (95)	4.68 (96)	4.87 (100)
	2 bare	0.338 (100)	0.338 (100)	0.323 (96)	0.357 (106)	0.338 (100)
Run 10	1 low	0.013 (65)	0.025 (125)	0.023 (115)	0.018 (90)	0.02 (100)
	2 low	0.672 (98)	0.66 (97)	0.684 (100)	0.72 (105)	0.684 (100)
Run 11	1 bare	2.89 (106)	2.74 (100)	2.61 (96)	2.69 (98)	2.73 (100)
	2 bare	8.3 (105)	7.88 (100)	7.59 (96)	7.88 (100)	7.91 (100)
Run 12	1 low	0.124 (83)	0.138 (92)	0.182 (121)	0.157 (105)	0.15 (100)
	2 low	0.248 (98)	0.283 (99)	0.285 (99)	0.305 (106)	0.289 (100)
Run 13	1 bare	0.544 (98)	0.562 (101)	0.553 (100)	0.556 (100)	0.556 (100)
	2 low	0.13 (105)	0.122 (98)	0.117 (94)	0.128 (103)	0.124 100
Run 14	1 bare	4.83 (104)	4.71 (101)	4.47 (96)	4.62 (99)	4.65 (100)
	2 bare	1.46 (100)	1.45 (99)	1.49 (102)	1.46 (100)	1.46 (100)

(continued...)

Table A3.1 continued...

Run no	test section		Rf at the end of Run (m2K/W*10^4) Relative magnitude of Rf (%)				
			top	side 1	bottom	side 2	average
Run 15	1	bare	0.803 (101)	0.776 (97)	0.819 (103)	0.774 (97)	0.797 (100)
	2	bare	-0.767 (103)	-0.755 (102)	-0.742 (100)	-0.707 (95)	-0.743 (100)
Run 16	1	low	0.04 (77)	0.048 (92)	0.064 (123)	0.056 (108)	0.052 (100)
	2	low	0.422 (100)	0.401 (95)	0.423 (101)	0.433 (103)	0.42 (100)
Run 17	1	bare	2.48 (108)	2.3 (101)	2.12 (93)	2.23 (98)	2.29 (100)
	2	low	0.336 (98)	0.353 9103)	0.354 (104)	0.325 (95)	0.342 (100)
Run 18	1	low	0.139 (90)	0.149 (97)	0.168 (109)	0.158 (103)	0.154 (100)
	2	low	0.472 (99)	0.45 (94)	0.472 (99)	0.517 (108)	0.478 (100)
Run 19	1	bare	0.643 (104)	0.643 (104)	0.614 (99)	0.586 (95)	0.619 (100)
	2	low	0.271 (103)	0.259 (98)	0.251 (95)	0.271 (103)	0.263 (100)

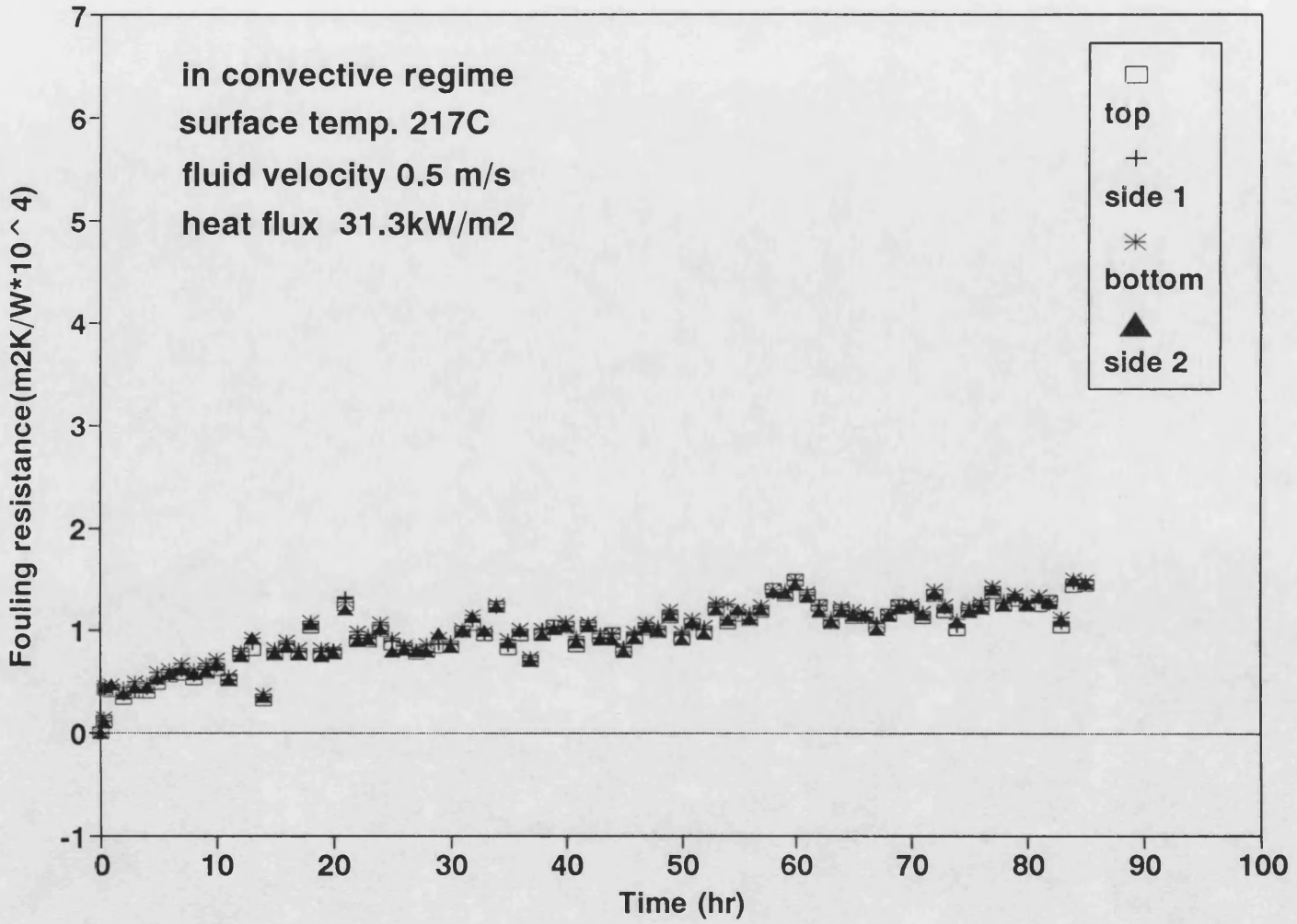

Figure A3.5 Circumferential variation of fouling resistance for the bare tube in Run 14-2

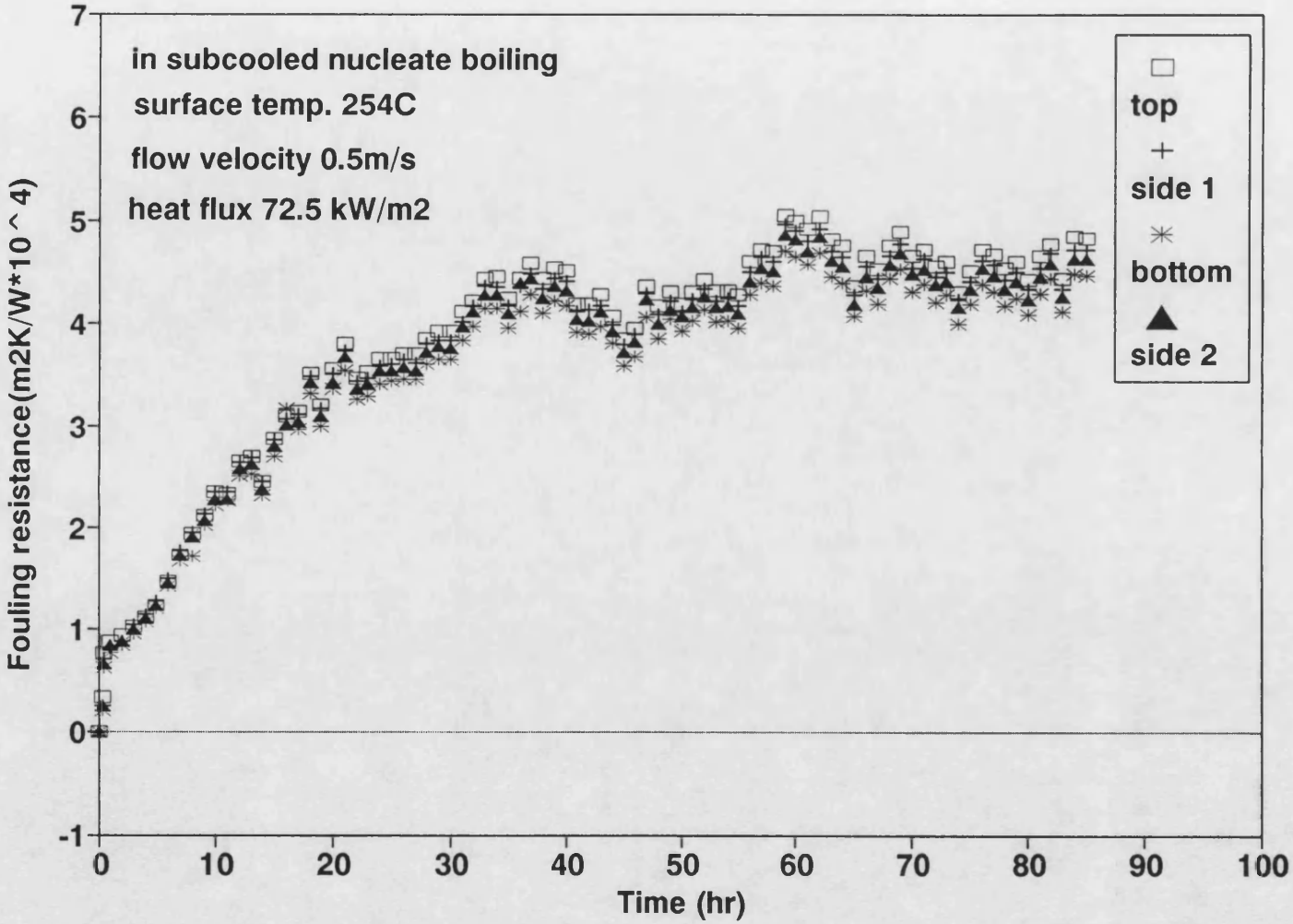

Figure A3.6 Circumferential variation of fouling resistance for the bare tube in Run 14-1

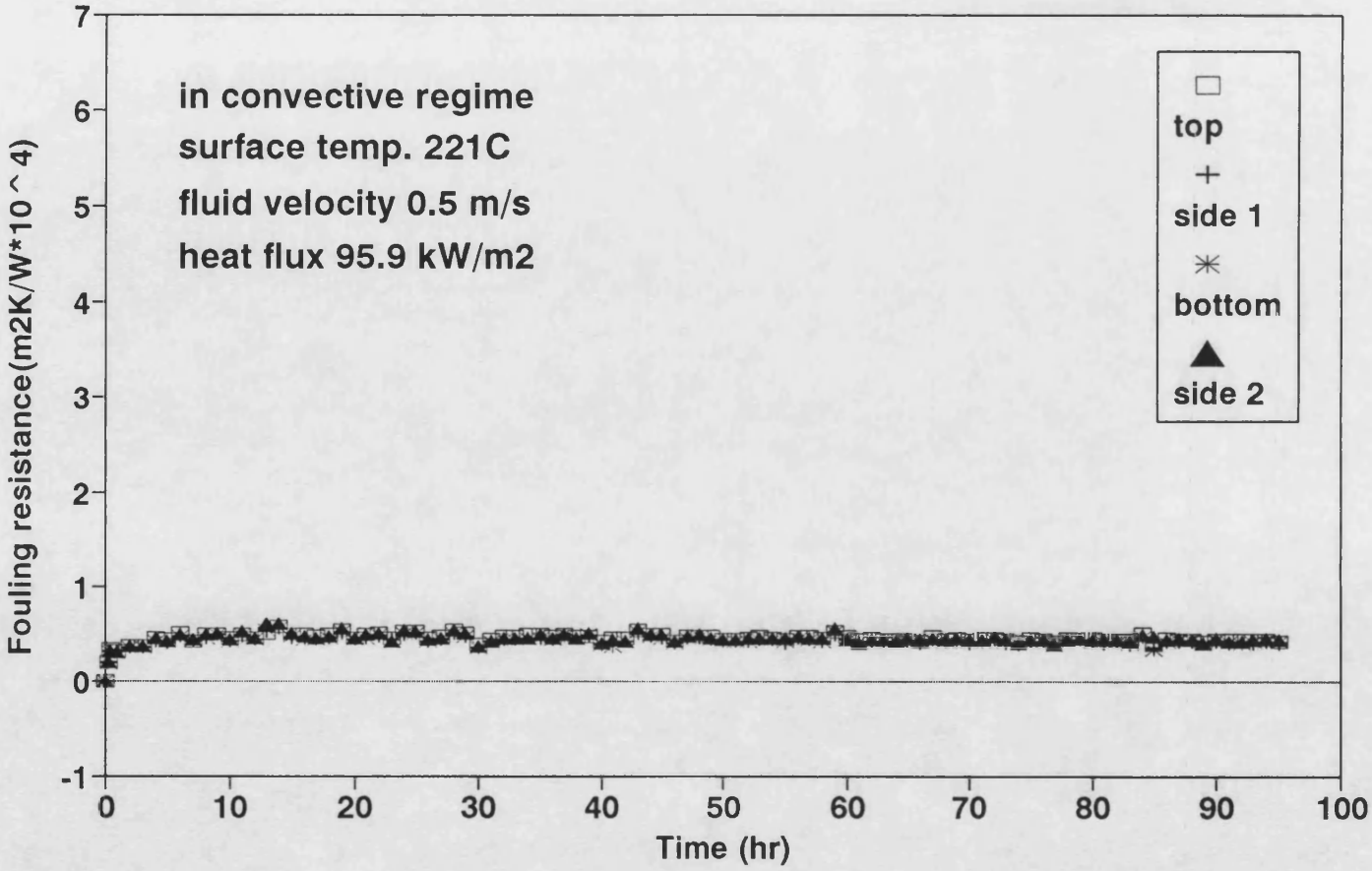

Figure A3.7 Circumferential variation of fouling resistance for the tube fitted with the low density insert in Run 16-2

APPENDIX 4 ESTIMATION OF THE MAGNITUDE OF HEAT CONDUCTION THROUGH THE WIRES OF AN INSERT

When an insert is fitted inside a tube, heat may be transferred by conduction through the wires which contact the tube wall. A calculation was therefore carried out to estimate the magnitude of heat conduction through the wires. The loops of the insert are designed to be sprung on the tube wall and therefore heat could be conducted along a wire through the area that it contacts with the tube wall. The crude oil flows in the pipe and heat is taken from the wire by the flowing fluid.

To simplify the estimation, the following assumptions are made:

(1) Steady-state conditions

(2) One dimensional conduction along the wire

(3) Constant physical properties

(4) Contact resistance between wire and wall is zero

(5) Heat transfer coefficients between fluid and tube and between fluid and wire are equal.

The round straight fin of uniform cross section, shown in Figure A4.1, is considered as a model of half a loop. Applying the conservation of energy requirement to the differential element of Figure A4.2, q_x is given by:

$$q_x = q_{x+dx} + dq_{conv} \qquad \text{(A4.1)}$$

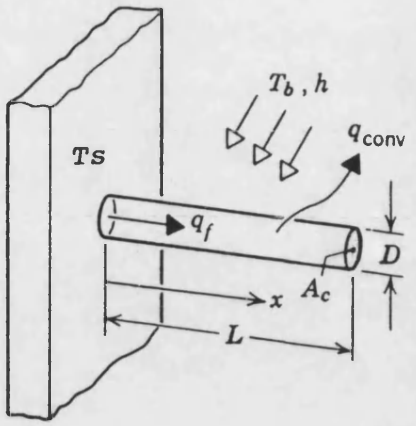

Figure A4.1 Straight fin of uniform cross section

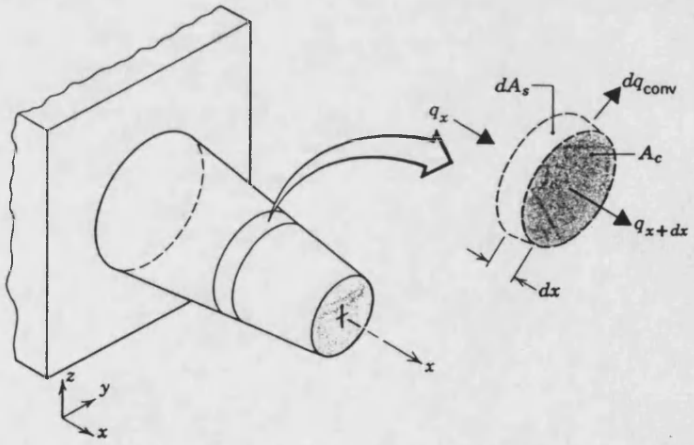

Figure A4.2 Energy balance for an extended surface

in which q_x and q_{x+dx} are the heats transferred to the fluid at the positions x and x + dx respectively and dq_{conv} is the heat transferred by convection from length dx of the wire fin.

From Fourier's law, q_x is given by:

$$q_x = -kA_c\frac{dT}{dx} \qquad \text{(A4.2)}$$

in which A_c is the cross sectional area of the fin and k is the fin thermal conductivity

Using Taylor's expansion, the conduction rate at x + dx may be expressed as:

$$q_{x+dx} = q_x + \frac{dq_x}{dx}\,dx \qquad \text{(A4.3)}$$

It follows that

$$q_{x+dx} = -kA_c\frac{dT}{dx} - k\,\frac{d}{dx}\left(A_c\frac{dT}{dx}\right)dx \qquad \text{(A4.4)}$$

The convection heat rate may be expressed as:

$$dq_{conv} = h\,dA_s(T-T_b) \qquad \text{(A4.5)}$$

in which dA_s is the surface area of the differential element, T_b is the bulk temperature and h is the heat transfer coefficient between fluid and wire.

From equations (A4.1) and (A4.3)

$$\frac{dq_x}{dx}\,dx = dq_{conv} \tag{A4.6}$$

Substituting equations (A4.2) and (A4.5) into equation (A4.6).

$$\frac{d}{dx}\left(A_c\frac{dT}{dx}\right) - \frac{h}{k}\frac{dA_s}{dx}(T-T_b) = 0 \tag{A4.7}$$

For the fin considered, A_c is a constant with x and A_s is equal to πDx in which D is the diameter of the fin.

Accordingly,

$$\frac{dA_c}{dx} = 0 \tag{A4.8}$$

and

$$\frac{dA_s}{dx} = \pi D \tag{A4.9}$$

Thus, equation (A4.7) reduces to:

$$\frac{d^2T}{dx^2} - \frac{\pi Dh}{kA_c}(T-T_b) = 0 \qquad \text{(A4.10)}$$

For convenience, the temperature difference is defined by:

$$\theta(x) = T(x) - T_b \qquad \text{(A4.11)}$$

Temperature T_b is assumed to be constant, thus

$$\frac{d\theta}{dx} = \frac{dT}{dx} \qquad \text{(A4.12)}$$

Substituting equation (A4.11) into equation (A4.10)

$$\frac{d^2\theta}{dx^2} - m^2\theta = 0 \qquad \text{(A4.13)}$$

in which

$$m^2 = \frac{h\pi D}{kA_c} \qquad \text{(A4.14)}$$

A general solution for equation (A4.13) is of the form

$$\theta(x) = C_1e^{mx} + C_2e^{-mx} \qquad \text{(A4.15)}$$

The constants C_1 and C_2 may be determined from the boundary conditions. One may be specified in terms of the temperature at the position x = 0.

$$x = 0 \ , \ T = T_s \tag{A4.16}$$

in which T_s is the surface temperature of the wall.

Thus θ (0) is given by:

$$\theta(0) = T_s - T_b = \theta_s \tag{A4.17}$$

The second one may be specified at the position L shown in Figure A4.1. Assuming that the temperature difference at the position L is equal to zero, the fin length should be considered to be very long.

$$\theta(L) \rightarrow 0 \ , \ L \rightarrow \infty \tag{A4.18}$$

Using equation (A4.15) and boundary conditions (A4.17) and (A4.18), the temperature profile θ (x) is given by:

$$\theta = \theta_s e^{-mx} \tag{A4.19}$$

Applying Fourier's law at the position x = 0, the total heat transferred by the fin (q_f) may be expressed as:

$$q_f = -kA_c \frac{d\theta}{dx} \Big|_{x=0} \tag{A4.20}$$

From equations (A4.19) and (A4.20), q_f is given by:

$$q_f = (h\pi DkA_c)^{1/2}\,\theta_s \qquad \text{(A4.21)}$$

The heat transferred by conduction was estimated as a function of surface temperature using equation (A4.21) for the following conditions:

	low density insert	high density insert
h (Wm^{-2} K^{-1})	2300	3300
	(velocity 0.5 ms^{-1})	(velocity 0.5 ms^{-1})
A_c (m^2)	6.622×10^{-5}	1.183×10^{-4}
	(86 loops per element)	(169 loops per element)

A_c is assumed to be equal to the cross sectional area of the wire for each half of a loop. This assumption probably leads to an over estimate of the amount of heat transferred by conduction because in theory the wire should only make a line contact with the wall.

wire diameter (D)	0.0007 m
thermal conductivity of the wire	17 W m^{-1} K^{-1}
(stainless steel 304)	(Touloukian and Ho (1972))

At a velocity of 0.5 ms^{-1}

$$q_f \ (low) = (2300 \ x \ \pi \ x \ 0.0007 \ x \ 17 \ x \ 6.622 \ x \ 10^{-5})^{1/2} \ (T_s - T_b)$$

$$= 0.0755 \ (T_s - T_b) \qquad (W) \qquad \text{(A4.22)}$$

$$q_f \ (high) = (3300 \ x \ \pi \ x \ 0.0007 \ x \ 17 \ x \ 1.183 \ x \ 10^{-4} \ )^{1/2} (T_s - T_b)$$

$$= 0.121 \ (T_s - T_b) \qquad (W) \qquad \text{(A4.23)}$$

For Run 7-1 (high density insert)

T_s = 197°C, T_b = 149°C and heat input 2000W

From equation (A4.23)

q_f = 0.121 x (197 - 149) = 5.8 (W)

Therefore the contribution of conduction to the total heat transferred is given by:

$$\frac{5.8 \ x \ 100}{2000} = 0.3\%$$

For Run 18-1 (low density insert)

T_s = 218°C, T_b = 149°C and heat input 2000W

From equation (A4.22)

$q_f = 0.0755 \times (218 - 149) = 5.2$ (W)

Therefore the contribution to the total heat transferred is given by:

$$\frac{5.2 \times 100}{2000} = 0.3\%$$

Thus it can be concluded that heat transferred by conduction is negligible compared with the heat transferred by convection when a HiTRAN insert is fitted within a tube. This is essentially because of the small contact area between wire and tube wall.

APPENDIX 5 PAPER ACCEPTED FOR

PRESENTATION AT THE 29TH AICHE

HEAT TRANSFER MEETING, ATLANTA

8 - 11, AUGUST, 1993

USE OF IN-TUBE INSERTS TO REDUCE FOULING FROM CRUDE OILS

B D Crittenden, S T Kolaczkowski and T Takemoto
Hydrocarbon Processing and Fouling Laboratory
School of Chemical Engineering, University of Bath
Bath BA2 7AY, United Kingdom

Abstract

Fouling experiments have been carried out with light Arabian crude oil (containing 10% waxy residue from a crude oil tank) flowing inside 3/4 inch OD, 14 BWG heat exchanger grade tubes of a pilot-scale recycle flow test rig. Use of two identical parallel test sections maintained at constant heat fluxes has allowed direct comparisons to be made in the same Run of the effect of heat flux, surface temperature, flowrate and the presence of HiTRAN inserts. The presence of an insert reduces substantially the extent of fouling and the effect seems not to be simply one of reducing the surface temperature. A greater reduction in fouling appears to occur with insets of higher loop density and it seems that the presence of an insert can alter the hydrodynamics in a beneficial manner. Crucial factors could be enhanced shear removal of deposits, suppression of nucleation as well as reductions in both the residence time and the volume of fluid which is at a temperature in excess of that of the bulk fluid. Further pilot-scale experiments, complemented by field trials on crude preheat trains, are required to elucidate further the actual mechanisms of fouling reduction and to optimise insert configurations.

Fouling from crude oils in the preheat exchanger trains of atmospheric distillation units remains a severe operating problem, with plant data revealing fouling resistances increasing substantially above TEMA recommended design values in relatively short periods of time [1]. The fouling process is undoubtedly complex with rates being dependent on crude oil compositions, storage conditions and processing parameters such as heat flux, temperature and flowrate [1]. Most of the fundamental mechanisms of fouling defined by Epstein [2] are believed [3] to be involved, including chemical reactions of organics, corrosion of surfaces, crystallisation of aqueous fractions, particulate deposition, asphaltene precipitation, etc. It is not surprising therefore that control of crude oil fouling through the use of chemical additives can be difficult to achieve reliably.

Evidence exists to indicate that in general the fouling rate from crude oils can be reduced by reducing skin temperatures and by increasing oil velocities [1, 4]. The latter can help to achieve the former. In-tube inserts as retrofits can also be used to reduce skin temperatures by increasing in-tube film heat transfer coefficients [5, 6]. Their installation reduces both the volume and the residence time of fluid which is exposed to temperatures which are greater than that of the fluid bulk, aspects believed by Nelson [4] to be particularly important in the control of hydrocarbon fouling. Installation of in-tube inserts also increases the degree of turbulence close to the tube wall. Whether this would lead to an increase in fouling rate by promoting the rate of mass transfer of fouling precursors to the hot surface or to a decrease in fouling rate by encouraging deposit removal through fluid shear has stimulated this study of the overall effect of HiTRAN inserts. Belief that the overall effect would be in favour of a reduction in fouling is supported by their success in virtually eliminating fouling in steam heated tar oil heaters [7].

University of Bath
Bath, Avon
United Kingdom

EXPERIMENTAL APPARATUS

The apparatus, comprising a recycle flow loop, a pressure control system and a safety system, is shown in simplified schematic form in Figure 1. The recycle loop consists of a feed stock reservoir (0.105 m^3), two identical horizontal tubular test sections in parallel, a variable speed centrifugal feed pump, valves and flowmeters. Two identical test sections are used for comparative experiments to determine the effects of HiTRAN inserts and process variables on fouling. Each test section comprises a thick wall carbon steel sleeve 0.27m long that has been heat shrunk tightly around a commercial grade heat exchanger tube (d_i = 0.01483 m ID and d_o = 0.01905 m OD). Electrical

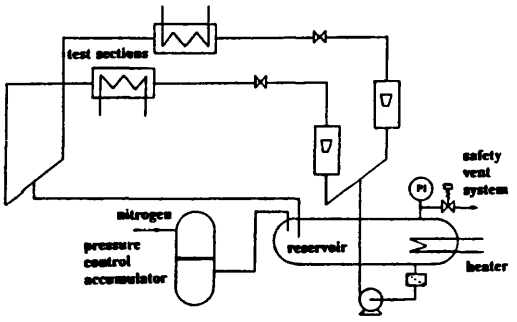

Fig. 1 Simplified schematic of apparatus

heating elements are wound into grooves cut into the surface of the sleeve, into which chromel alumel thermocouples are fitted at known positions close to the fluid outlet end. In order to calculate the local inside surface temperature of a test section the average total resistance R_w between the inner surface of the tube and the thermocouples positioned in the sleeve (which includes the contact resistance between the sleeve and the tube) has been determined by conducting Wilson plot experiments [8]. Figure 2 shows the nomenclature pertaining to a test section.

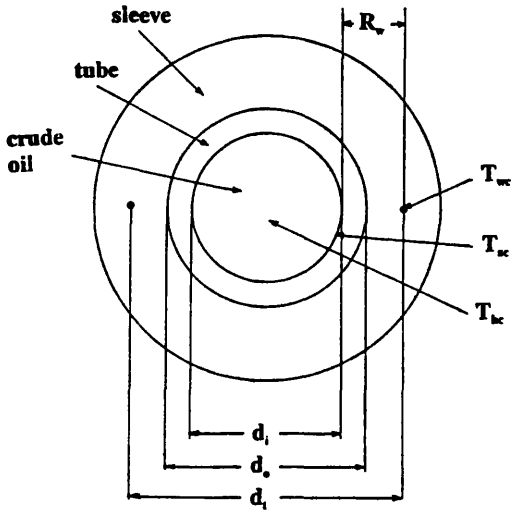

Fig. 2 Nomenclature for a clean test section

R_w is based on d_t, the distance between two diametrically opposed thermocouples (d_t = 0.02345 m). The physical properties of the system were assumed to be independent of temperature in deriving the Wilson plots. The excellent straight lines which were obtained therefore indicate that over the range of conditions studied, the values of R_w were unlikely to be affected by temperature as fouling proceeded.

Crude oil is recycled through the two test sections to be returned to the reservoir. The oil temperature into and out of each test section is measured using sheathed chromel-alumel thermocouples protruding into the centre of the flow tube. System pressure regulation is provided by a piston accumulator, the inside of which is divided into gas and liquid sides by a rigid but movable piston. The crude oil pressure is controlled to 15 ± 0.1 bar by maintaining the pressure of the gas side of the accumulator which is connected to a nitrogen cylinder via a pressure reducing valve.

EXPERIMENTAL PROCEDURE

Experiments have been carried out using Arabian light crude oil to which has been added 10% waxy residue from a crude oil storage tank. The base oil contained around 36% saturated hydrocarbons, 43% aromatics, 19% resins and 2% asphaltenes. It had a gravity of about 31°API, a Watson characterisation factor of 11.4 and an initial bubble point of about 70°C. After the addition of the residue the feed comprised around 28% saturated hydrocarbons, 49% aromatics, 19.5% resins and 3.5% asphaltenes. To start an experiment, the apparatus is filled with oil and the accumulator is pressurised to 15 bar (gauge). The crude oil is then passed through the test sections at maximum flowrate whilst the reservoir is heated by an electrical immersion heater to 140±2°C within about 5 hours. By maintaining high flowrates during the warm-up phase the inside surface temperature of test sections is kept to a minimum to prevent premature fouling. Prior to each fouling run, heat transfer measurements are made to ensure that repeatable heat transfer characteristics (with or without inserts, as appropriate) are obtained. The fouling run is then started at the desired flowrate and the heat fluxes to the parallel test sections kept constant, but not necessarily equal, by means of power controllers and wattmeters. Heat losses from the apparatus were estimated so that the net power supplied to the crude oil could be obtained. About fifteen minutes is required to reach the initial steady state which is deemed to be the clean condition.

Sleeve and bulk temperatures, pressure drops, flowrates and power inputs are recorded typically at

hourly intervals. At the end of a run, the test sections are dismantled and visually inspected. The inside of each test section is cleaned by a repetitive procedure of brushing and wiping with cloth, a procedure possible because the deposits currently have been found to be relatively soft and loosely adhering. Inserts, when removed from the tubes at the end of each Run, are cleaned in toluene. The repeatability of the heat transfer experiments before each fouling run confirm the effectiveness of the cleaning method.

DATA REDUCTION

The clean inside surface temperature T_{sc} of each test section is obtained from Equation (1):

$$T_{sc} = T_{wc} - R_w \phi_c \qquad (1)$$

in which T_{wc} is the temperature of the thermocouple in the sleeve and ϕ_c is the heat flux (based on the area at diameter d_i) under clean conditions. The fouling resistance R_f (based on the area at diameter d_i) is obtained from Equation (2):

$$R_f = \frac{1}{U_d} - \frac{1}{U_c} \qquad (2)$$

in which the clean and dirty overall heat transfer coefficients, U_c and U_d, (based on the area at diameter d_i) are given by Equations (3) and (4), respectively:-

$$\phi_c = U_c (T_{wc} - T_{bc}) \qquad (3)$$

$$\phi_d = U_d (T_{wd} - T_{bd}) \qquad (4)$$

T_{wd} is the temperature of the thermocouple in the sleeve and ϕ_d is the heat flux (based on the area at diameter d_i) under fouled conditions. T_{bc} and T_{bd} are the local bulk temperatures under clean and fouled conditions, respectively. Hence

$$R_f = \frac{(T_{wd} - T_{bd})}{\phi_d} - \frac{(T_{wc} - T_{bc})}{\phi_c} \qquad (5)$$

At any time the thermal coefficient H_i for the heat transfer film and the fouling layer combined is obtained from Equation (6):

$$H_i = \frac{1}{\left(\frac{1}{h_i} + R_f \frac{d_i}{d_t}\right)} = \frac{1}{(\frac{1}{U_d} - R_w)\frac{d_i}{d_t}} \qquad (6)$$

At clean conditions Equation (6) becomes

$$H_i = h_i = \frac{1}{(\frac{1}{U_c} - R_w)\frac{d_i}{d_t}} \qquad (7)$$

in which d_i is the inside tube diameter and h_i is the inside film heat transfer coefficient. Since R_w for the two test sections are numerically quite different, H_i defined by Equation (6) allows direct comparison of the thermal performance of the two test sections to be made. Circumferential variations in H_i and R_f are quite small. Averaged values are presented in this paper.

RESULTS

A summary of the experimental conditions for the four runs described in this paper is provided in Table 1. The same batch of Arabian light crude oil (containing the waxy residue) was used for all the runs and thus it is possible that continued recirculation at elevated temperature and pressure could affect its composition and lead to a loss of, or further formation of, fouling precursors [9]. Such changes might create fouling resistances and fouling rates different from those found in actual refinery heat exchangers. The heat transfer experiments carried out prior to each fouling run seemed to indicate that there was a progressive loss of gases or light ends from the crude oil from run to run. This was manifested by a progressive increase in the minimum temperature at which the heat transfer coefficient began to be increased significantly by an increase in heat flux, a symptom of surface nucleation. Whether or not surface nucleation was believed to be occurring in a test section is reported in Table 1.

An important aspect of the equipment design was that the recycle nature of the experiments allowed

Table 1 Experimental operating conditions

bulk velocity = 0.5 ms^{-1}; Re = 6800

Run	Test section	Insert	Heat Flux * kWm^{-2}	Clean surface temperature °C	Surface nucleation likely
A	1	none	55.9	216	yes
A	2	low density	55.9	198	no
B	1	none	55.9	216	yes
B	2	none	55.9	216	yes
C	1	low density	103.6	218	no
C	2	low density	93.3	218	no
D	1	high density	103.6	197	no
D	2	low density	77.7	197	no

* multiply by d_i/d_o (.02345/.01905) for the flux based on outside tube surface.

operating conditions of temperature, flowrate and heat flux similar to those found in oil refineries to be used in heat exchanger grade tubes within the University's laboratory environment. As a consequence, the heat transfer coefficients for bare tubes and for tubes fitted with HiTRAN inserts should be similar to those used in oil refineries. It is with the above comments in mind that the value of the HiTRAN inserts in controlling fouling must be judged.

Insert used as a retrofit

Figure 3 shows the comparison between a bare tube and one fitted with a low density HiTRAN insert operating under the same conditions of bulk temperature, velocity and heat flux (Table 1). Since the presence of an insert increases the film heat transfer coefficient (in this case from 1030 $Wm^{-2}K^{-1}$ for the bare tube to 1380 $Wm^{-2}K^{-1}$ for the tube fitted with the insert) the clean surface temperature has been reduced from 216°C to 198°C with the insert in place. Figure 3 shows that the consequence of fitting an insert simply as a retrofit is to reduce considerably the rate of fouling. As noted below the fouling resistance ultimately obtained with this insert is low (0.0001 $m^2K.W^{-1}$). The fouling resistance vs. time plot for the bare tube is only beginning to tend towards an asymptotic shape after 90 hours to give an ultimate

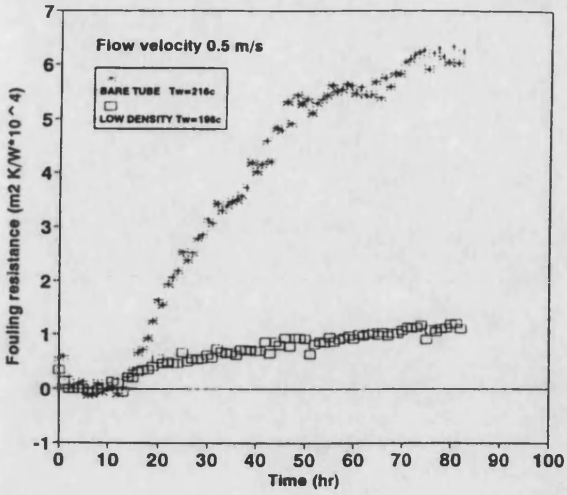

Fig. 3 Fouling data for Run A

resistance at least six times that of the tube fitted with the insert.

Induction periods of around 10 hours are seen for both test sections. Several plausible reasons are available to account for the existence of induction periods:

- the metal surface may require conditioning before deposits will adhere
- a certain amount of time may be required for deposit precursors to be formed in the fluid
- roughening of the heat transfer surface by the deposition process may increase the film heat transfer coefficient to an extent just sufficient to counteract the additional thermal resistance of the deposit itself [10]
- nucleation on the heat transfer surface may increase the film heat transfer coefficient to an extent just sufficient to counteract the additional thermal resistance of the deposit itself [11]

Reproducibility (with bare tubes)

For reasons given above, a comparison of Figures 3 and 5 confirms that some doubt could be expressed about reproducibility from Run to Run. However Figure 4 confirms the excellent reproducibility as expected between the two test sections (in this case without inserts) operating under identical conditions of

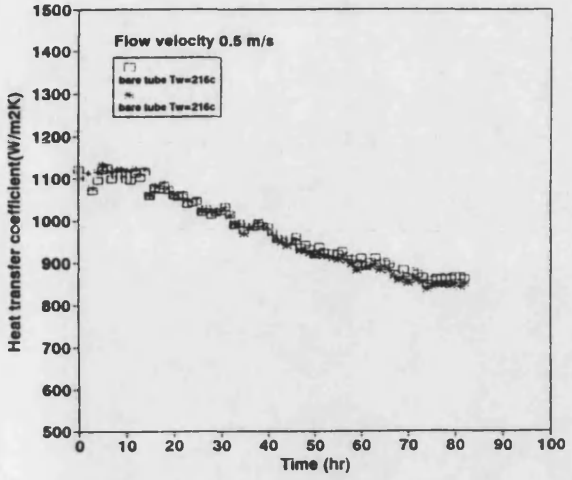

Fig. 4 Thermal coefficient H_i for Run B

flow velocity and heat flux in the same Run B. Clean surface temperatures were both 216°C and the thermal coefficients, H_i, decreased almost identically with time. The corresponding fouling resistances are shown in Figure 5 from which it can be seen that the fouling rate, after the initial induction period, is about 1.79 x 10^{-9} m^2 $K.J^{-1}$ based on d_t (or 1.13 x 10^{-9} $m^2K.\ J^{-1}$ based on d_i). Chenoweth [12] has recently published information on the final report of the HTRI/TEMA Joint Committee to review the fouling section of the TEMA standards.

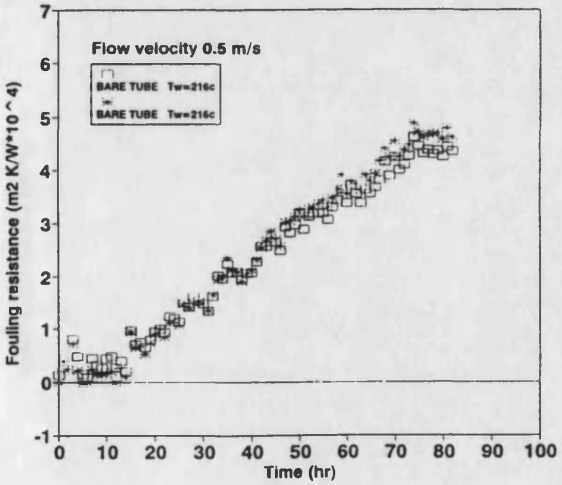

Fig. 5 Fouling data for Run B

Table 2 shows values for crude oil. Thus the test sections in this study would reach the design R_f (0.0007 to 0.00088 at 216°C) in less than 220 hours. One possible reason for this high rate of fouling is the use of a relatively low velocity in this study (0.5 $m.s^{-1}$) compared with that which would normally be used in a refinery heat exchanger (>1$m.s^{-1}$). Even so, previous comparisons with plant data [1, 13] have shown that TEMA design resistances can be exceeded in very short operating periods. Samples of deposit removed at the end of this Run were found to contain 18% ash.

Reproducibility (with inserts)

Figure 6 shows the H_i values for the two parallel test sections fitted with nominally identical low density HiTRAN inserts operated with the same flow velocity (0.5 $m.s^{-1}$) and the same clean surface temperature (218°C) in Run C. The clean film heat transfer coefficients (h_i = H_i at zero time) differ by about 320 $W.m^{-2}K^{-1}$ and as a consequence Table 1 shows that the heat flux for test section 1 needed to be about 11% higher than for test section 2 in order to provide the same clean surface temperature for both sections. The reason for this is believed to be due to a difference in the exact positioning of an insert within a test section tube. Sleeve temperature measurements, used in Equations (1), (3), (4) and (5) are made at a fixed axial location for both test sections. The corresponding calculated H_i values and fouling resistances are therefore local values, rather than values averaged over the length of the heated test sections. The need for

Table 2 Proposed design fouling resistances for crude oil, desalted at ~ 120°C (selected from Chenoweth, 1990)

temperature	velocity	design R_f
°C	$m.s^{-1}$	m^2 $K.W^{-1}$
120	>1.22	0.00035 to 0.0007
120 - 177	>1.22	0.00053 to 0.0007
177 - 232	>1.22	0.0007 to 0.00088
>232	>1.22	0.00088 to 0.00106

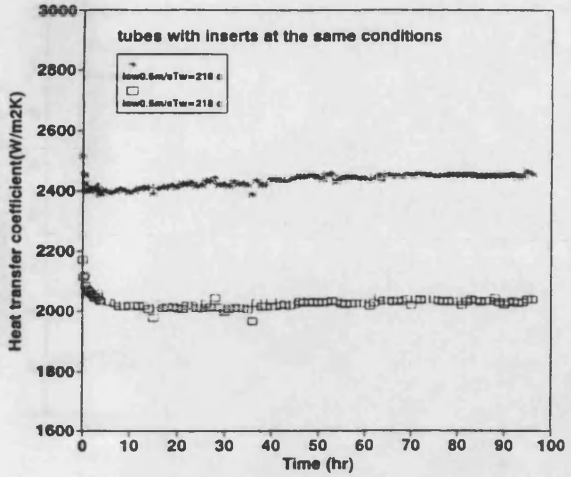

Fig. 6 Thermal coefficient H_i for Run C

higher heat fluxes for Run C compared with Run B is due to the higher film heat transfer coefficients with surface nucleation in Run B.

Comparison of Figures 4 and 6 shows the increase in clean film heat transfer coefficient, h_i, which can be obtained by use of a HiTRAN insert, in this case for a relatively low velocity of 0.5 ms^{-1}. Comparison of conditions for Runs B and C in Table 1 shows that with inserts the heat flux can be increased by a factor of about two without exceeding the surface temperature

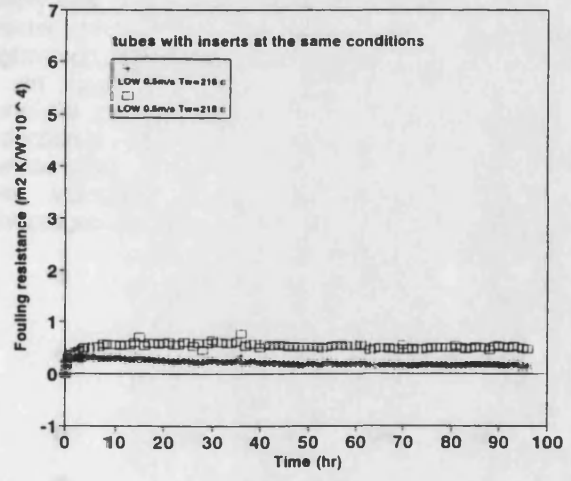

Fig. 7 Fouling data for Run C

of the bare tube case. Clearly the size of a new heat exchanger could be reduced substantially if its tubes were fitted with inserts.

The fouling resistance-time curves for run C are shown in Figure 7. For the same clean surface temperatures and flow velocities a comparison of Figures 5 and 7 reveals several noteworthy features obtainable with inserts. Firstly there are no induction periods. Their lack of existence in Run C could be ascribed to the many hours from the start of Run A of surface conditioning and foulant precursor formation with the same feedstock. Secondly Figure 7 shows a rapid approach of the fouling resistances in both test sections to asymptotic values. With bare tubes, operation up to 80 hours (Figure 5) provides no indication of when , if at all, the fouling resistance-time curves will show a decline in the net fouling rate. Figure 7 shows that with inserts, asymptotes are reached within 10 hours after start-up. The third noteworthy feature of Figure 7 is asymptotic fouling resistances (based on d_i) which are between only about 2 to 7% of the TEMA design values given in Table 2. The fourth noteworthy feature of Figure 7 is that, despite the use of the same velocity, the same clean surface temperature and nominally the same insert, the fouling resistance-time curves are not identical. The difference is not believed to be due simply to experimental error and the propagation of errors in calculating R_f. The higher fouling resistance (test section 2) is obtained with the insert which provides the lower film heat transfer coefficient (Figure 6). The film heat transfer coefficient is inversely proportional to the heat transfer film thickness. Thus a tentative conclusion is that the fouling is related in some way to the volume of fluid which is exposed to a temperature higher than that of the bulk, a simple model of hydrocarbon fouling suggested originally by Nelson [4]. Another possible explanation is that the deposit shear removal rates, if this mechanism indeed operates, could be different in the two test sections, especially since the film heat transfer coefficient is higher for test section 1 which has the lower fouling resistance.

Effect of insert density

Figure 8 provides a comparison between low and high density inserts operated at the same velocity and clean surface temperature. The initial film heat transfer coefficients were 2200 and 3390 $W.m^{-2}K^{-1}$ for the low and high density inserts respectively. The insert with

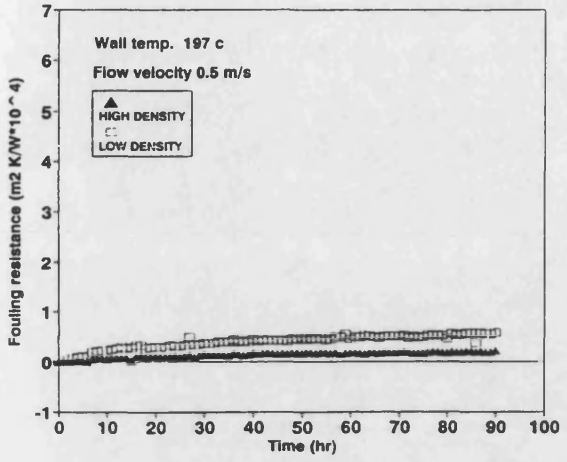

Fig. 8 Fouling data for Run D

the higher film coefficient, which would provide both the lower film thickness and/or the greater deposit removal rate, has again yielded the lower fouling resistance, almost equal to zero.

DISCUSSION AND CONCLUSIONS

The results from the first phase of experimentation demonstrate that HiTRAN inserts can be used to reduce substantially the extent of fouling from Arabian light crude oil to which 10% waxy residue from a crude oil tank has been added. The effect of an insert is not simply one of reducing the surface temperature. A greater reduction in fouling is found with inserts of higher loop density. Thus it appears that the presence of an insert also alters the hydrodynamics in a beneficial manner. The results indicate that a large reduction in fouling is achievable by use of an insert of low density. The additional turbulence close to the heat transfer surface provides four potentially advantageous effects:

- a reduction in the residence time of fouling precursors close to a hot surface, and
- a reduction in the volume of fluid which is heated to a temperature in excess of that of the bulk fluid, and
- the elimination of nucleation at the surface, and
- an increase in the rate of removal or release of deposits at or close to the wall.

Much more pilot-scale experimentation is required to elucidate the relative importance of these mechanisms. In the meantime, the early results now confirm that field trials with inserts in crude oil refinery preheat exchangers should be carried out. Process design studies are also required to obtain the optimum combination of fouling resistance, pressure drop and exchanger size.

ACKNOWLEDGEMENTS

The authors are grateful to Cal Gavin Ltd for sponsorship of the project and for supplying the in-tube inserts. The sponsorship by Asahi Chemical Company of one of the authors (TT) is gratefully acknowledged.

NOTATION

d_i inside tube diameter	m
d_t distance between jacket thermocouples	m
h_i inside film heat transfer coefficient	$W.m^{-2}K^{-1}$
R_f fouling resistance	$m^2K.W^{-1}$
R_w wall resistance	$m^2K.W^{-1}$
T_{bc} temperature, bulk clean	°C
T_{bd} temperature, bulk, fouled	°C
T_{sc} temperature, inner surface, clean	°C
T_{wc} temperature, jacket, clean	°C
T_{wd} temperature, jacket, dirty	°C
U_c overall coefficient, clean	$W.m^{-2}K^{-1}$
U_d overall coefficient, dirty	$W.m^{-2}K^{-1}$
ϕ_c heat flux, clean	$W.m^{-2}$
ϕ_d heat flux, dirty	$W.m^{-2}$

LITERATURE CITED

1 Crittenden B D, Kolaczkowski S T and Downey I L Fouling of crude oil preheat exchangers, Trans IChemE, 70A, 547-557 (1992)

2 Epstein N Fouling in heat exchangers. In Heat Transfer 1978 - Proc 6th Int Heat Transfer Conference, vol 6, Hemisphere, New York (1979)

3 Crittenden B D Basic science and models of reaction fouling. In Fouling Science and Technology, eds Melo LF, Bott TR and Bernardo CA, Kluwer Academic Publishers, Dordrecht, 293-313 (1988)

4 Nelson W L Fouling of heat exchangers, Refiner and Nat Gas Man 13 (7), 271-276 (1934)

5 Gough M J and Rogers J V 1 CPI strive to improve heat transfer in tubes, Chem Eng 93, (3

Feb), 22-25 (1986)
6 Oliver D R and Aldington R W J. Heat transfer enhancement in round tubes using wire matrix turbulators: Newtonian and non-Newtonian liquids. Chem Eng Res Des 66, 555-565 (1988)
7 Gough M J and Rogers J V Reduced fouling by enhanced heat transfer using wire matrix radial mixing elements. AIChE Symp Series 83 (No 257), 16-21 (1987)
8 Wilson E E A basis for rational design of heat transfer apparatus. Trans ASME, 37, 47-89 (1915)
9 Wilson D I and Watkinson A P Mechanism and solvent effects in chemical reaction fouling. IChemE Symp Series 129, 987-994 (1992)
10 Crittenden B D and Alderman N J Negative fouling resistances: the effect of surface roughness. Chem Eng Science 43, 829-838 (1988)
11 Shalhi A M Use of HiTRAN inserts to enhance heat transfer and control fouling from hydrocarbons, PhD Thesis, University of Bath (1993)
12 Chenoweth J M Final report of the HTRI/TEMA Joint Committee to review the fouling section of the TEMA standards. Heat Transfer Eng 11, 73-107 (1990)
13 Bott T R and Walker R A Fouling in heat transfer equipment. The Chemical Engineer (London) No 255, 391-395 (1971)